Insulin-regulated signalling proteins involved in GLUT4 trafficking

Pryor, Paul Robert

Award date:
1999

Awarding institution:
University of Bath

Insulin-regulated Signalling Proteins Involved in GLUT4 Trafficking

Submitted by

Paul Robert Pryor

for the degree of PhD at the University of Bath 1999

ProQuest LLC
789 East Eisenhower Parkway
P.O. Box 1346
Ann Arbor, MI 48106-1346

Abstract

The roles of early signalling intermediates in insulin-stimulated GLUT4 trafficking were investigated in insulin-resistant adipocytes. Chronic-insulin treatment of rat adipocytes reduced insulin receptor tyrosine phosphorylation, PI 3-kinase activation and PKB activation. Despite significant reductions in the activation of early signalling intermediates, GLUT4 exocytosis was calculated to have remained unaffected. However, reduced plasma membrane GLUT4 in chronic-insulin treated adipocytes, was accounted for by an increase in the rate of GLUT4 endocytosis. The chronic-insulin treatment on GLUT4 was reversed by the anti-hyperglycaemic drug metformin, which appeared to act at the level of insulin receptor phosphorylation.

Using periodate-oxidised GTP, it was shown that both Ras-like and heterotrimeric GTP-binding proteins are activated by insulin, downstream of PI 3-kinase. Furthermore, the GTPase ARF was shown to associate directly with GLUT4 vesicles. Since ARF1 recruits adaptor proteins onto vesicles, it is likely to facilitate the trafficking of GLUT4 from the plasma membrane back to the insulin-responsive GLUT4 storage pool.

The possibility of a role of PKB in insulin-stimulated GLUT4 trafficking to the plasma membrane in adipocytes was examined. PKB was not required for contraction-stimulated GLUT4 translocation to the plasma membrane in muscle. A study of PKB and the phosphatase inhibitor, okadaic acid, suggested that okadaic acid may stimulate the exocytosis of recycling endosomes by a PKB-independent route, or may act downstream of PKB.

It is postulated that the lipid products of PI 3-kinase are involved in downstream processes leading to GLUT4 translocation. Heparin and Ins(1,3,4,5)P4 chromatography were used to isolate PI(3,4)P2-/PIP3-binding proteins from adipocytes. Identification of PI(3,4)P2-/PIP3-binding proteins from adipocytes isolated aldolase. Aldolase has been reported to bind phosphoinositides, actin, and the C-terminus of GLUT4. Whether PI 3-kinase regulates aldolase binding to GLUT4, and hence the cytoskeleton, remains to be determined. Other PIP3 binding proteins that were labelled currently remain unidentified but might include centaurin-α and Gap1^{m}.

Acknowledgements

I would especially like to thank Professor Geoff Holman for all the helpful discussions throughout the time within his laboratory and for a critical reading of this thesis. I would further like to thank all past and present members of Geoff's lab for all their help and advice during my time in the lab.

Special thanks goes to all my friends and family who supported me during both the experimental work, and more importantly in the writing of this thesis.

I am also grateful to the MRC and SmithKline Beecham Pharmaceuticals for funding of my PhD studentship.

Publications

Lund, S., **Pryor, P. R.,** Østergaard, S., Schmitz, O., Pederson, O. & Holman, G. D. (1998) Evidence against protein kinase B as a mediator of contraction-induced glucose transport and GLUT4 translocation in rat skeletal muscle. FEBS Lett **425**: 472-474.

Tosh, D., Clark, A. E., **Pryor, P. R.,** Yang, J. & Holman, G. D. (1997) Altered GLUT4 subcellular trafficking in primary cultures of rat adipocytes. Biochem Soc Trans **25**: 469S.

Pryor, P. R., Young, P. W. & Holman, G. D. (1997) In situ labelling of insulin stimulated GTP-binding proteins in adipocytes. Biochem Soc Trans **25**: 475S.

Pryor, P. R., Liu, S. C. H., Clark, A. E., Yang, J., Holman, G. D. & Tosh, D. (1999) Chronic-insulin effects on insulin signaling and GLUT4 endocytosis are reversed by metformin. *Submitted for publication.*

Gillingham, A. K., Koumanov, F., **Pryor, P. R.,** Reaves, B. J. & Holman, G. D. (1999) Formation of GLUT4-enriched vesicles by interactions with AP-1 and AP-3 adaptor complexes. *Submitted for publication.*

Abbreviations

AP-1/2/3	-	adaptor protein-1/2/3
ARF	-	ADP-ribosylation factor
ATB-BMPA	-	2-*N*-[4-(1-azi-2,2,2-trifluoroethyl)benzoyl]-1,3-bis(D-mannos-4-yloxy)-2-propylamine
[^{3}H]BZDC	-	4-benzoyl-[2,3-^{3}H]-dihyrocinnamoyl
BFA	-	brefeldin A
BSA	-	bovine serum albumin
DAB	-	3,3'-diaminobenzidine
DMEM	-	Dulbecco's modification of Eagle's medium
2-DOG	-	2-deoxyglucose
GAP	-	GTPase activating protein
GDI	-	GDP-dissociation inhibitor protein
GEF	-	guanine nucleotide exchange factor
GLUT1/4	-	glucose transporter 1/4
GST	-	glutathione-S-transferase
GSV	-	GLUT4 storage vesicle
GTP	-	guanosine triphosphate
GTPγS	-	guanosine-5'-*O*-(3-thiotriphosphate)
HDM	-	high density microsome(s)
HRP	-	horseradish peroxidase
Ins(1,3,4)P3	-	inositol 1,3,4-trisphosphate
Ins(1,3,4,5)P4	-	inositol 1,3,4,5-tetrakisphosphate
IRS	-	insulin receptor substrate
k_{en}	-	endocytosis rate constant
k_{ex}	-	exocytosis rate constant
KRH	-	Kreb's Ringer's HEPES
LDM	-	low density microsome(s)
NIDDM	-	non-insulin dependent diabetes mellitus
NSF	-	N-ethylmaleimide-sensitive factor
OA	-	okadaic acid
3-OMG	-	3-*O*-methyl-D-glucose
PDGF	-	platelet derived growth factor

PDK1	-	PIP3-dependent protein kinase-1
PH	-	pleckstrin homology
PI 3-kinase	-	phosphatidylinositol 3-kinase
PKB	-	protein kinase B
PKC	-	protein kinase C
PM	-	plasma membrane
PMA	-	phorbol 12-myristate 13-acetate
PTB	-	phosphotyrosine binding
SDS-PAGE	-	sodium dodecyl sulphate polyacrylamide gel electrophoresis
SH2/3	-	Src-homology-2/3
Staph cells	-	*Staphylococcus aureus* Cowan I cells
TBS	-	Tris-buffered saline
TES	-	Tris EDTA sucrose
t-/v-SNARE	-	target-/vesicle-SNAP receptor
TGN	-	*trans*-Golgi network
VAMP	-	vesicle associated membrane protein

Lipid terminology and abbreviations:

PI	-	phosphatidylinositol
PI(3)P	-	phosphatidylinositol 3-phosphate
PIP2	-	phosphatidylinositol 4,5-bisphosphate
PI(3,4)P2	-	phosphatidylinositol 3,4-bisphosphate
PIP3	-	phosphatidylinositol 3,4,5-trisphosphate

The term 'phosphatidylinositide' has been used to encompass the various phosphorylated forms of phosphatidylinositol e.g. PIP2, PI(3,4)P2 and PIP3.

'Phosphoinositide' has been used to include the various phosphorylated forms of inositol e.g. inositol 1,4,5-trisphosphate.

Contents

CHAPTER 1

INTRODUCTION

Glucose plays a pivotal role in cellular homeostasis and metabolism. Hormones such as glucagon and insulin tightly regulate the level of blood glucose. Of central importance in the control of glucose homeostasis is insulin's ability to lower the blood glucose concentrations by promoting glucose uptake into muscle and adipose tissues. A defect in insulin's ability to promote glucose uptake seems to underlie conditions such as non-insulin dependent diabetes mellitus (NIDDM).

Glucose uptake into most mammalian cells occurs *via* facilitative glucose transporters (GLUTs), which are integral membrane proteins. Several GLUT isoforms are known to exist, which are variably expressed in different tissues (reviewed by Gould & Holman, 1993). It is the unique regulation of glucose transporter 4 (GLUT4) in insulin-sensitive tissues (muscle, heart and adipose tissue) which primarily allows insulin to lower blood glucose levels. In the presence of insulin, specialised intracellular GLUT4 storage vesicles (GSVs) rapidly translocate and fuse with the plasma membrane (PM), thereby increasing the cell surface levels of GLUT4. Since the discovery of insulin-regulated GLUT4 trafficking, much research has been undertaken to understand the mechanisms regulating the trafficking process. Research has concentrated primarily on the signalling mechanisms that follows insulin's binding to the insulin receptor, and the subsequent generation of intracellular signalling cascades leading to GLUT4 vesicle translocation. Whilst significant progress has been made in discerning the signalling molecules involved in regulating GLUT4 trafficking in adipose, and more recently, in muscle tissues, many aspects of the proposed signalling cascade require clarification and further molecules still need to be identified.

The thesis has therefore focussed on the role of insulin-regulated signalling molecules implicated in GLUT4 trafficking. Furthermore, research has been aimed at identifying new signalling molecules that may be involved in insulin-regulated GLUT4 trafficking.

Glucose Transporter 4

Following the cloning of GLUT1/2 and 3, there appeared in 1989 five separate reports of the cloning and sequencing of the GLUT4 isoform. (James *et al.*, 1989; Birnbaum, 1989; Charron *et al.*, 1989; Kaestner *et al.*, 1989; Fukumoto *et al.*, 1989).

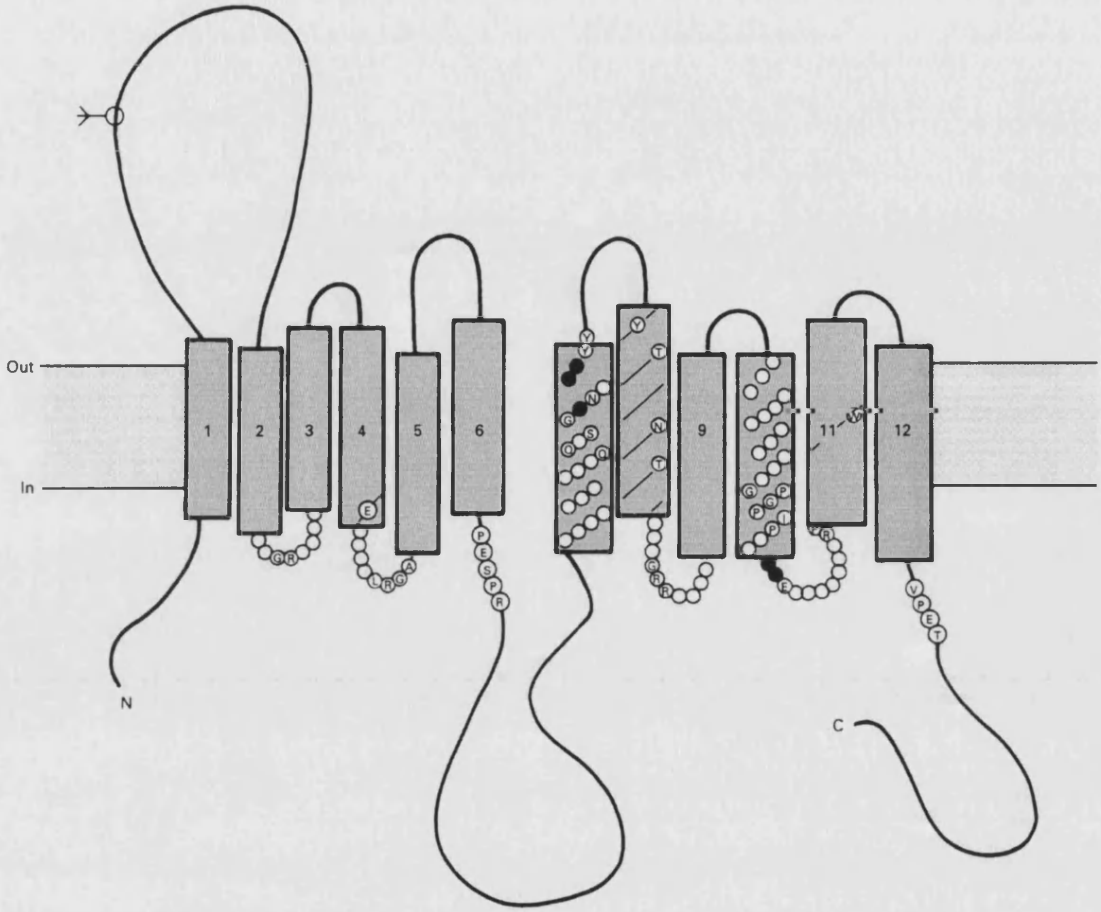

Figure i. Hypothetical model for the structure of glucose transporters (Gould & Holman, 1993). Conserved amino acids are indicated by the appropriate single letter code. Filled circles indicate conservative substitutions. Both the N- and C-terminus of GLUT4 appear to be important in the trafficking and sequestration of GLUT4 to an intracellular location.

Analysis of the predicted amino acid sequences of the mammalian glucose transporters shows that they are highly homologous with one another. Hydropathic analysis predicts 12 amphipathic helices arranged so that both the N- and C-termini are at the cytoplasmic surface (figure i). There is a large loop between helices 1 and 2 which can be glycosylated, and a large loop between helices 6 and 7. The loops between the remainder of the helices of the cytoplasmic surface are very short which places severe constraints on the possible tertiary structures and suggests very close packing of the helices at the inner surface of the membrane in each half of the protein (Gould & Holman, 1993).

Unique to GLUT4 is its intracellular sequestration in unstimulated (basal) adipose, cardiac and muscle tissues. In an attempt to define the relevant targeting domains that direct the intracellular sequestration of GLUT4, studies were performed in which reciprocal domains were exchanged between GLUT4 and GLUT1 and the subcellular distributions of these chimeras analysed in a variety of cellular systems. The chimera studies together with specific amino acid mutations have identified two important domains in the N- and C-termini (F5QQI and L489L490 respectively) involved in GLUT4 intracellular localisation (reviewed by Gould, 1997). Whilst the FQQI and di-leucine motifs appear to be important for GLUT4 internalisation from the plasma membrane, and for trafficking between intracellular compartments, neither of these two domains are entirely sufficient for targeting GLUT4 to the GSV compartment and other targeting domains remain to be discovered (Melvin *et al.*, 1999).

PART A - GLUT4 vesicle biogenesis and trafficking

Insulin-stimulated glucose transporter translocation was first described by two independent groups, Suzuki & Kono (1980) and Cushman & Wardzala (1980). The former group isolated rat adipose cells and stimulated cells with insulin. Cell populations were then homogenised, and a crude microsomal fraction was generated by differential and density gradient centrifugation. Protein fractions taken from sucrose density gradients were then reconstituted into liposomes, and the liposomes assayed for D-[^{3}H]glucose uptake. Glucose uptake into the liposomes was calculated by subtracting cytochalasin B-insensitive uptake (cytochalasin B will inhibit glucose uptake by binding to glucose transporters) from the total glucose uptake activity. The glucose uptake studies identified two glucose transport peaks on the sucrose gradients. One of the two peaks coincided with a marker for the PM, whereas the other peak coincided with a marker for the Golgi apparatus. Insulin-stimulation of the adipose cells decreased the glucose transport peak corresponding to the internal membrane site, with a concomitant increase in the glucose transport peak corresponding to the PM. Since the K_m values for the two glucose transport peaks were roughly similar, it was concluded that insulin facilitates translocation of the transport activity from an intracellular storage site to the PM.

The same conclusion derived by Suzuki & Kono (1980) was obtained by Cushman & Wardzala (1980). The latter authors showed that the number of cytochalasin B binding sites in plasma membranes, isolated from insulin-stimulated cells, increased to 24.4 pmol/mg of membrane protein, compared to 7.8 pmol/mg of membrane protein in basal cells. In contrast, the average number of D-glucose-inhibitable cytochalasin B-binding sites in a microsomal membrane fraction decreased from 37.8 to 21.2 pmol/mg microsomal membrane upon insulin treatment.

Whilst both Suzuki & Kono (1980) and Cushman & Wardzala (1980) determined the translocation of a glucose transporter to the PM in insulin-stimulated rat adipose cells, the intracellular glucose transporter compartment and the trafficking of the glucose transporter remained ill-defined. Part A of this introduction primarily describes the research undertaken since 1980 to address these issues.

1.1 Quantification of GLUT1 and GLUT4

Differential ultracentrifugation of adipocyte homogenates was shown to fractionate adipose cell membranes into four distinct subcellular components (Simpson *et al.*, 1983; Weber *et al.*, 1988). Using marker proteins, the isolated membrane fractions were characterised as the plasma membrane (PM), high-density microsomes (HDM), low-density microsomes (LDM) and a mitochondria and nuclei enriched fraction. Simpson *et al.* (1983) determined that following fractionation of basal rat adipose cells, the levels of D-glucose-inhibitable cytochalasin B-binding sites per mg protein was greatest in the LDM fraction. Insulin-stimulation of the adipose cells decreased the levels of cytochalasin B-binding sites in the LDM enriched fraction, with a concomitant increase in cytochalasin B binding sites in the PM.

Using the fractionation procedure developed by Simpson and colleagues, Zorzano *et al.* (1989) showed that using agarose conjugated to an anti-GLUT4 monoclonal antibody (1F8), ~80% of the GLUT4-containing vesicles in the LDM fraction could be immunoprecipitated. Whilst the GLUT4 vesicles were retained by the agarose pellet, >90% of GLUT1 (unlike GLUT4 which is expressed in adipose, cardiac and muscle tissues, GLUT1 is ubiquitously expressed) was found in the non-adsorbed supernatant. This result suggested that GLUT4 and GLUT1 resided in two (or more) distinct intracellular compartments. Zorzano *et al.* then set out to determine whether both GLUT4 and GLUT1 translocate to the PM in response to insulin. Immunoblotting data showed a 2-fold and 8-fold increase in PM GLUT1 and GLUT4 respectively in adipose cells stimulated by insulin. The insulin-stimulated glucose transporter increase in the PM was consistent with decreases observed in both GLUT1 and GLUT4 from the LDM fraction. To quantitate the relative contributions of GLUT4 and GLUT1 to glucose transport, Zorzano *et al.* photolabelled adipose LDM fractions with [^{3}H]cytochalasin B. Solubilisation of the photolabelled-LDM fraction and immunoadsorption using the 1F8-agarose conjugate, resulted in the retention of ~90% of the radiolabel into the agarose pellet. This result suggested that GLUT4 was the predominant glucose transporter in rat adipose cells. Furthermore, photolabelling of PM glucose transporters (the photolabel used was 3-[^{125}I]iodo-4-azidophenethylamido-7-*O*-succinyldeacetyl-forskolin) resulted in 75% of the photolabel being retained by the 1F8-agarose conjugate. Together the results suggested that GLUT4 is the major glucose transporter in rat adipose cells and can account for the majority of the increase in insulin-stimulated glucose transport.

Further studies (described below), using a novel glucose transporter photolabel, namely 2-*N*-[4-(1-azi-2,2,2-trifluoroethyl)benzoyl]-1,3-bis(D-mannos-4-yloxy)-2-propylamine (ATB-BMPA) (Clark & Holman, 1990) (figure 1), agreed with the data by Zorzano *et al.* (1989).

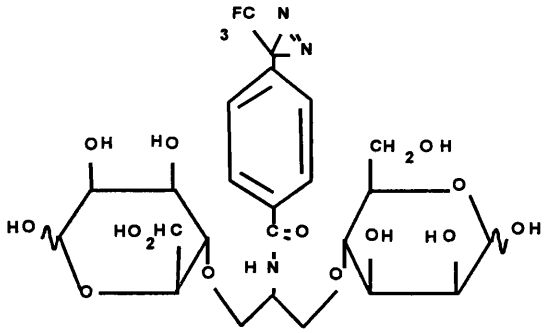

Figure 1. ATB-BMPA. ATB-BMPA consists of two mannose groups linked by a propyl-2-amine bridge. The diazirine generating photolabel is then attached to the bridge between the two sugars. Upon irradiation with 300 nm light, the diazirine loses nitrogen and generates a short-lived carbene that can form a covalent bond with any adjacent proteins. Hence, only the ligand that is bound to an active site is cross-linked to the protein. Tritium incorporation into the photolabel allows the detection of the ATP-BMPA.

ATB-BMPA was used to quantitate cell surface GLUT1 and GLUT4 in 3T3-L1 adipocytes (a differentiated fibroblast with properties similar to adipocytes) (Calderhead *et al.*, 1990). Western blotting of 3T3-L1 adipocyte lysates revealed that GLUT1 was expressed at a higher level than GLUT4, however, ATB-BMPA photolabelling of insulin-stimulated 3T3-L1 adipocytes showed 6.5- and 17.1-fold increases in PM GLUT1 and GLUT4, respectively. The increases in glucose transporters in the PM corresponded to a 21-fold increase in 2-deoxyglucose uptake. It was assumed that if GLUT4 has a higher intrinsic activity compared to GLUT1, then the translocation of GLUT4 could account for the insulin effect on hexose transport.

While 3T3-L1 adipocytes have a higher level of expression of GLUT1 than GLUT4, photolabelling in rat adipocytes revealed that the GLUT4 levels were 9 times higher than the GLUT1 levels (Holman *et al.*, 1990). Photolabelling studies also revealed that insulin stimulated a 15-20-fold increase in PM GLUT4 levels, whilst GLUT1 increased by approximately 3-5-fold. Again, glucose transport activity corresponded to the appearance of GLUT4 on the cell surface (Holman *et al.*, 1990). Studies by Nishimura *et al.* (1993) using ATB-BMPA, in rat adipocytes, demonstrated that GLUT4 has a 6-fold higher intrinsic activity (turnover number/K_m) than that of GLUT1 (turnover for both transporters were found to be

20,000 min^{-1}, and the K_ms for GLUT1 and GLUT4 were 26.2 mM and 4.3 mM, respectively). Studies in 3T3-L1 adipocytes, using ATB-BMPA, also determined that GLUT4 has a higher intrinsic activity than GLUT1 (Palfreyman *et al.*, 1992). Hence, ATB-BMPA photolabelling in rat and 3T3-L1 adipocytes determined that GLUT4 is generally the major contributor to insulin-stimulated glucose transport activity in these cells.

1.2 Kinetic studies of GLUT4 trafficking

ATB-BMPA photolabelling was used by Satoh *et al.* (1993) to dissect the trafficking of GLUT4 between the PM and LDM fractions in rat adipocytes. This study involved a combination of Western blotting of adipocyte sub-cellular fractions for GLUT4, ATB-[2-^{3}H]BMPA photolabelling, and measurements of the rates of glucose uptake into adipocytes. The trafficking kinetic studies were carried out on adipocytes under three conditions, which were as follows: cells were stimulated by the continuous presence of insulin, or cells were stimulated with insulin and then treated with collagenase to remove insulin from the cell surface, or finally insulin-stimulated cells were treated with collagenase and then subsequently re-challenged with insulin. Cells maintained in the continuous presence of insulin retained high levels of PM GLUT4. In this latter condition, the levels of GLUT4 protein in the PM as determined by Western blotting remained constant in the continuous presence of insulin. However, there was a slight loss of ATB-BMPA-photolabelled GLUT4 (a decrease of 55% from maximal levels, to a 45% steady state) from the PM. The $t_{½}$ for the decrease in ATB-BMPA labelled GLUT4 from the PM was similar to cells where the insulin stimulation was removed by collagenase treatment. This indicated that GLUT4 undergoes a constant rapid re-cycling between the PM and intracellular membranes even in the continuous presence of insulin.

After ATB-BMPA photolabelling of insulin-stimulated rat adipocytes, removal of the insulin by collagenase treatment showed a decrease in the amount of ATB-BMPA-tagged GLUT4 in the PM fraction ($t_{½}$ = 9.4 ± 0.8 min). The decrease in PM ATB-BMPA-labelled GLUT4 was fully accounted for by reciprocal changes in the LDM levels of ATB-BMPA-labelled GLUT4. These results correlated with both the rates of glucose uptake, and Western blotting of the levels of GLUT4, in both the PM and LDM fractions.

Finally, the third treatment showed that a subsequent re-challenge by insulin following collagenase treatment increased the ATB-BMPA labelled GLUT4 levels in the PM to a steady

state of 45% of the initial fully insulin-stimulated level. This latter process occurred with a $t_{½}$ = 2.7 ± 0.3 min, which correlated with immunodetectable PM GLUT4, but was slightly faster than the increase in glucose transporter activity. Together the results were consistent with the possibility that in the presence of insulin the entire complement of GLUT4 in adipocytes is involved in a recycling process between the PM and microsomal fraction.

The study by Satoh *et al.* (1993) showed that at 37°C the $t_{½}$ for GLUT4 translocation to the PM as measured by Western blotting and photolabelling with ATB-BMPA was slightly faster than the increase in glucose transport activity. These differences between immunodetectable PM GLUT4 and glucose transport were more noticeable at 20°C. The lower temperature studies showed that the rates of appearance of GLUT4 detected by ATB-BMPA photolabelling ($t_{½}$ = 9 min) and by Western blotting ($t_{½}$ = 5 min), were both faster than the rates of increase in glucose transport activity, which occurred with a $t_{½}$ of 12 min. These data are similar to studies by Yang *et al.* (1992), using 3T3-L1 adipocytes. The discrepancies between the rates of increase in GLUT4 in the PM and the increase in glucose transport were interpreted as being due to the presence of occluded GLUT4 vesicles docked at the PM, and partially occluded GLUT4 vesicles existing as a consequence of membrane fusion (Satoh *et al.*, 1993). Indeed this is consistent with the idea that GLUT4 vesicles fuse with plasma membranes via SNARE complexes (*section 1.4*) which would involve both docking and fusion events.

If GLUT4 is undergoing constant recycling between the PM and a single intracellular compartment, then the distribution between these two compartments will depend upon the relative balance of the rate constant for internalisation (endocytosis) and that of the re-externalisation (exocytosis), the rate constants k_{en} and k_{ex}, respectively. Using the redistribution of ATB-BMPA-labelled GLUT4 (and Western blotting for GLUT4) under steady state and non-steady state conditions, the effects of insulin on k_{en} and k_{ex} can be calculated. The calculation of k_{en} and k_{ex} using adipose cells under the three conditions described above, showed that insulin has little effect on k_{en}, but increases k_{ex} by approximately 10 fold (Satoh *et al.*, 1993).

Similar trafficking kinetic studies were also undertaken in 3T3-L1 adipocytes (Yang & Holman, 1993). Following the redistribution of ATB-BMPA-labelled GLUT1 and GLUT4 in basal and insulin-stimulated steady states, insulin reduced the endocytosis of the two glucose transporters by approximately 30% compared to the basal state. In the insulin-stimulated state,

the rate constants for GLUT4 and GLUT1 exocytosis (0.086 and 0.096 min^{-1} respectively) were similar to those of endocytosis. In contrast, the k_{ex} of GLUT4 and GLUT1 in the basal state were found to be 0.01 and 0.035 min^{-1}. It was therefore concluded that the main effect of insulin in 3T3-L1 adipocytes is to increase GLUT4 and GLUT1 k_{ex} by approximately 9- and 3-fold, respectively. Hence, the unique feature of the GLUT4 isoform is the very slow rate of exocytosis in the basal state.

In a two-pool model, of GLUT4 trafficking, this protein is assumed to be localised to the PM and only one intracellular vesicular site. The half time (which is only dependent upon k_{ex} and k_{en}) for both insulin-stimulated GLUT4 translocation to the cell surface and internalisation, in the continuous presence of insulin, should be the same. However, this is not observed experimentally (Satoh *et al.*, 1993): insulin-stimulated GLUT4 translocation to the PM has a faster half-time (2.7 min) than internalisation of GLUT4 in the continuous presence of insulin (10.6 min). These data were found to be better explained by the computer simulation of a three-pool model (Holman *et al.*, 1994). Here, there are two intracellular pools: the tubulo-vesicular system and the early endosomes (consistent with morphological data, *section 1.3*). It is therefore conceivable that GLUT4 is rapidly internalised from the PM to the early endosomes without a major contribution from k_{ex} to the half time for this process. The early endosomes may represent a site for sorting and recycling back to the tubulo-vesicular system, which could markedly slow the half time for internalisation back to the insulin-stimulated GLUT4-vesicle pool.

Hence, use of ATB-BMPA photolabelling has determined that the major-insulin responsive glucose transporter isoform in adipocytes is GLUT4 and that the main effect of insulin on GLUT4 is to increase the rate of exocytosis of GLUT4 from a reservoir compartment with only small changes in endocytosis.

1.3 Subcellular localisation of GLUT4

The idea that GLUT4 vesicles may represent a specialised compartment was derived from the observation that the GLUT4 vesicle compartment comprises ~3% or less of the LDM, has a limited protein composition, and does not contain the bulk of the insulin-like growth factor II receptor (Zorzano *et al.*, 1989).

The characteristics of the specialised GLUT4 vesicle population are still not clearly defined. By using immunoelectron microscopic analysis of GLUT4 in rat brown adipose tissue, Slot *et al.* (1991) made significant progress in forwarding the understanding of the intracellular compartments involved in GSV biogenesis. Cathepsin D was used as a marker of late endosomes/pre-lysosomes and internalised rat albumin (which is not synthesised in brown adipose tissue) was used as a marker for the endosome to lysosome pathway. The changes in the immunolocalisation of GLUT4 in brown adipose tissue from basal and insulin-stimulated cells were compared with these markers. Under basal conditions, 99% of GLUT4 was located intracellularly. The intracellular structures consisted of tubulo-vesicular structures (both near the PM and in areas close to the *trans*-Golgi network (TGN)) and small vesicular structures distributed throughout the cytoplasm. Only the outermost *trans*-cisterna of the TGN contained a small amount of GLUT4. A small proportion of GLUT4 (<3%) was observed in clathrin-coated pits at the PM and in early endosomes, under basal conditions. Upon insulin treatment, 50% of the GLUT4 was found associated with the PM. GLUT4 levels also increased within coated pits at the PM and early endosomes. The early endosomes were often observed to be continuous with tubular extensions (distinct from the tubulo-vesicular structures mentioned above) in which GLUT4 and albumin were enriched in the tubular extensions. The tubular extensions arising from early endosomes, enriched in GLUT4, suggested a sorting of GLUT4 from other endosomal proteins. The insulin-stimulated increase in GLUT4 localisation at the PM was consistent with a re-distribution of the GLUT4 from the tubulo-vesicular structures to the cell surface. No significant level of GLUT4 was found to be localised to late endosomes, under either basal or insulin-stimulated conditions. A model was therefore postulated for GLUT4 trafficking between intracellular compartments and the PM in basal and insulin-stimulated brown adipose tissue (figure 2)(Slot *et al.*, 1991).

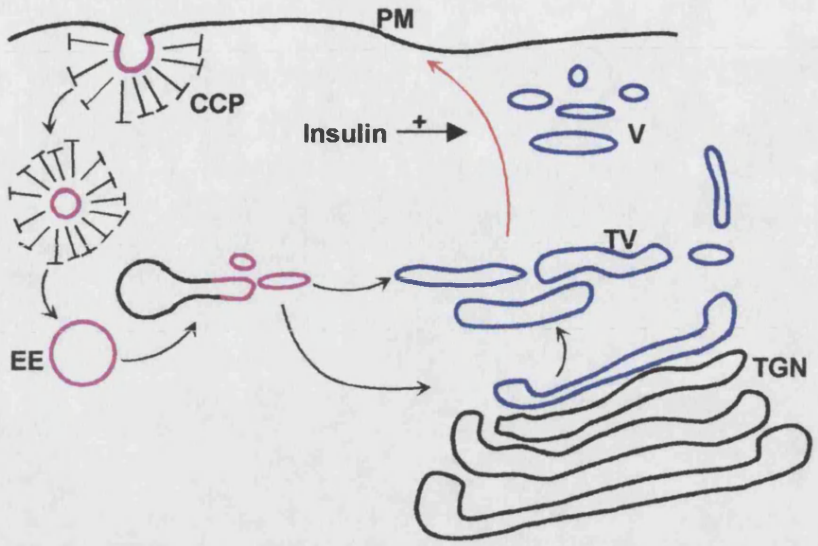

Figure 2. Model for GLUT4 trafficking between intracellular compartments (modified from Slot *et al.*, 1991). In the presence of insulin, GLUT4 is targeted from intracellular-vesicular structures (blue structures; *trans*-Golgi network (TGN), tubulovesicular-vesicles (TV), small vesicular structures (V)) to the plasma membrane (PM). The GLUT4 can then recycle between the PM and the endosomal system (purple structures). GLUT4 is primarily endocytosed *via* clathrin-coated pits (CCP) which fuse with early endosomal (EE) vesicles. GLUT4 is extruded from these vacuoles at an early step *via* tubular extensions. GLUT4 positive tubulo-vesicular structures may originate directly from the early endosomes or via the TGN/secretory route.

The model of GLUT4 trafficking between intracellular compartments proposed by Slot *et al.* (1991), has essentially held true, with refinements to the model being proposed as a result of further research by others (discussed below). As discussed previously (*section 1.2*), it is clear that GLUT4 continuously recycles between the PM and intracellular vesicle compartments, both under basal and insulin-stimulated conditions. To further define the GLUT4 storage compartment a technique referred to as compartment ablation analysis (Livingstone *et al.*, 1996) was employed. This method loads the recycling pathway of the transferrin-receptor with transferrin conjugated to horseradish peroxidase (HRP). In the presence of hydrogen peroxide and 3,3'-diaminobenzidine (DAB), the HRP converts DAB into a dense polymer. Integral membrane and soluble proteins present in the transferrin-HRP containing endosomes become cross-linked by the DAB polymerisation reaction and are subsequently ablated. Using endosomal ablation in conjunction with vesicle immunoisolation in 3T3-L1 adipocytes, Livingstone *et al.* (1996) showed that ~40% of the GLUT4 could be ablated in the recycling-endosomal pool. However, a larger proportion of GLUT4 (~60%) resides in a distinct 'non-

ablatable' pool which is devoid of transferrin receptors and other endosomal recycling proteins. In rat adipocytes however, only 10% of the cellular GLUT4 appears to co-localise with transferrin receptors, as analysed by glycerol gradient density centrifugation (Gillingham *et al.*, 1999). Furthermore, wortmannin (a fungal metabolite which inhibits PI 3-kinase (*section 1.9*)) treatment of basal adipocytes, induces the appearance of large vacuolar structures containing endosomal markers such as the transferrin receptor, and blocks GLUT4 trafficking to the PM, without affecting the morphology of GLUT4 tubulo-vesicular structures (Malide & Cushman, 1997). Treatment of adipocytes initially with insulin and then by wortmannin, induced the formation of large vacuolar structures containing both early endosomal markers and GLUT4. This suggested that internalisation of GLUT4 involves early endosomes and wortmannin treatment traps these proteins in this location. These latter studies are in contrast to results published by Kandror & Pilch (1998). Using rat adipocytes, Kandror & Pilch used sucrose velocity gradients in an attempt to separate GLUT4 compartments from endosomal systems containing transferrin receptors. However, transferrin-receptor containing compartments and GLUT4 vesicles were found to co-sediment in the sucrose velocity gradient system. Based on these *in vitro* data, Kandror and Pilch suggested that in unstimulated adipocytes, GLUT4 is inseparable from the recycling endosomal system and that insulin's effects on GLUT4 trafficking is entirely accounted for by a proposed reduction of retention within this endosome system. To date however, the majority of research tends to support the hypothesis that the localisation of insulin-responsive GLUT4 vesicles in basal adipocytes is distinct from that of the recycling-endosomal pool. However, GLUT4 molecules traffic through this compartment upon insulin stimulation and subsequent internalisation from the PM. The recycling endosomal pool is also subject to regulation by insulin. Insulin can increase, by 2- to 4-fold, the cell surface levels of many recycling receptors including the transferrin receptor. Ablation studies in 3T3-L1 adipocytes have shown that GLUT1 and the transferrin receptor can be ablated to a similar extent (Livingstone *et al.*, 1996). Hence, a hypothesis has been proposed whereby insulin promotes the exocytosis of proteins from the recycling endosomal pool, where GLUT1 and a proportion of GLUT4 is localised (Livingstone *et al.*, 1996), in addition to the exocytosis of GLUT4 from the specialised GSV compartment.

It is not clear whether the insulin-responsive GSV compartment may bud directly from the early/recycling endosomal compartment or whether GLUT4 may traffic back to the *trans*-Golgi network (TGN), with the subsequent budding of the storage compartment from this organelle. Evidence for the latter is derived from the observation that 13% of immunoreactive

GLUT4 is found in the TGN in basal adipocytes (Slot *et al.*, 1991). Additionally, confocal microscopy has shown that GLUT4 partially co-localises with γ-adaptin, a subunit of the adaptor complex, AP-1 (Malide *et al.* 1997), found associated with clathrin-coated vesicles budding from the TGN (Hirst & Robinson, 1998). Moreover, Gillingham *et al.* (1999) have found that AP-1 can co-sediment with GLUT4 on glycerol density gradients, and can associate directly with immunoisolated GLUT4 vesicles. As only 10% of GLUT4 has been found to co-localise with TGN38 (a marker of the *trans*-Glogi network) (Martin *et al.*, 1994), this pool probably does not represent the major steady-state localisation of intracellular GLUT4 pool within adipocytes. However, these data suggest that the GSV may be derived from the TGN. In cultured skeletal myotubes, GLUT4 has also been found associated with the TGN (Ralston & Ploug, 1996). GLUT4 is also targeted in atrial cardiomyocytes to the TGN and subsequently to atrial natriuretic factor (ANF) secretory granules, which only become GLUT4 positive in the TGN (Slot *et al.*, 1997). Cyclohexamide treatment does not prevent colocalisation of GLUT4 with the ANF-containing secretory granules in the TGN. Therefore GLUT4 enters the ANF secretory granules at the TGN via the recycling pathway and not via the biosynthetic pathway. Whether the insulin-responsive GLUT4 storage pool is derived directly from both early/recycling endosomes and the TGN still requires further investigation.

The subcellular trafficking of GLUT4 is likely to require signalling motifs to regulate the internalisation of GLUT4 via clathrin-coated pits, sorting at the TGN and sorting and/or retention into the storage compartment. Indeed, by studying GLUT4/GLUT1 chimeric, truncated, or point-mutated transporters, two discrete motifs have been identified (reviewed by Rea & James, 1997). These motifs include an aromatic-based motif found in the GLUT4 N-terminus (FQQI), and a di-leucine motif in the cytoplasmic C-terminus. Interestingly, vp165 (which is also found in GLUT4 vesicles; Keller *et al.* 1995), contains two di-leucine motifs and several acidic regions in its N-terminus cytoplasmic domain, similar to those which occur in the extreme GLUT4 C-terminus. Furthermore, the introduction of a glutathione S-fusion protein containing the cytosolic portion of vp165 results in GLUT4 translocation to the PM in basal 3T3-L1 adipocytes (Waters *et al.*, 1997). This suggests that the N-terminus of vp165 interacts with a retention/sorting protein that also regulates the distribution of GLUT4. However, current evidence suggests that neither the di-leucine and FQQI motifs of GLUT4 are entirely sufficient for targeting GLUT4 to the GSV compartment and other targeting signals remain to be identified (Haney *et al.*, 1995; Melvin *et al.*, 1999).

1.4 GLUT4 vesicle fusion with the plasma membrane

By 1993, the *N*-ethylmaleimide-sensitive factor (NSF) protein and soluble NSF attachment proteins (SNAPs) were shown to be essential components for various intracellular membrane fusion events. The discovery of SNAP receptors (SNAREs) by Söllner *et al.* (1993) led to the SNARE hypothesis for vesicle targeting and fusion. The SNARE hypothesis suggested that SNAP receptors are contained on both donor/vesicular membranes (v-SNAREs) and on target membranes (t-SNAREs). The SNARE hypothesis suggested that selective v- and t-SNARE interactions leads to membrane fusion mediated by the binding of NSF and SNAPs to the SNAREs.

Recently it has been suggested that SNAREs be reclassified as R-SNAREs or Q-SNAREs based on structural data which suggests that SNAREs either contribute an arginine (R-SNARE) or glutamine (Q-SNARE) to the SNARE complex (Fasshauer *et al.*, 1998). In the neuron, Söllner *et al.* (1993) identified the v-SNARE on synaptic vesicles as the vesicle associated membrane protein-2 (VAMP2), and t-SNARES on target membranes, now identified as SNAP25 and syntaxin1a. The SNARE hypothesis, also predicted that a family of v- and t-SNAREs should exist to account for targeting of vesicles to their correct location within a cell, and that particular v- and t-SNAREs would be localised to particular membranes. Whilst structural homologues of SNAP25, syntaxin and VAMP have been identified, it is still not yet known whether every transport step involves a set of three proteins that functionally correspond to the synaptic VAMP2, syntaxin1a and SNAP25. Furthermore, whilst NSF and α-SNAP appear to be necessary for synaptic fusion, the point at which NSF and α-SNAP act in this fusion process remains to be clearly defined. The original SNARE hypothesis suggested that NSF and α-SNAP assemble onto the docked SNARE complex and lead to rearrangements of protein-protein interactions to allow membrane fusion. However more recent data suggests that NSF and α-SNAP may also be required for priming of SNARE docking and SNARE-complex dissociation (reviewed by Hay & Scheller, 1997).

The discovery in 1992 by Cain *et al.* (1992) that GLUT4 vesicles from rat adipocytes contained VAMPs suggested that the genesis and/or the exocytosis of GLUT4 vesicles might be similar to that found for synaptic vesicles. In 3T3-L1 adipocytes, the v-SNAREs VAMP2 and the endosomal protein cellubrevin/VAMP3 were found to be associated with GLUT4 vesicles and showed a redistribution from the LDM fraction to the PM upon insulin treatment

(Volchuk *et al.,* 1995). However, antibodies to VAMP3 immunoprecipitated vesicles containing GLUT4 but not VAMP2. This suggests that VAMP2 and VAMP3, may be present in different subsets of GLUT4 containing vesicles. The differences in VAMP2 and VAMP3 localisation in adipocytes and their role in targeting of GLUT4 to the PM has been further studied by Martin *et al.* (1998). In this study by Martin and colleagues, 3T3-L1 adipocytes were permeabilised using streptolysin–O, and GST-fusion proteins encompassing the cytoplasmic tails of VAMP1, VAMP2 and VAMP3 were then introduced into the permeabilised cells. Out of the three GST-fusion proteins tested, only the VAMP2 fusion protein inhibited insulin-stimulated GLUT4 translocation (35% inhibition). Interestingly, the GST-VAMP2 fusion protein had no effect on insulin-stimulated GLUT1 translocation. Additionally, ablation of the recycling endosomal system using a transferrin-horseradish peroxidase conjugate with hydrogen peroxide and DAB (Livingstone *et al.*, 1996), inhibited insulin-stimulated GLUT1 trafficking but had no effect on insulin-stimulated GLUT4 translocation to the PM (Martin *et al.*, 1998). Overall, the experiments indicated that VAMP2 plays a part in regulating insulin-stimulated GLUT4 vesicle translocation to the PM, whilst VAMP3 is more likely to be involved in a constitutive GLUT4 trafficking pathway. Furthermore, the ablation studies and the use of the GST-v-SNARE fusion proteins substantiated the idea that GLUT1 and GLUT4 undergo insulin-stimulated translocation to the PM from different intracellular compartments.

The SNARE hypothesis suggests that fusion between vesicles and target membranes involves both v-SNAREs such as VAMP2 and t-SNAREs. Since VAMP2 appears to play a role in GLUT4 trafficking to the PM in adipocytes, it was not unexpected to find t-SNAREs in the PM. Indeed, antisera against t-SNAREs in rat adipocyte plasma membranes identified syntaxins 2 and 4 as the predominant t-SNAREs, with a small amount of syntaxin3 (Timmers *et al.*, 1996). To determine which of the adipocyte PM t-SNAREs might interact with GLUT4 vesicles and the corresponding v-SNAREs, solubilised membranes from low density microsomes or immunoisolated GLUT4 vesicles were added to solubilised plasma membranes in the presence of myc-epitope-tagged NSF and recombinant α-SNAP. Immunopecipitation of the myc-epitope using anti-myc antibodies and analysis of bound proteins showed that NSF complexes contained VAMPs 2 and 3 and syntaxin4, but not syntaxins 2 or 3. Furthermore, a 4- to 6-fold increase in v- and t-SNARE complex formation was observed when membranes were generated from insulin-stimulated cells, indicating that insulin can regulate SNARE complex formation. Whilst the latter study by Timmers *et al.* (1996) showed that syntaxin4, and VAMP 2/3 from GLUT4 vesicles can form a complex, the data did not indicate whether

syntaxin4 was necessary for GLUT4 vesicle fusion with the PM. The question of whether syntaxin4 is involved in GLUT4 vesicle fusion with the PM was further assessed by two subsequent studies. The first study used microinjection of a syntaxin4 peptide into 3T3-L1 adipocytes (Macaulay *et al.*, 1997), which resulted in a 40% inhibition of insulin-stimulated GLUT4 translocation. Microinjection of a VAMP2 peptide inhibited insulin-stimulated GLUT4 translocation by 54%, whereas a syntaxin1c peptide had no effect. These data suggested that syntaxin4 and VAMP2 are important for GLUT4 trafficking. In a second study, a recombinant GST-fusion protein encoding the cytoplasmic tail of syntaxin4 (Cheatham *et al.*, 1996), was added to streptolysin O permeabilised 3T3-L1 adipocytes, and was found to inhibit insulin-stimulated GLUT4 translocation.

Data therefore suggests that both VAMP2 and syntaxin4 are necessary for GLUT4 vesicle fusion with the PM, and that VAMP2 and syntaxin4 can bind to each other to form a stable complex (Timmers *et al.*, 1996). More recently, Rea *et al.* (1998) have shown that syndet/SNAP23 (a murine homologue of SNAP25) from 3T3-L1 adipocytes can form a SDS-resistant SNARE complex with VAMP2 and syntaxin4. Additionally, microinjection of anti-syndet peptides into 3T3-L1 adipocytes inhibited insulin-stimulated GLUT4 translocation by 40% (Rea *et al.*, 1998). These results therefore suggest that the t-SNAREs necessary for GLUT4 vesicle fusion include both syndet and syntaxin4.

Whilst it is likely that VAMP2/syndet/syntaxin4 complexes are important for GLUT4 vesicle fusion with the PM, further proteins involved in this complex may provide the acute insulin-regulation of GLUT4 vesicle translocation and fusion with membranes. For instance, the homologues of the yeast Sec1-like family, namely Munc-18 proteins, have been identified in 3T3-L1 adipocytes (Tellam *et al.*, 1995). In particular, Munc-18c was shown to bind to syntaxin4 in 3T3-L1 adipocytes and prevent VAMP2/syntaxin4 interactions (Tellam *et al.*, 1997). It has been subsequently shown that adenovirus mediated overexpression of Munc-18c in 3T3-L1 adipocytes inhibited insulin-stimulated glucose transport by 50% (Tamori *et al.*, 1998). A role for Munc-18 isoforms in regulating SNARE complexes is further implied by the observations that Munc-18a binding to syntaxin1a is inhibited by protein kinase C phosphorylation of Munc 18a (Fujita *et al.*, 1996), and that the DOC2 protein regulates the formation of Munc-18a-syntaxin1 complexes by binding to the Munc protein (Verhage *et al.*, 1997). Furthermore, recent studies have shown that a protein called synip can bind to syntaxin4 (Min *et al.*, 1999). The synip/syntaxin4 complex was found to dissociate in insulin-

stimulated adipocytes. In addition, the C-terminus of synip can bind to syntaxin4 and inhibit insulin-stimulated GLUT4 translocation. Evidence for the masking of SNAREs by regulatory proteins is further provided by the observations that in yeast, the Rab-like GTPase Ypt1p transiently interacts with the t-SNARE Sed5p, displacing the Munc-18 homologue Sly-1 (Lupashin & Waters, 1997). This also suggests that small GTP binding-proteins may be involved in SNARE complex formation (*section 1.14*).

The current view now emerging is that the targeting of vesicles to the correct membrane destination involves more than just SNAREs (reviewed by Pfeffer, 1999). Briefly, vesicle targeting is thought to require molecular motors and the actin and/or microtubule-based cytoskeleton to bring a vesicle from one part of the cell to another. 'Tethering/docking' proteins collect and restrain vesicles at or near their cognate target membranes. Finally, the SNAREs can bring vesicle membranes in close apposition with their cognate target membranes, thereby driving membrane fusion. Each of these processes may be subject to regulation by other proteins which enhance the degree of specificity to the membrane trafficking processes. Using models of synaptic vesicle fusion with the PM, and including vesicle and target SNAREs in adipocytes, a model for GLUT4 vesicle fusion with the PM can be postulated (figure 3).

Legend for figure 3. (A) GLUT4 vesicles may bud from the insulin-responsive GLUT4 storage pool. This process of budding may require the activation of small molecular weight GTP-binding proteins such as Rab4 (cyan)(*section 1.14*). The budding to form vesicles that can fuse with the PM is likely to be subject to regulation by insulin, via activation/inhibition of signalling intermediates such as phosphatidylinositol 3-kinase (*section 1.9*). The vesicles thus formed are likely to contain the SNARE protein VAMP2 that gives a degree of selectivity to the fusion process. **(B)** The movement of 'fusion competent' GLUT4 vesicles to the PM is likely to require the cytoskeleton. Unidentified proteins are likely to regulate the 'loose tethering' of the GLUT4 vesicles with the PM. Insulin regulation of proteins such as synip (not shown) and Munc-18c allows SNAREs to form complexes. SNARE complexes involve a complex of four α-helices provided by the syntaxin4, VAMP2 and syndet (which provides two α-helices). **(C)** SNARE complex formation and possibly the involvement of α-SNAP/NSF and/or a GTP-binding protein might drive membrane fusion. Membrane fusion exposes GLUT4 on the cell surface allowing increased glucose uptake into the cell. α-SNAP/NSF may then participate in separating SNAREs to allow recycling of the SNARE proteins.

Key: Undefined accessory proteins are unlabelled, GDP-dissociation inhibitor (GDI), GDI dissociation factor (GDF), guanidine nucleotide exchange factor (GEF), guanosine trisphosphate (GTP), guanosine diphosphate (GTP).

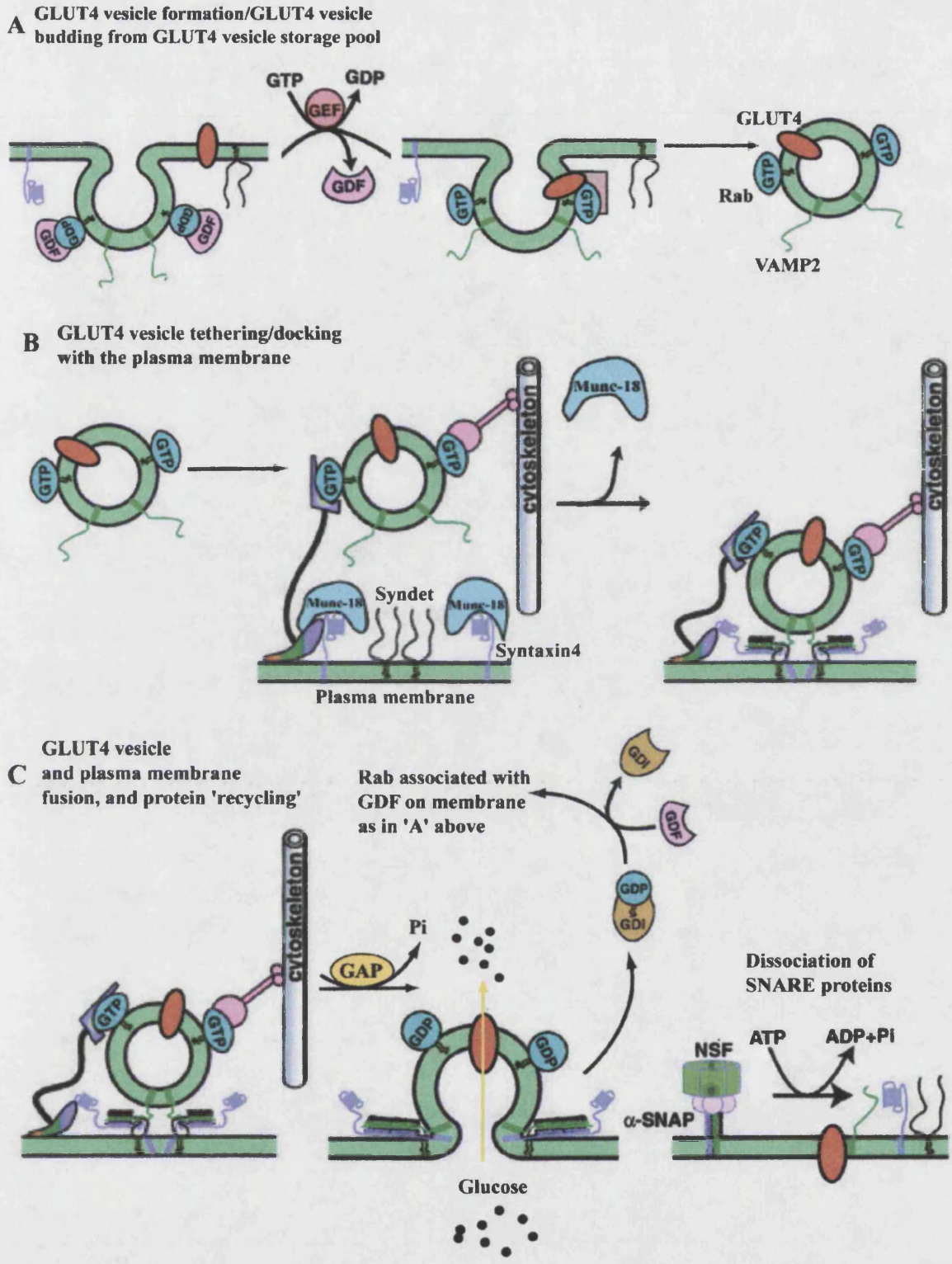

Figure 3. Model of GLUT4 vesicle fusion with the plasma membrane.
See previous page for figure legend (figure adapted from Gonzalez & Scheller, 1999).

PART B - Insulin signalling

The binding of insulin to plasma membrane insulin receptors represents the initial signalling event which ultimately leads to translocation of GLUT4 vesicles to the plasma membrane. Intracellular signalling events downstream of the insulin receptor which are linked to GLUT4 trafficking have been intensely researched for over a decade. It is the insulin-regulated signalling molecules and their roles in GLUT4 trafficking which constitutes the remaining text of the introduction.

1.5 The Insulin receptor

The insulin receptor is a heterotetrameric transmembrane glycoprotein composed of two extracellular α-subunits and two transmembrane β-subunits (White, 1997) (figure 4). The α-subunits contain the insulin-binding domains. The transmembrane β-subunits function as tyrosine-specific protein kinases which mediate both *trans*-autophosphorylation between the β-subunits (Lee *et al.*, 1993), and tyrosine phosphorylation of receptor substrates. α-Subunit crosslinking by insulin induces a conformational change in the intracellular β-subunits which leads to the activation of the kinase (Lemmon & Schlessinger, 1994).

Insulin receptor kinase activity is crucial for glucose uptake, since a site-directed point mutation in the ATP binding domain ($lysine_{1018}$ to alanine) destroys receptor kinase activity, insulin-receptor substrate-1 (IRS-1) phosphorylation (*sections 1.6.1* & *1.7*) and 2-deoxyglucose (2-DOG) uptake (Chou *et al.*, 1987; McClain *et al.*, 1987).

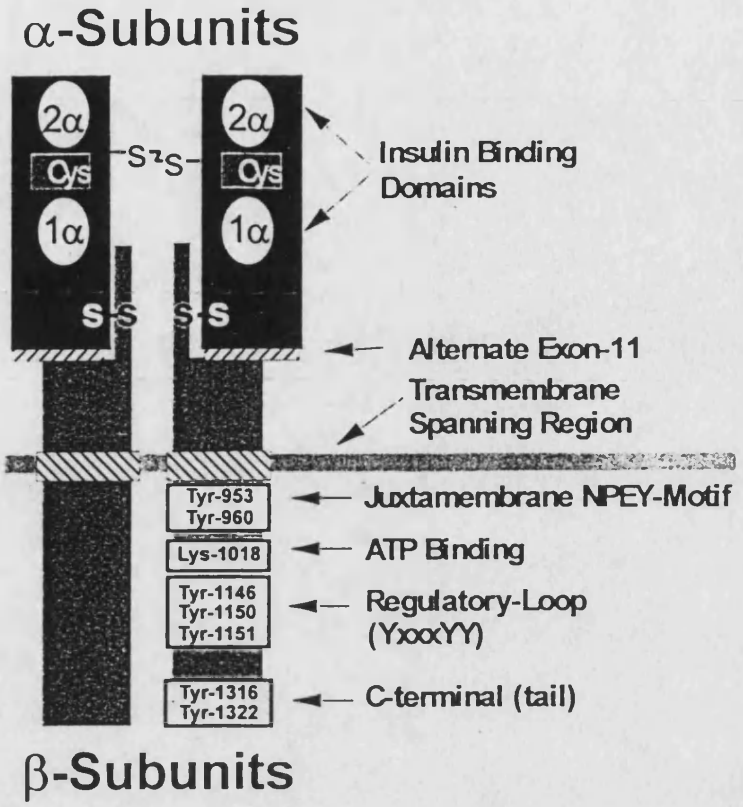

Figure 4. Schematic structure of the insulin receptor, White (1997). De Meyts (1994) describes a model for α-subunit crosslinking by insulin. Each α-subunit contains two distinct insulin-binding domains, designated as site-1α and site-2α, both of which can contribute independently to insulin binding. The insulin molecule itself has two distinct receptor binding domains. It is hypothesised that α-subunit crosslinking is achieved by insulin binding to site-1α on one α-subunit, with the other binding site of the insulin molecule binding to site-2α on the other α-subunit. The transmembrane spanning region is postulated to be important for stabilising the insulin-induced conformational change, since a single mutation in the transmembrane spanning domain of the insulin receptor has been shown to increase both β-subunit autophosphorylation and glucose transport (Longo *et al.*, 1992). The importance of Tyr and Lys residues of the β-subunits for insulin signalling (indicated above) is discussed in the body of the text.

A lack of β-subunit kinase activity results in decreased receptor *trans*-autophosphorylation. Insulin-induced tyrosine (Tyr) phosphorylation on the receptor β-subunits occurs on a well defined set of Tyr residues. These include Tyr_{960} in the juxtamembrane region, residues Tyr_{1146}, Tyr_{1150} and Tyr_{1151} in the β-subunit regulatory loop and residues Tyr_{1316} and Tyr_{1322} in the C-terminus (White & Kahn, 1994) (figure 4). The importance of these tyrosine residues in insulin signalling has been investigated by using various insulin receptor mutations. For example, the combined mutation of tyrosine residues 1146, 1150 and 1151 (the autophosphorylation sites) to phenylalanine results in an inactive receptor tyrosine kinase, which reduces both thymidine incorporation and 2-DOG uptake (Murakami & Rosen, 1991). However, Tyr to Phe mutations of residue 953, or both the C-terminal residues 1316 and 1322, does not effect either insulin-stimulated receptor β-subunit phosphorylation, thymidine incorporation, or 2-DOG uptake. Furthermore, a truncated insulin receptor (lacking the last 82 amino acids of the β-subunit C-terminus) exhibiting reduced autophosphorylation gave normal IRS-1 phosphorylation and 2-DOG uptake (Yamamoto-Honda *et al.*, 1993). Together these data suggests that autophosphorylation of the receptor within the kinase domain is required for normal insulin receptor kinase activity, and that kinase activity is necessary for phosphorylation of endogenous substrates. The aforementioned studies by Yamamoto-Honda *et al.* (1993) indicate that it is the phosphorylation of endogenous substrates which correlates more closely with the biological effects of insulin, rather than the phosphorylation state of the insulin receptor itself.

Insulin receptor substrate binding is an important process for mediating the effects of insulin. Disruption of substrate targeting to the receptor has been shown to reduce insulin action. Substrate targeting to the insulin receptor is thought to be mediated in part *via* the phosphotyrosine binding (PTB) domains of substrates like Shc and IRS-1 which associate with Tyr_{960} in the juxtamembrane region of the receptor β-subunit. Mutations of the insulin receptor at Tyr_{960} leads to the failure of receptor phosphorylation of IRS-1 and Shc (White *et al.*, 1988; Kaburagi *et al.*, 1993; Chen *et al.*, 1995). Overexpression of IRS-1 with these mutant receptors rescues the insulin response, suggesting that the juxtamembrane region plays a role in sensitising substrate targeting (Chen *et al.*, 1995).

The insulin receptor undergoes endocytosis following binding to insulin (Marshall *et al.*, 1981). Studies by Kublaoui *et al.* (1995) have shown that endosome associated insulin receptors exhibit increased autophosphorylation and exogenous substrate tyrosine kinase activity

compared to PM associated receptors. It was therefore hypothesised that the endosome associated insulin receptor population is responsible for the activation of intracellular signalling pathways. However, incubation of both 3T3-L1 adipocytes and Chinese hamster ovary cells (transfected with the human insulin receptor) at 4°C, prevents insulin receptor internalisation, despite IRS-1 phosphorylation remaining comparable to cells incubated at 37°C (Heller-Harrison *et al.*, 1995). A dominant-interfering mutant of dynamin also inhibits receptor internalisation but is without effect on insulin-stimulated glucose (Ceresa *et al.*, 1998). The effects of insulin are therefore not wholly dependent upon insulin receptor internalisation. This suggests that receptor substrates can associate with plasma membrane-located receptors. These data however do not rule out the possibility that internalised receptors can still phosphorylate substrates. Whilst IRS-1 is generally not found associated with either plasma membranes or the insulin receptor (Kelly & Rudeman, 1993), IRS-1 must be allowed access to the insulin receptor for IRS-1 phosphorylation to occur. Recent research suggests that IRS-1 may be associated with the membrane cytoskeleton in close proximity to the insulin receptor (Clark *et al.*, 1998).

Endocytosis of the insulin receptor downregulates insulin signalling since insulin becomes dissociated from the receptor following fusion of the internalised receptor compartment with an acidic endosome. The insulin receptor is then free to recycle back to the plasma membrane. Additionally, downregulation of the insulin signal is achieved by dephosphorylation of receptor phosphotyrosine residues by phosphatases. At least two phosphatases are known to interact with the insulin receptor. These include the protein tyrosine phosphatase 1B (PTP1B) (Seely *et al.*, 1996), and the transmembrane leukocyte common antigen-related (LAR) protein tyrosine phosphatase (Ahmad & Goldstein, 1997). The interaction of phosphatases with the insulin receptor may also be of importance in cases of insulin resistance, since increased phosphatase expression may reduce the insulin receptor signal. In obese individuals, reduced insulin receptor kinase activity and increased expression of LAR have been observed (Ahmad *et al.*, 1995). Conversely, antisense inhibition of LAR expression augments the insulin signal (Kulas *et al.*, 1995), and reduces receptor dephosphorylation (Mooney *et al.*, 1997).

Unlike the insulin receptor, most other receptor tyrosine kinases interact directly with Src-homology-2 (SH2) domain-containing signalling molecules (Pawson, 1995). It is the tyrosine phosphorylation of IRS proteins which allows the subsequent activation and/or localisation of

SH2-containing signalling molecules such as phosphatidylinositol 3-kinase (PI 3-kinase) (*section 1.9*).

Overall then, the kinase activity of the insulin receptor (which is the initial event in insulin signalling) is crucial for mediating phosphorylation of substrates that mediate the plethora of effects of insulin.

1.6 Insulin receptor substrates

1.6.1 Insulin receptor substrate-1 (IRS-1)

The open reading frame for the IRS-1 gene, predicts that IRS-1 has a molecular weight of 131 kDa and the potential for multiple phosphorylation on serine, threonine and tyrosine residues (White, 1997). IRS-1 analysis has shown that at least eight tyrosine residues undergo tyrosine phosphorylation by the activated insulin receptor, including tyrosine residues contained within motifs (YXXM and YMXM) which are predicted to bind to SH2 containing proteins (Sun *et al.*, 1993). In addition to phosphorylation sites, IRS-1 also contains a pleckstrin homology (PH) domain (*section 1.11)* and a phosphotyrosine-binding (PTB) domain.

1.6.2 Insulin receptor substrate-2 (IRS-2)

Mice lacking IRS-1 (*section 1.8*) only exhibit mild insulin resistance. Therefore it was thought that another IRS-signalling protein might exist. The concept of another IRS signalling protein existing led to the cloning of IRS-2 (Sun *et al.*, 1995). Amino acid sequence alignment between murine IRS-1 and IRS-2 revealed a highly conserved amino terminus containing PH and PTB domains (69% and 75% identical to IRS-1), with a less conserved C-terminus (35% identical to IRS-1). Like IRS-1, IRS-2 contains about 20 putative tyrosine phosphorylation motifs, nine of which are YXXM motifs and four that are YMXM motifs.

The homology between IRS-1 and IRS-2 at the amino terminus is likely to indicate a conserved mechanism whereby the substrates recognise the insulin receptor. Whilst the PTB domain appears to be important for recognition of the $NPXY^{960}$ of the insulin receptor (Sawke-Verhelle *et al.*, 1996), it is likely that more than one site on the insulin receptor is involved in receptor/substrate recognition. Indeed, deletion of the PH domain of IRS-1 reduces the level of IRS-1 tyrosine phosphorylation and signal propagation (Myers *et al.*, 1995). Thus, the PH domain possibly plays a role in coupling IRS-1 to the insulin receptor. However direct interactions between the PH domain of IRS-1 and the insulin receptor have not been

observed (Voliovitch *et al.*, 1995). It is therefore postulated that perhaps other domains within IRS or even other proteins are involved in the recognition between the insulin receptor and its substrates. Evidence for other proteins mediating interaction between IRS proteins and the insulin receptor is more recently shown by Burks *et al.* (1998). This study has indicated that IRS PH domains bind to acidic motifs in proteins. However, it was found that IRS-1 and IRS-2 PH domains bound acidic motifs of various proteins to different extents, indicating differences in selectivity between IRS-1 and IRS-2. Direct interactions between IRS-2 and the insulin receptor may occur through a region corresponding to residues 591 to 786 (the kinase regulatory loop binding (KRLB) domain) which binds the regulatory loop of the insulin receptor (Sawke-Verhelle *et al.*, 1996). This interaction between IRS-2 and the insulin receptor requires all three tyrosine residues of the regulatory loop of the receptor to be phosphorylated. Since this KRLB domain is not present in IRS-1 this region may be important for receptor substrate discrimination.

1.6.3 Insulin receptor substrate-3 (IRS-3)

A 60 kDa protein (pp60) that binds to PI 3-kinase (*via* phosphotyrosine residues) following insulin stimulation was identified by Lavan & Lienhard (1993). The purification of pp60 and the cloning of its cDNA from a rat adipocyte cDNA library were subsequently described Lavan *et al.* (1997). The sequence of pp60 revealed a polypeptide of 494 residues, and like IRS-1 and –2 it has an amino terminal PH domain (50% and 45% identical respectively), a PTB domain (48% and 53% identical respectively), followed by putative tyrosine phosphorylation sites (four with YXXM motifs). Thus based on its similarity to IRS-1 and –2, pp60 was designated as IRS-3. Immunoprecipitation of p85 (the regulatory subunit of PI 3-kinase) from rat adipocyte membrane fractions followed by immunoblotting with anti-phosphotyrosine revealed a 60 kDa band located predominantly in the PM (Kelly & Ruderman, 1993). It has subsequently been shown that IRS-3 is localised primarily to the PM (Anai *et al.*, 1998). This is in contrast to IRS-1 and IRS-2 which tend to localise to intracellular membranes (Anai *et al.*, 1998; Inoue *et al.*, 1998). The significance of the different localisation of IRS-1/2 compared to IRS-3 are not clear since IRS-1/2 also need to be in close proximity to plasma membrane insulin receptors to be phosphorylated. Anai and colleagues (1998) and Inoue *et al.* (1998) do suggest however that differences in the subcellular compartments of IRS-1, -2 and-3 and their downstream utilisation can contribute to the diversity of the insulin response.

1.6.4 Insulin receptor substrate-4 (IRS-4)

The IRS-4 sequence was obtained following purification of a 160 kDa protein using anti-phosphotyrosine immunoaffinity chromatography of lysates from human embryonic kidney (HEK) 293 cells (Lavan *et al.*, 1997). Cloning revealed that like other IRS proteins, IRS-4 contains both N-terminus PH and PTB domains (~ 40% identical to other IRS proteins), and 12 potential tyrosine phosphorylation sites, 7 of which are in YXXM motifs. As with the other IRS proteins, IRS-4 was found to bind to both Grb2 and PI 3-kinase, but not Syp (Fantin *et al.*, 1998). Like IRS-3, IRS-4 appears to be mainly plasma membrane associated in HEK cells and with no apparent re-distribution upon cell stimulation by insulin. Currently, the mRNA for IRS-4 has been found in tissue culture cells but not in human tissues. Therefore it appears to be expressed only in certain specific cell types. IRS-1 and –2 and to a certain extent IRS-3 appear to be expressed with more widespread tissue distributions.

1.6.5 Shc

Another protein phosphorylated by the insulin receptor is Shc. The *shc* gene was originally identified by Pelicci *et al.* (1992) and was cloned because of its homology with SH2 containing gene sequences. The gene was also found to have stretches of homology to a glycine/proline-rich coding region of the α1 chain of the collagen gene, hence the gene was called *shc* (derived from SH2 and collagen). Pelicci *et al.* (1992) also showed that the *shc* gene codes for three proteins of about 46, 52 and 66 kDa, and are expressed in a wide range of mammalian cell lines. These authors also showed that Shc was tyrosine phosphorylated by the activated EGF receptor. Pronk *et al.* (1993) subsequently showed that the insulin receptor could phosphorylate both the 46 and 52 kDa Shc proteins. Like IRS-1, Shc is found to bind growth factor receptor-bound protein 2 (Grb2), which leads to activation of the mitogen activated protein kinase (MAPK) pathway.

1.6.6 Grb2-associated binder-1 (Gab1)

The ability of IRS proteins such as IRS-1 to bind to the SH2-domain containing protein Grb2 is discussed later in relation to the activation of the mitogen activated protein kinase (MAPK) pathway (*via* Sos). Using a ^{32}P-labelled Grb2-fusion protein to screen an expression cDNA library, Holgado-Madruga *et al.* (1996) isolated a protein termed Grb2-associated binder-1 (Gab1) which shared homology and structural features to IRS-1. Gab1 was found to contain an N-terminal PH domain, two SH3 binding domains and several tyrosine phosphorylation

sites (Gab1 contains no PTB domain). Like other IRS proteins, Gab1 was found to be phosphorylated on tyrosine by both the epidermal growth factor (EGF) and insulin receptors, and to bind Syp, phospholipase C-γ (PLC-$_\gamma$) and PI 3-kinase. Whilst Gab1 binds many of the same molecules as the EGF receptor, Gab1 is not membrane bound and could potentially target signalling molecules to specific intracellular sites.

1.7 Insulin signalling *via* IRS proteins

It is the tyrosine phosphorylation of insulin receptor substrates which allows SH2 containing proteins to bind to the receptor substrates. SH2-domain containing proteins that have thus far been found to bind to IRS-1 include the p21^{ras} activator complex - Grb2/Sos (Skolnik *et al.*, 1993), the protein tyrosine phosphatase SHPTP2 (Syp)(Sun *et al.*, 1993), the regulatory subunit of the serine/threonine/lipid kinase PI 3-kinase (Sun *et al.*, 1991) (class I_A regulatory subunits, *section 1.9*), the C-terminal Src kinase (Csk) (Tobe *et al.*, 1996), the Src-like kinase Fyn (Sun *et al.*, 1996) and the adaptor protein Nck (Lee *et al.*, 1993). The binding of numerous signalling molecules extends the notion made by Sun *et al.* (1991), that IRS-1 acts as a multisite 'docking protein' to engage various downstream regulatory elements during insulin signal transmission.

Grb2 can bind to phosphotyrosine residues on both Shc and IRS-1. Upon insulin-stimulation, Grb2 is recruited to IRS proteins and activates the cellular proto-oncogene p21^{ras} *via* Sos. Hence, p21^{ras} can be activated by an IRS-1 dependent and independent pathway. Whilst activation of p21^{ras} has been shown to activate the mitogen-activated protein kinase (MAPK) pathway, the activation of p21^{ras} via IRS-1 warranted investigation to see if p21^{ras} activation was necessary for GLUT4 translocation. Activated p21^{ras} was shown to have no effect on insulin-stimulated GLUT4 translocation when microinjected into 3T3-L1 adipocytes (Haruta *et al.*, 1995; Quon *et al.*, 1995). Furthermore, a dominant-negative mutant Ras also failed to affect insulin-stimulated GLUT4 translocation, but blocked the MAPK cascade (Quon *et al.*, 1995). These data therefore indicate that Ras is not likely to be involved in insulin-stimulated GLUT4 translocation.

Amongst the IRS-1 binding proteins is the protein tyrosine phosphatase Syp (SHPTP2, PTP1D) (Sun *et al.*, 1993). Microinjection of SH2 domains of Syp or anti-Syp antibodies into mammalian fibroblasts inhibits insulin-induced DNA synthesis (Xiao *et al.*, 1994). These results indicate that Syp acts as a regulator of mitogenic signals. Similarly, microinjection of fusion proteins encoding the N- and C-terminal SH2 domains of Syp, or anti-Syp antibodies

into 3T3-L1 adipocytes blocks insulin-induced DNA synthesis (including GLUT1 expression). However, translocation of GLUT4 to the cell surface is unaffected. These data therefore indicated that Syp appears to be necessary for mitogenic signals but not for the activation of the metabolic pathway leading to GLUT4 translocation (Hausdorff *et al.*, 1995).

Figure 5 shows a simplified diagrammatic representation of the binding of various signalling molecules to the IRS-1 molecule.

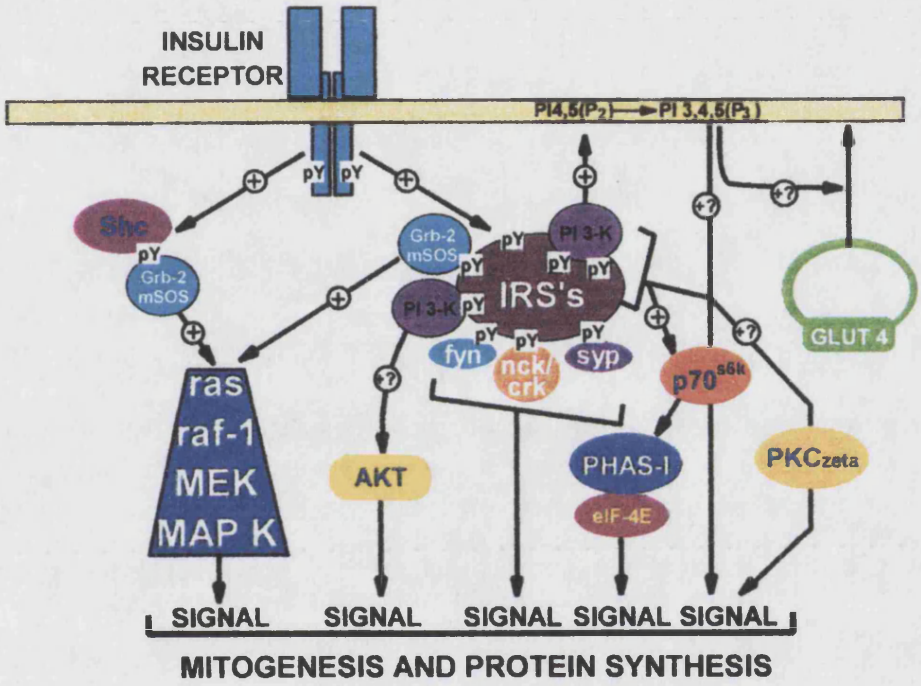

Figure 5. The role of IRS-1 as a multisite docking protein for SH2-domain containing proteins (Yenush & White, 1997). PI 3-kinase activation appears to be necessary for GLUT4 translocation (*section 1.9*), however the precise mechanism of this process is still largely unclear. PI 3-kinase is thought to regulate Akt (protein kinase B (PKB)), PKCζ, and the 70 kDa ribosomal S6 kinase ($p70^{S6k}$). Whilst $p70^{s6}$ kinase does not appear to be involved in GLUT4 translocation (Fingar *et al.*, 1993), roles for PKB and PKCζ in the regulation of GLUT4 translocation are implicated, and discussed later (*sections 1.12* & *1.13* respectively).

1.8 The role of insulin receptor substrates in GLUT4 trafficking

As will become apparent (*section 1.9*), PI 3-kinase activity appears to be necessary for insulin-stimulated GLUT4 translocation to the plasma membrane. Receptor substrates IRS-1, -2 and -3 have all been shown to bind PI 3-kinase but a definitive role of these insulin receptor substrates in insulin-stimulated GLUT4 translocation remains unclear. For example, microinjection of a fusion protein containing amino acid residues 108-516 of IRS-1 (residues important for IRS-1 binding to the insulin receptor) had no effect on GLUT4 translocation but inhibited membrane ruffling and mitogenesis (Morris *et al.* 1996). Microinjection of IRS-1 antibodies and tyrosine phosphorylated peptides corresponding to the $NPXY^{960}$ motif of the insulin receptor (*section 1.5*) produced similar results. Together, these data suggested that IRS-1 is not an essential component for insulin-stimulated GLUT4 translocation. Disruption of IRS-1 binding to the insulin receptor was also investigated by Sharma *et al.* (1997) who overexpressed IRS-1 protein domains in 3T3-L1 adipocytes. The overexpression of these IRS-1 protein domains resulted in a reduced IRS-1 phosphorylation, IRS-1 associated PI 3-kinase activity and insulin-stimulated mitogenesis, but had no effect on PKB activation (*section 1.12*) or GLUT4 translocation and glucose transport.

IRS-1 null mice have been generated by inserting a neomycin phosphotransferase gene (*neo*) cassette into the first exon of the IRS-1 gene (Tamemoto *et al.*, 1994; Araki *et al.*, 1994). The IRS-1 null mice show intra-uterine and postnatal growth retardation but only a mild degree of peripheral insulin resistance is observed. This indicates that there are IRS-1-independent signalling pathways. The IRS-1-independent pathways were postulated to occur *via* alternative substrates to IRS-1, since phosphotyrosine immunoprecipitates still show a significant insulin-induced phoshotyrosyl-associated PI 3-kinase activity. Furthermore, Araki *et al.* (1994) observed the phosphorylation of IRS-2 in IRS-1 null mice which suggested that IRS-2 may act as an alternative substrate to IRS-1. Studies in NIDDM patients observe a 70% decrease in IRS-1 expression in NIDDM patients, with IRS-2 becoming the main docking protein for PI 3-kinase (Rondinone *et al.*, 1997). However, a more recent study using IRS-1 null mice showed that IRS-1 deficiency leads to only a 50% reduction in glucose transport, and that IRS-3 is the major tyrosine phosphorylated protein associated with PI 3-kinase in fat tissue (Kaburagi *et al.*, 1997). Tyrosine phosphorylation of IRS-2 and association with PI 3-kinase in the adipose tissue was almost undetectable. The latter authors therefore suggested that IRS-3 plays a major role in insulin-induced glucose uptake in the absence of IRS-1.

The aforementioned studies suggest that the ability to retain insulin-sensitivity for glucose uptake may be mediated by alternative substrates such as IRS-2 and IRS-3. Whilst disruption of IRS-1 gene expression leads to only to a 50% reduction in glucose uptake, IRS-2 null mice show a progressive decline in glucose homeostasis (Withers *et al.*, 1998). The eventual hyperglycaemia is due to insulin resistance in both the liver and skeletal muscle, which is not compensated for by the β-cells of the pancreas (Withers *et al.*, 1998). Withers *et al.* (1998) therefore suggests that IRS-2 is more important for insulin-stimulated metabolic events such as glucose uptake, whilst other studies indicate IRS-1 is more important for mitogenic effects. Brüning *et al.* (1997) have shown that in IRS-1-deficient fibroblasts (derived from IRS-1 null mice), overexpression of IRS-2 cannot compensate for the lack of mitogenic responses (cell cycle progression) but can reconstitute immediate-early gene expression (*c-fos* and *erg-1*). It is therefore suggested that IRS-1 and IRS-2 are not functionally interchangeable signalling intermediates for stimulation of mitogenesis, but may mediate some common functions. Hence, whilst IRS-2 deficiency appears to be most important for glucose transport and IRS-1 in mitogenic responses, the role in metabolic signalling served by IRS-2 may, in part also be provided by alternative substrates such as IRS-1. The roles of IRS-3 and IRS-4 in insulin and growth factor signalling still remain to be determined.

1.9 Phosphatidylinositol 3-kinases

Phosphatidylinositol 3-kinases (PI 3-kinases) represent a family of kinases capable of phosphorylating phosphatidylinositides at the D-3 position of the inositol ring. Hence phosphatidylinositol (PI), phosphatidylinositol 4-phosphate (PI(4)P) and phosphatidylinositol 4,5-bisphosphate (PIP2) are converted to phosphatidylinositol 3-phosphate (PI(3)P), phosphatidylinositol 3,4-bisphosphate (PI(3,4)P2) and phosphatidylinositol 3,4,5-P_3 (PIP3) respectively. The family of PI 3-kinases all share significant homology within the catalytic domain but can be divided into three main classes based upon their *in vitro* lipid substrate specificity, structure and mode of regulation (figure 6) (reviewed by Vanhaesebroeck *et al.*, 1997).

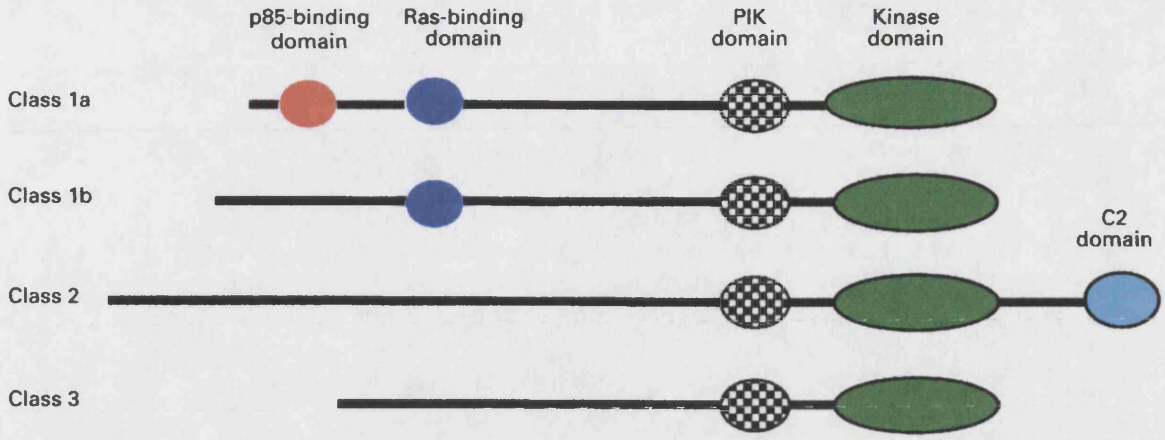

Figure 6. Schematic representation of the domain structure of the various classes of PI 3-kinase catalytic subunits (Shepherd *et al.*, 1998). Class I PI 3-kinases form heterodimeric complexes which consist of an adaptor/regulatory subunit tightly associated with the catalytic subunit. Depending upon the associated adaptor subunit, the class I PI 3-kinases are further subdivided into two subclasses (A and B). Class I_A PI 3-kinases are 110-130 kDa proteins that interact with adaptor subunits containing SH2 domains (linking class I_A PI 3-kinases to tyrosine kinase signalling pathways). Three highly homologous mammalian isoforms of the class I_A catalytic subunits have been cloned, and designated as p110α, p110β and p110δ. All contain the kinase domain at the C-terminus with adaptor-binding and Ras-binding domains towards the N-terminus. There is a phosphatidylinositide kinase (PIK) homology domain that is also found in phosphatidylinositide 4-kinases, but yet no role has been assigned to this domain. Class I_B PI 3-kinase catalytic subunits are similar in structure to class I_A PI 3-kinase catalytic subunits, but they lack the p85 binding domain and associate with a distinct family of adaptor subunits. The activity of class I_B PI 3-kinases are therefore regulated by βγ subunits of heterotrimeric G-proteins, although there is no current evidence to suggest that class I_B PI 3-kinases can be activated by insulin.

Further complexity is added by the occurrence of several splice variants of the class I_A PI 3-kinase adaptor subunits (reviewed by Shepherd *et al.*, 1998). Briefly, the class I_A PI 3-kinase adaptor subunits contain two SH2 domains and an inter-SH2 p110-binding domain. One adaptor gene generates five adaptor subunits termed as p85α, p55α/AS53, p50α and the splice variants of p85α and p55α termed $p85\alpha_i$ and $p55\alpha_i$ (an 8 amino acids insertion into the inter-SH2 domain). The p85α subunit contains an SH3 domain, a Bcr/Rac GTPase-activating protein (GAP) homology (BH) domain, as well as two proline-rich regions (P1 and P2) N-terminal to the SH2 domains. The p55α and p50α subunits are truncated versions of p85α and lack the SH3, BH and P1 domains. The second adaptor subunit gene generates p85β that differs only slightly in molecular mass to the p85α subunit. The third PI 3-kinase adaptor

differs only slightly in molecular mass to the p85α subunit. The third PI 3-kinase adaptor subunit gene product generates a 55 kDa protein, designated as p55γ, which is highly homologous in sequence and has an identical domain structure to the p55α splice variant of p85α.

It is unlikely that class II PI 3-kinases are involved in insulin-stimulated GLUT4-vesicle translocation to the plasma membrane, for two reasons. Firstly, class II PI 3-kinases are unable to use PIP2 as a substrate (Domin *et al.*, 1996; Virbasius *et al.*, 1996), but insulin activates PI 3-kinase in rat adipocytes (Kelly *et al.*, 1992) causing a rapid increase in PIP3 (also PI(3,4)P2). Secondly, class II PI 3-kinases are relatively resistant to the PI 3-kinase inhibitor wortmannin (Domin *et al.*, 1996; Virbasius *et al.*, 1996) at concentrations that inhibits insulin-stimulated GLUT4 translocation to plasma membranes (Okada *et al.*, 1994; Clarke *et al.*, 1994). PI(3,4)P2 and PIP3 production, which are thought to be necessary for further downstream signalling of PI 3-kinase, also rules out class III PI 3-kinases as being involved in insulin-stimulated GLUT4 trafficking, since class III PI 3-kinases are found to only use PI as a substrate. Whilst class II and III PI 3-kinases do not appear to be involved in insulin-stimulated GLUT4 trafficking, there is compelling evidence to suggest an involvement of class I_A PI 3-kinases (discussed below). Class III PI 3-kinases are homologous to Vps34p, the only PI 3-kinase present in yeast. Vps34p is important in yeast for trafficking of newly formed proteins from the Golgi to the vacuole (Rameh & Cantley, 1999), and the PI(3)P lipid product is hypothesised to regulate membrane trafficking and vesicle morphogenesis. It is possible that the lipid products of class I_A enzymes perform a similar role in membrane trafficking events in mammalian cells.

The PI 3-kinase inhibitor, wortmannin, has been shown to block glucose uptake and GLUT4 translocation in both rat adipocytes and 3T3-L1 adipocytes (Okada *et al.*, 1994; Clarke *et al.*, 1994). Furthermore, Hara *et al.* (1994) developed a p85 mutant which lacked the binding site for the catalytic p110 subunit. When expressed in CHO cells overexpressing the insulin receptor, these constructs led to attenuation in glucose transport, but not in $p21^{ras}$ activation. More recently introduction of the dominant negative p85α construct to 3T3-L1 adipocytes was shown to reduce PI 3-kinase activity, glucose transport and GLUT4 translocation (Katagiri *et al.*, 1997). Together these results suggest that PI 3-kinase is important for insulin-stimulated GLUT4 translocation to the plasma membrane, and that a class I_A PI 3-kinase

would appear to be the most likely isoform necessary for insulin-stimulated GLUT4 translocation.

Although PI 3-kinase activity is necessary for insulin-stimulated GLUT4 translocation to the plasma membrane, it is controversial as to whether the PI 3-kinase activity alone is sufficient to stimulate GLUT4 translocation. Evidence suggesting that endogenous PI 3-kinase activity alone is not sufficient for GLUT4 translocation is derived from two studies. Wiese *et al.* (1995) have shown that PDGF treatment of 3T3-L1 cells can activate PI 3-kinase activity to an extent that is comparable to insulin stimulation but does not produce a corresponding increase in glucose transport. Moreover, Herbst *et al.* (1994) introduced phosphopeptides corresponding to the sites of PI 3-kinase binding to IRS-1 into permeabilised 3T3-L1 adipocytes. The phosphopeptides activated PI 3-kinase to a similar extent as insulin stimulation without the normal increase in glucose transport.

Three groups have expressed constitutively active forms of p110 in 3T3-L1 adipocytes (Martin *et al.*, 1996a; Katagiri *et al.*, 1996; Tanti *et al.*, 1996). In each case, the extent of GLUT4 translocation to plasma membranes in cells expressing the constitutively active kinase was comparable to that occuring in cells stimulated by insulin. This contradictory result may be explained by the idea that PI 3-kinase should be targeted to a particular membrane compartment to stimulate GLUT4 translocation. This may not have been achieved by cell stimulation with either PDGF or phosphopeptides, however constitutively active over-expression of PI 3-kinase is likely to saturate any membranes with kinase activity and its lipid products. The idea of localisation of PI 3-kinase to a particular membrane compartment is discussed in *section 1.10.*

1.10 Localisation of IRS proteins and PI 3-kinase

Kelly & Rudeman (1993) have shown that in rat adipocytes the majority of the insulin-stimulated PI 3-kinase activity was localised to an intracellular LDM fraction, associated with tyrosine-phosphorylated IRS-1. A similar study by Yang *et al.* (1996) in 3T3-L1 adipocytes showed a similar subcellular distribution of insulin-activated PI 3-kinase activity. An increase in insulin-stimulated PI 3-kinase activity in the LDM fraction is also supported by the data of Kublaoui *et al.* (1995) and Inoue *et al.* (1998). However, analysis of the LDM fraction from 3T3-L1 adipocytes by hypertonic sucrose gradients, has suggested that IRS-1 and PI 3-kinase are not associated with an internal membrane structure or with GLUT4 vesicles (Clark *et al.*,

1998). Although PI 3-kinase-associated IRS-1 did not appear to be bound to any internal membrane, the signalling complex was found to be associated with fractions enriched in elements proposed to resemble cytoskeletal filaments (Clark *et al.*, 1998). One additional study to address the precise location of PI 3-kinase suggested that a small proportion of the adipocyte PI 3-kinase activity could associate with GLUT4 vesicles (Heller-Harrison *et al.*, 1996). However, unpublished data from our lab, suggests that this is less than 1% of the total insulin-stimulated PI 3-kinase activity in 3T3-L1 adipocytes. Furthermore, targeting of PI 3-kinase to GLUT4 vesicles by fusing the inter-SH2 domain of the p85α adaptor subunit to the N- and C-terminal cytoplasmic regions of GLUT4 failed to alter insulin-stimulated GLUT4 translocation, despite 11-13-fold increases in PI 3-kinase activity on the GLUT4 vesicles (Frevert *et al.*, 1998).

Whilst the majority of studies looked at PI 3-kinase activity associated with IRS-1 it may be more relevant to look at IRS-2 cell distribution and association with PI 3-kinase (*section 1.8*). IRS-2 compartmentalisation in 3T3-L1 adipocytes was studied by Inoue *et al.* (1998). Whilst IRS-1 was found to be mainly concentrated in a LDM fraction, IRS-2 was found to be mainly cytosolic. Upon insulin stimulation, IRS-2 was found to associate with the LDM fraction and with PI 3-kinase. The differences between IRS-1 and IRS-2 are potentially very important, and more work is required to define which IRS protein is important for insulin-stimulated GLUT4 translocation, and where the relevant PI 3-kinase activity resides.

1.11 Phosphatidylinositide-binding proteins

PI 3-kinase appears to be necessary for GLUT4 translocation, however the subsequent signalling events downstream of PI 3-kinase leading to GLUT4 translocation remain largely unclear. The most likely route for the generation of subsequent signalling processes is *via* the lipid products formed by the activated PI 3-kinase. Evidence for PI 3-kinase lipid products as mediators of signalling processes is provided by the observation that the transient production of PI(3,4)P2 and PIP3 in many cell types tends to correlate with the transient activation of downstream signalling processes. Further evidence for D-3-phosphatidylinositide signalling is shown by the ability of phosphatidylinositides to interact with signalling molecules. The PI 3-kinase lipid products can either act as an allosteric effector of the phosphatidylinositide-binding protein e.g. protein kinase C (PKC) (see below), change the conformation of phosphatidylinositide-binding proteins thereby revealing sites for phosphorylation e.g. PKB

(*section 1.12*), or regulate co-localisation with other phosphatidylinositide-binding proteins to form specific signalling complexes at membranes e.g. PKB and PDK1 (*section 1.12*).

The atypical PKC (aPKC) isoform PKCζ (which is not activated by either phorbol esters or diacylglycerol) was shown to be activated by 0.1 μM PIP3 (Nakanishi *et al.*, 1993), but not by PIP2 (only 11% of the PIP3 response). PI(3,4)P2 was only half as effective as PIP3 in stimulating PKCζ, and no significant effects of any lipid were seen on conventional PKC (cPKC) isoforms (α, β, and γ)(Nakanishi *et al.*, 1993). These results suggested that PKCζ might be a target for PIP3 and thus downstream of PI 3-kinase. Other isoforms additional to PKCζ have also been shown to be activated by PIP3 (Palmer *et al.*, 1995). In this study by Palmer *et al.*, the novel PKC (nPKC) isoforms PKCη and PKCε were activated to the same extent by both PIP3 and PIP2. aPKC isoforms, such as PKCζ, may therefore be potential targets for downstream signalling of PI 3-kinase, and their role in insulin stimulated GLUT4 translocation is discussed (*section 1.13*). The study by Palmer *et al.* emphasises an important point: to study a pathway that utilises PI 3-kinase, the downstream lipid-binding proteins need to be shown to have specificity for either PI(3,4)P2 and/or PIP3 relative to PIP2.

The PIP3 binding of PKCζ is unknown. Various PIP3 binding proteins are found to contain a PIP3 binding domain that has homology to pleckstrin (termed the PH domain; Tyers *et al.*, 1988). The PH domain consists of approximately 120 amino acids and was originally identified as an internal repeat present at the amino and C-termini of pleckstrin (the major substrate for PKC in platelets). Proteins that are found to contain PH domains include amongst others the serine/threonine kinase PKB (*section 1.12*), dynamin, and regulators of small molecular weight G-proteins (GEFs and GAPs; *section 1.14*). Despite a low similarity in sequence, the PH domains all share a similar core structure. This core structure consists of an antiparallel β-sheet of seven strands and a C-terminal amphiphilic α-helix (Harlan *et al.*, 1995). The β-strands form a cleft around a region of positive potential (provided by conserved lysine residues) which is critical for interaction with the negatively charged headgroup of phospholipids (Harlan *et al.*, 1995).

Early studies examined the interaction between PH domains and PIP2, however a subsequent study by Rameh *et al.* (1997) studied the interaction of PH domains with the products of PI 3-kinase activity. Rameh and colleagues compared the PH domains from six different proteins,

including Bruton's tyrosine kinase (Btk), the amino-terminal PH domain of T lymphoma invasion and metastasis protein (Tiam-1), Son-of-sevenless (Sos), β-adrenergic receptor kinase (βark), oxysterol binding protein (OSBP) and β-spectrin. The relative affinities of PIP2, PI(3,4)P2 and PIP3 for the various protein PH domains were determined by displacement of radiolabelled-C8-PI(3,4)P2 and –PIP3 bound to PH domains using unlabelled lipids. These binding studies demonstrated that the PH domain of Btk bound PIP3 with a higher affinity (K_d < 1 μM) than to PIP2 (K_d = 8 μM), PI(3,4)P2 or inositol 1,3,4,5-tetrakisphosphate (Ins(1,3,4,5)P4). Similar results were also obtained for Sos, Tiam-1 and βark, although these proteins showed less selectivity for PIP3 than the Btk PH domain. The PH domains of β-spectrin and OSBP bound PIP2 and PIP3 with similar affinities and with greater affinity that PI(3,4)P2. The PH domain of dynamin, the C-terminal PH domain of Tiam-1 and the phosphotyrosine binding (PTB) domain of IRS-1 (which has similarities to a PH domain) were found to bind the phosphatidylinositides poorly (Rameh *et al.*, 1997). A general hypothesis was therefore proposed for determining the phosphatidylinositide binding affinity of a PH domain. In general those PH domains with clusters of basic residues in the β1-β2 region (of the PH domain) tend to have higher affinity for PIP3 compared to PI(3,4)P2 (Btk, Tiam-1 N-terminal have 8 and 11 residues respectively). The PH domains with less than 5 basic residues in the β1-β2 loop tend to have a low affinity for PIP3. Hence, the results from Rameh *et al.* (1997) indicate that distinct PH domains might have evolved selectively for different phosphatidylinositides to provide discriminatory regulation.

The idea that PH domains might have evolved to provide discriminatory regulation is taken further by a more recent study by Kavran *et al.* (1998). Kavran *et al.* used a 'dot blot' approach to screen PH domain-containing proteins for specificity to particular phosphatidylinositides. The dot blot analysis used phosphatidylinositides spotted onto nitrocellulose that were subsequently incubated with ^{32}P-labelled GST-PH domain fusion proteins. The results of the dot blot analysis revealed a classification of PH-domain containing proteins that was similar to that obtained by Rameh *et al.* (1997). In the more recent classification by Kavran *et al.* (1998) the PH domain containing proteins were divided into three groups. These groups of proteins consist of proteins that specifically bind PIP3 relative to other phosphatidylinositides, proteins which bind PI(3,4)P2 and PIP3 with a higher affinity to PIP2 and finally proteins that have no particular specificity for a phosphatidylinositide relative to PIP2. The dot blot screening by Kavran *et al.* (1998) also revealed that of the 10 PH domain containing proteins analysed, only two proteins (Grp1 (*see below and section 1.14.2*) and phospholipase C-δ_1) showed clear

specificity for a single phosphatidylinositide. It was therefore suggested that many PH domain-containing proteins are likely to be regulated *in vivo* by the most abundant phosphatidylinositide to which they bind. Hence, Kavran *et al.* (1998) suggested that highly specific phosphatidylinositide binding may be a characteristic of relatively few proteins.

As indicated previously in consideration of PKCζ, not all proteins that bind PIP3 contain a PH domain. Proteins which bind PIP3 (in vitro) and which do not contain a PH domain include the adaptor proteins (APs) which are involved in vesicle trafficking. The dissociation constants for PIP3 binding to the adaptor proteins AP-2 and AP-3 are 350 nM and 5.8 μM respectively (Gaidarov & Keen, 1995; Falck *et al.*, 1997). Similarly, synaptotagmin, which is also involved in vesicle trafficking, regulates neurotransmitter release by a regulatory process involving the calcium induced exchange of PIP3 for PIP2 (Schiavo *et al.*, 1996). It is therefore interesting to speculate that PIP3-binding proteins may represent, in part, a family of proteins that are involved in regulating vesicle trafficking processes.

A link between PIP3-binding proteins and vesicle trafficking may also be provided by the observation that various PIP3-binding proteins (GRP-1, cytohesin-1, ARF nucleotide binding site opener (ARNO), SOS, tiam-1, neurogranin, centaurin-α) are found to be regulators of small GTP binding-proteins (*section 1.14*) (table 1). Small GTP binding-proteins include members of the Ras-related superfamily, consisting of Ras, Rho, Rab and ARF (*sections 1.14.1* & *1.14.2*) subfamilies (each family exhibits 30-50% similarity with Ras p21). As discussed in *section 1.14*, it is likely that small GTP binding-proteins are involved in insulin-stimulated GLUT4 translocation in insulin-sensitive tissues. Therefore, regulators of small GTP binding-proteins (GTPase activating proteins (GAPs) and GTP exchange factors (GEFs)) may play an important part in regulating the translocation of GLUT4.

PIP3-Binding Protein	Protein Function	Reference
Cytohesin-1	ARF GEF	Meacci *et al.*, 1997
GRP1	ARF GEF	Klarlund *et al.*, 1997
ARNO	ARF GEF	Peyroche *et al.*, 1996
Tiam-1	Rac GEF	Michiels *et al.*, 1995
Neurogranin	ARF GAP	Lu & Chen, 1997
Centaurin-α	ARF GAP	Hammonds-Odie *et al.*, 1996
SOS	Ras GEF	McCollam *et al.*, 1995

Table 1. PIP3-binding proteins with homology to small GTP binding-protein GAPs and GEFs.

In yeast, constitutive membrane trafficking into the vacuole and the sorting of newly synthesised proteins is dependent upon PI 3-kinase (reviewed by Rameh & Cantley, 1999). Additionally, the early-endosomal autoantigen (EEA1) is found to bind to PI(3)P (Patki *et al.*, 1997), and to Rab5 (Simonsen *et al.*, 1998), thereby linking small GTP binding-proteins and PI 3-kinase. Yeast trafficking processes are inhibited by the addition of wortmannin but may be overcome by activating Rab5 (Simonsen *et al.*, 1998). In a similar scenario, inhibition of GLUT4 translocation by wortmannin may be partially overcome by the addition of GTPγS (a non-hydrolysable analogue of GTP, which activates both small GTP-binding proteins and heterotrimeric G-proteins) in adipocytes (Clarke *et al.*, 1994). It is therefore interesting to speculate that a conserved mechanism may exist in which small GTP binding-proteins involved in vesicle trafficking processes such as GLUT4 translocation are linked to GTP binding-protein regulators which are also regulated by upstream PI 3-kinase.

Ultimately, identification of proteins which specifically bind the lipid products of PI 3-kinase activity, and which can be shown to be necessary for insulin-stimulated GLUT4 translocation may help to clarify subsequent downstream signalling processes that lead to the fusion of GLUT4 vesicles with the plasma membrane. Currently, PIP3 proteins identified in adipocytes include PKC isoforms (*section 1.13*), adaptor proteins, PKB (*section 1.12*), PDK1 (*section 1.12*), dynamin and proteins with Sec 7 homology domains (GRP1, ARNO) (*section 1.14.2*). The roles of some these proteins and their relationship to GLUT4 translocation are discussed further.

1.12 Protein kinase B

The serine/threonine kinase protein kinase B (PKB) (Coffer & Woodgett, 1991) is so named because of its similarity in its catalytic domain to the kinases PKA and PKC. This similarity has also given rise to the alternative name RAC-kinase ('related' to protein kinases 'A' and 'C') (Jones *et al.*, 1991). Additionally PKB is also known as c-Akt-kinase, since it is the cellular homologue of the viral oncogene v-Akt (Bellacosa *et al.*, 1991).

Three PKB isoforms have been identified, PKBα, PKBβ (Cheng *et* al., 1992) and PKBγ (Konishi *et al.*, 1995). Each PKB isoform has >80% sequence identity between each isoform and contains a PH domain amino-terminal to the catalytic domain. The major difference between the three PKB isoforms is that PKBγ is truncated at the C-terminus and hence lacks a serine phosphorylation site (present in the other two isoforms). PKBα and PKBβ are found to be ubiquitously expressed whereas PKBγ expression is generally found in greater amounts in brain and testicular tissue (Alessi & Cohen, 1998). PKBβ activation by insulin has been shown to be twice that of PKBα in adipocytes (Walker *et al.*, 1998), but surprisingly in skeletal muscle PKBα is the dominant isoform activated by insulin, and little activation of PKBβ is observed (Walker *et al.*, 1998). For glucose disposal, skeletal muscle is more relevant than adipose tissue since it represents 90% of the insulin-stimulated glucose uptake from the blood. Research is therefore still required to assess the roles of individual PKB isoforms in particular tissues and their relevance to GLUT4 translocation.

The current interest in PKB and glucose transport arises from the observations that PKB is activated by various growth factors, including insulin (Burgering & Coffer, 1995; Kohn *et al.*, 1995). Furthermore, PKB activity was shown to be blocked by PI 3-kinase inhibitors (Burgering & Coffer, 1995; Kohn *et al.*, 1995), implying that PKB activation is a downstream event of PI 3-kinase activity. Further evidence for PKB activity occurring downstream of PI 3-kinase was derived from the observations that overexpression of a constitutively active mutant of PI 3-kinase activated PKB (Didichenko *et al.*, 1996), whereas a dominant negative form of PI 3-kinase inhibited PKB activation (Burgering & Coffer, 1995). Although PI 3-kinase- independent mechanisms for PKB activation do exist (Sable *et al.*, 1997), the activation of PI 3-kinase appears to be the major factor regulating PKB activation. Early PKB research showed that both PI(3,4)P2 and PIP3 could activate PKB (Frech *et al.*, 1997; Klippel *et al.*, 1997). However, it has now been shown that PKB is not directly activated by PI(3,4)P2 and PIP3 (James *et al.*, 1996), but activation is mediated by phosphorylation (Kohn *et al.*, 1996a).

Indeed, early studies with PKB showed that PKB activation by growth factors (including insulin) was paralleled by phosphorylation of the kinase itself (Kohn *et al.*, 1995). PKB phosphorylation appears to be critical for PKB kinase activity as treatment of active PKB immune complexes with phosphatases abolishes the ability of the kinase to phosphorylate *in vitro* substrates (Kohn *et al.*, 1995). Insulin-induced phosphorylation of PKBα on residues Thr_{308} and Ser_{473} (both residues act synergistically to activate PKB) was shown to be blocked by wortmannin (Alessi *et al.*, 1996). The realisation that PKB activation is dependent upon phosphorylation led to the discovery of a kinase which phosphorylated PKB on Thr_{308} (Alessi *et al.*, 1997). This kinase was found to be dependent upon PI(3,4)P2 or PIP3 for activity and was therefore termed as PIP3-dependent protein kinase-1 (PDK1). Like PKB, PDK1 was shown to have a PH domain (C-terminal to its kinase domain) (Stephens *et* al., 1998). Overexpression of PDK1 enhanced PKB activation (Anderson *et al.*, 1998) whereas mutation of the PH domain of PDK1 significantly reduced PKB activation (Anderson *et al.*, 1998). Inhibitors of PI 3-kinase had no direct effect on PDK1 activity, suggesting that PDK1 is constitutively active and its activity and function is regulated by its subcellular localisation and substrate availability. The importance of the PH domains of both PKB and PDK1 appears to localise the two kinases to a membrane and thereby bring them together to allow PKB phosphorylation and activation. This model has been proposed for PKB activation by Downward (1998) and Alessi & Cohen (1998) (figure 7).

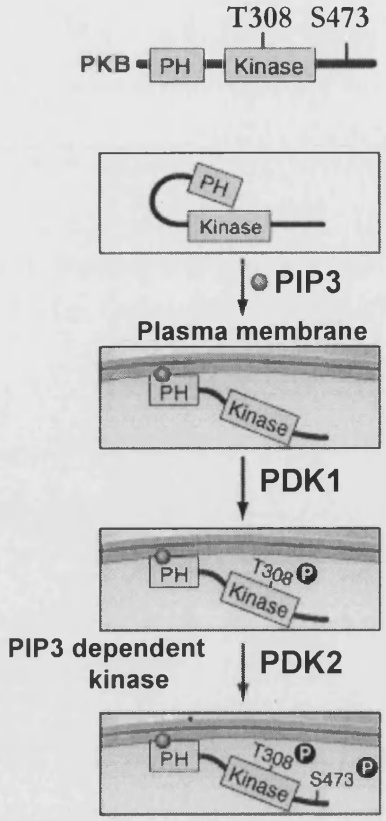

Figure 7. Mechanism of activation of PKB (Downward, 1998). PKBα is activated by phosphorylation of two residues by kinases PDK1 and PDK2. The initial event is the generation of either PI(3,4)P2 or PIP3, by PI 3-kinase, which allows targeting of both PKB and PDK1 to a particular membrane *via* their PH domains. PKB targeting to a membrane induces a conformational change in PKB, which allows PKB to become phosphorylated by PDK1 on Thr_{308} or the equivalent residue for PKBβ and PKBγ. The phosphorylation of Ser_{473} on PKBα (or Ser_{474} on PKBβ) is thought to be mediated by a kinase similar to PDK1, but remains unidentified and is simply termed as PDK2. A review on PKB (Coffer *et* al., 1998) has a note added in proof on results soon to be published, that integrin-linked kinase (ILK) can phosphorylate PKB on Ser473 and that this kinase may represent PDK2. The phosphorylated PKB molecule is now able to dissociate from the membrane and translocate to sites such as the nucleus (Meier *et al.*, 1997) and phosphorylate substrates independently of phosphatidylinositides.

Whilst various processes such as protein synthesis and apoptosis have been suggested to be downstream of PKB (reviewed by Coffer *et al.*, 1998), direct links remain to be established. Similarly PKB appears to be involved in regulating glucose metabolism, *via* glycogen synthase kinase 3 (GSK3) and the cardiac isoform of 6-phosphofructo 2-kinase (PFK-2), reviewed by Coffer et al. (1998). Given the dependency of GLUT4 translocation on PI 3-kinase activation, and the activation of PKB by insulin, it was therefore not surprising that the role of PKB in insulin-stimulated GLUT4 translocation was also investigated. The role of PKB activation in relation to GLUT4 translocation was initially studied by Kohn *et al.* (1996b). This group showed that PKBα lacking a PH domain but targeted to membranes by myristoylation, leads to a constitutively active kinase. Transfection of this PKB mutant into basal 3T3-L1 adipocytes increased glucose uptake to 70% of that occuring in insulin-stimulated cells. The increased glucose uptake was attributed to increases in GLUT1 and GLUT4 on the cell surface. Whilst this was evidence that PKB may be responsible for regulating GLUT4 translocation, these latter experiments only evaluated the long-term effects of PKB activation. They did not directly address the issue of whether acute-insulin stimulation of PKB is necessary for GLUT4 translocation. Without specific inhibitors of PKB this question is

difficult to address. However more recently, Kitamura *et al.* (1998) expressed a mutant PKBα in CHO cells and 3T3-L1 adipocytes in which the two phosphorylation sites were replaced by alanine. The construct produced a dominant negative effect on the endogenous PKB activity that was stimulated by insulin. Endogenous PKB activity was reduced by 80 to 95%, while p70 S6 kinase activity was reduced by 75% in CHO cells and 30% in 3T3-L1 adipocytes. However, there was no effect on glucose transport. The conclusion reached was that PKB activity is not required for glucose transport (Kitamura *et al.* 1998). While the double alanine PKB mutant was for PKBα, the polyclonal antibodies used to examine the endogenous PKB activity were capable of precipitating all three known PKB isoforms. Hence the data indicated that the PKB mutant inhibited all three of the PKB isoforms. In contrast, Calera *et al.* (1998) have shown that insulin stimulates an association of PKBβ with GLUT4 vesicles in 3T3-L1 adipocytes. This association was shown to be wortmannin sensitive. However, it is not clear whether GLUT4 vesicles represent a site of insulin-stimulated PI 3-kinase activation (*section 1.10*) and therefore the mechanism by which GLUT4 localised PKBβ is activated is not evident. The role of PKB in GLUT4 translocation remains unresolved and more work is required to determine if GLUT4 vesicles from muscle are associated with an active isoform of PKB.

1.13 Protein kinase C

PKC involvement in the regulation of GLUT4 vesicle trafficking has primarily been investigated by the use of phorbol esters such as phorbol 12-myristate 13-acetate (PMA). PMA is known to activate cPKC (α, β, and γ), nPKC (δ, ε, η, θ and μ), but not aPKC (ζ and ι/λ) isoforms. In rat adipocytes, PMA only partially raises cell surface levels of GLUT1 and GLUT4 (5.7- and 4-fold respectively) (Holman *et al.*, 1990). Whilst the GLUT1 increase in the plasma membrane caused by PMA is comparable to that observed by insulin-stimulation, the small PMA-induced increase in GLUT4 is not comparable to that seen by insulin-stimulation (20-fold). In a similar study by Gibbs *et al.* (1991), 3T3-L1 adipocytes stimulated by PMA only exhibited a 10% increase in plasma membrane GLUT4 levels compared to insulin stimulation. Furthermore, down-regulation of PKC by chronic treatment of 3T3-L1 adipocytes with PMA prevents elevation of glucose transport by acute and chronic PMA stimulation but does not inhibit insulin-stimulated glucose transport (Gibbs *et al.*, 1991). These data would therefore suggest that PMA-sensitive PKC proteins appear not to be necessary for insulin-stimulated GLUT4 translocation. However, a role for cPKC's and nPKC's cannot be entirely ruled out,

since PMA and insulin treatment appear to activate PKC isoforms differently (Farese *et al.*, 1992). Farese *et al.* (1992) have shown that PKCβ translocates to the plasma membrane in rat adipocytes following insulin stimulation, but not following PMA stimulation. More recently, Walaas *et al.* (1997) have shown that in Streptolysin-O (SLO)-permeabilised rat adipocytes, the PKC pseudosubstrate inhibitor peptide inhibited both PKC phosphorylation of an artificial peptide substrate, and GLUT4 translocation to the plasma membrane. Additionally, they showed that PKCβ translocates to the plasma membrane in response to insulin, and that neutralising antibodies to PKCβ inhibited the insulin-stimulated GLUT4 translocation to the plasma membrane in SLO-permeabilised rat adipocytes. This would therefore suggest that PKCβ may play a role in GLUT4 translocation, but whether PKCβ activation is sufficient to account for insulin-stimulated GLUT4 translocation remains to be determined.

Studies by Nave *et al.* (1996) have shown that PMA can stimulate PIP3 production in 3T3-L1 adipocytes by ~2-fold, and that this correlates with the 2-fold increase seen in glucose transport. However, PIP3 production and glucose transport were stimulated 6- and 8-fold respectively by insulin. This agrees with previous observations (as above) that PMA can partially stimulate GLUT4 translocation, but not to the same extent as insulin. Nave *et al.* (1996) also observed that the PMA-induced increases in PIP3 and glucose transport were inhibited by treatment of the cells with inhibitors of PI 3-kinase (wortmannin and LY294002). This therefore suggested that the partial stimulation of glucose transport by PMA was mediated by a downstream PI 3-kinase.

aPKC's are not activated by PMA and therefore need to be considered separately. Additionally the aPKC's are not inhibited by the pseudosubstrate inhibitor peptide (see above) since their pseudosubstrate domain differs from that of cPKC's and nPKC's. The possibility that aPKC's may be involved in signalling downstream of PI 3-kinase, comes from the observation that PKCζ can be activated *in vitro* by PIP3 (Nakanishi *et al.*, 1993; *section 1.2.6*). Furthermore, Standaert *et al.* (1997) have shown that insulin-stimulation of rat adipocytes results in the phosphorylation of PKCζ and a 4-fold increase in PKCζ activity. The insulin-induced activation of PKCζ is inhibited by both wortmannin and LY294002 (another inhibitor of PI 3-kinase) suggesting that PKCζ acts as a downstream effector of PI 3-kinase. Additionally, 10μM PI(3,4)P2, 10 μM PIP3 and 1 μM PIP2 directly stimulated PKCζ activity and autophosphorylation in immunoprecipitates, to the same extent as insulin. Furthermore, in

adipocytes transiently expressing haemagglutinin antigen-tagged GLUT4, co-transfection of wild-type or constitutive PKCζ stimulated haemagglutinin antigen-tagged GLUT4 translocation to the PM (Standaert *et al.*, 1997). Conversely, a dominant-negative PKCζ construct which was transiently transfected into adipocytes inhibited insulin-stimulated GLUT4 translocation to the plasma membrane by ~50%. These data therefore suggested that PKCζ might act as a downstream effector of PI 3-kinase and contribute to the activation of GLUT4 translocation (Standaert *et al.*, 1997).

Subsequent research by Kotani *et al.* (1998) have shown that 3T3-L1 adipocytes express the aPKC PKCλ and not PKCζ. Insulin was observed to cause a 3-fold increase in PKCλ activity which was inhibited by wortmannin. Additionally, 3T3-L1 adipocytes transfected with mutant PKCλ constructs, produced inhibition of insulin stimulated PKCλ activation. The dominant negative PKCλ constructs produced a 50-60% inhibition of glucose uptake, however no inhibition of PKB was observed. Complete inhibition of PKCλ activity in immunoprecipitates corresponded only to 50% inhibition in glucose transport. The lack of complete inhibition of glucose transport was explained by the possibility of their existing an alternative signalling pathway which may compensate for the lack of PKCλ activity. Alternatively, the discrepancy between PKC activity and glucose uptake may be explained if some lipid moduators that activate the kinase were limiting/removed from the experimental system. Indeed, Kotani *et al.* have shown that phosphatidylserine can further increase PKCλ activity in PKCλ immunoprecipitates from insulin stimulated cells (Kotani *et al.*, 1998). Whilst dominant-negative mutants of PKCλ can inhibit glucose transport, a constitutively active PKCλ construct (made by deletion of the pseudosubstrate domain) was found to activate GLUT4 translocation to the plasma membrane. The constitutively active PKCλ stimulated glucose transport to an extent comparable to that seen by insulin, in a wortmannin resistant manner, but had no effect on PKB activity (Kotani *et al.*, 1998). Hence, the authors suggested that insulin signalling diverges into at least two independent pathways downstream of PI 3-kinase, one pathway through PKB and the other pathway through PKCλ. They suggest that the latter pathway contributes to insulin stimulation of glucose uptake in 3T3-L1 adipocytes.

How PI 3-kinase modulates PKCλ and PKCζ activity is still uncertain, and this warrants further investigation, as does identification of the substrate of the aPKC isoforms. Whilst the significance of aPKC's activation by insulin in not known, studies by Sanchez *et al.* (1998) have

shown that aPKC isoforms are targeted to late endosomes through interaction a member of the src-kinase family ($p56^{lck}$). Furthermore, expression of a dominant negative PKCλ impaired the endocytic membrane transport of epidermal growth factor receptors but not the transferrin receptor. These results therefore suggest that aPKC's may be important in membrane trafficking, and possibly GLUT4 trafficking.

1.14 GTP-binding proteins

Guanosine nucleotide binding regulatory proteins (GTP-binding proteins) play a pivotal role in signal transduction. Evidence that GTP-binding proteins are involved in insulin-regulated GLUT4 trafficking comes from the observations that non-hydrolysable analogues of guanosine triphosphate (GTP) such as guanosine-5'-*O*-(3-thiotriphosphate) (GTPγS) can stimulate GLUT4 translocation (Baldini *et al.*, 1991) even in the presence of the PI 3-kinase inhibitor wortmannin (Clarke *et al.*, 1994). Furthermore, a small molecular weight GTP-binding protein has also been found on immunoisolated GLUT4 vesicles (Cormont *et al.*, 1993).

There is also evidence that GTP-binding proteins are involved in SNARE complexes (*section 1.4*) and in the endocytosis of plasma membrane GLUT 4 (Omata *et al.*, 1997; Al Hasani *et al.*, 1998; Volchuk *et al.*, 1998).

Discussed below is the evidence that GTP-binding proteins (heterotrimeric and small molecular weight ras-like GTP-binding proteins) are involved in both trafficking of GLUT4, to and from, the plasma membrane.

1.14.1 Small Ras-like GTP-binding proteins

Studies by Cormont *et al.* (1991) have shown that GLUT4 enriched vesicles contained small molecular weight GTP-binding proteins. These GLUT4 vesicle-associated GTP-binding proteins are likely to represent members of the Ras-like GTP-binding proteins which include ARF (*section 1.14.2*) and Rab families, which regulate vesicle trafficking processes (reviewed by Pfeffer, 1992 and Novick & Zerial, 1997)(table 2). Indeed, subsequent studies by Cormont *et al.* (1993) identified one of the proteins associated with GLUT4 vesicles as Rab4. In cardiac muscle, experiments undertaken by Uphues *et al.* (1994) similarly found GTP-binding proteins in a GLUT4-enriched membrane fraction, but found that only a single GTP-binding protein

(as assessed by one-dimensional gel electrophoresis), was associated with isolated GLUT4 vesicles, and that it was unlikely to be Rab4. Despite, the conflicting evidence on whether Rab4 is associated with GLUT4 vesicles (which may be due to differences in tissues), there is now strong evidence to suggest that Rab4 is involved in GLUT4 trafficking.

Protein	Localisation	Function
Rab3C	Synaptic vesicles	Unknown
Rab4A, Rab4B	Early endosomes	Recycling pathway from endosomes to plasma membrane
Rab5A, Rab5B, Rab5C	Plasma membrane, clathrin-coated vesicles; early endosomes	Plasma membrane to early endosome transport and homotypic fusion between early endosomes
Rab11	TGN; constitutive secretory vesicles; secretory granules; recycling endosomes	Transport through recycling endosomes

Table 2. Function of a variety of rab proteins involved in vesicular trafficking events in mammalian cells (adapted from Novick & Zerial, 1997).

Evidence for the involvement of Rab4 in GLUT4 trafficking comes from four sources. Firstly, studies by Cormont *et al.* (1996a) showed that a moderate and transient expression of Rab4 in rat adipocytes led to the retention of GLUT4 to intracellular membranes under basal conditions, with no effect on GLUT4 trafficking under insulin-stimulated conditions. However, overexpression of Rab4 led to a decrease in the insulin-stimulated GLUT4 trafficking to the plasma membrane. These data would therefore imply that Rab4 is involved in both the biogenesis of the insulin-sensitive GLUT4 intracellular compartment and may direct it to the PM under insulin-stimulated conditions. Secondly, electroporation of a peptide corresponding to the carboxy-terminus hypervariable region of Rab4 inhibited insulin-stimulated GLUT4 trafficking to the plasma membrane by 50% (Shibata *et al.*, 1996). The peptide was also capable of inhibiting GTPγS-stimulation of GLUT4 trafficking. Thirdly, coexpression of Rab4 and GLUT4 in *Xenopus* oocytes led to an increased intracellular retention of GLUT4 (Mora *et al.*, 1997). Fourthly, more recent studies by Shibata *et al.* (1997), have shown that insulin stimulates guanine nucleotide exchange on Rab4 in rat adipocytes. The increased nucleotide exchange by insulin treatment was inhibited by wortmannin. Hence,

it would seem that Rab4 is involved in GLUT4 vesicle trafficking events. How exactly Rab4 contributes to GLUT4 trafficking is still unclear, although it is likely that Rab4 is regulated by various nucleotide exchange factors and accessory proteins and effectors, such as GTPase activating proteins (GAPs) (reviewed by Scheffzek *et al.* 1998), GDP-dissociation inhibitor proteins (GDIs) and guanine nucleotide exchange factors (GEFs) (reviewed by Sprang & Coleman, 1998). The regulation of Rab activity by these various regulatory proteins is shown by figure 3. Briefly, Rab proteins exist in a membrane bound state regulated by GEF and GAP proteins, and in a cytosolic state bound to GDI proteins. The functional cycle of Rab proteins as shown by figure 3, can be applied to observations seen with Rab4.

Experiments involving Rab4 have shown that upon insulin stimulation, Rab4 undergoes nucleotide exchange (Shibata *et al.* 1997), hence it is possible that a GEF (figure 3-A) is activated by insulin which allows for 'activation' of Rab4 associated with GLUT4 vesicles. Generally, it is found that Rab4 translocates from GLUT4 vesicles to the cytosol (Cormont *et al.*, 1993), and preferentially binds to GDI-1 in the cytosol (Shisheva *et al.* 1997). However, in cardiac muscle, Uphues *et al.* (1994) found that upon insulin stimulation Rab4 shifted to the plasma membrane. Whilst GDI proteins normally extract Rab proteins from membranes in the GDP bound 'inactive state' (figure 3-C), it is possible, that experiments by Cormont and colleagues have disrupted any plasma membrane/Rab4 interactions. This is plausible, since the GAP activity for Rab4 is found to be enriched in the plasma membrane of 3T3-L1 adipocytes (Bortoluzzi *et al.*, 1996). Furthermore, if Rab4 is associated with GLUT4 it may represent a regulator of the SNARE complex (*section 1.4*). Thus, the C-terminal hypervariable region of Rab4 may be involved in masking VAMP2 under basal conditions, and thus regulating vesicle fusion.

Whilst, Rab4 is implicated in GLUT4 vesicle trafficking it is unlikely that it represents the only Rab protein involved in the trafficking process, although to date, no other Rab protein has been determined to be necessary for insulin-stimulated GLUT4 trafficking.

Other members of the Ras superfamily, which might be important for GLUT4 trafficking are the small GTP-binding proteins of the Rho family. The Rho family, includes Rac, Rho and Cdc42. Like other small-molecular weight GTP-binding proteins these cycle from GTP-bound active forms to GDP-bound inactive forms. Members of the Rho family can regulate the actin cytoskeleton (reviewed by Machesky & Hall, 1996) which has been implicated in being

important for GLUT4 trafficking (Wang *et al.*, 1998). Furthermore, Cdc42, has been shown in conjunction with the products of PI 3-kinase to regulate actin assembly in *Xenopus* cells (Ma *et al.*, 1998). As described in *section 1.11*, it is possible that GTP-binding proteins may be regulated by PI 3-kinase mediated events. Certainly, the more recent data by Clark *et al.* (1998) suggests that the insulin-stimulated PI3-kinase activity observed in adipocytes is associated with structures that could possibly be represented by the cytoskeleton. The observations that insulin promotes the wortmannin sensitive translocation of Rho to the plasma membrane in rat adipocytes, suggests that Rho might be involved in processes like GLUT4 trafficking (Karnam *et al.*, 1997). Furthermore, GTPγS-stimulated GLUT4 translocation in rat adipocytes can be inhibited by the use of *Clostridium botulinum* C3 transferase, an inhibitor of Rho (Standaert *et al.*, 1998). However, more work is still required to determine precisely the role of the cytoskeleton in GLUT4 trafficking, and the role that GTP-binding proteins have in the regulation of the cytoskeleton.

1.14.2 ARF

The ADP-ribosylation factor (ARF) family is a group of structurally related proteins. Like the Rab family these form a subset of the Ras superfamily of regulatory GTP-binding proteins. Six mammalian ARF genes have been identified, but only five proteins have been identified in humans, namely that of ARF1, 3, 4, 5 and 6. The role of these various isoforms appear to be as diverse as the Rab proteins, and ARF proteins have been shown to act in a variety of processes such as targeting recycling vesicles to the plasma membrane (D'Souza-Schorey *et al.*, 1998), regulating phospholipase D activity (Cockcroft, 1996), Golgi membrane budding (Elazar *et al.*, 1994) and targeting of adaptor proteins to membranes (West *et al.*, 1997). Brefeldin A has been shown to disrupt guanine nucleotide exchange on ARF (ARF 6 is brefeldin A insensitive) and thereby inhibit its function. However, whilst brefeldin A has been reported to inhibit insulin-stimulated GLUT4 translocation in rat adipocytes (Lachaal *et al.*, 1994), three further independent studies have shown that despite a small effect on basal glucose transport brefeldin A has little effect on the insulin-stimulated translocation of GLUT4 to plasma membranes in rat adipocytes (Chakrabarti *et al.*, 1994; Bao *et al.*, 1995; Kono-Sugita *et al.*, 1996). Despite this conflicting evidence from the use of brefeldin A, recent research by Rapoport *et al.* (1998) have shown that the adaptor protein AP-1 binds the carboxy dileucine motif of GLUT4. Furthermore, AP-1 binding to membranes has been shown to be dependent on ARF (Stamnes & Rothman, 1993). Hence it is possibile that ARF can associate with intracellular membranes enriched with GLUT4. Furthermore, unpublished

data from our lab (Gillingham *et al.*, 1999) have found both AP-1 and AP-3 (reviewed by Odorizzi *et al.*, 1998) co-localised with immunoisolated GLUT4 vesicles. Interestingly, AP-1 and plasma membrane associated AP-2 complexes have been shown to bind the products of PI 3-kinase (*section 1.11*). It is therefore plausible that both lipid products from PI 3-kinase together with ARF proteins can regulate assembly of AP complexes and regulate GLUT4 vesicle trafficking.

Moreover, the PIP3 binding proteins cytohesin-1, GRP-1 and ARNO (*section 1.11*) contain Sec7 domains which catalyses the exchange of GDP to GTP on ARF, promoting ARF association with membranes. It is likely that one or more of these ARF GEFs are involved in regulating ARF activity. Indeed, both ARF and ARNO translocate from the cytosol to the PM upon insulin stimulation of adipocytes (Karnam *et al*, 1997; Venkateswarlu *et al.*, 1998), the translocation of ARNO being blocked by wortmannin (Venkateswarlu *et al.*, 1998). Therefore the translocation of ARNO to the PM appears to be dependent upon PIP3 production. This raises further questions about the localisation of insulin-stimulated PI 3-kinase activity in adipocytes, since the work by Venkateswarlu *et al.* (1998) would suggest that insulin-stimulated PI 3-kinase activity is at the PM. Further work is therefore still required to determine the role of ARF in GLUT4 trafficking events.

1.14.3 Heterotrimeric G-proteins

There is evidence that vesicle trafficking is also regulated by heterotrimeric GTP-binding proteins. For example, heterotrimeric GTP-binding proteins are found to be involved in the organisation and formation of secretory vesicles from the Golgi complex (Barr *et al.*, 1992; Yamaguchi *et al.*, 1997). Whilst adipocytes are found to express a variety of heterotrimeric GTP-binding proteins (Denis-Henriot *et al.*, 1996), very few reports have implicated these proteins in GLUT4 trafficking. One possible candidate for regulating GLUT4 trafficking is $G_{i\alpha_2}$. Antisense RNA expression of the gene encoding $G_{i\alpha_2}$ in mice gave characteristics of non-insulin-dependent diabetes mellitus (*section 1.16*) such as hyperinsulinaemia, impaired glucose tolerance, insulin-resistance and impaired insulin-stimulated GLUT4 translocation to plasma membranes (Moxham & Malbon, 1996). This therefore implicates $G_{i\alpha_2}$ as a positive regulator of insulin action. The latter study also suggested that the deficiency of $G_{i\alpha_2}$ was upstream of IRS-1, since IRS-1 tyrosine phosphorylation was reduced. The reduction in tyrosine phosphorylation of IRS-1 was explained by the observations that the lack of $G_{i\alpha_2}$ expression

also led to increased cellular tyrosine phosphatase activities. Further experiments will hopefully clarify the role of $G_{i\alpha_2}$ in GLUT4 trafficking.

1.15 Phosphatases

In intracellular signalling pathways signalling events are regulated by a balance between kinase and phosphatase activities. As has already been mentioned in previous sections, recent reports on the serine/threonine kinases PKB and PKC have implicated these proteins in insulin-regulated GLUT4 trafficking. However earlier studies involving the use of phosphatase inhibitors such as okadaic acid (OA) also implied that serine/threonine kinases may be important for insulin-regulated GLUT4 trafficking.

OA is a potent inhibitor of protein phosphatases 1 and 2A. Initial studies in adipocytes with okadaic acid by Haystead *et al.* (1989) have shown that OA increases the phosphorylation state of many cellular proteins, and more importantly increases 2-deoxyglucose uptake, to an extent that is comparable to insulin-stimulation. However, subsequent studies have shown that OA only elicits a partial insulin-like response on glucose transport (approximately 20% of the insulin response) in rat adipocytes (Lawrence *et al.*, 1990; Corvera *et al.*, 1991; Rondinone *et al.*, 1996). The precise targets of OA targets in rat adipocytes are not clear. Although the small OA-stimulated increase in glucose transport is due to an increase in the rate of GLUT4 exocytosis from intracellular vesicles to the PM (Rampal *et al.*, 1995). Whilst, insulin stimulation of GLUT4 translocation to the plasma membrane appears to have a requirement for PI 3-kinase, OA does not stimulate PI 3-kinase in rat adipocytes (Rondinone *et al.*, 1996). This would imply that okadaic acid acts either on a pathway downstream of PI 3-kinase or by a distinct pathway which eventually converges with a pathway downstream of the PI 3-kinase which is acted upon by insulin.

Inhibition of tyrosine phosphatases by pervanadate ions can also stimulate GLUT4 translocation to the plasma membrane (Shisheva & Shechter, 1993). Pervanadate-stimulation of glucose transport is thought to occur by inhibition of tyrosine phosphatases that are associated with the insulin receptor. This causes receptor phosphorylation and initiates the insulin intracellular signalling cascade that leads to glucose transport. Furthermore, pervanadate stimulation of 2-deoxyglucose uptake in 3T3-L1 adipocytes has been shown to be partially both wortmannin and LY294002 resistant (Ida *et al.*, 1996). This suggests that stimulation of tyrosine kinases occurs either on a pathway distinct to those activated by insulin

or on a pathway downstream of PI 3-kinase that is normally activated by insulin which can lead to glucose transport. Further evidence for tyrosine kinases acting downstream of PI 3-kinase activity have been shown by Elmendorf *et al.* (1998) and Haruta *et al.* (1998). These studies have shown that in the presence of wortmannin, GTPγS can elicit tyrosine phosphorylation of various cellular proteins in addition to increased glucose uptake.

Overall, it would appear that serine/threonine and tyrosine phosphatases are likely to play a critical role in the regulation of GLUT4 trafficking.

1.16 Non-insulin-dependent diabetes mellitus (NIDDM)

Insulin's effects on glucose metabolism is primarily due to repression of gluconeogenesis and glucose uptake in the liver, acceleration of the rate of glucose uptake across the cell membrane of adipose and muscle tissue, and enhancement of glucose incorporation into glycogen. However, in NIDDM patients there tends to be a loss of peripheral sensitivity to insulin (insulin resistance). Hence, to maintain normoglycaemia, there is an increase in insulin secretion from the β-cells of the pancreas, resulting in hyperinsulinaemia. Eventually the increased demand placed on the pancreatic β-cells to maintain normoglycaemia results in progressive loss of β-cell function. The eventual hyperglycemia results from both a defect in insulin secretion as well as from a loss of peripheral sensitivity to insulin. Whilst NIDDM appears to be due to both a combination of genetic and environmental factors (Kahn, 1994), it is likely that the insulin resistance which is associated with the onset of NIDDM is responsible for the subsequent hyperinsulinaemia. Since it would appear that a diminished insulin-stimulated glucose transport in skeletal muscle is not a consequence of reduced GLUT4 expression (Pederson *et al.*, 1990), it is likely that the defect in glucose transport in NIDDM is due to alterations in insulin signalling, insulin-stimulated targeting of GLUT4 to the PM or alterations in the sequestration of GLUT4 (Garvey *et al.*, 1998). Therefore, by obtaining a greater understanding of the normal insulin-regulation of GLUT4 translocation in adipose and muscle tissues, the precise defects which result in insulin-resistance may become apparent and could possibly be targeted for a cure of NIDDM.

PART C - Aims of the thesis

A model representing insulin resistance as an indicator of NIDDM was studied. The aims in this study were to discern whether the reduced insulin-stimulated glucose transport in insulin-resistant adipocytes (Kozka *et al.*, 1993) results from alterations in the insulin signal transduction pathway or in trafficking processes that lead to GLUT4 translocation.

Further aims were to study the involvement of insulin-regulated signalling intermediates already implicated in insulin-regulated GLUT4 trafficking. Therefore the role of PKB in okadaic acid stimulated glucose transport in both rat and human adipocytes was examined. Additionally, the role of PKB in muscle was examined to determine whether insulin- and contraction-stimulated glucose transport utilise the same signalling pathway

Other aims of the thesis were to develop methods for identifying new signalling molecules involved in GLUT4 trafficking. The signal transduction pathway from the insulin receptor leading to GLUT4 translocation remains only partially elucidated. Given the involvement of PI 3-kinase, and the potential involvement of GTP-binding proteins in insulin-stimulated GLUT4 translocation, research was aimed at identifying both phosphatidylinositide-binding proteins and insulin-regulated GTP-binding proteins. The identification of new phosphatidylinositide-binding proteins may help clarify the site of action of insulin-stimulated PI 3-kinase lipid products and the subsequent downstream molecules required for insulin-stimulated GLUT4 translocation to the PM. Molecules downstream of PI 3-kinase are likely to involve GTP-binding proteins. Therefore identification of insulin-regulated GTP-binding proteins which are sensitive to the activation state of PI 3-kinase can hopefully also give further elucidation of regulation of GLUT4 trafficking processes.

CHAPTER 2

MATERIALS & METHODS

2.1 Laboratory chemicals

Unless otherwise stated general laboratory chemicals were of analytical grade and purchased from either Sigma-Aldrich Company Ltd., Fisons Scientific UK Ltd. or BDH Laboratory Supplies.

Bovine Albumin Cohn Fraction V powder, pH 5.2 (BSA), was purchased from Intergen Co. (Newark, NJ). A 10% (w/v) solution was prepared at 4°C and the pH adjusted with 10 M NaOH to pH 7.4. The BSA solution was filtered through Millipore type A (mixed cellulose esters) membrane filters (0.8μm pore size), aliquoted and stored at -20°C.

Monocomponent porcine insulin was a kind gift from Dr. G. Danielson, Novo Nordisk. 1 mg of insulin was initially dissolved in 1 ml of 30 mM HCl, then diluted to 3 ml with distilled H_2O. 1 ml of this stock solution was then diluted to 50 ml with 1% (w/v) BSA/KRH buffer (*section 2.2*), and the resulting 1 μM solution aliquoted and stored at -20°C. 100 μM sterile stocks were also made in a similar fashion for adipocyte rat culture.

Tritiated phosphatidylinositide photoprobes, phosphatidylinositide lipids and phosphoinositide affinity resins (Ins(1,3,4)P3 and Ins(1,3,4,5)P4 linked to Bio-Rad Affi-Gel 10) were generous gifts from Prof. G. Prestwich, University of Utah, USA (Prestwich, 1996) Phosphatidylinositides used in PI 3-kinase experiments were purchased from Sigma.

2-*N*-4-(1-azi-2,2,2-trifluoroethyl)benzoyl-1,3-[^{3}H]bis-(D-mannos-4-yloxy)-2-propylamine (ATB-[^{3}H]BMPA), approximately 10 Ci/mmol was synthesised by Prof. G. D. Holman, University of Bath, UK (Clark & Holman, 1990).

Radiochemicals, ECL Western blotting detection reagents and Amplify were purchased from Amersham International plc.

Collagenase Type 1 from *Clostridium histolyticum* was purchased from Worthington Biochemical Corporation (Freehold, NJ). Before purchase of the collagenase, individual lots were tested for their suitability to maintain adipocyte insulin responses (as measured by glucose uptake studies, *section 2.10*). Lots used varied in their collagenase activity from 183-296 U/mg dry weight.

4-(2-aminoethyl)benzenesulfonylfluoride (AEBSF) and α-toxin from *Staphylococcus aureus* were purchased from Calbiochem.

Guanosine 5'-[γ-thio]triphosphate (GTPγS) and Thesit® ($C_{12}E_9$) were purchased from Boehringer Mannheim UK Ltd.

Protein G (Sepharose 4 Fast Flow) and Pharmolytes were purchased from Pharmacia Biotech.

Okadaic acid (sodium salt) was purchased from Alexis Corporation Ltd.

2.2 Buffers

Buffers used routinely were as follows:

Kreb's Ringer's HEPES (KRH) buffer	140 mM NaCl, 4.7 mM KCl, 2.5 mM $CaCl_2$, 1.25 mM $MgSO_4$, 2.5 mM NaH_2PO_4, 10 mM HEPES pH 7.4
TES buffer	5 mM EDTA, 255 mM Sucrose, 10 mM Tris-HCl pH 7.2
Adipocyte lysis buffer	50 mM HEPES pH 7.0, 150 mM NaCl, 1 mM EGTA, 100 mM NaF, 10 mM $Na_4P_2O_7$, 10% (v/v) glycerol, 1.5 mM $MgCl_2$, 1 mM Na_3VO_4, 1% (v/v) Triton X-100
Phosphate buffered saline (PBS) buffer	12.5 mM $Na_2HPO_4.12H_2O$ pH 7.2, 154 mM NaCl
TBS-T buffer	10 mM Tris-HCl pH 7.4, 154 mM NaCl, 0.1% (v/v) Tween-20
SDS-PAGE sample buffer	Final concentrations after addition to samples: 62.5 mM Tris-HCl pH 6.8, 2% (w/v) SDS, 10% (v/v) glycerol, 0.01% (w/v) bromophenol blue. The reducing agent was 10% (v/v) 2-mercaptoethanol unless otherwise stated

Protease inhibitors were added to buffers when appropriate, to give final concentrations of leupeptin, aprotinin, pepstatin A and antipain at 1 μg/ml, and AEBSF at 100 μM.

2.3 Sources of antibodies

The source of antibodies used, and where appropriate the dilution's used in Western blotting (*section 2.29*), and the amounts for immunoprecipitation (*section 2.15*) are given in table 3.

Anti-IRS-1 rabbit serum was a kind gift from Dr G. Murphy, SmithKline Beecham Pharmaceuticals, Harlow. The peptide used for immunisation corresponded to residues 652-666 of rat liver pp185 (Sun *et al.*, 1991).

Anti-dynamin II rabbit serum used for immunoprecipitation was a kind gift from Dr M. Kasuga, Kobe University School of Medicine, Kobe, Japan. The antibody was raised against a synthetic peptide corresponding to the proline-rich region of rat dynamin II.

Anti-VAMP2 rabbit serum (Timmers *et al.*, 1996) and anti-GLUT4 rabbit serum were gifts from Dr S. W. Cushman (National Institutes of Health, Bethesda, USA). Anti-GLUT4 antibodies were raised against the C-terminal 13 amino acids of GLUT4 (a cysteine was attached to the N-terminus for conjugation to keyhole limpet haemocyanin). The peptide for immunisation was produced at Bath University (Holman *et al.*, 1990).

Anti-syntaxin4 rabbit serum was raised against recombinant syntaxin4 (construct a gift from Dr M. K. Bennett, University of California, Berkeley) by Dr S. Oldfield, Bath University.

Antibody	Polyclonal/Monoclonal Purified/Serum	Source	WB dilution/ IP quantity
Goat anti-Akt1 (PKB1)	Polyclonal Purified	Santa Cruz Biotechnology	WB 1:1000 IP: 2 µg/ml cell lysate
Mouse anti-phosphotyrosine agarose conjugate	Monoclonal (PT66) Purified	Sigma-Aldrich	IP: 30 µl agarose suspension/ml cell lysate
Mouse anti-ARF	Monoclonal (1D9) Purified	Alexis Corporation	WB 1:500
Mouse anti-dynamin II	Monoclonal (27) Purified	Transduction Laboratories	WB 1:250
Mouse anti-$G_{i\alpha 2}$	Monoclonal (L5) Purified	Serotec	WB 1:1000
Mouse anti-GLUT4	Monoclonal (1F8) Purified	Jackson Laboratories	WB 1:1000
Rabbit anti-insulin receptor β-subunit	Polyclonal Purified	Santa Cruz Biotechnology	WB 0.2 µg/ml
Mouse anti-phosphotyrosine	Monoclonal (4G10) Purified	Upstate Biotechnology	WB 1:1000
Rabbit anti-p85 (PI 3-kinase)	Polyclonal Purified	Transduction laboratories	WB 1:250 IP: 4 µg/ml cell lysate
Rabbit anti-dynamin II	Polyclonal Serum	M. Kasuga, Kobe, Japan	IP: 20 µl/ml cell lysate
Rabbit anti-$G_{i\alpha 1/2}$	Polyclonal Serum	G. Holman Laboratory, Bath University	WB 1:1000 IP: 20 µl/ml cell lysate
Rabbit anti-GLUT4	Polyclonal Purified (WB) Serum (IP)	G. Holman Laboratory, Bath University	WB 1:1000 IP: 50 µl serum/ 1 rat equivalent of post-HDM supernatant
Rabbit anti-IRS-1	Polyclonal Serum & Purified	SmithKline Beecham Pharmaceuticals & Upstate Biotechnology	IP: 20 µl serum/ml cell lysate WB 1µg/ml
Rabbit anti-syntaxin4	Polyclonal Serum	G. Holman Laboratory, Bath University	WB 1:5000
Rabbit anti-VAMP-2	Polyclonal Serum	S. Cushman, NIH, Bethesda, USA	WB 1:1000

Table 3. Sources of antibodies used for Western blotting (WB) and immunoprecipitation (IP).

2.4 Production of antibodies to $G_{i\alpha 1/2}$

A 10 amino acid peptide (KENLKDCGLF) corresponding to the C-terminal region of transducin, with homology to G-protein α_i subunits (Goldsmith *et al.*, 1987) was synthesised. using a Milligan 950 automatic peptide synthesiser. The synthesised peptide was cleaved from the resin and purified by high-performance liquid chromatography, with confirmation of the sequence by mass spectroscopy (S. Phillips, Bath University). The peptide was lyophilised and stored at -20°C.

20 mg of keyhole limpet haemocyanin (KLH; Sigma) and 6 mg of peptide (as above) were dissolved in 2 ml PBS, to which was added 1 ml of 21 mM glutaraldehyde in PBS (dropwise with stirring). The combined 3 ml was incubated for 24 h at room temperature. An equal volume of Freund's complete adjuvant was added to the KLH-peptide conjugate, an emulsion was formed, and 1 ml injected into multiple subcutaneous sites in New Zealand White rabbits. Booster injections were then performed every four weeks after the initial immunisation, using half the amount of peptide and KLH, initially in Freund's incomplete adjuvant, and then in PBS.

A 5 ml test bleed was taken in week 6, then every 4 weeks to monitor the titre of specific antibodies by ELISA. Bleeds were from ear veins of rabbits under anaesthetic. Rabbits were bled out at 12 weeks following from the first immunisation. Sera from rabbits were allowed to clot for 1 h at room temperature then overnight at 4°C. Sera were then removed from blood clots and any cells in the sera removed by centrifugation. The sera were stored at -20°C. Sera from rabbits were obtained prior to immunisation (pre-immune sera) for use as negative controls in experiments.

2.5 Affinity purification of GLUT4 antibodies

12 ml of Reacti-gel 6X (6%, cross-linked agarose, Pierce) was filtered through Whatman number 1 filter paper on a Buchner funnel and washed with ice-cold distilled water. The beads were then rotated with 66 mg of GLUT4 peptide (as used for immunisation) in 0.1 M sodium borate pH 8.5 for 48 h at 4°C. The mixture was then filtered and the beads added to 24 ml of 1 M ethanolamine in borate buffer for 3 h at room temperature with rotation. The beads were then packed into a column and washed successively with 1 M NaCl, distilled water and PBS. 15 ml of anti-GLUT4 rabbit serum was circulated through the column for 12 h at 4°C. The

column was extensively washed with PBS, then with 2M NaCl in 10 mM $Na_2HPO_4.12\ H_2O$, pH 7.2. The anti-GLUT4 antibodies were then eluted with 3.5 M NaSCN in 10 mM $Na_2HPO_4.12\ H_2O$, pH 6.6, and immediately dialysed against PBS. The antibody solution was concentrated using polyethyleneglycol 20,000. The antibody was stored at -20°C in the presence of 40% (v/v) glycerol and 0.02% (w/v) sodium azide. Purification of antibodies was monitored by ELISA.

2.6 Isolation of rat adipocytes

Adipose cells were obtained from the whole epididymal fat pads of male Wistar rats (180-200 g). The necks of the rats were broken and tissue was quickly removed and briefly washed in 1% (w/v) BSA/KRH buffer at 37°C. Tissue was finely chopped (using scissors) in digestion buffer (3.5% (w/v) BSA/KRH buffer supplemented with 5 mM glucose and 700 μg/ml collagenase), at a ratio of 4 fat pads/5 ml. Tissue was digested with vigorous shaking for 40-50 min at 37°C, until a fine tissue suspension was achieved. Tissue digestion was performed in 25 ml Sterilin clear-polystyrene tubes with the maximum amount of digestion buffer in any one tube being 5 ml. The resulting cell suspensions in each tube were filtered through 250 μm nylon mesh (Lockertex) into separate 23 ml polystyrene flat-bottomed tubes (Sarstedt). Adipocytes were allowed to float at 37°C. The infranatant buffer was removed using a 13 gauge x 10 cm needle attached to a syringe and then 20 ml 1% (w/v) BSA/KRH buffer was added to each tube. Cells were resuspended and allowed to float at 37°C. This washing procedure was generally repeated 4 times until the BSA/KRH buffer became clear and the layer of floating cells became white in appearance. Tubes of cells were pooled together and the cell suspension adjusted to 40% cytocrit.

2.7 Isolation of human adipocytes

Human adipocytes were prepared from human subcutaneous adipose tissue of female patients undergoing gynaecological surgery (Kozka *et al.*, 1995). Briefly, 10-30 g of tissue was excised at the beginning of surgery and placed in 1% (w/v) BSA/KRH buffer supplemented with 5 mM glucose. Tissue was transported to the laboratory in a thermos flask within 30 min. Adipose cell preparation was essentially as described for rat adipose cells (*section 2.6*), with a few modifications. Approximately 2 g of tissue (free of clotted blood and connective tissue) was digested in 3.5 ml digestion buffer. The digestion buffer was the same as for the rat buffer but with an increase in the BSA to 4% (w/v). Tissue digestion was achieved in approximately 30

min. The cell suspension was then filtered through nylon mesh with a pore size of 400 μm. The washing of the human cells was as described for the rat cells but using 4% (w/v) BSA/KRH buffer and was continued until the BSA/KRH buffer became clear and the cells were bright yellow in appearance. Finally, cell suspensions were adjusted to a cytocrit of 40%.

2.8 Maintenance of rat adipocytes in culture

Rat adipocytes were prepared as previously described (*section 2.6*) but using sterile solutions and techniques where possible. The isolated adipocytes were added to Dulbecco's Modification of Eagle's Medium (DMEM (with 25 mM glucose, without L-glutamine; ICN)) supplemented with 1% (w/v) BSA, 25 mM HEPES pH 7.6, 2 mM L-glutamine, 100 U/ml penicillin and 100 μg/ml streptomycin. Initially, 2 ml aliquots of cells were added to 40 ml culture medium in 100 ml sterile polyethylene pots (Sarstedt). Later experiments utilised 70 ml sterile polystyrene pots (Sarstedt), which increased the subsequent recovery of cells following the overnight culture. Cells were incubated at 37°C in a 5% CO_2 atmosphere for 20 h in the absence or presence of 500 nM insulin with or without 1 mM metformin. Cells were subsequently recovered by removing the culture medium and washing 4 times with 1% (w/v) BSA/KRH buffer (*section 2.2*) supplemented with either 500 nM insulin with or without 1 mM metformin as appropriate. Cell suspensions were adjusted to a cytocrit of 40%. The recovery of cells was approximately 75% after the 20 h culture period. A fraction of cells cultured without insulin or metformin were acutely insulin-stimulated with 20 nM insulin for 30 min at 37°C. Cells without any additions were termed basal (B). Cells treated with 20 nM insulin for 30 min were termed insulin-acute (Ia). Cells with 500 nM insulin for 20 h were termed insulin-chronic (Ic). Cells with 500 nM insulin and 1 mM metformin for 20 h were termed as insulin-chronic metformin (IcM).

2.9 Stimulation rat adipocytes with insulin and isolation of cell lysates

Adipose cells were generally stimulated with 20 nM insulin at 37°C for 30 min unless otherwise stated. Cells treated with okadaic acid were either incubated with okadaic acid for 20 min alone, or treated with okadaic acid for 20 min before insulin stimulation.

Cell lysates from cells at 40% cytocrit were concentrated by briefly centrifuging cell aliquots at 1,000*g* for 10 seconds and removing excess buffer. Cells were then lysed with a volume equal

to the original cell suspension volume, with ice cold lysis buffer containing protease inhibitors. Lysates were incubated on ice for 20 min then centrifuged at 20,000*g* for 10 min at 4°C. Triton X-100-soluble lysates were separated from the fat layer, and passed through 0.2 μm Minisart filters (Sartorius).

Soleus muscle (samples from Dr. S. Lund, Aarhus, Denmark) lysates were generated by homogenising samples in 1.25 ml of 10 mM Tris-HCl pH 7.2, 5 mM EDTA, 255 mM sucrose, 10 mM NaF, 0.2 mM Na_3VO_4, 1 mM sodium molybdate, plus protease inhibitors. Triton X-100 was added to the homogenates to give a final concentration of 1% (v/v) and then the samples were rotated for 30 min at 4°C. Homogenates were centrifuged at 20,000*g* for 10 min and detergent-soluble fractions were removed from the insoluble material.

2.10 3-*O*-Methyl-D-glucose transport assays

Glucose transport activity in both rat and human adipocytes was determined by measuring the uptake of 3-*O*-methyl-D-glucose (3-OMG). Uptake was initiated by the addition of 50 μl of a 40 % adipocyte suspension to 10 μl of 200 μM 3-OMG containing 0.15 μCi of 3-*O*-methyl-D-[U-^{14}C]glucose, all in KRH buffer. Uptake studies were performed in 4 ml (50 mm x 13 mm) polypropylene tubes (Nunc/Gibco). Uptake was terminated by the rapid addition of 3 ml of 300 μM phloretin in KRH. The phloretin was initially dissolved in ethanol, such that the final concentration of ethanol on dilution in KRH was 0.5% (v/v). Uptake was measured for 3 seconds for insulin-stimulated cells and 120 seconds in basal cells. For cells treated with inhibitory or stimulatory compounds of GLUT4 translocation, timings were altered appropriately so as to allow uptake in the 30-60% cell fractional filling range. These timings are given in the results section where appropriate. Uptake for each condition was measured in triplicate. For uptake times less than 10 seconds a metronome was used, set at 2 beats/second. Background values (cpm_{bg}) corresponding to extracellular trapped radioactivity were determined by adding the phloretin solution to the 3-OMG before the addition of the cells. Infinity values (cpm_{∞}) (indicating equilibrium distribution of the radioactivity) were determined by incubating insulin-treated cells with the 3-OMG for 30 min at 37°C. Cells were recovered by oil floatation following addition of approximately 1 ml of Dow Corning 200/100 cs silicon oil to the tubes and centrifugation at 2,500 rpm for 45 seconds (MSA bench centrifuge, swing-out rotor). Cells were removed from the top of the oil by using small pieces of pipe-cleaner and were placed in scintillation vials. Scintillation fluid was added to the vials

and radioactivity uptake (cpm) counted by liquid scintillation counting (Packard 1500 scintillation counter). The rate constant of 3-OMG uptake v/s (s^{-1}) was calculated from the fractional filling (f). The rate constant v/s (s^{-1}) = -ln(1-f)/t, where t = time of uptake in seconds, and f = (cpm-cpm_{bg}) / (cpm_{∞}-cpm_{bg}), which assumes that filling follows a single exponential time function (Taylor & Holman, 1981).

2.11 3-*O*-Methyl-D-glucose transport in adipocytes following a 24 h maintenance in tissue culture

3-OMG uptake was measured in adipocytes following a 20 h maintenance in tissue culture (*section 2.8*), either directly (*section 2.10*) or after the addition of 1 μM wortmannin. The rate constant of 3-OMG uptake was measured at time points after wortmannin addition, t = 0, 3, 6, 9, 20, 30 and 60 min. To enable the amount of fractional filling to be calculated at each time point, the uptake times (used for estimating the rate constant for 3-OMG) varied, and are given in table 4.

Culture / Condition	Time in seconds of measurement of 3-OMG uptake at time (t) following wortmannin treatment			
	t = 0 & 3	t = 6 & 9	t = 20 & 30	t = 60
Basal	30	40	50	60
Insulin-acute	5	7	10	30
Insulin-chronic	10	15	20	40
Insulin-chronic /Metformin	5	7	10	30

Table 4. Time used for measuring 3-OMG uptake in cultured adipocytes following wortmannin treatment.

The measurements of the 3-OMG uptake rate constants following wortmannin treatment allowed an estimate of the rates of endocytosis and exocytosis rate constants for GLUT4 to be calculated as follows:

It was assumed that GLUT4 exists in only two pools, one in the low-density microsomes and one in the plasma membrane. The process of redistribution between these two pools can be described by a single exponential function (eqn. 1)

$$\frac{dT_P}{dt} = k_{ex}.(1-T_P) - k_{en}.T_P \qquad \text{(Eqn. 1)}$$

where T_P is the plasma membrane GLUT4 pool expressed as a fraction of the total cellular GLUT4 pool, and k_{ex} and k_{en} represent the exocytosis and endocytosis rate constants for movement between the two pools of GLUT4. Integration of equation 1, where $T_P = T_{P0}$ at t = 0 gives

$$T_P = \frac{k_{ex} \cdot (1-\exp(-t(k_{ex} + k_{en})))}{k_{ex} + k_{en}} + T_{P0} \cdot \exp(-t(k_{ex} + k_{en})) \qquad \text{(Eqn. 2)}$$

For the analysis of transport data, the rates of transport for all conditions were normalised to the unperturbed acute insulin-treatment transport rate and this ratio was multiplied by the T_{P0} value (0.5) for cell-surface GLUT4 in the acute-insulin treatment (Yang *et al.*, 1992). The rate constants k_{ex} and k_{en} were calculated by least-squares fitting (non-weighted fit) to equation 2, using the PRISM software (GraphPad Software, Inc., San Diego).

2.12 Subfractionation of rat adipocytes

Adipocytes were washed twice in TES buffer (plus protease inhibitors) at 18°C, and resuspended to give a suspension of 1.0 ml cells at approximately 80% cytocrit. Cells were then homogenised with 10 strokes in a 55 ml Potter-Elvehjem homogeniser (Thomas Scientific). The specific clearance of the homogeniser was 150 μm. Unless otherwise stated, the homogenate and all subsequent fractions were centrifuged in a Beckman TL-100 benchtop ultracentrifuge at 4°C, using a TLA-100.3 fixed angle rotor. Centrifugation of homogenates at 17,500g_{max} for 20 min gave a crude membrane pellet, a microsomal/cytosol fraction and a layer of fat. The microsomal and cytosol fraction was centrifuged at 49,000g_{max} for 9 min to pellet the high-density microsomes (HDM). The HDM pellets were resuspended in TES and stored at -20°C until required. The post-HDM supernatant was centrifuged at 541,000g_{max} for 17 min to pellet the low-density microsomes (LDM) containing GLUT4 vesicles. The LDM pellet was also resuspended in TES and stored at -20°C until required. Following the removal of the solid fat layer from centrifuge tubes, membrane pellets were resuspended in TES and homogenised with 5 strokes in a 10 ml homogeniser tube (Braun) and centrifuged at 17,500g_{max} for 20 min. Membrane pellets were resuspended in 300 μl of TES and loaded on top of 600 μl of a sucrose cushion (1.12 M sucrose, 10 mM Tris-HCl pH 7.2, 5 mM EDTA). These were then centrifuged at 105,000g_{max} for 20 min in a Beckman TLS-55 swing-out rotor. The plasma membranes were collected at the cushion interface and resuspended in 3 ml of

TES. The collected plasma membranes were pelleted by centrifugation at 74,000g_{max}, resuspended in TES and stored at -20°C.

2.13 Photolabelling of GLUT4 in rat adipocytes

1 ml aliquots of adipose cells at a cytocrit of 40% in KRH buffer were added to 0.5 mCi of ATB-[^{3}H]BMPA in 35 mm-diameter polystyrene dishes (Nunc/Gibco) and irradiated for 1 min using 300 nm lamps in a Rayonet RPR-100 photoreactor. Following irradiation, cells were washed 3 times with 1% (w/v) BSA/KRH at 18°C and lysed with 1% (w/v) Thesit in PBS (with protease inhibitors). Cells were solubilised for 20 min at room temperature and then centrifuged at 20,000*g* for 20 min at 4°C. GLUT4 was immunoprecipitated from the detergent soluble lysate (*section 2.15*) and analysed by SDS-PAGE and liquid scintillation counting of proteins extracted from gel slices (*section 2.26*).

2.14 *In Situ* periodate-oxidised GTP labelling

Freshly isolated adipocytes (200 µl of 40% cytocrit suspension) were permeabilised with α-toxin (8 µg/ml) in the presence of 25 µCi [α-^{32}P] GTP (3000 Ci/mmol). Permeabilisation was performed in 0.1% (w/v) BSA/KRH with 4 mM Mg-ATP and 3 mM sodium pyruvate, at 37°C for 15 min. Appropriate aliquots of cells were then stimulated with 20 nM insulin for 5 min followed by centrifugation through silicone oil at 1,000*g* for 10 seconds. Excess buffer and silicon oil was removed and cells were then incubated with 1 mM $NaIO_4$ for 1 min, then 1 mM $NaCNBH_3$ for 1 min and finally 20 mM $NaBH_4$ for 1 min (all freshly made up in KRH buffer). This was followed by a 10 min incubation at 4°C. Cells were then lysed in ice cold lysis buffer with protease inhibitors. The lysates were centrifuged at 13,400*g* in a microfuge for 5 min and detergent-soluble lysates were added to SDS-PAGE sample buffer. Samples were then analysed by either SDS-PAGE or two-dimensional electrophoresis, followed by autoradiography.

2.15 Immunoprecipitation of proteins

Dried Protein A immobilised on Sepharose CL-4B (Sigma) was rehydrated with PBS for 15 min on ice. The rehydrated Protein A-Sepharose was resuspended to give a 50% (v/v) suspension. Protein G-Sepharose was supplied hydrated, and was washed 3 times with PBS to remove preservatives. The Protein G-Sepharose was resuspended to give a 50% (v/v)

suspension. Rabbit and the majority of mouse antibodies were conjugated to Protein A, mouse IgG_1 and goat antibodies were coupled to Protein G.

Antibodies were coupled to 20-30 µl (50% suspension) of either Protein A-Sepahrose or Protein G-Sepharose in 1 ml of PBS for 2 h at 4°C with rotation. The amounts of antibody used are given in table 3. The antibody-Sepharose conjugates were pelleted by centrifugation at 13,400*g* for 1 min and were washed with PBS. This washing was repeated a further 2 times. Cell lysates were then added to the antibody-Sepharose conjugate pellets. Generally 1 ml of adipocyte cell lysate (*section 2.9*) was added to each pellet. The lysates were rotated with the Sepharose conjugates for 2 h at 4°C. The Sepharose conjugates were pelleted and either washed 3 times with lysis buffer for SDS-PAGE, or with appropriate buffers for the kinase assays (*section 2.17, section 2.18).* Immunoprecipitation of phosphotyrosine containing proteins was as described above, but no antibody conjugation was required since the anti-phosphotyrosine antibody was covalently coupled to the agarose suspension supplied.

2.16 Immunoprecipitation of GLUT4 vesicles

GLUT4 vesicles were isolated using *Staphylococcus aureus* Cowan I cells (Staph cells) expressing Protein A on the surface membranes (Sigma). Staph cells were initially prepared by heating to 95°C for 30 min in an extraction buffer (50 mM Tris-HCl pH 7.2, 150 mM NaCl, 104 mM SDS, 10% (v/v) 2-mercaptoethanol), at a ratio of 50 mg Staph cells/ml buffer. Staph cells were then pelleted by centrifugation at 13,400*g* for 1 min, the supernatants removed, and the resuspended again in extraction buffer. Cells were again heated to 95°C for 30 min, pelleted and washed 3 times with TES buffer. Cells were finally resuspended in TES at 50 mg/ml and aliquots stored at -20°C until required.

Aliquots of the Staph cells (40 µl) which were used for immunoprecipitation experiments were rotated (2 h at 4°C) with either rabbit serum or anti-GLUT4 rabbit serum (50 µl serum) in 1 ml TES buffer. Staph cells were then washed 3 times with 1 ml of TES buffer and then mixed with adipocyte post-HDM supernatants as appropriate. The equivalent of 1 rat post-HDM supernatant was added to each 40 µl of Staph cell suspension. Adipocyte post-HDM supernatants were initially pre-cleared using Staph cells bound with rabbit IgG for 30 min at 4°C (with rotation). Supernatants were then transferred to Staph cells bound with rabbit IgG (pre-immune controls) or rabbit anti-GLUT4 IgG (GLUT4 vesicle isolation) for 2 h at 4°C

with rotation. Staph cells were washed 3 times with TES buffer and vesicle proteins solubilised with 1% (v/v) Thesit in TES (20 min at room temperature). Following removal of solubilised vesicle proteins from the Staph cell pellets, IgG and GLUT4 molecules still bound to the Staph cells, were recovered from the Staph cells by heating in SDS-PAGE sample buffer (20 mM dithiothreitol (DTT) as the reducing agent) to 95°C for 2-3 min.

2.17 Measurement of PI 3-kinase activity

PI 3-kinase activity was measured in immunoprecipitates isolated from adipocyte cell lysates. Following immunoprecipitation, Protein A-Sepharose pellets were washed twice with 12.5 mM $Na_2HPO_4.12H_2O$, pH 7.2, 154 mM NaCl, 1% (w/v) Thesit, 1 mM DTT, then twice with 0.1 M Tris-HCl pH 7.4, 0.5 M LiCl, 1 mM DTT, and finally twice with 10 mM Tris-HCl pH 7.4, 100 mM NaCl, 1 mM DTT (1 ml for each wash). Immunoprecipitates were resuspended in a final volume of 50µl containing 20 mM HEPES pH 7.1, 0.4 mM EGTA, 0.4 mM $Na_2HPO_4.12H_2O$, 10 mM $MgCl_2.6H_2O$, 40 µM ATP with 10 µCi [γ-^{32}P]ATP and 10 µg of either phosphatidylinositol (PI) or phosphatidylinositol 4,5-bisphosphate (PI 4,5-P_2). After 20 min at room temperature, the assay was stopped by the addition of 30 µl 4 M HCl. 130 µl of chloroform/methanol 1:1 (v/v) was then added to each tube. The tubes were vortexed briefly and centrifuged at 13,400*g* for 10 min to separate the chloroform and aqueous phases.

TLC polyester plates coated with silica gel (layer thickness 250 µm, particle size 5 to 17 µm, pore size 60 Å) were pre-treated for 10 seconds with *trans*-1,2-diaminocyclohexane-N,N,N',N'-tetraacetic acid (CDTA) in 0.6% (v/v) 10 M NaOH, 66 % (v/v) ethanol. Plates were left to air-dry before baking in an oven at 80°C for 1 h. 10 µl samples from the lower chloroform phase were spotted on to the TLC plates and lipids separated by the following solvent system: 75 ml methanol, 60 ml chloroform, 45 ml pyridine, 12 g dissolved boric acid, 7.5 ml distilled water, 3 ml 88 % (v/v) formic acid, 0.375 g 2,6-di-*tert*-butyl-4-methylphenol (BHT) and 75 µl ethoxyquin. After separation, the plates were dried and then exposed to autoradiography film. Radiolabelled phosphatidylinositides were then excised from the TLC plates and counted by liquid scintillation counting.

2.18 Measurement of PKB activity

PKB activity was immunoprecipitated from cell lysates (*section 2.9*), and Sepharose pellets were washed 3 times with lysis buffer (with protease inhibitors) and then 3 times with kinase assay

buffer (50 mM Tris-HCl pH 7.5, 10 mM $MgCl_2.6H_2O$). Immunoprecipitates were incubated in 50 µl kinase assay buffer containing 1 mM DTT, 100 ng protein kinase A (PKA) inhibitor peptide, 25 µg protamine sulphate, 5 µM ATP and 2 µCi [γ-^{32}P]ATP. The reaction was allowed to proceed for 20 min at 30°C. Supernatants were then removed and 40 µl of 2% (w/v) SDS was added to the pellets. After a further 10 min, this supernatant was removed. The two supernatants were pooled and 20 µl of the combined mixture in duplicate samples were spotted onto a 2 cm x 2 cm area of phosphocellulose paper. The phosphocellulose paper was washed five times, each for 5 min and with a large excess of 75 mM phosphoric acid, and then once with distilled water and once with acetone. The dried paper was cut into squares, scintillation fluid was added and then the radioactivity was estimated by liquid scintillation counting.

2.19 Benzophenone-phosphatidylinositide photolabelling

Initially, subcellular protein fractions were photolabelled using the benzophenone-phosphatidylinositide photolabels (*section 6.2*). Subsequent experiments on isolated rat adipocyte cytosol, used the benzophenone-phosphatidylinositide photolabels either before, or after chromatography purification steps (*section 2.20, section 2.21*). Initial photolabelling experiments used 0.2 µCi (42.5 Ci/mmol) of the appropriate photolabel with 50 µg of protein. After chromatography purification steps, the photolabelling experiments used 0.1 µCi of the appropriate benzophenone-based phosphatidylinositide photolabel with 50 µg of protein. Photolabelling reactions in which the competition with non-radioactive phosphatidylinositides was studied, contained a 1000-fold molar excess of non-radioactive phosphatidylinositide to radioactive phosphatidylinositide-photolabel.

Protein samples for photolabelling (50 µg) were incubated with the appropriate phosphatidylinositide-photolabel for 10 min on ice, in a final volume of 50 µl in either TES buffer or TE buffer (10 mM Tris-HCl pH 7.2, 1 mM EDTA). Following the 10 min incubation on ice, protein samples to be photolabelled were transferred to flat-bottomed, clear, polystyrene 96 well plates (Falcon), and irradiated with 350 nm light using a Rayonet RPR-100 photoreactor (maximum intensity 9,200 µWatts/cm^2), for 30 min at 4°C. SDS sample buffer was then added to the samples and the proteins were separated by SDS-PAGE on 10% Laemmli gels. Gels were then stained with Coomassie brilliant blue, destained, and were then incubated with Amplify for 30 min. The gels were then dried down and the radioactivity was imaged by exposure to autoradiography film for 4-60 days (*section 2.26*).

2.20 Binding to heparin-agarose

Adipose cells were isolated from the epididymal fat pads from 20 rats, and the cytosol fractions were obtained (containing approximately 30 mg protein). These samples were diluted 5 fold with 10 mM Tris-HCl pH 7.2. The diluted cytosol fractions were then incubated (2 h at 4°C with rotation) with 5 ml of heparin-agarose type I (Sigma) (per 20 rats), which had been previously washed with 10 mM Tris-HCl pH 7.2, 1 mM EDTA. NaCl was added to the heparin-agarose plus cytosol fraction to give a final NaCl concentration of 50 mM. Following the 2 h incubation of the cytosol fractions with the heparin-agarose, the agarose resins were washed with 20 volumes of 10 mM Tris-HCl pH 7.2, 1 mM EDTA, at 4°C. The heparin-agarose was then incubated for 2 h at 4°C with 10 mM Tris-HCl pH 7.2, 1 mM EDTA containing 175 mM NaCl (approximately 50 ml). The heparin-agarose eluates were then removed and the agarose was washed as previously described but using 10 mM Tris-HCl pH 7.2, 1 mM EDTA, with 300 mM NaCl. Eluate fractions were then repeatedly concentrated (using Macrosep and Microsep centrifugal concentrators (Pall Filtron), MWCO = 10K) and then diluted with 10 mM Tris-HCl pH 7.2, 1 mM EDTA, to remove the NaCl from the eluates. Concentrated heparin-agarose eluates were then either photolabelled using benzophenone-phosphatidylinositide photolabels (*section 2.19*), or were further purified by phosphoinositide affinity chromatography (*section 2.21*).

2.21 Phosphoinositide affinity columns

Phosphoinositide affinity resins (Ins(1,3,4)P3 and Ins(1,3,4,5)P4 linked to Bio-Rad Affi-Gel 10) were washed with 10 column volumes of 10 mM Tris-HCl pH 7.2, 1 mM EDTA and packed into C 10/10 columns with AC 10 adapters (Pharmacia Biotech). The heparin-agarose eluates (300 mM NaCl elution fractions) were continuously circulated through the phosphoinositide affinity resin columns overnight at 4°C using a peristaltic pump. The affinity columns were then washed with 10 mM Tris-HCl pH 7.2, 1 mM EDTA and those proteins which bound to the phosphoinositide affinity resins were eluted using a NaCl gradient, (0-2 M) with a flow rate of 0.2 ml / min (all at 4°C). Thirty 1 ml fractions were collected. Protein concentrations from the fractions eluted from the affinity columns were estimated by measuring the absorbance at 280 nm. Fractions were concentrated using Microsep centrifugal concentrators (as previously described, *section 2.20*).

2.22 Protein assays using BCA

Protein concentrations were determined using the Pierce bicinchoninic acid (BCA) protein assay. Protein samples for protein determination were diluted with 0.2 M NaOH to give a final concentration of 0.1 M NaOH. 10 µl of protein samples were then mixed with 200 µl aliquots of BCA reagent, in the wells of microplates (Labsystems). Protein concentrations were calculated from a standard calibration curve using 0-10 µg BSA. Colour development due to Cu^{+1} and BCA complex formation was allowed to proceed for 30 min at 37°C. This was followed by measurement of the absorbance at 595 nm in a microplate spectrophotometer.

2.23 Chloroform and methanol protein precipitation

Proteins were precipitated by adding 1 ml methanol and 250 µl chloroform to 250 µl of protein sample in polypropylene tubes. Tubes were centrifuged at 9,000*g* for 10 s and then 750 µl H_2O was added to each tube. Tubes were further centrifuged at 9,000*g* for 1 min. The upper aqueous phases were removed (being careful not to remove precipitated proteins from the chloroform/aqueous phase interface) and a further 750 µl methanol was added to the chloroform/protein samples. This was followed by centrifugation at 9,000*g* for 2 min. The supernatants were discarded and protein pellets were dried under vacuum with centrifugation.

2.24 Enzyme linked immunosorbant assay (ELISA)

ELISA's were performed in 96-well ELISA plates (Labsystems). For assaying anti-$G_{i\alpha 1/2}$ and -GLUT4 antibodies, wells were coated with the corresponding immunising peptide (20 ng/well) in 100 µl of PBS overnight at 4°C. After the binding of the peptides to the wells, the ELISA plates were washed 3 times with 100 µl of 0.05 % (v/v) Tween-20 in PBS (PBS-T) at room temperature and then incubated for 30 min at 37°C with 100 µl of 5 % (w/v) BSA in PBS. Wells were again washed 3 times with PBS-T, then incubated for 2 h at 37°C with 100 µl of the appropriate antibody solution, diluted appropriately in PBS-T. Following the incubation with the primary antibody, ELISA plates were washed 3 times with PBS-T, then incubated with 100 µl of a 1:2000 dilution of goat anti-rabbit peroxidase conjugate (Sigma) in PBS-T for 2 h at 37°C. Wells were then washed 3 times with PBS-T and 100 µl of substrate (0.1 M sodium acetate, pH 6.0, 100 µg/ml tetramethylbenzidine, 0.005 % (v/v) H_2O_2) was added to each of the ELISA plate wells. ELISA plates were then incubated at 37°C until a blue colour

developed. The reaction was stopped by the addition of 25 µl of 1 M H_2SO_4 to each well. The absorbance of the resulting yellow colour was read at 450 nm in a microtitre plate reader (Labsystems).

2.25 SDS-polyacrylamide gel electrophoresis (SDS-PAGE)

Protein samples to be resolved by SDS-PAGE were added to sample buffer (*section 2.2*) and heated to 95°C for 2-3 min, before loading onto Laemmli gels.

Discontinuous polyacrylamide gels (lower resolving gel and upper stacking gel) were produced using either the Bio-Rad minigel apparatus (Mini-PROTEAN II electrophoresis cell) or the Bio-Rad PROTEAN II xi slab cell system (all gels were 1.5 mm in thickness). The following solutions were used to make the gels: resolving gel buffer (1.5 M Tris-HCl pH 8.8, 0.4 % (w/v) SDS), stacking gel buffer (0.5 M Tris-HCl pH 6.8, 0.4 % (w/v) SDS), 10% (w/v) ammonium persulfate, N,N,N',N'-tetramethylethylenediamine (TEMED) and acrylamide/bis (30.8% T, 2.6% C; Protogel, National Diagnostics). For both systems resolving gels were made to 0.375 M Tris-HCl and 0.1 % (w/v) SDS with acrylamide concentrations in the range of 7 to 15 %. Stacking gels were made to 0.125 M Tris-HCl and 0.1% (w/v) SDS with acrylamide concentrations at 6%, or 4% when using 7% resolving gels. Acrylamide polymerisation was initiated by the addition of TEMED and ammonium persulfate to give final concentrations of both TEMED and ammonium persulfate at 0.05%. The electrode buffer was 25 mM Tris-HCl pH 8.3, 0.1 % (w/v) SDS, 192 mM glycine.

Minigels were run at a constant 200 mA. PROTEAN II xi gels were generally run at low current overnight (10-13 mA constant current), or with a maximum constant current of 25 mA through stacking gels and 35 mA through resolving gels. Gels were run until the bromophenol blue dye front eluted from the bottom of the gels. Broad range molecular weight markers (New England Biolabs) were run on each gel for molecular weight determination.

2.26 Gel staining, imaging and analysis

Proteins separated by SDS-PAGE were either transferred onto nitrocellulose (*section 2.28*) or fixed within the polyacrylamide gel matrix. Gels were either stained for 30 min with 0.2 % (w/v) Coomassie Blue R-250 in fixative (30% (v/v) methanol, 10% (v/v) glacial acetic acid)

and destained for a few hours in fixative only. Alternatively, more sensitive staining was obtained using silver staining-reagent (Bio-Rad, Silver Stain Plus kit).

Protein-fixed gels containing tritium (from [^{3}H]BZDC-phosphatidylinositide photolabelled proteins) were incubated with Amplify for 30 min at room temperature with gentle agitation. These gels were briefly rinsed in water and dried down onto 3M filter paper using a Labconco gel dryer attached to a vacuum pump. Drying was at 60-80°C for 2 h. The photolabelled/tritiated proteins were visualised by exposure to autoradiography film (BioMax MR film, Kodak) placed directly on the gels for 4-60 days at -80°C. ^{32}P-labelled proteins were also detected by liquid scintillation counting of gel slices. In these instances, lanes from the gels were cut into 6.5 mm slices and dried individually in open scintillation vials at 80°C. Dried gel slices were then solubilised with 0.5 ml 2% (v/v) NH_4OH in 30% (w/w) H_2O_2 in sealed vials at 80°C. Following solubilisation of the gel slices, scintillation fluid was added to each vial and the radioactivity detected by liquid scintillation counting. Gels containing ^{32}P-labelled proteins were also dried down (as above) and labelled proteins visualised by exposure to autoradiography film at -80°C.

2.27 Two-dimensional gel electrophoresis

Two-dimensional gel electrophoresis was performed using Pharmacia Biotech Immobiline DryStrips and ExcelGel SDS gradient gels with the Pharmacia Multiphor II Electrophoresis Unit. Immobiline strip preparation and the conditions for running both the first and second dimension gels was as described in the manufacturer instructions.

Adipocyte cell lysates (generated following periodate-oxidised GTP-labelling, *section 2.14*) were chloroform/methanol precipitated and re-dissolved in 40 µl of lysis buffer. To each sample, 60 µl of 2D-gel electrophoresis sample buffer was added (9 M Urea, 0.02 % (v/v) Triton X-100, 0.02 % (v/v) 2-mercaptoethanol, 0.02% (v/v) Pharmalyte 3-10, 100 µM AEBSF). Samples were then applied to 180 mm Immobiline strips, with linear pH (3-10) gradients. Isoelectric focusing was then achieved in two phases: 3 hr at 500 Volts then 17.5 h at 3500 Volts. Following the isoelectric focussing, Immobiline strips were then run on ExcelGel 12-14 % gradient polyacrylamide gels (245 x 180 mm). Gels were run stepwise at 20 mA for 45 min, then 40 mA for 5 min, and finally 40 mA for 160 min. Gels were then stained by Coomassie Blue, destained and then ^{32}P-labelled proteins visualised using a Molecular Dynamics

phosphorimager. Molecular weight and pI values of gel proteins were determined by comparison with 2D SDS-PAGE molecular weight standards (Bio-Rad).

2.28 Electrophoretic transfer of proteins to nitrocellulose

Following SDS-PAGE, polyacrylamide gels were soaked in transfer buffer (0.0375 % (w/v) SDS, 48 mM Tris-HCl pH 8.8, 39 mM glycine, 20 % (v/v) methanol) for 5 min at room temperature. Gels were then placed onto nitrocellulose (BioTrace, 0.45μm pore size, Gelman Sciences) wetted with transfer buffer, and sandwiched between electrode- paper soaked in transfer buffer. Transfers were carried out using the Pharmacia Multiphor II NovaBlot unit, with a field strength of 0.8 mA/cm^2 membrane for 110 min. After transfer, nitrocellulose membranes were rinsed in distilled water and then stained with 0.1% (w/v) Ponceau S in 3% (w/v) trichloroacetic acid. Molecular weight markers were identified and marked on the nitrocellulose with pencil.

2.29 Western blotting

Nitrocellulose membranes were briefly rinsed in TBS-T (*section 2.2*) to remove any excess Ponceau S stain. These membranes were then blocked with 5% (w/v) dried skimmed milk in TBS-T for 30 min at room temperature. For phosphotyrosine blotting, the milk was exchanged for 5% (w/v) BSA. Nitrocellulose membranes were briefly rinsed in TBS-T and then incubated with appropriate primary antibodies in 1% (w/v) BSA in TBS-T for 1 h at room temperature. The dilutions used for the primary antibodies are given in table 2.1. Following incubation with the primary antibodies, nitrocellulose membranes were washed with TBS-T for 30 min with frequent changes of buffer. After washing, the nitrocellulose was incubated with the secondary antibody (1:4000 anti-rabbit or anti-goat (Sigma), or 1:1000 anti-mouse (Sigma) IgG conjugated to horseradish peroxidase) in 5% (w/v) dried skimmed milk in TBS-T for 30 min at room temperature. Alternatively, membranes were incubated with ^{125}I-Protein A (0.1 μCi/ml in TBS-T) for 90 min at room temperature. Nitrocellulose membranes were then washed with TBS-T for 30 min as previously described. Membranes were incubated for 1 min with ECL detection reagents (0.125 ml/cm^2 membrane) and exposed to autoradiography film for 5 s - 10 min. ^{125}I-Protein A detection was carried out using air-dried membranes wrapped in cellophane which were exposed to autoradiography film at -80°C, for 2-3 days.

2.30 N-terminal protein sequencing

For proteins to be N-terminally sequenced from membranes, modifications were made to the SDS-PAGE and electrophoretic transfer protocols in order to minimise N-terminal blocking of proteins.

Protein samples were added to sample buffer and heated to 65°C for 30 min (not 95°C for 2-3 min). Polyacrylamide gels were made at least 12 h before use, using acrylamide deionised with Amberlite MB-1A (a spatula-full of Amberlite into the acrylamide stock). Additionally, 2 mM sodium thioglycolate was included in the cathode buffer, and SDS-PAGE gels were pre-run for 10 min before the loading of protein samples.

Proteins were transferred onto polyvinylidene difluoride membranes (PVDF, ProBlott, Applied Biosystems) and not nitrocellulose. The PVDF membrane was prepared by soaking in methanol for 10 seconds followed by equilibration in transfer buffer for 5 min. The transfer buffer was modified and was 25 mM Tris-HCl pH 8.3, 190 mM glycine, 10 % (v/v) methanol. Following transfer, the PVDF was washed 3 times with distilled H_2O containing 130 μM DTT (10 min per wash), then 3 times with just distilled H_2O. Protein bands were visualised by Ponceau S staining and membranes were dried overnight in a vacuum dessicator.

Protein bands were excised from membranes and sequenced using an ABI 477A Pulsed liquid protein microsequencer with 120A on-line analyser (Applied Biosystems). Sequencing was done by J. Gilroy and R. Croy at the Department of Biological Sciences, University of Durham.

2.31 Protein sequencing by tryptic digestion

Proteins (as indicated in *section 6.7*) were sequenced by a process of tryptic digestion followed by MALDI-TOF (matrix assisted laser description ionisation-time of flight) mass spectroscopy. Masses of spectroscopy fragments were compared with the theoretical tryptic digestion masses of proteins held in databases. Matches between mass fragments from the unknown sample and the databases were confirmed by Edman degradation. Tryptic digests and their subsequent analysis were all done by M. Skehel, Bioinformatics, SmithKline Beecham Pharmaceuticals, Harlow using the following method:

Protein bands on PVDF were excised from membranes using a razor blade, and the membranes were washed with distilled water for 1 h at room temperature. The water was removed from the PVDF membranes and the membranes were washed with 4% (w/v) CHAPS for 1 h at room temperature. The PVDF membranes were further washed with 20 mM Tris-HCl pH 8.0 for 30 min at room temperature. The Tris-HCl was removed from the PVDF membranes, and the membranes were then covered with a solution of 20 mM Tris-HCl pH 8.0, containing 10 mM DTT. The PVDF membranes were then incubated at 55°C for 1 h. After cooling to room temperature, the DTT solution was removed and replaced with a solution of 55 mM iodoacetamide in 20 mM Tris-HCl pH 8.0. The PVDF membranes were incubated in the iodoacetamide solution for 45 min in the dark at room temperature. The PVDF membranes were then washed twice with 20 mM Tris-HCl pH 8.0, then incubated overnight at 37°C with a solution of 20 mM Tris-HCl pH 8.0, containing 5 mM $CaCl_2$ and 12.5 ng/µl sequencing grade trypsin (Boehringer). The digestion solution was removed from PVDF membranes and transferred to Eppendorf tubes. Peptides were then extracted from the PVDF membranes by covering membranes with 5.0% (v/v) formic acid for 1 h at room temperature with occasional vortexing. Peptides were further recovered from PVDF membranes by covering membranes with 60% acetonitrile in 5.0% (v/v) formic acid for 1 h at room temperature with occasional vortexing. The latter extraction was repeated, and then all extracts were combined and concentrated down in a Speed-vac to 10-20 µl.

Tryptic digests were analysed by mass spectroscopy on a Micromass TOF Spec E research grade spectrometer. Briefly, 1µl of the peptide solution obtained from a tryptic digest was mixed with 0.5 µl of 1% α-cyano-4-hydroxycinnamic acid matrix solution in 70% acetonitrile containing 0.1% trifluoroacetic acid and 200 fmole/µl insulin β-chain as internal standard. The mixture was allowed to air dry and then spectra were collected.

The remaining peptide solution obtained from a tryptic digest was separated out on a Beckman Gold HPLC system using a reverse phase column (Brownlee Aquapore RP300 7µm 100 x 1 mm) on a gradient of 5-65 % methylcyanide containing 0.08% trifluoroacetic acid, at a flow rate of 0.2 ml/min. A dual wavelength Beckman 167 detector monitoring at 215 nm and 280 nm was used to detect cleavage products, which were collected for further analysis. The resulting peptide peaks were reduced in volume by drying partially in a Speed-Vac and were analysed by MALDI mass spectroscopy prior to Edman degradation and sequencing. Edman

degradation and sequencing used an Applied Biosystems 477A pulsed liquid automated protein sequencer.

2.32 Data analysis

Data were plotted using GraphPad PRISM v 2.1 (GraphPad Software, Inc., San Diego). Statistical analysis was carried out using the PRISM program with unpaired t tests.

CHAPTER 3

INSULIN-RESISTANCE IN RAT ADIPOCYTES

PART A – Insulin signalling in insulin-resistant rat adipocytes

Large decreases in insulin-responsive glucose transport occurs in rat adipocytes maintained in culture for 20 h in the continuous presence of insulin (Kozka & Holman, 1993). Although the total cellular content of GLUT4 is unaltered, or changes very little in the chronic insulin condition, the cell surface levels of GLUT4 are reduced by up to 60% and the adipocytes are poorly responsive (measuring glucose uptake) to an additional acute-insulin treatment. This defect may be due to either impaired/altered signalling, impaired/altered trafficking of the GLUT4 or a combination of both. Hence, the roles of early signalling intermediates and the trafficking of GLUT4 were investigated in these insulin-resistant adipocytes. Additionally, the effect of the oral anti-hyperglycaemic drug metformin on both signalling and GLUT4 trafficking was studied under these conditions.

3.1 Glucose transport in rat adipocytes chronically treated with insulin

Following a 20 h culture of rat adipocytes in the absence of insulin, a subsequent acute insulin stimulation (20 nM) for 30 min produced a 5.6-fold increase in 3-OMG transport (figure 8). However, when the cells were cultured in the presence of 500 nM insulin, the levels of glucose transport activity were only 3-fold above those in basal cells, a 40-50% reduction in comparison with acutely insulin-stimulated cells. This reduction in insulin-stimulatable glucose transport following chronic-insulin treatment was alleviated when cells were cultured in the presence of both 500 nM insulin and 1 mM metformin. In this case, the subsequently measured levels of 3-OMG transport were 7.4-fold higher than in basal cells.

3.2 Protein levels of intracellular signalling intermediates

To investigate whether the reduced glucose transport activity in adipose cells that have been chronically treated with insulin was associated with reduced levels of known insulin signalling proteins, Western blotting was carried out on whole cell lysates for the regulatory subunit of PI 3-kinase (p85), IRS-1 and the β-subunit of the insulin receptor. The blots for p85, IRS-1 and the β-subunit of the insulin receptor are shown in figure 9(A-C) respectively. The Western blotting shows that the levels of these signalling molecules does not alter with the chronic-insulin treatment, or following chronic-insulin treatment in the presence of metformin.

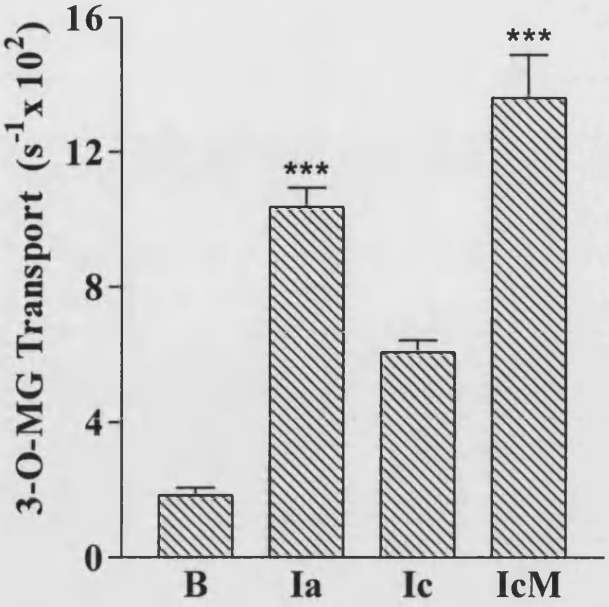

Figure 8. 3-OMG transport in rat adipocytes following a 20 h culture. Isolated rat adipocytes were cultured with either no additions (basal; B), in the presence of 500 nM insulin (chronic; Ic), or with 500 nM insulin and 1 mM metformin (chronic metformin; IcM). All cells were washed and adjusted to 40% cytocrit. A portion of the basal cells were acutely stimulated with 20 nM insulin for 30 min (acute stimulation; Ia). The rates of uptake of 50 μM 3-OMG were then determined. Data are means ± SEM from 6 separate experiments. *** $P<0.001$ vs. Ic.

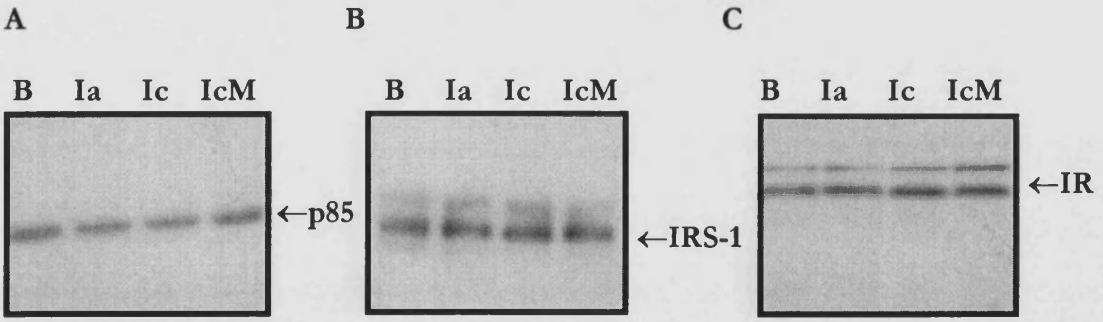

Figure 9. Western blot analysis of the levels of signalling proteins in adipocyte whole cell lysates. Freshly isolated adipocytes were cultured for 20 h either with no additions (B), or with 500 nM insulin (Ic), or with 500 nM insulin and 1 mM metformin (IcM). Cells were subsequently washed and adjusted to 40% cytocrit. A portion of basal cells were stimulated with 20 nM insulin for 2 min (Ia). 0.5 ml portions of the cells from each condition were then directly lysed with sample buffer and 20 μg of lysate protein was loaded onto 8% SDS-PAGE minigels. Proteins were transferred onto nitrocellulose and blotted for either p85 (**A**), IRS-1 (**B**) or the β-subunit of the insulin receptor (**C**). The blots shown are representative of 3 separate experiments.

3.3 Phosphorylation of the insulin receptor β-subunit

Since the reduced glucose transport activity following chronic-insulin treatment did not correlate with reduced protein levels of either the insulin receptor, IRS-1 or p85, the extents of activation of these intermediates were investigated. The extent of tyrosine phosphorylation of the insulin receptor was analysed in phosphotyrosine immunoprecipitates obtained from detergent lysates. Immunoprecipitated proteins were separated by SDS-PAGE, transferred onto nitrocellulose and blotted for phosphotyrosine (figure 10A). Scanning densitometry of autoradiograms (figure 10B) showed that insulin, within 2 min, produced extensive phosphorylation of tyrosine residues of the receptor β-subunit, the 97 kDa band on the SDS-PAGE gels. However chronic-insulin treatment of the cells produced a 70% decrease in the levels of tyrosine phosphorylation on the receptor β-subunits. This decrease was partially reversed when metformin was included in the chronic-insulin culture. There was then a 2-fold increase in β-subunit tyrosine phosphorylation compared to the response to chronic-insulin treatment, but to a level that was still only ~60% of the acute stimulation.

3.4 Levels of PI 3-kinase activity associated with tyrosine phosphorylated proteins

Downstream effects that may occur as a consequence of the reduced level of tyrosine phosphorylation of the insulin receptor include reduced coupling of PI 3-kinase to tyrosine phosphorylated proteins. The PI 3-kinase activity that was associated with tyrosine phosphorylated proteins was therefore determined in anti-phosphotyrosine agarose immunoprecipitates. PI 3-kinase activities were assessed directly in the immunoprecipitates. The phosphatidylinositol [^{32}P]3-phosphate (PI [^{32}P]3-P) generated in the assay was separated from reaction components by TLC. This major product was quantified by autoradiography. An autoradiogram image is shown in figure 11A. The kinase activity was estimated by cutting out the PI [^{32}P]3-P spots from the TLC plate, counting the radioactivity and relating this to the radioactivity of the ATP substrate (figure 11B). Following overnight culture of the adipose cells without insulin, a subsequent acute stimulation with insulin increased the kinase activity ~20-fold (from 0.57 ± 0.13 fmol/min/ml 40% cells in the basal cells to 13.43 ± 2.18 fmol/min/ml 40% cells following the insulin treatment). By contrast, the PI 3-kinase activity observed in adipose cells which were cultured in the continuous presence of insulin was only 3.48 ± 1.082 fmol/min/ml 40% cells, a 6-fold increase over the basal levels, but only 26% of

A

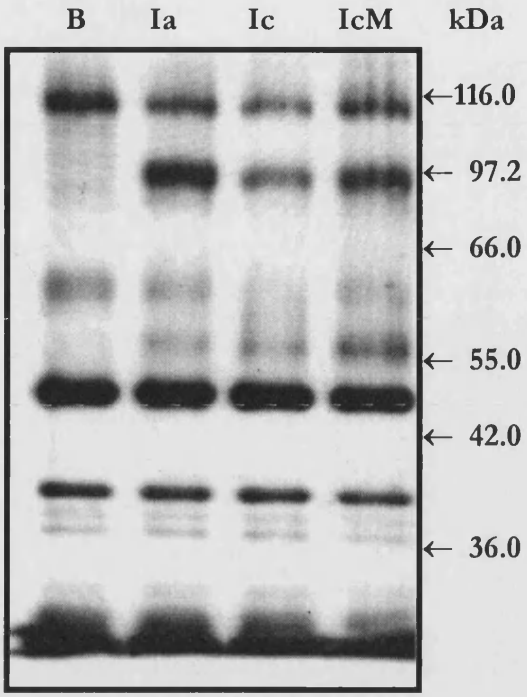

B

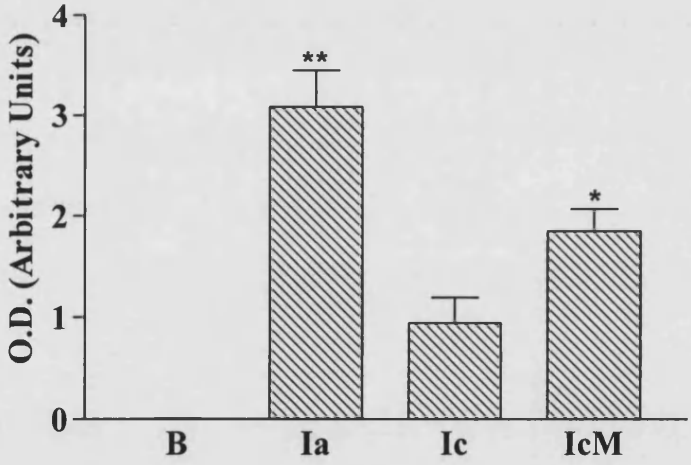

Figure 10. Tyrosine phosphorylation of the insulin receptor β-subunit following chronic-insulin treatment. Adipocytes were cultured for 20 h either with no additions (B), or with 500 nM insulin (Ic) or with 500 nM insulin and 1 mM metformin (IcM). A portion of the cells cultured under basal conditions were acutely stimulated with 20 nM insulin for 2 min (Ia). Cells were lysed and phosphotyrosine containing proteins were immunoprecipitated with anti-phosphotyrosine agarose and then resolved by SDS-PAGE. The gels were then Western blotted using an anti-phosphotyrosine antibody. The autoradiogram shown is a typical blot (**A**). The phosphorylation of the β-subunit was quantified by scanning densitometry (**B**), and represents the mean ± SEM from 5 separate experiments. In comparison with Ic, *P<0.05, **P<0.01.

the response observed in cells that were acutely treated with insulin. Treatment with both insulin and metformin during the culture period prevented the lowering of PI 3-kinase activity. The PI 3-kinase activity was 11.81 ± 3.08 fmol/min/ml 40% cells, 88% of the acute response. The PI 3-kinase activity measurements correspond closely with the levels of the p85 regulatory subunit of the enzyme that was found to be associated with phosphotyrosine immunoprecipitates. The Western blot analysis of the p85 is shown in figure 11C.

3.5 PI 3-kinase activity associated with IRS-1

PI 3-kinase activity associated with IRS-1 immunoprecipitates was investigated to determine whether IRS-1 associated PI 3-kinase activity correlated with PI 3-kinase activities observed in anti-phosphotyrosine immunoprecipitates. PI 3-kinase activities were assessed directly in the IRS-1 immunoprecipitates. As in previous experiments the PI [^{32}P]3-P generated in the assay was separated from reaction components by TLC. A typical autoradiogram of the PI [^{32}P]3-P spots is shown in figure 12A. The PI 3-kinase activity associated with IRS-1 is shown by figure 12B. Following overnight culture of the adipose cells without insulin, the acute stimulation with insulin increased the kinase activity ~10-fold (from 0.11 ± 0.09 fmol/min/ml 40% cells in the basal cells to 1.08 ± 0.09 fmol/min/ml 40% cells following the insulin treatment). As observed in the anti-phosphotyrosine immunoprecipitates, the PI 3-kinase activity associated with IRS-1 was reduced in adipose cells cultured in the presence of insulin to only 0.42 ± 0.03 fmol/min/ml 40% cells. This was a ~60% reduction in activity compared with acute-insulin treatment. However, in contrast to the results obtained with the phosphotyrosine antibody, 1 mM metformin had no effect on the PI 3-kinase activity associated with IRS-1 in cells maintained in culture overnight in the presence of 500 nM. Under these latter conditions the PI 3-kinase activity was 0.46 ± 0.11 fmol/min/ml 40% cells.

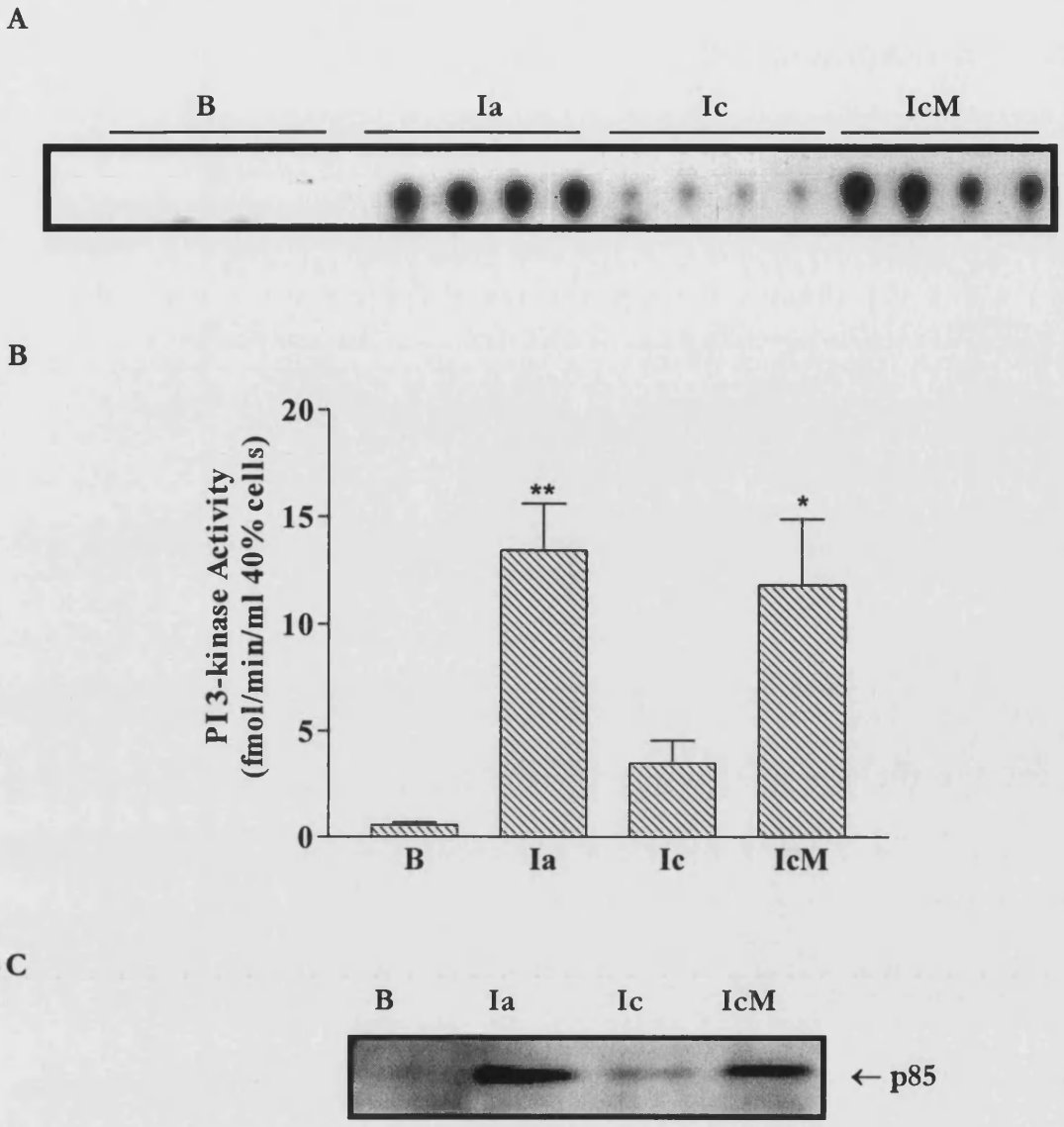

Figure 11. PI 3-kinase activity associated with tyrosine phosphorylated proteins. Adipocytes were cultured for 20 h either with no additions (B), or with 500 nM insulin (Ic), or with 500 nM insulin and 1 mM metformin (IcM). A portion of the cells cultured under basal conditions were acutely stimulated with 20 nM insulin for 2 min (Ia). 1 ml aliquots of the cells at 40% cytocrit were lysed, and the tyrosine phosphorylated proteins immunoprecipitated with anti-phosphotyrosine agarose. The pellet material was then directly assayed for PI 3-kinase activity. PI [^{32}P]3-P produced in the assay was resolved on TLC plates and visualised by autoradiography. The kinase activity was assayed in duplicate for each condition, with each reaction mix analysed by spotting twice on the TLC plate (**A**). The kinase activity was quantified by counting of PI [^{32}P]3-P radioactivity (**B**). The autoradiogram shown is representative of 5 separate experiments. The kinase activity measurements in (**B**) are the mean ± SEM of 5 separate experiments. **P<0.01, *P<0.05 vs. Ic. The levels of the p85 subunit of PI 3-kinase that were associated with the anti-phosphotyrosine immunoprecipitates were analysed by Western blotting and detection using ECL (**C**).

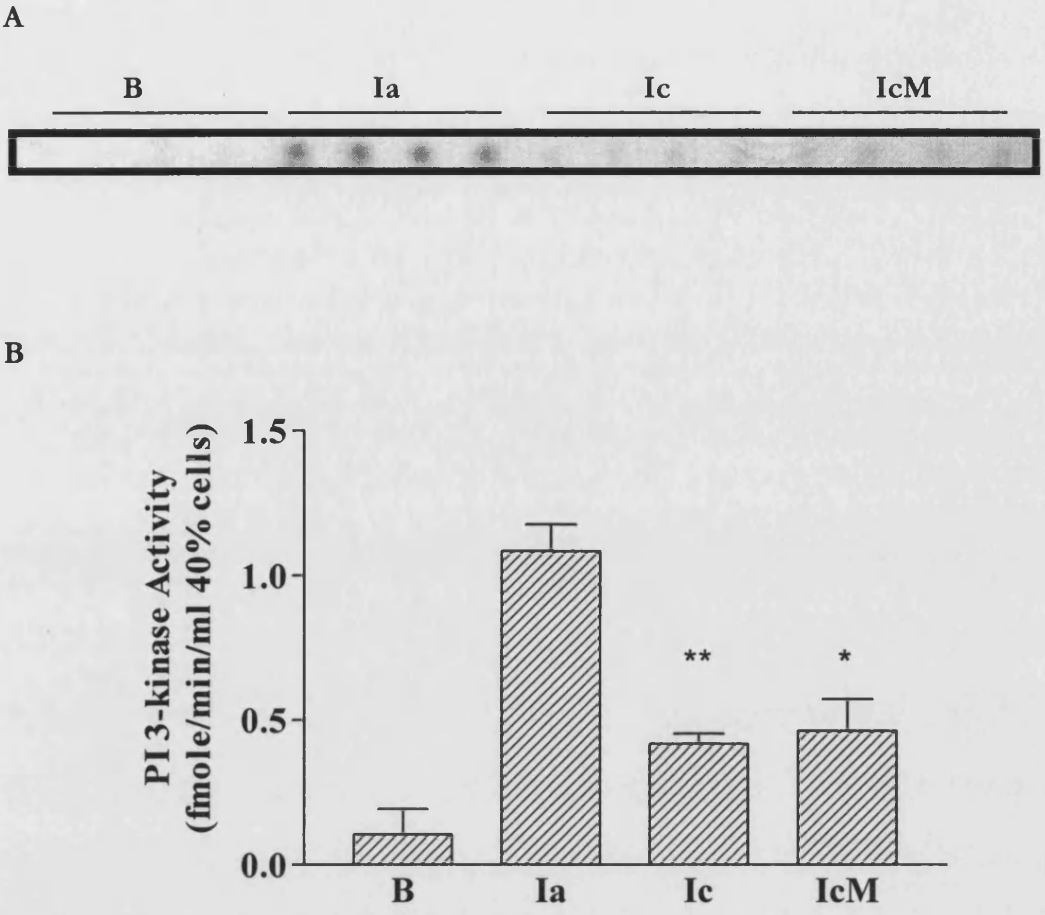

Figure 12. PI 3-kinase activity associated with IRS-1. Adipocytes were cultured for 20 h either with no additions (B), or with 500 nM insulin (Ic), or with 500 nM insulin and 1 mM metformin (IcM). A portion of the cells cultured under basal conditions were acutely stimulated with 20 nM insulin for 2 min (Ia). 1 ml aliquots of the cells at 40% cytocrit were lysed, and the IRS-1 was immunoprecipitated from lysates. The pellet material was then directly assayed for PI 3-kinase activity. PI [^{32}P]3-P produced in the assay was resolved on TLC plates and visualised by autoradiography. The kinase activity was assayed in duplicate for each condition, with each reaction mix analysed by spotting twice on the TLC plate (**A**). The kinase activity was quantified by counting of PI [^{32}P]3-P radioactivity (**B**). The autoradiogram shown is representative of 3 separate experiments. The kinase activity measurements in (**B**) are the mean ± SEM of 3 separate experiments. **P<0.01, *P<0.05 vs. Ia.

3.6 Levels of PI 3-kinase activity associated with p85 immunoprecipitates

Studies on synthetic peptides that interact with the SH2 domains of the p85 subunit of PI 3-kinase suggest that an activating conformational change in p85 occurs following the binding of phosphotyrosine ligands (*section 1.9*). To determine whether chronic-insulin treatment can alter the PI 3-kinase through this type of mechanism, the changes that occur in PI 3-kinase activity in p85 immunoprecipitates have been measured (figure 13A). From the quantitation of a series of these experiments (figure 13B) it is evident that a relatively small, less than 2-fold, increase above basal levels of PI 3-kinase activity occurs in the p85 precipitates from cells acutely treated with insulin. This effect is likely to be due to the increased association of PI 3-kinase with insulin receptor substrates such as IRS-1 which enhance the activity through the conformational change mechanism. However, these data also suggest that the large (20-fold) effects of insulin on activity determined in anti-phosphotyrosine immunoprecipitates occur because of a large increase in the levels of tyrosine phosphorylated proteins that associate with PI 3-kinase rather than to extensive activation through the conformational change mechanism. Likewise, neither the chronic-insulin treatment nor metformin produce a significant alteration in PI 3-kinase activity through the latter mechanism.

3.7 Levels of PKB activity following maintenance of adipocytes in culture

To explore whether signalling changes are transmitted downstream of PI 3-kinase, PKB was immunoprecipitated from cell lysates and the kinase activity determined (figure 14A). A 2 min acute insulin stimulation of the cells produced a 4.7-fold increase in activity over that in basal cells. The activity was increased from 16.23 ± 1.76 fmol/min/ml 40% cells in cells cultured without insulin to 87.75 ± 20.35 fmol/min/ml 40% cells in cells which were acutely treated with insulin after culture. The chronic-insulin treatment reduced this activation to 34.90 ± 2.48 fmol/min/ml 40% cells, only 40% of the acute stimulation. This chronic effect was partially alleviated by inclusion of metformin in the culture medium. The PKB activity was 61.0 ± 9.28 fmol/min/ml 40% cells. This represents 69% of the acute response and a 1.7-fold increase over the activity in chronically-treated cells. Western blot analysis of the levels of PKB in whole cell lysates (figure 14B) indicated that the protein levels of the enzyme were not reduced by the chronic-insulin treatment. However in comparison with the PKB signal from basal

A

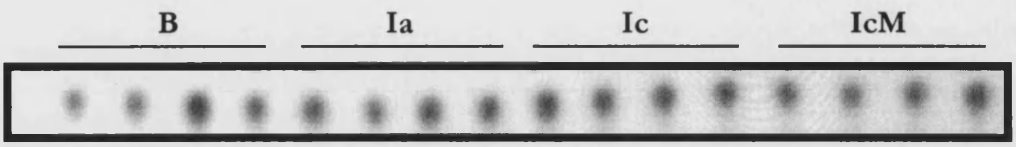

B

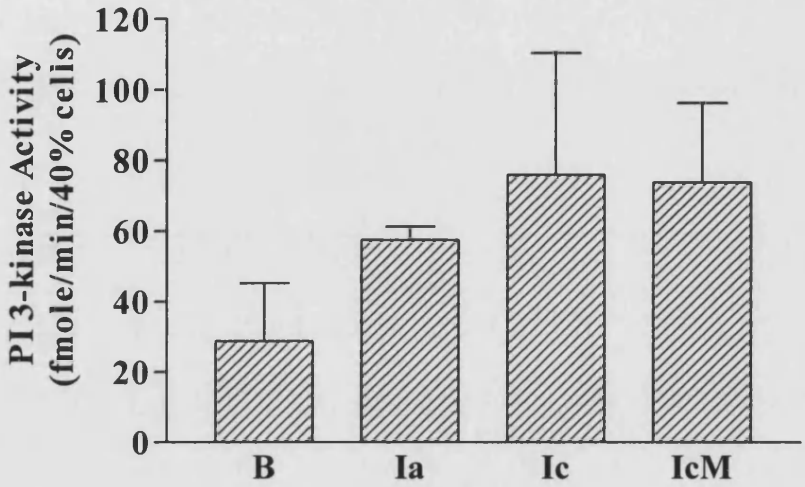

Figure 13. PI 3-kinase activity associated with p85 immunoprecipitates. Adipocytes were cultured for 20 h either with no additions (B), or with 500 nM insulin (Ic), or with 500 nM insulin and 1 mM metformin (IcM). Cells were subsequently washed and adjusted to 40% cytocrit. A portion of the cells cultured under basal conditions were stimulated with 20 nM insulin for 2 min (Ia). 1 ml aliquots of the cells were lysed and p85 was immunoprecipitated from the detergent soluble lysates. The immune pellets were then directly assayed for PI 3-kinase activity. PI [^{32}P]3-P produced in the assay was resolved on TLC plates and visualised by autoradiography. The kinase reaction was performed in duplicate for each condition, with each reaction mix analysed by spotting twice on the TLC plate (**A**). The kinase activity was determined by counting the PI [^{32}P]3-P radioactivity (**B**). The results are the mean ± SEM from 5 separate experiments.

cells, there were slight band shifts in the position of the PKB signal in the gel lanes from the cells that had been acutely treated with insulin and in those cells that had been chronically treated with insulin in the presence of metformin. The band shift was less marked in the samples obtained from cells that had been chronically treated with insulin. This band shift occurs because of a PI 3-kinase dependent phosphorylation of the enzyme that is associated with the activation of PKB by insulin treatment (*section 1.12*). Therefore, these band shift changes correspond to the direct measurements of enzyme activity shown in figure 14A.

A

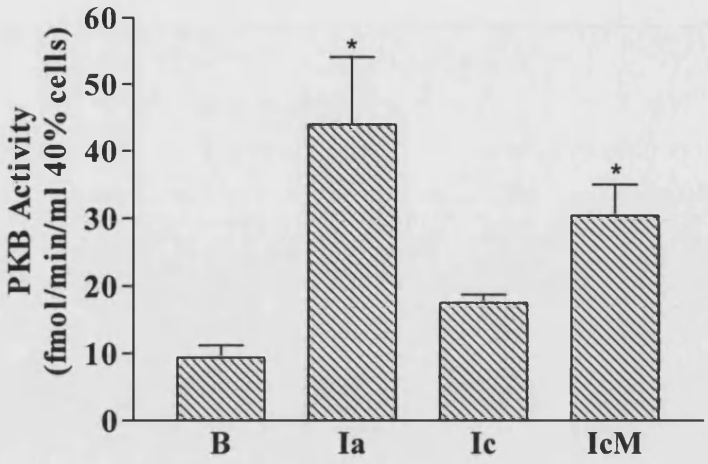

B

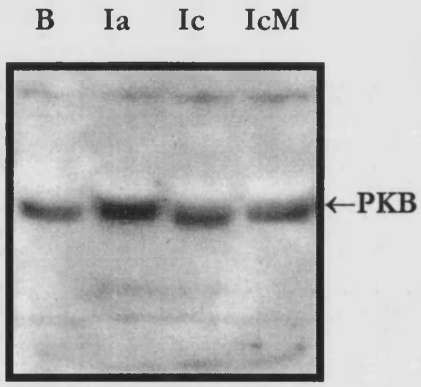

Figure 14. PKB activity following maintenance of adipocytes in culture. Adipocytes were cultured for 20 h either with no additions (B) or with 500 nM insulin (Ic) or with 500 nM insulin and 1 mM metformin (IcM). A portion of the cells cultured under basal conditions were stimulated with 20 nM for 2 min (Ia). Cells were lysed and PKB immunoprecipitated from the detergent soluble lysates. PKB activity was directly measured in immune pellets (**A**). The kinase activity measurements are means ± SEM from 4 separate experiments. *$P<0.05$ vs. Ic. Cell lysates were also subjected to Western blot analysis for PKB. This was detected by enhanced chemiluminescence (**B**). The Western blot is representative of 3 separate experiments.

PART B – Trafficking measurements in insulin-resistant rat adipocytes

3.8 Measurements of GLUT4 endocytosis and exocytosis in wortmannin treated adipocytes following a 20 h culture

As in previous experiments, adipocytes were maintained in culture for 20 h either with no additions to the culture medium, with 500 nM insulin, or with 500 nM insulin and 1 mM metformin. Cells were subsequently recovered by removing the culture medium and washing 4 times with 1% (w/v) BSA/KRH buffer supplemented with either 500 nM insulin with or without 1 mM metformin as appropriate. Cell suspensions were then adjusted to a cytocrit of 40 %. A fraction of the cells maintained in culture without insulin or metformin were then acutely insulin-stimulated with 20 nM insulin for 30 min. 1 μM wortmannin was then added to the four cell populations and the rate constants of 3-OMG uptake were measured at 0, 3, 6, 9, 20, 30 and 60 min after the addition of the wortmannin (*section 2.11*). The decrease in transport activity (related to decreased cell surface GLUT4) as shown by figure 15A can be fitted to an exponential rate equation (*section 2.12*) to determine the trafficking rate constants (figure 15B). As in previous reports (Yang *et al.*, 1996) the exocytosis rate constant (k_{ex}) was found to be negligible in all of the cell conditions after the addition of wortmannin (figure 15B). However, analysis of the endocytosis rate constant (k_{en}) revealed that the chronic-insulin treatment results in a 3-fold increase in the endocytosis rate constant compared with cells cultured without insulin and then subsequently acutely stimulated (0.127 ± 0.011/min for cells treated with 500 nM insulin for 20 h compared to 0.039 ± 0.008/min for cells acutely stimulated with 20 nM insulin for 30 min following a 20 h maintainance in culture) (figure 15B). Addition of metformin to the culture medium together with insulin reversed the effects of the chronic-insulin treatment on the endocytosis rate constant (0.043 ± 0.010/min) (figure 15B).

A

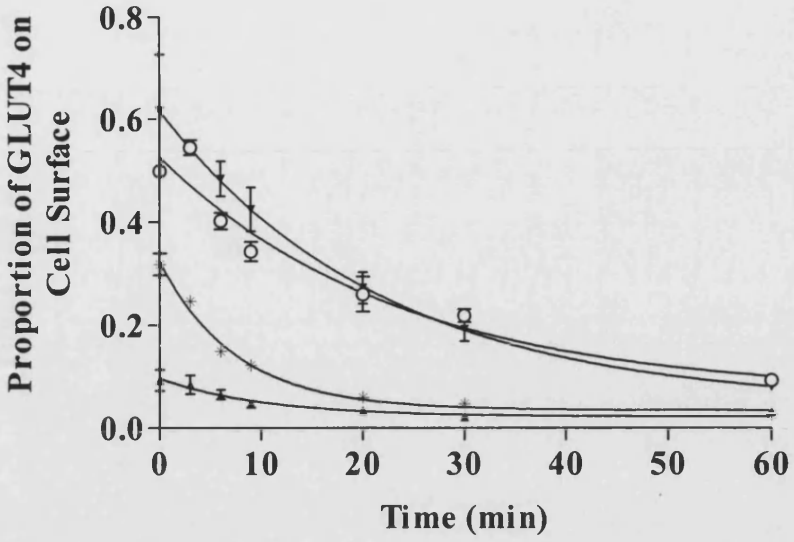

B

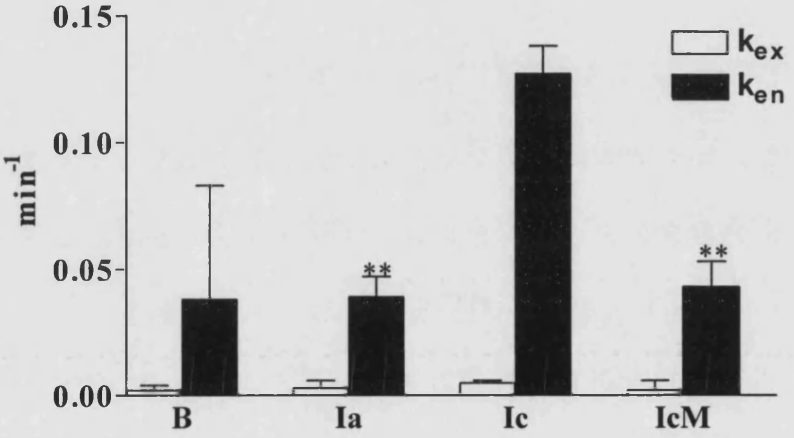

Figure 15. Reduction in cell surface GLUT4 in rat adipocytes following a 20 h maintenance in culture and wortmannin treatment, and determination of GLUT4 trafficking kinetics. Isolated rat adipocytes were cultured with either no additions (basal; B), in the presence of 500 nM insulin (chronic; Ic), or with 500 nM insulin and 1 mM metformin (chronic metformin; IcM). All cells were washed and adjusted to 40% cytocrit. A portion of the basal cells were acutely stimulated with 20 nM insulin for 30 min (acute stimulation; Ia). The rates of uptake of 50 μM 3-OMG were then determined at times 0, 3, 6, 9, 20, 30 & 60 min following the addition of 1 μM wortmannin (time of 3-OMG uptake at each time point varied for each cell condition and time after the addition of the wortmannin – see table 4, *section 2.11*). The data are plotted as the fractional reduction of the initial activity (**A**). ▲ - B, O - Ia, ✳ - Ic, ▼ - IcM. The rate constants k_{ex} and k_{en} were calculated by least-squares fitting (non-weighted fit) to equation 2 (*section 2.11*) (**B**). Data are means ± SEM from three separate experiments. ** $P < 0.01$ vs Ic.

3.9 Chapter 3 discussion

It has previously been observed that a large decrease in insulin-responsive glucose transport occurs in rat adipocytes maintained in culture for 20 h in the continuous presence of insulin (Kozka & Holman, 1993). The reduction of glucose transport activity induced by chronic-insulin treatment is found to be independent upon the total cellular levels of both GLUT1 and GLUT4 (Kozka & Holman, 1993; Pryor *et al.*, 1999). It was therefore investigated to observe whether impairments in signalling and/or altered trafficking of the GLUT4 could account for the downregulation of PM GLUT4.

The oral biguanide metformin is used clinically to alleviate insulin resistance (Davidson & Peters, 1997). *In vivo* metformin treatment has been found to ameliorate insulin resistance by inducing transporter translocation in obese (fa/fa) Zucker rats (Matthaei *et al.*, 1993) and streptozotocin diabetic rats (Rossetti *et al.*, 1990). It has previously been observed that inclusion of metformin in the culture medium during the chronic-insulin treatment of rat adipocytes can alleviate the downregulation of glucose transport activity (Kozka & Holman, 1993). Hence, we addressed the question of whether the metformin effect is related to the reversal of early signalling and/or trafficking events induced by chronic insulin treatment.

The initial event in insulin intracellular signalling is the activation of the insulin receptor kinase. Chronic-insulin treatment of the rat adipocytes caused a significant reduction in receptor β-subunit tyrosine phosphorylation (figure 10). The reduction in insulin receptor phosphorylation is fully accountable by reduced receptor kinase activation and not by a reduction in the levels of receptor protein (figure 9C). Furthermore, the levels of PM insulin receptors did not alter with the chronic-insulin treatment (data not shown). The reduced receptor phosphorylation is likely to result in a reduced kinase activity towards IRS molecules, and therefore a reduction in the intracellular signalling pathway leading to GLUT4 translocation to the PM. Indeed, downstream signalling of the insulin receptor was markedly reduced in the chronic-insulin treatment model of insulin resistance. Chronic-insulin treatment resulted in the reduction of IRS-1- and phosphotyrosine-associated PI 3-kinase activity (figures 12 and 11 respectively) and PKB phosphorylation/activation (figure 14). The results also suggest that chronic-insulin treatment does not alter PI 3-kinase catalytic activity directly, but alters the coupling of PI 3-kinase to upstream phosphotyrosine intermediates (figure 13). Hence, these data show that impaired signalling at the level of receptor phosphorylation,

transmitted to downstream signalling molecules, is associated with the chronic-insulin treatment model of insulin resistance.

Reduced PKB and glucose transport activities have been observed in human muscle from NIDDM patients (Krook *et al.*, 1998). Similarly, the activity of PKB following chronic-insulin treatments *in vitro* (in the absence and presence of metformin) correlates with the changes occurring at the levels of insulin receptor phosphorylation and phosphotyrosine associated PI 3-kinase. In turn, the changes in PKB also correlate with the changes observed in glucose transport activity but this may occur because both of these processes are related to the same early signalling changes. These data suggest that alterations in PKB activity are a consequence of the early processes and that there are probably no additional effects of these treatments (insulin or metformin) on enzyme activity. This correlation does therefore not provide evidence either for or against the possibility that changes in transport are mediated by PKB.

Reduced insulin receptor kinase activity has also been observed in other insulin-resistant systems (Handgerg *et al.*, 1993; Goodyear *et al.*, 1995; Saad *et al.*, 1997). Reductions in insulin receptor activation are possibly due to either reduced intrinsic tyrosine kinase activity or to an increased receptor associated phosphatase activity. Reduced receptor intrinsic kinase activity has not been assessed here, but it is possible that the chronic-insulin treatment has directly affected the receptor kinase. However, a more likely scenario is that increased expression and/or activity of one or more insulin receptor-tyrosine phosphatase has been altered with the chronic-insulin treatment. Studies with purified enzymes and recombinant catalytic domains have revealed several protein tyrosine phosphatases are active against the autophosphorylated insulin receptor (Goldstein, 1993). These phosphatases include the transmembrane phosphatases CD45, LAR and leukocyte common antigen-related protein tyrosine phosphatase (LRP), and cytosolic protein tyrosine phosphatases PTP1B and TC-PTP (Goldstein, 1993). The role of LAR in insulin receptor dephosphorylation has been studied by both overexpression in insulin-responsive CHO cells (Zhang *et al.*, 1996), and by knocking out LAR expression in a rat hepatoma cell line using antisense RNA (Kulas *et al.*, 1995). Overexpression of LAR, reduced insulin receptor autophosphorylation, whilst antisense inhibition of LAR increased both insulin receptor autophosphorylation and PI 3-kinase activity (150 and 350 % respectively). Furthermore, in obese human subjects with reduced receptor tyrosine phosphorylation, the levels of LAR expression in adipose tissue is elevated (Ahmad *et al.*, 1995). However, a study of LAR expression in the major human insulin target

tissues revealed that LAR expression in skeletal muscle is extremely low (Norris *et al.*, 1997). Additionally, overexpression of LAR in insulin-responsive hamster kidney cells has no effect on insulin-stimulated insulin receptor autophosphorylation (Moller *et al.*, 1995). Moreover, overexpression of LRP and PTPε in the hamster kidney cells significantly reduced the insulin responses. Whilst PTP1B overexpression in hamster kidney cells has no effect on receptor phosphorylation, overexpression in Rat-1 fibroblast inhibits insulin-stimulated autophosphorylation. These conflicting observations may reflect the use of different cell lines where relative levels of overexpressed protein tyrosine phosphatases and the insulin receptor vary. Since *in vitro* studies suggest that different protein tyrosine phosphatases may dephosphorylate specific tyrosine residues on the insulin receptor (Goldstein, 1993), it is possible that a complex regulatory process exists whereby receptor dephosphorylation may involve several phosphatases acting in tandem to regulate insulin receptor signalling (Drake & Posner, 1998). Further work needs to be carried out using phosphorylated insulin receptors to determine whether the chronic-insulin treatment of the adipose cells results in an elevation of insulin receptor-tyrosine phosphatase activity.

Inclusion of metformin has been found to reverse the chronic-insulin effects on receptor phosphorylation (figure 10). There are reports that metformin treatment of obese (fa/fa) Zucker rats (Matthaei *et al.*, 1993) and a 2 h metformin treatment of rat adipocytes (Matthaei *et al.*, 1991) have no effect on the insulin receptor phosphorylation. However, there is contradictory evidence suggesting that metformin can produce increases in the receptor tyrosine phosphorylation in streptozotocin diabetic rats (Rossetti *et al.*, 1990), erythrocytes (Santos *et al.*, 1995), *Xenopus* oocytes (Stith *et al.*, 1996), and basal insulin receptor tyrosine phosphorylation in vascular smooth muscle (Dominguez *et al.*, 1996). It is possible that metformin can either directly activate the receptor kinase or alternatively metformin may act as an insulin receptor tyrosine phosphatase inhibitor. The action of metformin on phosphatases can readily be tested. This may provide some evidence for the mechanism of action of metformin, which currently remains largely unresolved.

Not assessed in this study, is which particular insulin receptor tyrosine residues have reduced phosphorylation with the chronic-insulin treatment. Substrate targeting to the insulin receptor is thought to be mediated in part *via* the PTB domain of substrates like IRS-1 and Shc (*section 1.5*), the KRLB domain of IRS-2 (*section1.6.2*) and even perhaps other proteins linking the substrates and receptor (Burks *et al.*, 1998). Dephosphorylation of particular insulin receptor

tyrosine residues by specific phosphatases may differentially alter the binding efficacy of receptor substrates. Hence, IRS-2/3 may become a better substrate than IRS-1. The partial reversal of the chronic-insulin effect by metformin on receptor phosphorylation may be a result of metformin acting as a phosphatase inhibitor on one or more phosphatases. However, whilst metformin can reverse the chronic-effect on phosphotyrosine-associated PI 3-kinase, this reversal was not due to an association with IRS-1 (figure 12). This suggests that another phosphotyrosine protein is binding PI 3-kinase under the chronic-insulin metformin treatment. This further supports the hypothesis that another IRS molecule such as IRS-2 may be more important for glucose transport than IRS-1 (*section 1.8*). Obviously, it has not been shown here whether the tissue culturing of the adipose cells has altered the levels of the IRS proteins relative to each other, and more work is therefore required to determine whether this is the case, and whether IRS-2/3 can account for the increased PI 3-kinase activity under the chronic-insulin metformin treatment. Certainly, the tyrosine phosphorylation of a 60 kDa protein is shown to be increased by the insulin-chronic and metformin treatment (figure 10), and this protein is probably IRS-3. Whether IRS-3 phosphorylation can account for the metformin reversal of the chronic-insulin treatment on phosphotyrosine-associated PI 3-kinase requires further investigation.

There appears to be spare receptor and signalling capacity in the normal system leading to the elevation of GLUT4 translocation. The concentration of insulin required to activate glucose transport maximally corresponds to only 14% of the maximal receptor kinase activity (Klein *et al.*, 1991). Furthermore, in 3T3-L1 adipocytes only 10% of the insulin-stimulated PI 3-kinase activity is required to give full glucose uptake that is comparable to maximal insulin stimulation (unpublished data). However, only rather moderate deficiencies in receptor phosphorylation and the subsequent intracellular signalling processes produces insulin resistance and the downregulation of PM GLUT4. This appears to apply to both *in vitro* model systems and in human NIDDM (Bjornholm *et al.*, 1997).

Wortmannin appears to have little or no effect on endocytosis as the values for k_{en} derived here are similar to those previously obtained in cells not treated with wortmannin (Yang & Holman, 1993; Satoh *et al.*, 1993; Yang *et al.*, 1996). As in 3T3-L1 cells (Yang *et al.*, 1996), GLUT4 exocytosis is inhibited by wortmannin since values for k_{ex} (figure 15B) are much lower than those previously obtained in cells not treated with wortmannin (Yang & Holman, 1993; Satoh *et al.*, 1993; Yang *et al.*, 1996). These comparisons therefore suggest that it is the

inhibition of exocytosis and not acceleration of endocytosis that leads to the perturbation of glucose transport and reduction of levels of cell-surface GLUT4 following wortmannin treatment. A rate constant for unperturbed GLUT4 exocytosis (k_{ex}) can be calculated if we assume (and as suggested above) k_{en} is unaltered by wortmannin. To do this the steady-state GLUT4 distributions (k_{ex}/k_{en}) are used. These ratios (k_{ex}/k_{en}) are ~0.81 and 0.33 for acute- and chronic-insulin treatments respectively (Kozka & Holman, 1993; Holman *et al.*, 1994). For acute- and chronic-insulin treatments, the derived exocytosis rate constants are therefore ~0.032 min^{-1} and 0.042 min^{-1}, respectively. From this analysis, it is apparent that the calculated rate of GLUT4 exocytosis in the absence of wortmannin is not markedly altered by chronic-insulin treatment, despite a reduction in insulin signalling. However, the down-regulation of cell surface GLUT4 is associated with a 3-fold increase in the rate of endocytosis of GLUT4 (figure 15) and this effect is reversed by metformin. It is the increase in endocytosis of GLUT4 that correlates with the reductions in insulin receptor phosphorylation and PI 3-kinase activity. The effects on endocytosis persist under conditions in which exocytosis is blocked by wortmannin treatment. This suggests that, once elevated, the endocytosis rate is not dependent upon signalling *via* a wortmannin-sensitive PI 3-kinase. Therefore, an explanation for the apparent poor correlation between high insulin sensitivity/signalling capacity and insulin signalling resistance may be that the former is associated with GLUT4 exocytosis while the latter is associated with GLUT4 endocytosis. Regulation of the endocytosis limb of the translocation pathway may involve a divergent signalling route or branch with a different insulin and PI 3-kinase dependence.

Previous studies have shown that GLUT4 exocytosis is increased over 9-fold by insulin (Satoh *et al.*, 1993; Yang & Holman, 1993) while endocytosis is slightly decreased by insulin under normal conditions (Satoh *et al.*, 1993; Yang & Holman, 1993; Jhun *et al.*, 1992). It appears that the relatively small effect of acute-insulin treatment to reduce endocytosis is lost following prolonged insulin treatment. However, as the endocytosis process appears to be more sensitive to perturbations in signalling, an acceleration of endocytosis may be an important component of the pathophysiological changes leading to insulin resistance.

Shibata *et al.* (1995) have suggested that GLUT4 endocytosis requires the hydrolysis of GTP by a GTP-binding protein. It may therefore be of interest to study the effects of chronic-insulin treatment on the activity of GTP-binding proteins involved in the endocytosis of GLUT4 from the PM. One candidate GTP-binding protein might be Rab5, which has been

shown to regulate endocytosis (Bucci *et al.*, 1992; Li *et al.*, 1995) and whose distribution in 3T3-L1 adipocytes is altered upon insulin treatment (Cormont *et al.*, 1996b). Further experiments are required to determine how insulin regulates the endocytosis of GLUT4 and whether proteins such as rab5 might be involved in this process.

We have found that metformin can reverse both signalling and the related GLUT4 trafficking defects associated with chronic-insulin treatment. The metformin reversal appears to be primarily associated with altered insulin receptor tyrosine phosphorylation. Although its precise mechanism of action remains to be fully elucidated, the secondary effects on GLUT4 endocytosis provide a rationale for the therapeutic use of this compound in the treatment of insulin resistance in human NIDDM.

CHAPTER 4

GTP-BINDING PROTEINS

Guanosine nucleotide binding regulatory proteins (GTP-binding proteins) play a pivotal role in signal transduction. Evidence for the involvement of GTP-binding proteins in insulin-regulated GLUT4 trafficking comes from the observations that non-hydrolysable analogues of guanosine triphosphate (GTP) such as guanosine-5'-*O*-(3-thiotriphosphate) can stimulate GLUT4 translocation (Baldini *et al.*, 1991) even in the presence of the PI 3-kinase inhibitor wortmannin (Clarke *et al.*, 1994). Furthermore, small molecular weight GTP-binding proteins have been found on immunoisolated GLUT4 vesicles (Cormont *et al.*, 1993; Uphues *et al.*, 1994). Since GTPγS activation of GTP-binding proteins does not distinguish between small molecular weight Ras-like and heterotrimeric GTP-binding proteins, it is possible that both families of GTP-binding proteins are involved in the insulin-stimulated translocation of GLUT4 vesicles to the plasma membrane (*section 1.14*). Experiments were therefore undertaken to identify possible GTP-binding protein targets of acute insulin stimulation.

4.1 Periodate-oxidised [α-^{32}P]GTP as a probe for identifying GTP-binding proteins

Two methods have been described which use [α-^{32}P]GTP to detect GTP-binding proteins. One method involves an incubation of proteins which have been electrophoretically transferred onto a membrane. In this procedure the proteins are allowed to renature on the membrane and then [α-^{32}P]GTP-binding to the proteins is measured. The second method involves photo-crosslinking of the [α-^{32}P]GTP to cell extracts following irradiation of samples with an intensive ultraviolet light source. However, both of these techniques have their limitations (Huber & Peter, 1994). For instance, only proteins with very high binding affinities are detectable and proteins which do not renature on nitrocellulose after SDS-PAGE cannot be detected. A limitation of the GTP photo-crosslinking method is that often the levels of incorporation of the radionucleotide into GTP-binding proteins is found to be low. Hence, a technique of *in situ* periodate-oxidised GTP labelling has been developed by Peter *et al.* (1993) (figure 16). This technique introduces [α-^{32}P]GTP into permeabilised cells, with the subsequent addition of sodium periodate to oxidise the GTP. The addition of the sodium periodate leads to oxidative cleavage of the nucleotide ribose and formation of a reactive dialdehyde. This can form an unstable condensate with an ε-amino group of a nearby lysine residue (a lysine residue tends to be conserved in the nucleotide binding pocket of GTP-binding proteins, Löw *et al.*, 1992). Subsequent addition of sodium cyanoborohydride stabilises the covalent bond, thereby labelling the protein. Any unbound oxidised-GTP is reduced with sodium borohydride. Using this technique, it has been found that stimulation of the T-cell

receptor (TCR) in Jurkat cells leads to an increase in GTP-binding of the TCR-ξ chain (Sancho *et al.*, 1993). The aim of the work described here was therefore to use the technique of periodate-oxidised GTP labelling to tag GTP-binding proteins in basal and insulin-stimulated rat adipocytes.

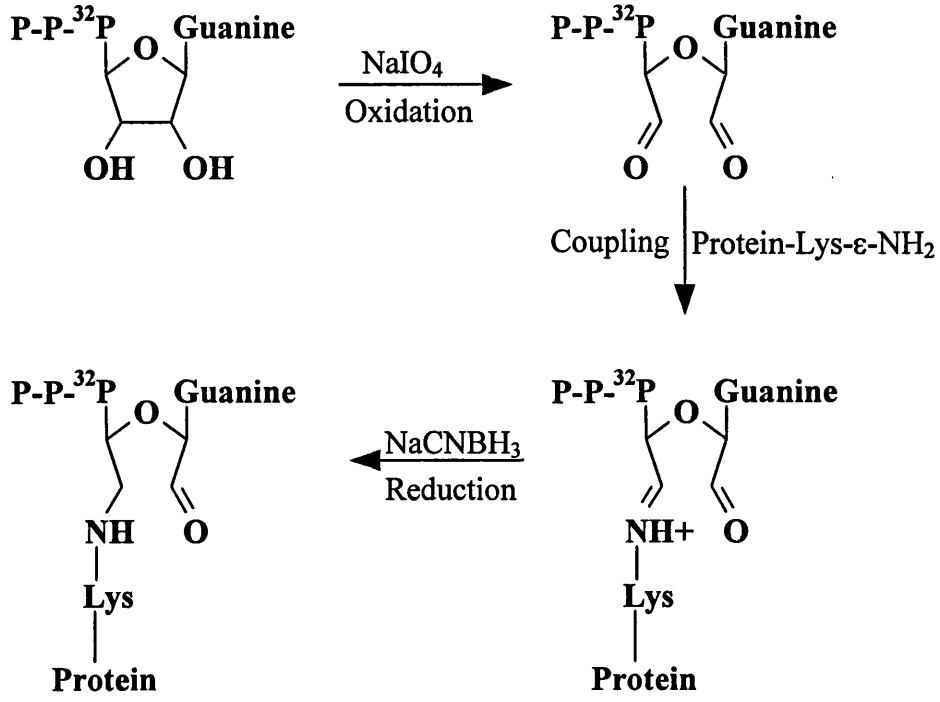

Figure 16. Reaction scheme for covalent linking of [α-^{32}P]GTP to GTP-binding proteins. [α-^{32}P]GTP non-covalently bound to a protein is oxidised with $NaIO_4$ to produce a reactive dialdehyde. This forms an unstable imine with the ε-NH_2 of a nearby lysine residue. Reduction of the imine with $NaCNBH_3$ gives rise to a stable covalent bond and thereby radiolabels the GTP-binding protein.

4.2 Retention of insulin-responsive GLUT4 translocation to the plasma membrane of permeabilised rat adipocytes as determined by ATB-BMPA photolabelling

Cells are impermeable to [α-^{32}P]GTP and therefore need to be permeabilised to allow access of the [α-^{32}P]GTP to the intracellular GTP-binding proteins. Since the aim of the *in situ* periodate-oxidised GTP labelling of rat adipocytes was to observe differences between GTP-labelling in basal and insulin-stimulated cells the rat adipocytes needed to be permeabilised under conditions that still maintained an insulin-stimulated GLUT4 translocation to plasma membranes.

Rat adipocytes were permeabilised using α-toxin from *Staphylococcus aureus* cells. The conditions for permeabilisation were essentially as described by Baldini *et al.* (1991). Permeabilised cells were tested for a functional insulin response by stimulating with 20 nM insulin for 20 min and then by photolabelling the cell-surface GLUT4 with the cell impermeant ATB-[2-^{3}H]BMPA photolabel. Although the photolabel is likely to gain access to the cell cytosol (since the cells are permeabilised) the photolabel tends only to bind to the exofacial side of the glucose transporter and probably does not permeate the intracellular vesicles. Therefore labelling of GLUT4 in permeabilised cells is mainly indicative of the levels of plasma membrane GLUT4. Photolabelling followed by immunoprecipitation of GLUT4 in intact basal and insulin-stimulated adipocytes showed a 20-fold difference in the levels of GLUT4 in the PM (figure 17). In permeabilised cells, the insulin-induced increase in PM GLUT4 was reduced to 6-fold, but the experiment indicated that the permeabilised cells were still partly insulin responsive (figure 17). Additionally, 600 μM GTPγS was also capable of stimulating the translocation of GLUT4 to the PM in permeabilised cells, to the same extent as permeabilised cells stimulated by insulin (figure 17). Since normally cells are not permeable to GTPγS, the GTPγS-induced stimulation of labelling indicated that the adipocytes had been permeabilised. The photolabelling experiment therefore showed that under the experimental conditions described, the adipose cells were permeable to small molecules such as GTP and were still insulin responsive.

By washing permeabilised cells after the addition of α-toxin, small molecular weight intracellular molecules may be removed and thereby reduce the insulin response. Hence, the adipose cells were left continuously in the presence of the α-toxin during the periodate-oxidised GTP-binding procedure. However, the adipose cells were sensitive to prolonged incubation with the α-toxin. This is shown in figure 17, where adipose cells which had been permeabilised for 35 min, instead of 15 min, showed no translocation of GLUT4 to the plasma membrane in response to insulin-stimulation. With cells other than adipocytes, α-toxin can be bound to cell membranes at 0°C thus preventing damaging effects but allowing excess toxin to be removed. However, this was not practical with the adipose cells due to their high fat content. The fat solidifies at 0°C, with a subsequent reduction in insulin responsiveness of the cells.

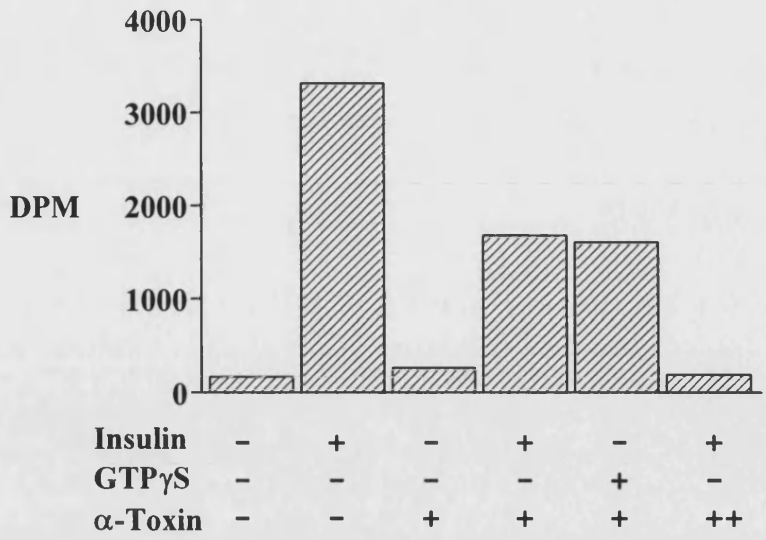

Figure 17. ATB-BMPA photolabelling of plasma membrane GLUT4 in α-toxin permeabilised rat adipocytes. Intact, or permeabilised rat adipocytes (8 μg/ml α-toxin for 15 min, or 35 min (++)) were stimulated with, or without 20 nM insulin, or with 600 μM GTPγS for 20 min at 37°C. Cell surface GLUT4 was then photolabelled with the glucose transporter photolabel ATB-[2-^{3}H]BMPA. Cells were then lysed and total cell GLUT4 immunoprecipitated. Immunoprecipitates were subjected to SDS-PAGE and the total amount of radiolabelled GLUT4 determined by liquid scintillation counting of gel slices corresponding to the molecular mass of GLUT4 on SDS-PAGE gels.

4.3 *In situ* periodate-oxidised GTP labelling of GTP-binding proteins in permeabilised rat adipocytes

200 μl aliquots of adipose cells at a cytocrit of 40% were permeabilised in the presence of [α-^{32}P]GTP (*section 2.14*) and then stimulated with 20 nM insulin for 15 min at 37°C. Sodium periodate was then added to the cells for 1 min, followed by the subsequent additions of sodium cyanoborohydride for 1 min, then sodium borohydride for 10 min on ice. Cells were then lysed in a 1% (v/v) Triton X-100 lysis buffer (*section 2.2*). The lysates were briefly centrifuged in a microfuge and the detergent-soluble infranatant added to SDS-PAGE sample buffer for gel electrophoresis. Radiolabelled proteins were visualised by autoradiography of the gels. Initially, the radiolabelling of the proteins resulted in GTP-incorporation into proteins as shown by figure 18. Numerous proteins in cells treated with or without α-toxin were labelled by GTP. This indicates that there was some non-specific labelling. Nonetheless, there was more labelling in cells treated with the α-toxin, and differences between basal and insulin-stimulated cells could be seen. In particular, in insulin-stimulated cells there appeared

to be an increased labelling of proteins at ~25 kDa and 50 kDa (indicated by arrows - figure 18) than in basal permeabilised adipocytes.

In order to reduce the non-specific labelling, the protocol was modified to reduce the amount of free [α-^{32}P]GTP present before the addition of the sodium periodate. This was achieved by centrifuging the cells through 100 µl of silicone oil and by removing the labelling solution before the addition of the periodate. The effect of this was to markedly reduce the labelling in the unpermeabilised cells compared with the permeabilised cells (figure 19 - lane 1 vs. lanes 2 - 4).

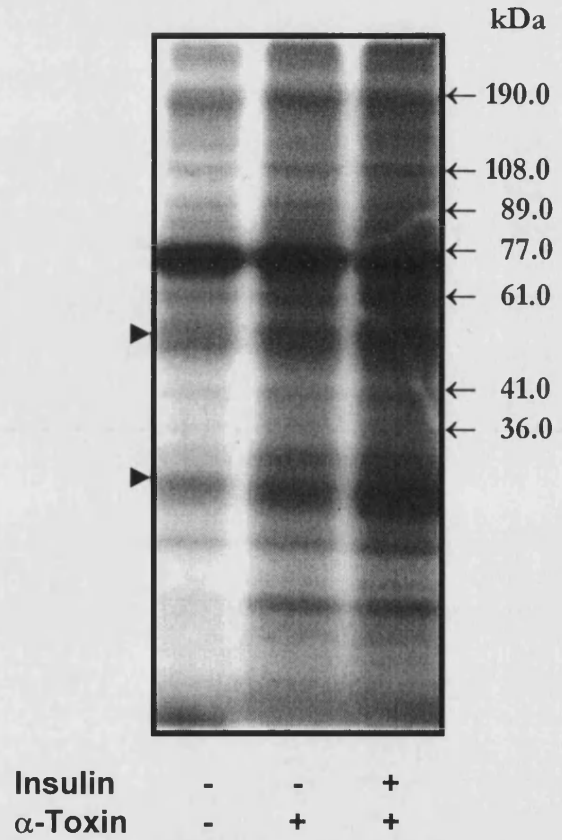

Figure 18. *In situ* periodate-oxidised GTP labelling of proteins in α-toxin permeabilised rat adipocytes. Rat adipocytes in 0.1% BSA/KRH were incubated either with or without α-toxin for 15 min at 37°C in the presence of 25 µCi [α-^{32}P]GTP. Cells were then incubated for 20 min, either with or without 20 nM insulin, at 37°C. Cells were subsequently incubated for 1 min each with 1 mM $NaIO_4$, 20 mM $NaCNBH_3$ and then 20 mM $NaBH_4$. Cells were lysed in a detergent lysis buffer and infranatants subjected to SDS-PAGE. Gels were dried and imaged by autoradiography.

Specificity of GTP-labelling was determined by including 100 μM cold GTP in the labelling solution. This reduced the labelling to a level that was similar to that seen in unpermeabilsed cells (figure 19 - lanes 5 & 6). In the development of the GTP-labelling technique, 4 mM Mg-ATP and 3 mM sodium pyruvate were included in the labelling solution to help maintain insulin responses (not shown). The inclusion of the ATP had no effect on the extent of the GTP labelling, which further implies that the GTP labelling is specific for GTP-binding proteins. By removing excess radionucleotide before periodate addition, and with the inclusion of the ATP and pyruvate, a clear difference in GTP-labelling between basal and insulin-stimulated adipocytes could be observed (figure 19 - lanes 2 & 3). In particular proteins at ~ 22-24 kDa and ~ 43 kDa showed a marked increase in GTP-labelling.

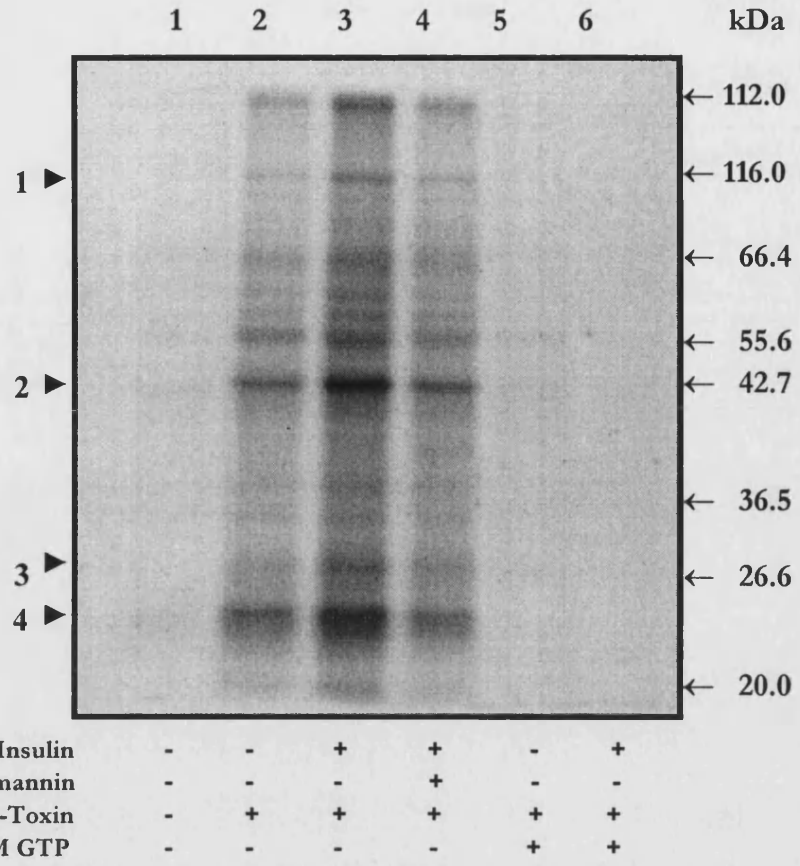

Figure 19. *In situ* periodate-oxidised GTP labelling of proteins in α-toxin permeabilised rat adipocytes. Rat adipocytes in 0.1% BSA/KRH were incubated either with or without α-toxin for 15 min at 37°C in the presence of 4 mM ATP, 3 mM sodium pyruvate and 25 μCi [α-^{32}P]GTP. Cells were then incubated for 20 min either with or without 20 nM insulin at 37°C, and with or without 1 μM wortmannin. As a control for specific labelling, basal and insulin-stimulated permeabilised samples were incubated additionally with 100 μM cold GTP. Cells were centrifuged through silicone oil and excess labelling solution removed. Cells were subsequently incubated for 1 min each with 1 mM $NaIO_4$, 20 mM $NaCNBH_3$ and then 20 mM $NaBH_4$. Cells were lysed in a detergent lysis buffer and infranatants were subjected to SDS-PAGE. The gel was dried and imaged by autoradiography. Bands labelled 1-4 were quantified for radioactivity by liquid scintillation counting (figure 20). The differences observed between basal and insulin-stimulated samples is representative of at least 3 separate experiments.

The insulin-induced increase in labelling was inhibited by the inclusion of 1 μM wortmannin during the insulin stimulation (figure 19 - lane 4). Quantification of the extent of insulin-stimulation of GTP-labelling and of inhibition by wortmannin was achieved by excision of bands (labelled 1-4 on figure 19) and by liquid scintillation counting of the radioactivity. The background radioactivity for each lane, was obtained by scintillation counting of a gel slice area at ~120 kDa from each lane on the gel (figure 20).

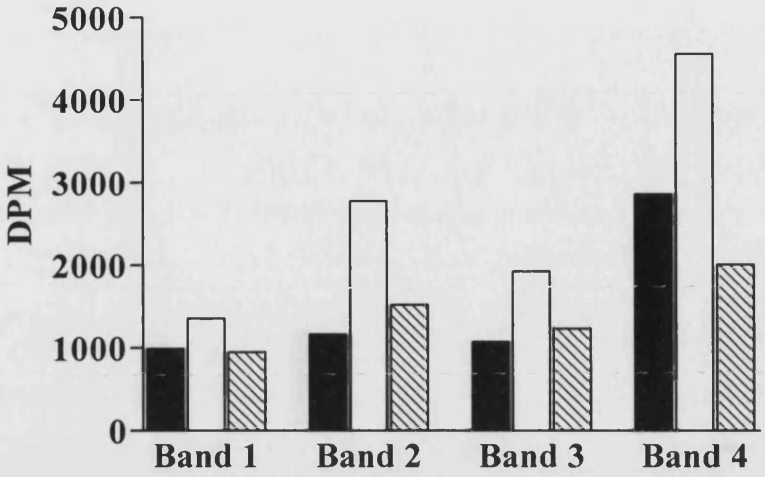

Figure 20. Quantification of [α-^{32}P]GTP labelled proteins in α-toxin permeabilised rat adipocytes. Protein bands corresponding to [α-^{32}P]GTP labelled proteins (determined by autoradiography, figure 19) were excised from gels and the radioactivity was estimated by liquid scintillation counting. Background labelling has been subtracted from each value. ■ - Basal, □ - Insulin, ▨ - Insulin + Wortmannin.

Scintillation counting of radiolabelled-protein bands showed that whilst band 1 only showed a slight increase (~1.5-fold) in labelling with insulin, band 2 (region corresponding to α-subunits of heterotrimeric GTP-binding protiens) showed a ~2.5-fold increase in labelling. Bands 3 and 4 (region corresponding to small molecular weight GTP-binding proteins) showed 1.8- and 1.6-fold increased labelling respectively.

4.4 Time-dependent increases in periodate-oxidised GTP-labelling following insulin treatment

To determine whether the increased GTP-labelling that followed insulin stimulation was time dependent, permeabilised adipocytes were stimulated with 20 nM insulin for varying times before the addition of the sodium periodate and the oxidation of the [α-^{32}P]GTP. Cells were then treated with $NaCNBH_3$ and $NaBH_4$ as in previous experiments, and radiolabelled-proteins analysed by SDS-PAGE and autoradiography (figure 21).

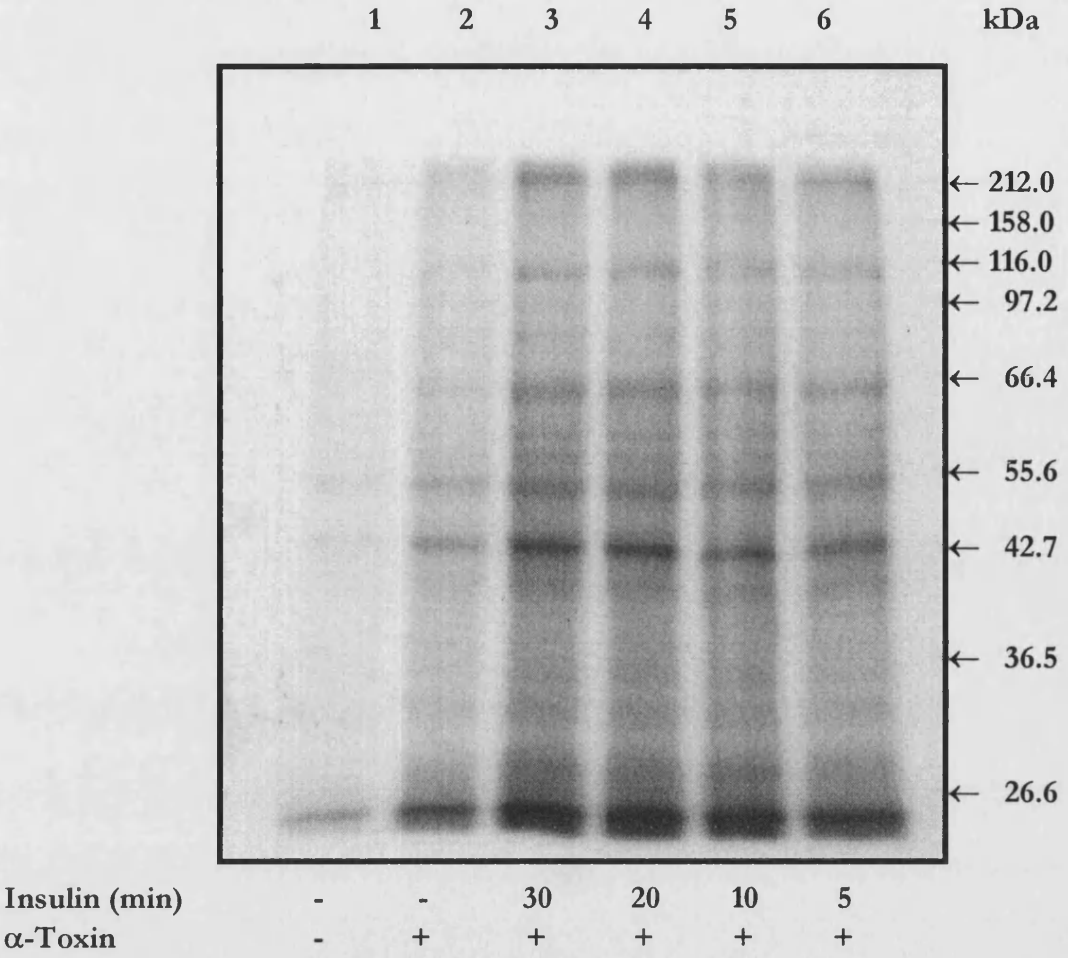

Figure 21. Time course for periodate-oxidised GTP labelling in insulin-treated, rat adipocytes. Rat adipocytes in 0.1% BSA/KRH were incubated either with or without α-toxin for 15 min at 37°C in the presence of 4 mM ATP, 3 mM sodium pyruvate and 25 μCi [α-^{32}P]GTP. Cells were then stimulated with 20 nM insulin for 5-30 min at 37°C. The total time in the presence of α-toxin was constant for each condition. Cells were then incubated for 1 min each with 1 mM $NaIO_4$, 20 mM $NaCNBH_3$ and then 20 mM $NaBH_4$. Cells were then lysed in a detergent lysis buffer and infranatants were subjected to SDS-PAGE. The gel was dried and radioactivity was imaged by autoradiography.

The time course of insulin-stimulation shows that the GTP labelling of the proteins at ~25 kDa and ~45 kDa occurs rapidly within 5 minutes of insulin stimulation. Scanning densitometry of the autoradiogram (data not shown) revealed that maximum labelling of the ~25 and ~45 kDa proteins was achieved 20 min after insulin stimulation.

4.5 Analysis of GTP-labelled proteins by two-dimensional gel electrophoresis

The previously described GTP-labelling experiments have shown that insulin-stimulation of the permeabilised adipose cells increases the [α-^{32}P]GTP-labelling of at least two groups of proteins (25 and 45 kDa), as analysed by one-dimensional SDS-PAGE and autoradiography. The radiolabelling of proteins at approximately 25 kDa corresponds to the expected migration of small-molecular weight Ras-like GTP-binding proteins on SDS-PAGE. Moreover, the GTP-radiolabelling of proteins at approximately 45 kDa is in a region expected on SDS-PAGE gels for α-subunits of heterotrimeric G-proteins. Since one-dimensional SDS-PAGE only separates proteins by molecular weight, it is possible that the periodate-oxidised GTP-labelling of proteins at 25 and 45 kDa represents several Ras-like and α-subunit GTP-binding proteins. Hence, labelled GTP-binding proteins were analysed by two-dimensional electrophoresis.

Two-dimensional (2D) electrophoresis was performed using the Pharmacia Multiphor II system (*section 2.27*). Rat adipocytes from basal, insulin-stimulated and cells treated with 1 μM wortmannin and 20 nM insulin, were covalently labelled with [α-^{32}P]GTP as described for previous experiments. The cell lysates generated from labelling experiments were then chloroform/methanol precipitated (*section 2.23*) and the precipitated proteins solubilised in 40 μl of lysis buffer and 60 μl of 2D-gel electrophoresis sample buffer (*section 2.27*). The solubilised proteins were then applied to Immobiline strips for isoelectric focusing, followed by SDS-PAGE (*section 2.27*). The ^{32}P-labelled proteins were then visualised using a Molecular Dynamics phosphorimager. A typical 2D gel of periodate-oxidised GTP-labelled proteins is shown by figure 22. It was observed that the high degree of radiolabelling in the 20-25 kDa region by one dimensional SDS-PAGE was resolved into a cluster of at least 7 radiolabelled proteins, with pIs of approximately 5.0-5.5. From examination of a map of small GTP-binding proteins separated by 2D-PAGE (Huber *et al.*, 1994) it was concluded that the small molecular weight proteins Rab2, 8, 10, 17 and 18 would be expected to run in this area.

When analysing the cluster of radiolabelled proteins at 20-25 kDa, pI 5.0 – 5.5, it was difficult to discern whether there were any differences between basal, insulin-stimulated, or insulin and wortmannin treated cells (figure 23). While differences in GTP-labelling between basal, insulin, and insulin and wortmannin treated cells were noticeable on one-dimensional

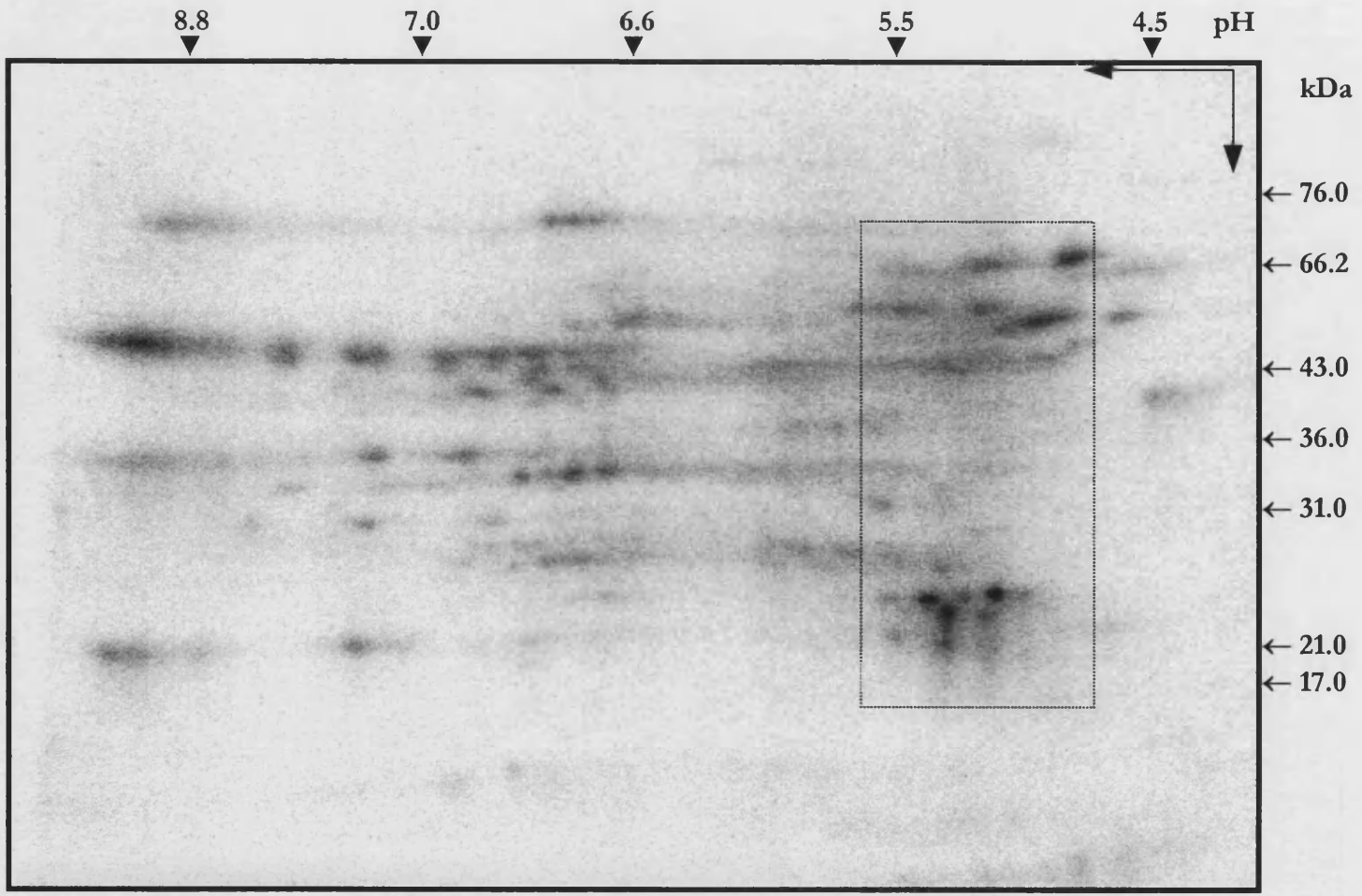

Figure 22. Two dimensional electrophoresis of [α-^{32}P]GTP-labelled proteins from insulin-stimulated rat adipocytes. Rat adipocytes were labelled with periodate-oxidised [α-^{32}P]GTP, and then lysed. Infranatants were chloroform/methanol precipitated and then solubilised in lysis buffer. Samples were added to 2D electrophoresis sample buffer and subjected to 2D electrophoresis (*section* 2.27). Radiolabelled proteins were visualised by a Molecular Dynamics phosphorimager.

Figure 23. Analysis of small molecular weight proteins labelled by periodate-oxidised [α-^{32}P]GTP from permeabilised rat adipocytes by two-dimensional electrophoresis. GTP-binding proteins in basal, insulin-stimulated and insulin-stimulated cells in the presence of 1 μM wortmannin, were labelled with [α-^{32}P]GTP as in previously described experiments. Lysates were then subjected to 2D-gel electrophoresis. Areas shown are representative of the boxed area (figure 22) and from representative gels from two separate experiments.

polyacrylamide gels, two-dimensional electrophoresis revealed that this difference could not be accounted for by any one particular protein. Differences in labelling between the various conditions could not be observed for any proteins in the 45 kDa region. Using the schematic diagram below (figure 24), which represents the small molecular weight proteins that appeared to be distinctly labelled, it appeared that protein spots 1 and 3 showed the highest degree of labelling. It was however difficult to discern whether insulin had any effect on the extent of labelling of protein spots 1,3,5 and 7. However, it did appear that wortmannin reduced the labelling of protein spots 5 and 7, and to a lesser degree spots 2 and 6.

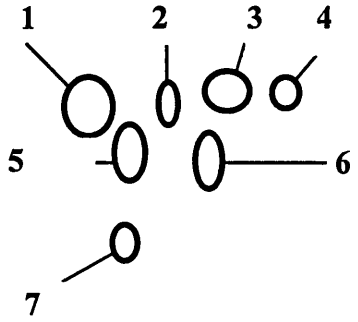

Figure 24. Schematic representation of the small molecular weight proteins labelled by periodate-oxidised [α-^{32}P]GTP (20-25 kDa, pI 5.0 - 5.5).

A single Coomassie stained spot was observed in the region that was represented by the GTP-radiolabelled proteins at 20-25 kDa, pI 5.0-5.5. The Coomassie stained protein was excised from 18 2D-gels and the protein digested by trypsin (*section* 2.31). The peptides resulting from the tryptic digest were analysed by mass spectroscopy (*section 2.31*). The mass spectroscopy data were compared to the theoretical mass spectroscopy peaks obtained from tryptic digests of sequenced proteins held in databases (mass finger printing). Unfortunately the mass finger printing failed to generate results that allowed identification of the protein.

4.6 Generation of antibodies to periodate-oxidised GTP

One disadvantage of the *in situ* periodate-oxidised GTP labelling technique is that GTP binding proteins that exhibit slow nucleotide exchange kinetics do not become radiolabelled. Hence antibodies to oxidised and reduced GTP ($GTP_{ox\text{-}red}$) were generated. Generation of antibodies to $GTP_{ox\text{-}red}$ should therefore allow the isolation of GTP-binding proteins which have GTP in the nucleotide binding site, but which have a slow rate of nucleotide exchange. The antibodies were generated by following a protocol described Peter *et al.* (1993). Briefly,

100μM GTP was oxidised with 20 mM sodium periodate in the presence of 5 mg keyhole limpet haemocyanin (KLH). The KLH and GTP mixture was then treated with 100 mM sodium cyanoborohydride and then 100 mM sodium borohydride. Reducing reagents and free nucleotides were then removed with a NAP-25 column (Pharmacia). The modified KLH was then injected subcutaneously into two New Zealand White rabbits in Freund's complete adjuvant (amounts and booster injections as for antibodies to $G_{i\alpha 1/2}$, *section 2.4*). 3 months after the initial immunisation, the sera from the two rabbits (S188 and S189, and pre-immune sera NS188 and NS189) were used to detect GTP-binding proteins in adipocyte whole cell lysates, by Western blotting. The cell lysates used in the Western blotting were pre-treated with or without 1 mM $NaIO_4$ and subsequently with 20 mM $NaCNBH_3$ before SDS-PAGE to generate GTP-labelled proteins. The results of the Western blotting are shown by figure 25.

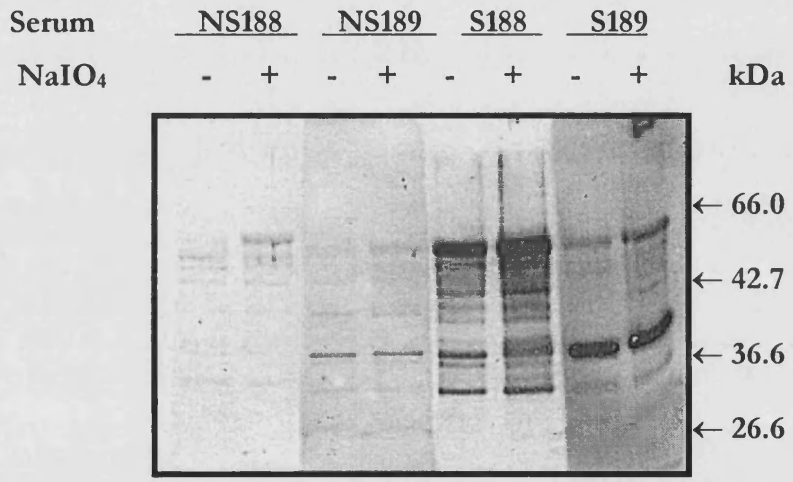

Figure 25. Western blotting of $NaIO_4$ and $NaCNBH_3$ treated proteins from rat adipocytes with anti-$GTP_{ox\text{-}red}$ antibodies. Rat adipocytes were permeabilised with α-toxin as previous experiments for 15 min at 37°C. Adipocytes were then treated with or without 1 mM $NaIO_4$. All samples were then treated with 20 mM $NaCNBH_3$. Cells were then lysed with lysis buffer, and 20 μg aliquots of the lysates were subjected to SDS-PAGE and electrophoretic transfer onto nitrocellulose. Membranes were then Western blotted (1:50 dilution in TBS-T) using antisera S188 and S189 (raised against $GTP_{ox\text{-}red}$) or the respective pre-immune sera (sera from rabbits before immunisation) NS188 and NS189.

Both of the anti-$GTP_{ox\text{-}red}$ sera (S188 and S189) were found to detect numerous proteins by Western blotting. These proteins were not detected using pre-immune sera (NS188 and NS189). However, no significant differences could be seen by Western blotting for $GTP_{ox\text{-}red}$ protein samples that had been treated with or without $NaIO_4$. This result contrasts with results described for anti-$GTP_{ox\text{-}red}$ antibodies generated by Peter *et al.* (1993). Few bands were observed by Western blotting in samples which were not treated with the $NaIO_4$,

compared with samples treated with $NaIO_4$. Additionally, Peter and co-authors reported significant reductions in the number of proteins that were detected by their anti-$GTP_{ox\text{-}red}$ antiserum by incubating the primary antibody with 300 μM GTP. Using sera S188 and S189, inclusion of 300 μM GTP had no effect on the number of proteins detected by the two antisera to the $GTP_{ox\text{-}red}$, (figure 26). The Western blotting also showed that ATP also had no effect on the number of proteins detected by the two antisera, indicating that the antibodies raised were not specific to any oxidised-reduced nucleotide.

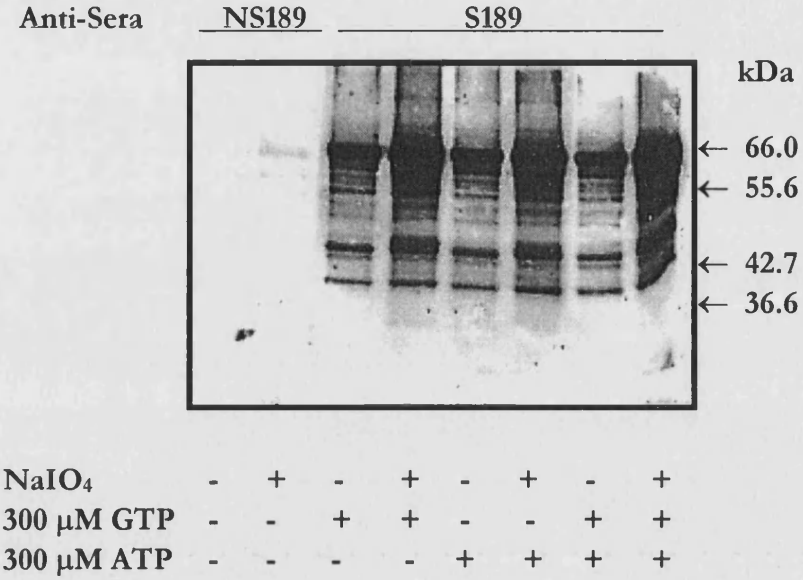

Figure 26. Western blotting of $NaIO_4$ and $NaCNBH_3$ treated proteins from rat adipocytes with anti-$GTP_{ox\text{-}red}$ serum S189 in the presence of GTP and/or ATP. Rat adipocytes were permeabilised with α-toxin for 15 min at 37°C, as previously described. Adipocytes were then treated with or without 1 mM $NaIO_4$. All samples were then treated with 20 mM $NaCNBH_3$. Cells were then lysed with lysis buffer and 20 μg aliquots of the cell lysates were subjected to SDS-PAGE and electrophoretic transfer onto nitrocellulose. Membranes were then Western blotted (1:50 dilution in TBS-T) using antiserum S189 (raised against $GTP_{ox\text{-}red}$) or the pre-immune serum (serum from the rabbit before immunisation) NS189, in the presence of 300 μM GTP and/or 300 μM ATP.

4.7 Generation of antibodies to $G_{i\alpha 1/2}$ and immunoprecipitation of periodate-oxidised GTP-labelled proteins

The 2D-gel electrophoresis of GTP-labelled proteins did not show any major differences between samples labelled with periodate-oxidised GTP, under basal and insulin-stimulated conditions. Nonetheless, attempts were made to immunoprecipitate GTP-binding proteins possibly implicated in the regulation of GLUT4 trafficking. One such GTP-binding protein

that has been implicated in regulating GLUT4 trafficking is $G_{i\alpha 2}$, (Moxham & Malbon, 1996; *section 1.14.3*). Hence, antibodies to $G_{i\alpha}$ were generated to enable $G_{i\alpha}$ to be immunoprecipitated following periodate-oxidised [α-^{32}P]GTP labelling.

An antibody was raised against the C-terminal region of transducin, which shares homology to heterotrimeric G-protein α-subunits (Goldsmith *et al.*, 1987). Antibodies raised to this region of homology recognise both $G_{i\alpha 1}$ and $G_{i\alpha 2}$. Two New Zealand White Rabbits (designated G182 and G183) were immunised with the C-terminal transducin peptide. An ELISA showed that good immune responses had been raised to the peptide by both of the rabbits, 6 weeks after immunisation, with the antibody titre further increasing by week 11 (figure 27).

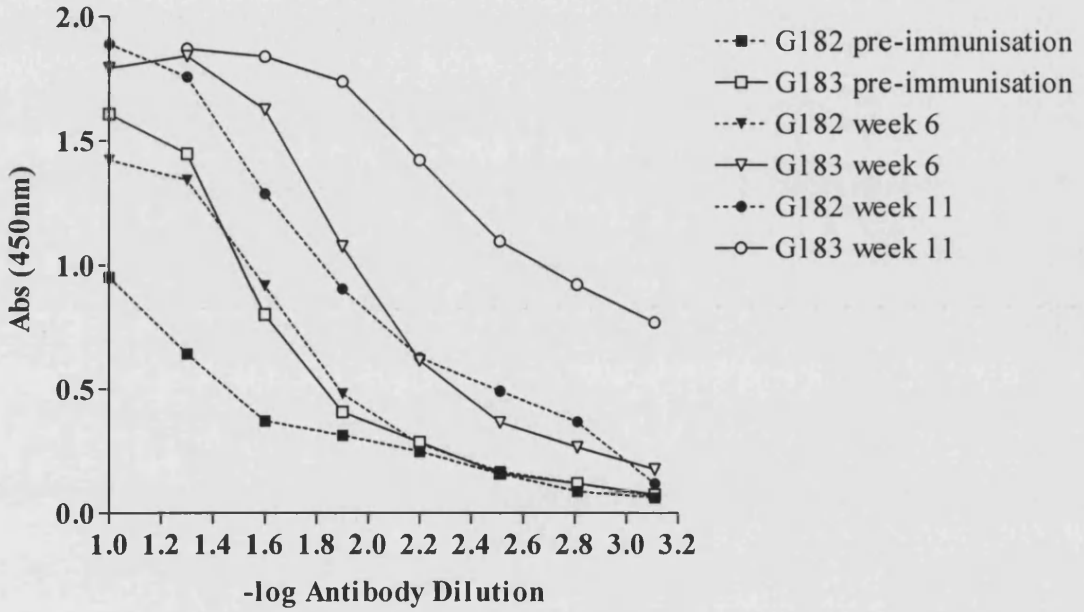

Figure 27. ELISA for antibodies raised against $G_{i\alpha 1/2}$. Sera from rabbits (G182 and G183) before immunisation, and after immunisation at weeks 6 and 11 were tested for antibody reactivity to the immunising peptide (homologous to the C-terminal region of $G_{i\alpha 1/2}$) by ELISA (*section 2.24*).

Using a commercially available antibody to $G_{i\alpha 1/2}$ (Serotec) it had been shown that the majority of $G_{i\alpha 1/2}$ is to be found localised to the plasma membranes in rat adipocytes (figure 28). Hence, using the anti-$G_{i\alpha 1/2}$ sera from the week 11 bleeds, plasma membranes obtained

from rat adipocytes were Western blotted for $G_{i\alpha 2}$ (recombinant $G_{i\alpha 2}$ from Santa Cruz Biotechnology was included on the gel as a positive control) (figure 29).

Figure 28. Western blotting of rat adipocyte subcellular fractions for $G_{i\alpha 1/2}$ using a commercially available antibody. Basal (B) and insulin-stimulated (I) rat adipocytes were homogenised and subcellular fractions isolated by ultracentrifugation. 20 μg aliquots of each sample were subjected to SDS-PAGE and electrophoretic transfer onto nitrocellulose membrane. The membrane was then Western blotted for $G_{i\alpha 1/2}$, using a commercially available antibody (Serotec).

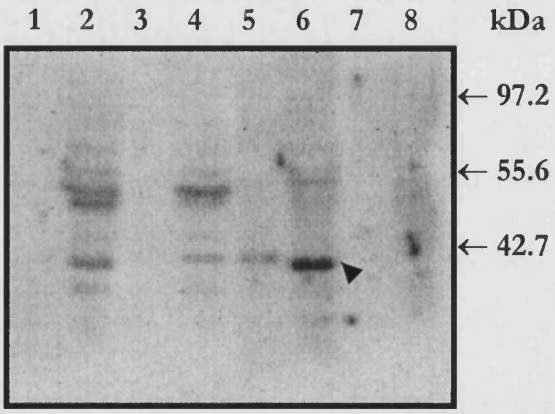

Figure 29. Western blotting of adipocyte plasma membranes using anti-$G_{i\alpha 1/2}$ sera (G182 and G183). 20 μg of adipocyte plasma membranes (lanes 2, 4, 6 & 8) or recombinant $G_{i\alpha 2}$ (lanes 1, 3, 5 & 7) were Western blotted for $G_{i\alpha 2}$ using antiserum G182 (lanes 1 & 2), or antiserum G183 (lanes 5 & 6). Serum from rabbits before immunisation were also used as a negative control (pre-immune serum G182 - lanes 3 & 4, pre-immune serum G183 - lanes 7 & 8).

The two anti-$G_{i\alpha 1/2}$ sera confirmed the ELISA result, with antiserum G183 (used at the same dilution as G182) detecting more $G_{i\alpha 1/2}$ than antiserum G182 (compare lanes 2 & 6, figure 29). Antiserum G183 also detected recombinant $G_{i\alpha 2}$ to a greater extent than antiserum G182 (lanes 1 & 5; the recombinant $G_{i\alpha 2}$ has a slightly higher molecular weight than the predicted molecular weight of native $G_{i\alpha 2}$). In both cases the pre-immune sera did not detect any $G_{i\alpha 1/2}$ (lanes 3, 4, 7 & 8).

Anti-$G_{i\alpha 1/2}$ serum G183 was then used to immunoprecipitate $G_{i\alpha 1/2}$ from rat adipocyte membranes (figure 30). However, as figure 30 shows, the antiserum did not immunoprecipitate the $G_{i\alpha 1/2}$ with high efficiency. Lane 1 represents 20 μg of plasma membrane protein, whereas 150 μg of plasma membrane protein was used for the immunoprecipitations (lanes 2 - 5). Protein samples used for immunoprecipitations were either solubilised in Triton X-100, lanes 4 & 5 (native conditions), or heated in a Tris-HCl buffer with 1% (w/v) SDS, lanes 2 & 3 (denatured conditions). Under both native and denatured conditions a protein band was detected specifically for the $G_{i\alpha 1/2}$ serum compared to the pre-immune serum (lanes 2 and 5), but only to the same extent as the positive control (lane 1). Increasing the amount of antiserum (and Protein A) had no effect on the amount of $G_{i\alpha 1/2}$ that could be detected. Similar results were produced by antiserum G182. Overall, it is concluded that whilst the antisera worked well in Western blotting, they were inefficient at immunoprecipitation.

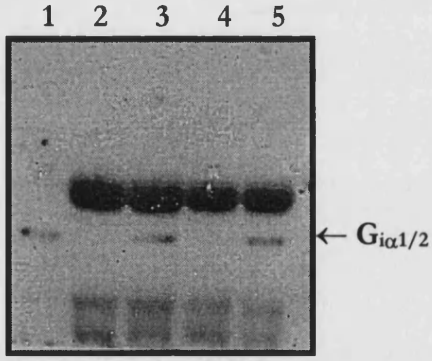

Figure 30. Immunoprecipitation of $G_{i\alpha 1/2}$ from adipocyte plasma membranes. 150 μg isolated plasma membranes were either denatured by heating to 95°C in a Tris-HCl buffer containing 1% (w/v) SDS (lanes 2 & 3) or solubilised in a 1% Triton X-100 solubilisation buffer (lanes 4 & 5). $G_{i\alpha 1/2}$ was then immunoprecipitated using antiserum G183 (lanes 3 & 5) or the respective pre-immune serum (lanes 2 & 4). Immunoprecipitates were then subjected to SDS-PAGE and Western blotting using G183 and Protein A-^{125}I for detection. Lane 1 is 20 μg of purified plasma membrane.

In situ periodate-oxidised GTP labelling followed by immunoprecipitation of $G_{i\alpha 1/2}$ from cell lysates failed to reveal any bands that could be assigned to the immunoprecipitated G-protein α-subunit. Similarly, immunoprecipitations of dynamin (which could be immunoprecipitated with a higher efficiency than $G_{i\alpha 1/2}$) also failed to reveal any bands that could be assigned to the GTPase. A typical result from an immunoprecipitation experiment which followed a periodate-oxidised GTP labelling is shown by figure 31. The left-hand panel shows the typical basal and insulin differences in labelling, whilst the right-hand panel shows the non-specific bands obtained from immunoprecipitation experiments.

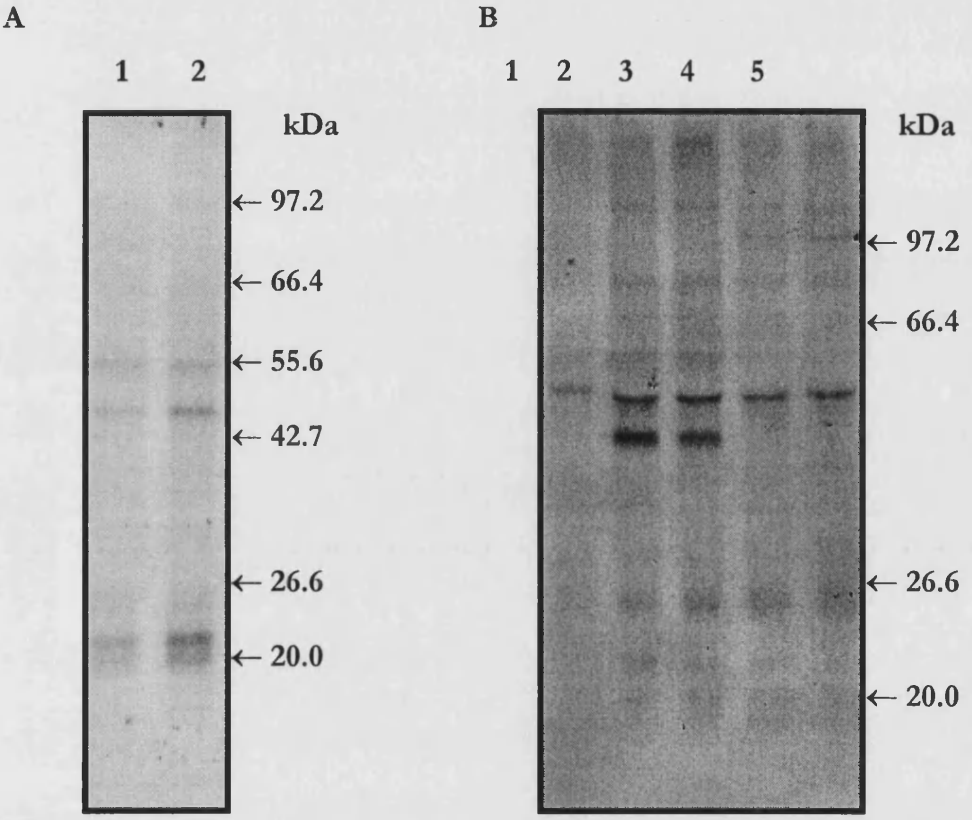

Figure 31. Immunoprecipitation of GTP-binding proteins following *in situ* periodate-oxidised GTP-labelling in rat adipocytes. Basal and insulin-stimulated rat adipocytes were permeabilised and labelled with periodate-oxidised [α-^{32}P]GTP. The typical basal and insulin responses as seen previously are shown (**A**) (lane 1- basal, lane 2 -insulin). Detergent soluble samples were immunoprecipitated for various GTP-binding proteins (see text) and the immunoprecipitates subjected to SDS-PAGE and autoradiography (**B**). Lane 1 represents non-specific bands associated with Protein A alone, lanes 2 & 3 - immunoprecipitates using pre-immune serum from basal and insulin-stimulated adipocytes respectively, lanes 4 & 5- immunoprecipitates using anti-GTP-binding protein serum (dynamin in this case) from basal and insulin-stimulated adipocytes respectively. Panel A represents a 4 h exposure, panel B a 3 day exposure.

4.8 Periodate-oxidised GTP-labelling of isolated GLUT4 vesicles.

It has been previously reported that use of the [α-^{32}P]GTP ligand blotting technique revealed that GLUT4 vesicles contain low molecular weight GTP-binding proteins (Cormont *et al.*, 1991). Hence, to compare the periodate-oxidised GTP labelling method with the ligand blotting method, GLUT4 vesicles were isolated and subsequently any associated GLUT4-vesicle GTP-binding proteins were labelled using periodate-oxidised [α-^{32}P]GTP. However no labelled proteins were detected by this method. Whilst immunoglobulins bound to the *Staphylococcus aureus* cells (*section 2.16*) could be seen by Coomassie staining on SDS-PAGE gels, it is uncertain whether the GLUT4 vesicles remained intact following the oxidation with the sodium periodate and the subsequent reductions with the borohydride compounds.

4.9 ADP-ribosylation factor (ARF)

Given the role of ARF isoforms in membrane trafficking processes (*section 1.14.2*) and the report of ARF translocation to plasma membranes in insulin-stimulated rat adipocytes (Karnam *et al.*, 1997), there is perhaps a precedence for the involvement of ARF in GLUT4 trafficking processes. Therefore, experiments were designed to identify whether ARF truly does translocate to plasma membranes as reported. Additionally experiments described below investigated the role of an association of ARF with GLUT4 vesicles.

4.9.1 ARF cellular localisation in basal and insulin-stimulated rat adipocytes

Basal and insulin stimulated rat adipocytes were subfractionated (*section 2.12*), to produce PM, LDM, HDM and cytosol fractions. Equal amounts of plasma membranes (20 μg) from basal and insulin-stimulated cells were Western blotted for GLUT4, syntaxin4 and ARF (figure 32). The blotting for GLUT4 clearly shows the increase of GLUT4 in the PM under insulin stimulated conditions. As a marker for protein loading on the SDS-PAGE gel, the plasma membranes were Western blotted for syntaxin4. Unlike GLUT4, syntaxin4 is found to be mainly localised to the plasma membrane, with plasma membrane concentrations remaining constant under insulin-stimulated conditions. The Western blot for syntaxin4 showed an equal amount of syntaxin4 in both basal and insulin-stimulated plasma membranes, under conditions where GLUT4 translocation to the plasma membrane can be observed. Similarly, using an ARF polyclonal antibody that recognises ARF isoforms 1,3,4,5 and 6 an increase in ARF protein levels in plasma membranes of rat adipocytes stimulated with 20 nM insulin was detected. Whilst ARF appeared to increase in plasma membranes of insulin-stimulated rat

adipocytes, a concomitant decrease in ARF protein was observed in the cytosol of insulin-stimulated adipocytes, compared to basal cells. No differences between basal and insulin samples were observed for ARF in the HDM or LDM fractions. The levels of ARF protein observed in the LDM fraction were very small (data not shown) and may represent cytosolic contamination, since the LDM pellets were not washed after isolation.

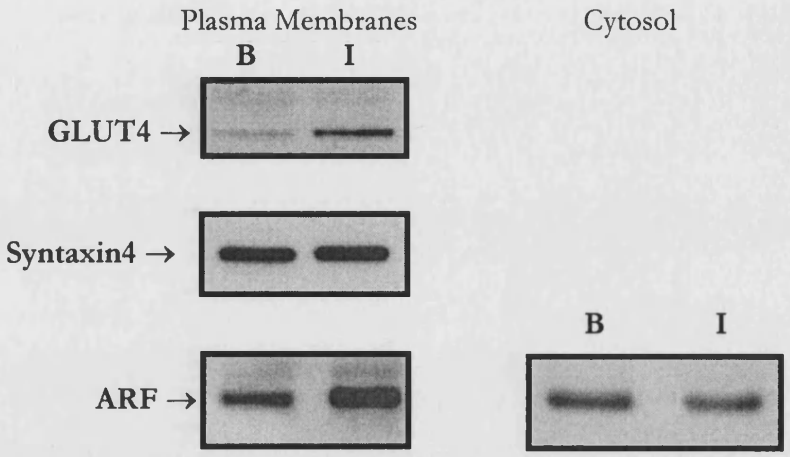

Figure 32. Western blotting of plasma membranes and cytosol fractions for ARF. Rat adipocytes were isolated and basal cells (B) or cells stimulated with 20 nM insulin for 20 min (I) were fractionated and the PM and cytosol fractions isolated. 20 µg aliquots of B and I samples were subjected to SDS-PAGE, followed by transfer onto nitrocellulose membrane. The nitrocellulose membrane was stained with Ponceau S and the nitrocellulose membrane cut to enable the blotting of GLUT4 at 45 kDa, syntaxin4 at 37 kDa and ARF at 20 kDa. No GLUT4 or syntaxin4 were found in cytosol preparations and therefore these results are not shown. The blots shown are from a single experiment, representative of three separate experiments.

4.9.2 ARF association with GLUT4 vesicles

To determine whether the translocation of ARF to plasma membranes upon insulin-stimulation is associated with GLUT4 vesicle translocation, GLUT4 vesicles were isolated and vesicle proteins Western blotted for ARF (figure 33). GLUT4 vesicles were isolated from the post-HDM supernatant of basal and insulin-stimulated adipocytes using *Staphylococcus aureus* cells pre-adsorbed with either rabbit serum containing anti-GLUT4 antibodies or with rabbit serum from non-immunised rabbits (pre-immune serum (PI)) (*section 2.16*). Vesicle proteins were solubilised in 1% Thesit. Bound immunoglobulins and GLUT4 were eluted from the *Staphylococcus aureus* cells with SDS-PAGE sample buffer heated to 95°C. To estimate the efficiency of GLUT4 vesicle isolation, 40 µg of the LDMs that remained after immunoprecipitation of the vesicles were also Western blotted for GLUT4. The various

immunoprecipitates were also Western blotted for the known GLUT4 vesicle protein, VAMP2. Western blotting for VAMP2 allows the integrity of the isolated GLUT4 vesicles to be determined. The top panel of figure 33, shows the Western blotting of GLUT4. The GLUT4 remains tightly associated with the anti-GLUT4 antibody bound to the *S. aureus* cells. Hence no GLUT4 were observed in samples solubilised by Thesit. However, the GLUT4 was eluted by SDS-PAGE sample buffer heated to 95°C. Under these conditions, rabbit serum containing anti-GLUT4 antibodies immunoprecipitated GLUT4 from both basal and insulin-stimulated post-HDM fractions. It could also be seen that since 50% of GLUT4 vesicles translocate to the plasma membrane under insulin-stimulated conditions, approximately 50% less GLUT4 vesicles were immunoprecipitated under insulin-stimulated conditions. The immunoprecipitation of the GLUT4 vesicles was found to be specific, since serum from non-immunised rabbits (pre-immune serum) failed to immunoprecipitate any GLUT4 as detected by Western blotting. The efficiency of the anti-GLUT4 serum compared to the pre-immune serum was determined by blotting a fraction of the remaining LDMs following the immunoprecipitations. Western blotting of these fractions showed that there was a greater reduction in the amount of GLUT4 in the LDM fraction following immunoprecipitation using specific anti-GLUT4 antibodies than using pre-immune serum. The efficiency of GLUT4 immunoprecipitation from this and other experiments was found to be approximately 60-70% for basal cells, and approaching 100% for insulin-stimulated cells (as determined by Western blotting and scanning densitometry). GLUT4 vesicle immunoprecipitation using 12 μg purified GLUT4 antibodies coupled to *S. aureus* cells was found to be more efficient and results in over 90 % efficiency for immunoprecipitation of GLUT4 from the LDM of basal cells (data not shown).

Figure 33. Isolation of GLUT4 vesicles and Western blotting for ARF and the known GLUT4 vesicle proteins GLUT4 and VAMP2. The post-HDM fraction was isolated from basal (B) and insulin-stimulated (I) rat adipocytes. Using *Staphylococcus aureus* cells pre-adsorbed with either pre-immune serum (PI) or rabbit serum containing anti-GLUT4 antibodies (GLUT4), GLUT4 vesicles were immunoprecipitated from the post-HDM fractions. Each immunoprecipitation used 50µl of serum conjugated to 40µl of *Staphylococcus aureus* cells and a post-HDM fraction equivalent to the post-HDM fraction obtained from one rat. Following a 2 h immunoprecipitation, *S. aureus* bound vesicle proteins were solubilised using 1% (v/v) Thesit in TES (Thesit soluble proteins), and immunoglobulins bound to the *Staphylococcus aureus* cells eluted with SDS-PAGE sample buffer heated to 95°C (Staph. cell bound proteins). The LDMs not bound to the *S. aureus* cells following immunoprecipitation were pelleted by centrifugation, of which 40µg was used in Western blotting (remaining LDMs). Thesit soluble protein fractions, Staph. cell bound proteins and remaining LDMs were then subjected to SDS-PAGE, and electrophoretic transfer onto nitrocellulose membrane. Nitrocellulose membranes were cut and Western blotted for either GLUT4 (top panel), ARF (middle panel) or VAMP2 (bottom panel). Positive blotting controls were included in the experiment; 50µg of rat basal low density microsomes (LDM) and cytosol (CYT).

The bottom panel of figure 33, shows that GLUT4 vesicles can be isolated intact, as shown by the Western blotting for VAMP2. VAMP2 was found in the Thesit solubilised fractions following GLUT4 immunoprecipitation, but not in fractions using pre-immune serum as the immunoprecipitating antibody. Like GLUT4, approximately 50 % less VAMP2 was observed in solubilised vesicle proteins from GLUT4 vesicles derived from insulin-stimulated cells, compared to basal cells. The solubilisation of vesicle proteins with Thesit was found to be 100% effective, since no VAMP2 was observed in any sample following the subsequent addition of sample buffer to the *S. aureus* cells and by heating to 95°C. Unlike GLUT4, it

appeared that 100% of VAMP2 containing vesicles were removed by immunoprecipitation of GLUT4 vesicles, whereas VAMP2 could still be observed in LDM fractions after immunoprecipitations using pre-immune rabbit serum.

Western blotting for ARF (middle panel, figure 33) showed that unlike VAMP2 no ARF could be detected in the Thesit solubilised fractions. This would indicate that ARF was not associated with the GLUT4 vesicles. This was confirmed by Western blotting of the remaining LDMs which showed that there were no differences between basal or insulin-stimulated samples. Furthermore, removal of GLUT4 vesicles by immunoprecipitation had no effect on the levels of ARF found in the LDM. A protein band was observed at the predicted molecular weight for ARF in samples removed from the *S. aureus* cells using SDS-PAGE sample buffer, but this is representative of a non-specific band, since no differences were seen between samples derived from either the pre-immune serum or anti-GLUT4 serum.

Inclusion of 600 μM GTP to the post-HDM supernatant had no effect on the association of ARF with GLUT4 vesicles (data not shown). However, inclusion of 600 μM GTPγS to the post-HDM supernatant resulted in the detection of ARF on GLUT4 vesicles (figure 34). There was also an association of ARF with immunoprecipiates that were obtained using pre-immune serum in the presence of GTPγS, but to a lesser extent to that obtained with specific immunoprecipitation of the GLUT4 vesicles. The effect of the GTPγS on ARF association with GLUT4 vesicles was also observed following inclusion of 20 μM GTPγS in the TES homogenisation buffer (figure 35).

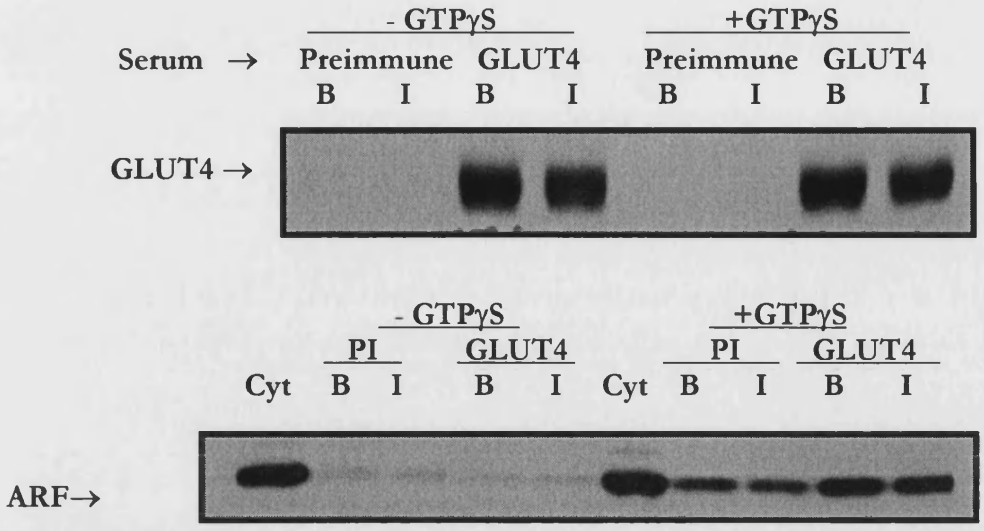

Figure 34. ARF association with GLUT4 vesicles with and without the presence of GTPγS. Post-HDM supernatants containing the low density microsomes (LDMs) were isolated from basal (B) and insulin-stimulated (I) rat adipocytes. Using *Staphylococcus aureus* cells pre-adsorbed either with rabbit serum from non-immunised rabbits (pre-immune serum (PI)), or rabbit serum containing anti-GLUT4 antibodies (GLUT4), GLUT4 vesicles were immunoprecipitated from the post-HDM supernatants, either with or without 600 μM GTPγS. Each immunoprecipitation used 50 μl of serum bound to 40 μl of *Staphylococcus aureus* cells with a post-HDM fraction equivalent to that obtained from one rat (an average of 300 μg of LDM protein). Following a 2 h immunoprecipitation, *S. aureus* bound vesicle proteins were solubilised using 1% (v/v) Thesit in TES, and immunoglobulins bound to the *Staphylococcus aureus* cells were eluted with SDS-PAGE sample buffer heated to 95°C. Thesit soluble proteins were Western blotted for ARF (lower panel; 40 μg of adipocyte cytosol (Cyt) was used as a positive control for blotting), and proteins were removed from the *S. aureus* cells by SDS-PAGE sample buffer and Western blotted for GLUT4 (upper panel).

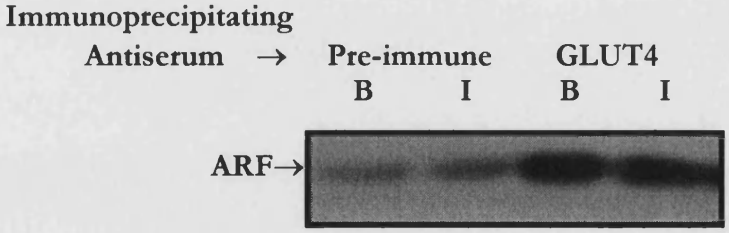

Figure 35. Western blotting for ARF associated with GLUT4 vesicles, isolated in the presence of 20 μM GTPγS. GLUT4 vesicles were immunoprecipitated from basal (B) and insulin-stimulated (I) rat adipocytes as described in previous experiments but with the inclusion of 20 μM GTPγS to the homogenisation buffer. Thesit soluble proteins from isolated vesicles were subjected to SDS-PAGE and electrophoretic transfer onto nitrocellulose. Membranes were then Western blotted for ARF.

4.10 Chapter 4 discussion

It is well established that GTP-binding proteins play important and diverse roles in membrane trafficking. In particular the Ras-like GTP-binding protein families, Rabs and ARFs, have been shown to be involved in numerous membrane trafficking events. GTP-binding proteins implicated in GLUT4 trafficking include Rab4 (*section 1.14.1*) and $G_{i\alpha 2}$ (*section* 1.14.3), but their roles in GLUT4 trafficking remain unclear.

Periodate-oxidised GTP-labelling. The method of periodate-oxidised GTP-labelling of GTP-binding proteins has several advantages over other methods ([α-^{32}P]GTP ligand binding and photocrosslinking of [α-^{32}P]GTP) to identify GTP-binding proteins. For instance, periodate-oxidised [α-^{32}P]GTP-labelling will radiolabel high molecular weight GTP-binding proteins, whereas [α-^{32}P]GTP ligand binding is restricted to the detection of low molecular weight GTP-binding proteins, since only small molecular weight proteins will renature upon transfer to nitrocellulose and form the GTP binding pocket. Additionally, periodate-oxidised GTP-labelling can be performed under equilibrium conditions which enables the labelling of low affinity nucleotide binding proteins, whereas GTP ligand binding only detects GTP-binding proteins that have very high binding affinities for GTP. The main advantage of periodate-oxidised GTP-labelling is that in addition to identifying GTP-binding proteins, under conditions where the exchange of GDP for GTP is stimulated i.e. GTP-binding protein activation, then the activation of GTP-binding proteins can be identified.

Using insulin-responsive permeabilised rat adipocytes, periodate-oxidised GTP-labelling revealed specific GTP-labelling of numerous proteins from ~20-120 kDa (figure 19). In particular, proteins at ~22-24 kDa and ~45 kDa showed marked increases in GTP-labelling upon insulin stimulation. The insulin-induced increased GTP-labelling of these latter proteins was reduced when the cells were treated with insulin in the presence of wortmannin. The GTP-labelling was consistently observed, and implied that GTP-binding proteins are activated by insulin downstream of a wortmannin sensitive PI 3-kinase. The molecular weight of the proteins, which showed increased GTP-labelling upon insulin stimulation, suggested that both Ras-like, and heterotrimeric GTP-binding proteins are activated by insulin downstream of PI 3-kinase. Whilst, insulin treatment increased GTP-labelling up to ~2.5-fold above basal GTP-labelling, 2D-gel electrophoresis failed to reveal any single protein that could account for the increased insulin-stimulated GTP-labelling. This latter result would suggest that more than one heterotrimeric GTP-binding protein and Ras-like protein are activated by insulin.

Unfortunately, the identification of these proteins was not possible using the techniques described.

The 2D-gel electrophoresis experiments showed that the highest degree of GTP-labelling was of proteins with a pI in the range ~4.0-5.5 and an apparent molecular mass of 21-25 kDa. It is likely that these labelled proteins are Ras-like GTP-binding proteins. However, it was difficult to interpret what the Ras-like GTP-binding proteins following periodate-oxidised GTP-labelling might be. This may be because periodate-oxidised GTP-labelling can cause a significant shift in the isoelectric focussing of proteins (Huber & Peter, 1994), and can shift the apparent molecular weight of proteins e.g. Ras on SDS-PAGE shifts from 21 to 25 kDa following periodate-oxidised GTP-labelling (Löw *et al.*, 1993).

Whilst numerous proteins were shown to be labelled by the periodate-oxidised GTP, there are some disadvantages of the technique. Firstly, the technique relied upon the covalent attachment of the oxidised GTP to an amino group, such as the ε-amino group of lysine. If an amino group is not present within, or close to, the GTP binding site, then GTP-labelling of the protein is unlikely to occur. Periodate-oxidised GTP-labelling of Ras was shown to covalently label two lysine residues namely K117 and K147, which are parts of the NKXD and SAK/L consensus elements of Ras-related proteins (Löw *et al*, 1993). The predicted amino acid sequences of Rab4 and $G_{i\alpha 2}$ both have the NKXD sequence in their predicted GTP-binding pocket (N^{121}KKD and N^{268}KKD respectively; protein accession numbers P05714 and P04696 respectively). Both Rab4 and $G_{i\alpha 2}$ would therefore be expected to be labelled by the periodate-oxidised GTP. However, immunoprecipitation of dynamin, Rab4 and $G_{i\alpha 2}$ following periodate-oxidised GTP-labelling failed to immunoprecipitate any of these proteins. These data raise a second limitation of the periodate-oxidised GTP-labelling technique. Whilst not assessed, it is possible that periodate-oxidation and borohydride reduction of proteins inflicts damage to an extent where they are no longer recognised by antibodies. Moreover, the excess borohydride added to samples was present on addition to Sepharose-conjugated antibodies that were used for immunoprecipitation reactions. Whilst experiments demonstrated that the antibodies remained attached to the Sepharose in the presence of the borohydride (25 and 50 kDa bands in Coomassie Blue stained gels) the reduction of the antibody by borohydride may have reduced antibody to antigen binding. Further experiments need to be undertaken to determine whether proteins such as Rab4 and

$G_{i\alpha 2}$ can still be immunoprecipitated under conditions which follow oxidation and reduction of proteins and borohydride reduction of antibodies.

The chemical crosslinking reaction probably destroys native protein structures, which can disrupt the association with other proteins. Hence, whilst Rab4 has been found associated with GLUT4 vesicles (Cormont *et al.*, 1993), GTP-labelling of immunoisolated GLUT4 vesicles may result in the dissociation of any GTP-binding protein with the GLUT4 vesicles. Therefore, it may be necessary to precipitate any proteins from the supernatant following GTP-labelling of proteins initially associated with the GLUT4 vesicles.

One final limitation of the periodate-oxidised GTP-labelling method is that proteins that have a slow rate of nucleotide exchange (exchange of GDP for GTP) are unlikely to become labelled. Many Ras-like proteins fall into this latter category. The action of accessory proteins, GEFs and GAPs, normally increase the rate of nucleotide exchange. Additionally, the concentration of free Mg^{2+} may alter the exchange of GDP for GTP. For instance, guanine nucleotide exchange rates on Ras are critically dependent on the Mg^{2+} concentration (Hall & Self, 1986). In high free Mg^{2+} nucleotide exchange rates on Ras are very slow and the half-life for nucleotide dissociation is around 60 min. In low free Mg^{2+} (0.1 μM) exchange is fast and the half-life is less than 1 min. The adipocytes were permeabilised in KRH buffer (containing 1.25 mM $MgSO_4$) supplemented with 4 mM Mg-ATP. Under these conditions the free Mg^{2+} concentration can be calculated to be ~1.6 mM (free Mg^{2+} was calculated using the freeware computer program BAD4 (v. 4.0) developed by Brooks & Storey, 1992). Hence, the relatively high free Mg^{2+} may have slowed guanine nucleotide exchange thereby reducing both insulin-responsiveness and periodate-oxidised GTP-labelling of GTP-binding proteins.

From the studies described here, it is difficult to know what proportion of GTP-binding proteins were labelled. If only a small proportion of GTP-binding proteins were labelled then a greater equilibrium incubation time with [α-^{32}P]GTP may result in increased labelling. However, an increased equilibrium incubation time with [α-^{32}P]GTP also means an increased time with α-toxin, which was shown to reduce adipocyte insulin-responsiveness.

The simplest procedure for labelling GTP-binding proteins is by u.v. irradiation of the labelled physiological ligand, [α-^{32}P]GTP. However, as mentioned previously, this method gives a low level of covalent incorporation and hence has low sensitivity. Photoaffinity labelling is usually

preferred over chemical affinity labelling because the photoaffinity label is generally more stable in solution, photoactivation is time controlled while chemical affinity labels usually react only with certain amino acids (as with periodate-oxidised GTP). Zor *et al.* (1995) describes the synthesis of a novel photoaffinity label, with high affinity, for GTP-binding proteins. The GTP-photolabel appears to have equal affinity for GTP-binding proteins compared to GTP, but unlike GTP the GTP-photolabel would appear not to be hydrolysed by GTP-binding proteins. The GTP-photolabel may therefore be a more powerful tool than periodate-oxidised GTP to identify GTP-binding proteins.

ADP-ribosylation factor (ARF). ARF proteins have been proposed to play several roles in the control of membrane traffic including endosome-endosome fusion (Lenhard *et al.*, 1992), formation of Golgi coated vesicles (Ktistakis *et al.*, 1996), adaptor protein recruitment to membranes (West *et al.*, 1997) and vesicular trafficking between the ER and the *cis*-Golgi compartment (Balch *et al.*, 1992).

Guanine nucleotide exchange on ARF is disrupted by the fungal metabolite, brefeldin A (BFA) (ARF6 is BFA insensitive). BFA has no inhibitory effects on insulin-stimulated translocation of GLUT4 to the PM in adipocytes (Chakrabarti *et al.*, 1994; Bao *et al.*, 1995; Kono-Sugita *et al.*, 1996). Although BFA treatment does not inhibit insulin-stimulated GLUT4 trafficking to the PM, it causes a 2-fold increase in basal glucose uptake (Bao *et al.*, 1995; Kono-Sugita *et al.*, 1996). BFA also interferes with the transport of some proteins between the PM, endosomes and the TGN (Lippincott-Schwartz *et al.*, 1991). Whilst GLUT4 internalisation from the PM does not appear to be affected by BFA treatment (Chakrabarti *et al.*, 1994), BFA may prevent GLUT4 trafficking from early-endosomes to the TGN. BFA treatment of adipocytes may therefore increase the levels of GLUT4 in the recycling endosomal pool, which may account for the small increase in glucose transport in basal BFA-treated adipocytes.

Experiments with BFA would suggest that the TGN is not the major functional source of GLUT4 undergoing insulin-mediated translocation to the PM. However, these data do not eliminate the TGN as a compartment utilised by GLUT4 *en route* to the formation of the major insulin-responsive GSVs. If BFA does inhibit GLUT4 trafficking between the PM and the TGN, then this can readily be tested. If GLUT4 is trapped within the recycling endosomal pool in cells treated with BFA, then removal of the insulin-stimulus from insulin and BFA treated cells would result in an elevated basal glucose transport compared to cells treated with

insulin alone. Furthermore, if GLUT4 is allowed to internalise following removal of the insulin stimulus in insulin and BFA treated cells, a subsequent insulin-stimulation may result in a reduced insulin-stimulated glucose transport. If reduced glucose transport occurs in this latter case it may be a direct result of GSVs not being regenerated, due to a lack of trafficking through the endocytic/TGN pathway.

Evidence for ARF being involved in GLUT4 vesicle trafficking is provided by data presented here, where ARF was found to associate with GLUT4 vesicles (figures 34 & 35). Smaller amounts of ARF were also found associated with Staph cells pre-adsorbed with non-specific rabbit serum. ARF loosely bound to Golgi membranes can be extracted with phosphatidylcholine (PC) liposomes (Helms *et al.*, 1993). PC liposomes failed to reduce ARF association with GLUT4 vesicles (data not shown), suggesting a strong interaction between ARF and GLUT4 vesicles. The interaction between ARF and GLUT4 vesicles was only apparent when GTPγS was added to the post-HDM supernatant or homogenisation buffer when isolating the vesicles. Inclusion of GTP to the post-HDM supernatant failed to cause an association between ARF and GLUT4 vesicles (data not shown). The association of ARF with GLUT4 vesicles that occurs in the presence of GTPγS but not GTP or under normal conditions, may be explained by the mechanism of ARF binding to membranes (Antonny *et al.*, 1997; Losonczi & Prestegard, 1998). In the GDP bound state ARF is mostly soluble but interacts transiently with membrane. The N-terminus of ARF is myristoylated and this enables it to insert into the bilayer. In addition, some basic residues of the N-terminus interact electrostatically with acidic phospholipids of the membrane. The weak interaction of ARF with membranes favours the interaction of ARF_{GDP} with an exchange factor. In the GTP-bound state, ARF is tightly bound to membranes. This longer-lived interaction is due to exposure of ARF N-terminal hydrophobic residues. These residues, which are buried in the GDP-bound state become available for anchoring ARF to the lipid bilayer when the protein switches to the GTP state. They provide the additional binding energy that, in addition to non-specific electrostatic interactions and insertion of the myristoyl group, permits a stable association of ARF with the membrane. Hence, non-hydrolysable GTPγS is likely to increase ARF association with membranes. Since GTP did not increase ARF association with GLUT4 vesicles then a high level of ARF GTPase activity is suggested. Whilst a small amount of ARF was found to bind non-specifically to the *S. aureus* cells, immunoprecipitation of GLUT4 vesicles using acrylamide beads instead of *S. aureus* cells reduced non-specific ARF binding (Gillingham *et al.*, 1999).

Further evidence for ARF association with GLUT4 vesicles is provided by the observations that GLUT4 vesicles can associate, with BFA sensitive, adaptor proteins, AP-1 and AP-3 (Gillingham *et al.*, 1999). Adaptor proteins appear to participate in two crucial events in trafficking processes, namely the physical formation of transport intermediates and the selection of cargo for transport (Hirst & Robinson, 1998). ARF1 has been shown to regulate the recruitment of both AP-1 and AP-3 to membranes (Zhu *et al.*, 1998; Ooi *et al.*, 1998). ARF and adaptor proteins are therefore likely to participate in the biogenesis of insulin-responsive GSVs.

Recently it has been shown that addition of myristoylated peptides corresponding to the N-terminus of ARF5 and ARF6 inhibited insulin-stimulated transferrin receptor and GLUT1 trafficking to the PM in permeabilised 3T3-L1 adipocytes (Millar *et al.*, 1999). Whilst myristoylated N-terminal ARF5 peptides did not significantly affect insulin-stimulated PM GLUT4 levels, the ARF6 peptide inhibited GLUT4 translocation to the PM by ~50%. Other studies have shown that overexpression of ARF6 can redistribute the transferrin receptor to the PM, while a dominant negative mutant of ARF6 was shown to redistribute transferrin receptors to intracellular membranes (D'Souza-Schorey *et al.*, 1995). Millar *et al.* (1999) have therefore suggested that ARF6 may be involved in insulin-stimulated GLUT4 trafficking to the PM, or alternatively ARF6 may be responsible for regulating GLUT4 internalisation from the PM. These data provide further evidence for the regulation of GLUT4 endocytosis by insulin (*section* 3.9).

ARF6 has been reported to be localised only to the PM in cultured mammalian cells (Cavenagh *et al.*, 1996). Furthermore the ARF-GEF, ARNO (*section 1.14.2*), has been shown to stimulate nucleotide exchange on both ARF1 and ARF6 (Paris *et al.*, 1997; Frank *et al.*, 1998). Insulin stimulation of 3T3-L1 adipocytes causes the translocation of ARNO to the PM (Venkateswarlu *et al.*, 1998). It was therefore suggested that the translocation of ARNO to the PM might activate ARF6 and regulate subsequent plasma membrane cycling events. If ARNO activates ARF6, and if active ARF6 blocks GLUT4 internalisation (Millar *et al.*, 1999), then ARNO translocation to the PM would cause a subsequent reduction of GLUT4 internalisation. Insulin treatment of adipocytes does inhibit GLUT4 endocytosis, but only to a small extent in comparison to the effects of insulin on GLUT4 exocytosis to the PM (Satoh *et al.*, 1993; Yang & Holman, 1993; Jhun *et al.*, 1992).

Insulin appeared to cause a redistribution of ARF from the cytosol to the PM (figure 32). This result is in agreement with Karnam *et al.* (1997) who also observed an insulin-stimulated translocation of ARF to the PM. Since BFA does not inhibit GLUT4 translocation to the PM, then the ARF translocated to the PM is unlikely to be ARF derived from GLUT4 vesicles. ARF association with GLUT4 vesicles, was only apparent in the presence of GTPγS and not GTP. This latter result suggests that under the conditions used to sub-fractionate the adipocytes ARF exhibits a high GTPase activity, probably due to the interaction with GAPs. A difference in the levels of PM ARF isolated from basal and insulin-stimulated adipocytes may have been detected as the PM was rapidly isolated from the cytosol (<30 min). Therefore cytosolic GAP activity associated with the PM may have been reduced thereby increasing the levels of GTP-bound ARF and hence a tighter association of ARF with the PM. A subfractionation of basal and insulin-stimulated adipocytes in the presence of GTPγS increased ARF association with all membrane fractions, with a reduction of ARF in the cytosol, however no major differences between basal and insulin-stimulated fractions were observed (data not shown). This indicates that since GTPγS increases ARF binding to membranes any differences that are due to insulin stimulation are no longer apparent. Both GDP and GTP bound to ARF will be exchanged for GTPγS resulting in the active conformation of all ARF isoforms. The translocation of ARF5 from the cytosol to the PM upon insulin stimulation of 3T3-L1 adipocytes has been observed (Millar *et al.*, 1999). Whether the translocation of ARF seen in figure 32 is due to ARF5 is difficult to assess without the use of specific ARF isoform antibodies.

In summary, it would appear from the GTP-oxidation and labelling experiments that in adipocytes both small Ras-like and heterotrimeric GTP-binding proteins are activated by insulin, and that in part these proteins are activated by insulin downstream of PI 3-kinase. ARF can associate with GLUT4 vesicles, and by recruiting adaptor proteins it is proposed that ARF can regulate the trafficking of GLUT4 from the PM back to the insulin-responsive GSVs. ARF was also observed to translocate from the cytosol to the PM upon stimulation of the adipocytes with insulin. It is possible that the observed translocation of ARF could be due to ARF5, and the ARF isoform associated with GLUT4 vesicles is ARF1. Isoform specific ARF antibodies are required to determine which ARF isoform can associate with GLUT4 vesicles, and which isoform translocates from the cytosol to the PM upon insulin stimulation. Further research is required to determine whether any of these events are BFA sensitive.

CHAPTER 5

PROTEIN KINASE B

PART A - The effects of okadaic acid on PKB activity in rat and human adipocytes

Whilst PKB activity has been shown to be dependent upon PI 3-kinase activation, it is still not clear whether PKB is necessary for insulin-stimulated GLUT4 translocation. Since the mode of activation of PKB is primarily by serine and threonine phosphorylation, the non-specific serine/threonine phosphatase inhibitor okadaic acid (OA) (*section 1.15*) was used to correlate the effects of phosphatase inhibition on both PKB activity and GLUT4 translocation in both human and rat adipocytes.

5.1 Glucose transport and PKB activity in human adipocytes treated with okadaic acid

Human adipocytes were isolated (*section 2.7*) and treated either with or without 20 nM insulin and/or 1 μM OA. Adipose cells were then either assayed for 3-OMG transport, or lysed and PKB immunoprecipitated for PKB activity measurements. Figure 36A shows that insulin stimulation of the human adipose cells produces a 3.5-fold increase in the 3-OMG transport rate (0.011 ± 0.001/s in insulin-stimulated cells compared to 0.0033 ± 0.0001/s in basal cells). This was mimicked by the OA, which produced a 3-OMG uptake rate constant of 0.0125 ± 0.002/s. Unlike experiments by Rondinone & Smith (1996), the 3-OMG transport rate in adipose cells treated with both OA and insulin were found not to be additive compared to insulin stimulation alone (0.0143 ± 0.008/s for cells treated with insulin and OA compared to 0.0125 ± 0.002/s for insulin-stimulated cells).

Insulin stimulation of human adipocytes produced a 14-fold increase in PKB activity (figure 36B) (46.76 ± 10.36 fmol/min/ml 40% cells in insulin-stimulated cells compared to 3.244 ± 0.908 fmol/min/ml 40% cells in basal cells). By contrast cells treated with OA alone, only exhibited a 2-fold increase in PKB activity (7.490 ± 2.520 fmol/min/ml 40% cells). Insulin and OA treatment together gave a 10- fold increase in PKB activity (31.17 ± 8.849 fmol/min/ml 40% cells) compared to basal cells. However PKB stimulation by both insulin and OA was significantly lower (approximately 35%) than adipocytes stimulated by insulin alone.

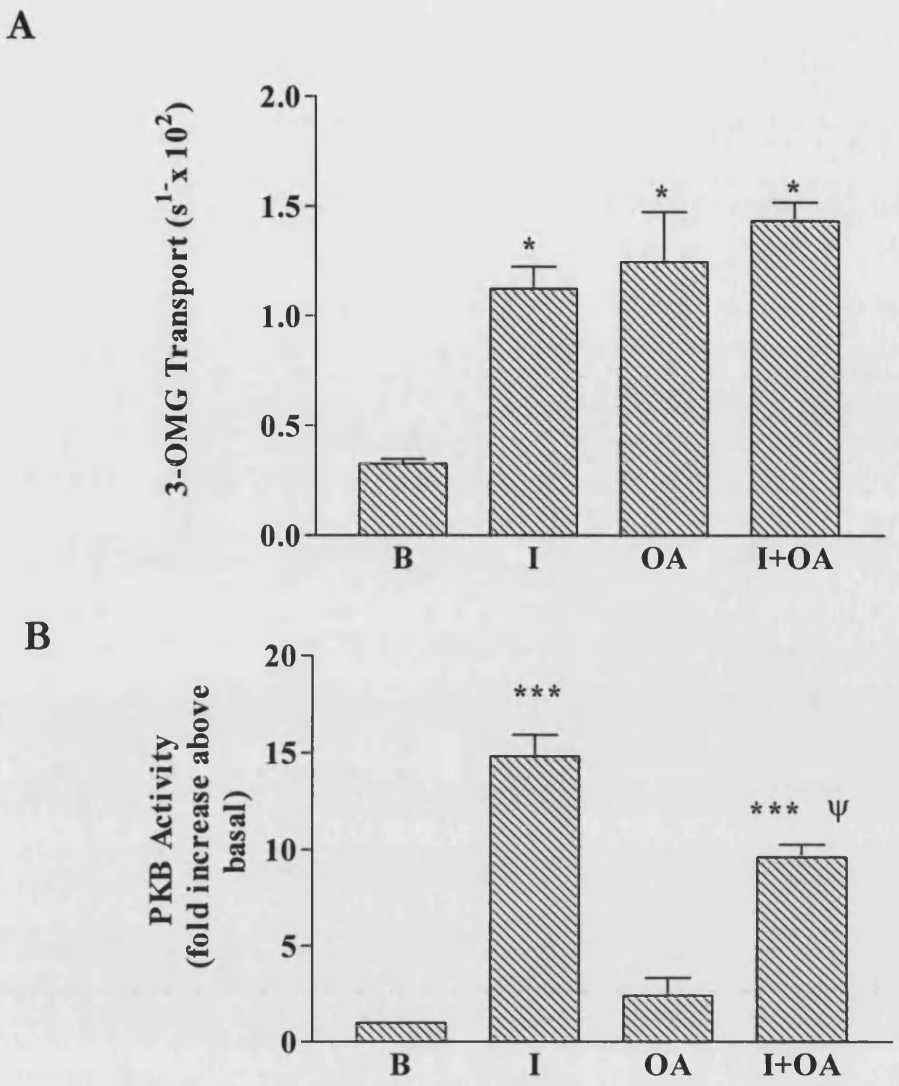

Figure 36. 3-OMG transport and PKB activity in human adipose cells treated with insulin and/or okadaic acid. Human adipocytes were isolated and treated with or without 1 μM okadaic acid (OA) for 20 min and then with or without 20 nM insulin (I) for 30 min. Adipose cells were then either directly used in determining the rate of uptake of 50 μM 3-OMG (**A**) or lysed and PKB immunoprecipitated for PKB activity measurements (**B**). Data are means ± SEM for 3 separate experiments. * $P < 0.05$ vs B, *** $P < 0.001$ vs B, ψ significantly different from insulin, $P < 0.05$.

5.2 Okadaic acid effects on 3-OMG transport and PKB activity in rat adipocytes

Whereas 1 μM OA stimulated 3-OMG transport in human adipocytes to an extent comparable with the insulin stimulation, this was not found for rat adipocytes. In rat adipocytes, OA stimulated the 3-OMG transport rate 10-fold above basal levels (from 0.003/s in basal cells to 0.030/s in okadaic acid treated cells). However the stimulation produced by OA was only 16% of that observed following insulin treatment (0.030/s for OA treated cells compared to 0.183/s for insulin treated cells) (figure 37).

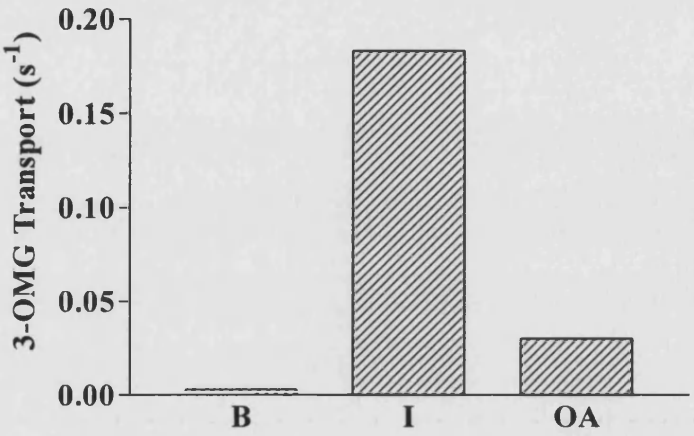

Figure 37. 3-OMG transport in rat adipocytes stimulated with 1 μM okadaic acid. Isolated rat adipocytes were either incubated with either 20 nM insulin (I) or 1 μM okadaic acid (OA) for 20 min, or with no additions (B). The rates of uptake of 50 μM 3-OMG were then determined. Data is from a single experiment.

Additionally, treatment of rat adipose cells with OA failed to significantly stimulate PKB. It was shown that while insulin stimulated PKB 7-fold over basal cells (88.73 fmol/min/ml 40% cells compared to 12.11 fmol/min/ml 40% cells in basal cells), OA only produced an ~2-fold increase in PKB activity (22.56 fmol/min/ml 40% cells) over basal cells (only 25% of the insulin stimulated activation) (figure 38).

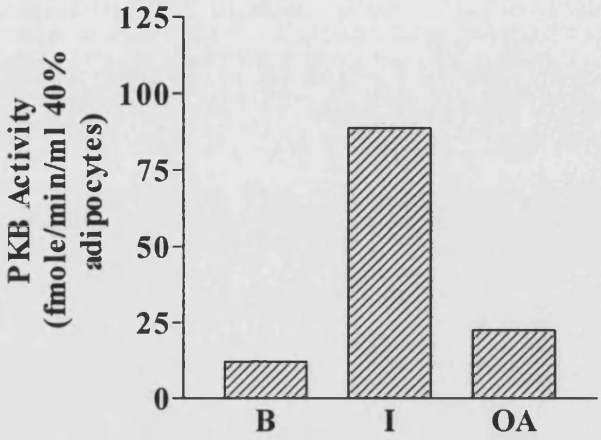

Figure 38. PKB activity in insulin and okadaic acid stimulated rat adipose cells. Isolated rat adipocytes were stimulated with either 20 nM insulin (I) or 1 μM okadaic acid (OA), for 20 min at 37°C, or incubated with no additions (B). Cells were then lysed and PKB immunoprecipitated from detergent soluble lysates. The measurements of the PKB activity were performed directly on the immunoprecipitates. Results are means from 2 separate experiments.

PART B - PKB activity in contraction- and insulin-stimulated soleus muscle

In contrast to the insulin-mediated signalling leading to GLUT4 translocation in adipocytes, little is known about intracellular signalling mechanisms through which muscle contraction elicits glucose transport and GLUT4 translocation. Whilst muscle contraction appears to be independent of PI 3-kinase activation (Lund *et al.*, 1995; Yeh *et al.*, 1995), it is conceivable that muscle contraction stimulates a pathway that utilises common steps to that of insulin signalling. Hence further studies were undertaken to see if PKB may be a candidate for a common mediator of insulin- and contraction-stimulated glucose transport.

5.3 PKB activity in isolated rat soleus muscles

To investigate whether muscle contraction and insulin stimulate GLUT4 translocation, *via* PKB, rat soleus muscles were stimulated *in vitro* with either insulin, insulin following a pre-treatment with wortmannin (100-1000 nM), or by contraction (5 min at 10 Hz with square-wave pulses of 0.5 ms duration and 10 V amplitude). This part of the experiment was carried out by Dr Sten Lund (Aarhus, Denmark). Muscles were then frozen. Muscles were subsequently homogenised and solubilised in a 1% (v/v) Triton X-100 buffer (*section 2.9*). PKB was immunoprecipitated from the detergent-soluble lysates and the PKB activity was directly measured in the immunoprecipitates. Figure 39 shows that insulin stimulated PKB activity ~4-fold above basal levels in muscle samples (15.2 ± 0.5 fmole/min/mg compared to 3.9 ± 0.3 fmole/min/mg for basal muscles). Addition of 100 nM or 1 μM wortmannin inhibited the insulin-stimulated increase in PKB activity in the soleus muscles. The resulting levels of activity were below those of basal muscles (1.1 ± 0.1 and 0.8 ± 0.1 fmole/min/mg respectively).

In contrast to insulin stimulation, muscle contraction did not induce activation of PKB activity above basal levels (3.9 ± 0.3 fmole/min/mg in basal muscles compared to 4.2 ± 0.5 fmole/min/mg in contracted muscles). The combined effect of insulin and contraction also failed to stimulate PKB activity above that already activated by insulin alone (insulin 15.2 ± 0.5 fmole/min/mg compared to insulin and contraction 13.55 ± 3.1 fmole/min/mg). The PKB activity in muscles treated with either insulin or wortmannin corresponded to both 3-OMG transport and GLUT4 photolabelling with ATB-[^{3}H]BMPA (Lund *et al.*, 1998). However, whilst the PKB activity in contraction-stimulated muscles were not higher than basal PKB activity levels, muscles stimulated by contraction were observed to have 3-fold higher levels of

both 3-OMG transport and GLUT4 photolabelling compared to basal muscle samples (Lund *et al.*, 1998).

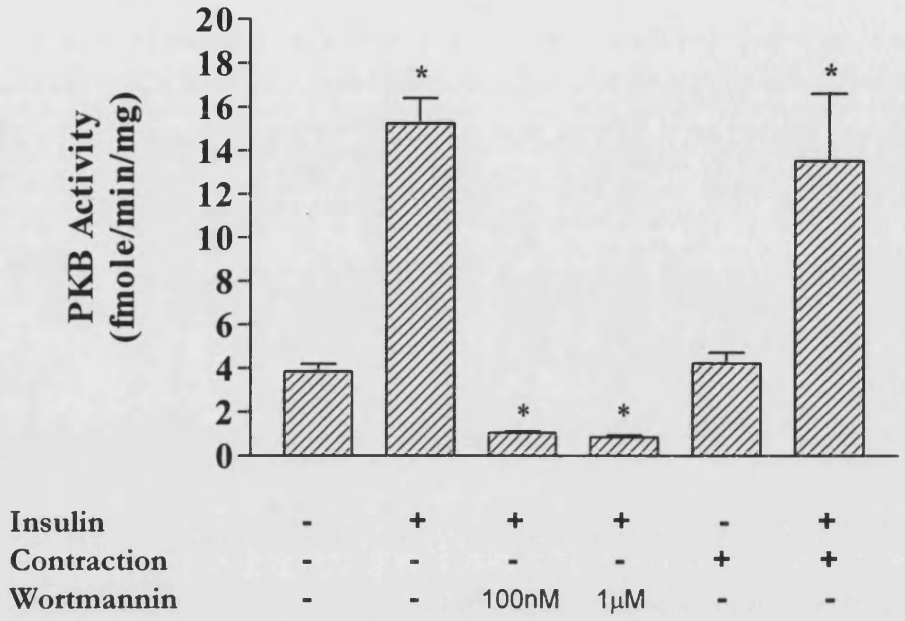

Figure 39 PKB activity in isolated rat soleus muscles. Soleus muscles from Wistar rats were either stimulated with insulin and/or by contraction. Some muscles were stimulated by insulin following a 10 min pre-treatment with either 100 nM or 1 μM wortmannin. Following these treatments, muscle samples were homogenised and the PKB activity was measured in PKB immunoprecipitates from detergent-soluble lysates. Data are means ± SEM from six separate experiments. * $P < 0.001$ vs. basal samples.

5.4 Chapter 5 discussion

PKB and glucose transport in rat and human adipocytes treated with OA. It is unclear as to whether PKB activation is necessary for insulin-stimulated GLUT4 translocation to the PM (*section 1.12*). The phosphorylation of serine and threonine residues on PKB is required for PKB activation. The non-specific serine/threonine phosphatase inhibitor, okadaic acid (OA), has been shown to elicit a partial insulin-like response on glucose transport in rat adipocytes (Lawrence *et al.*, 1990; Corvera *et al.*, 1991; Rondinone *et al.*, 1996) and a full insulin response on glucose transport in human adipocytes (Rondinone & Smith, 1996). It was therefore hypothesised that inhibition of PKB dephosphorylation may elevate PKB activity and possibly cause an increase in GLUT4 translocation to the PM.

In both human adipocytes and rat adipocytes, treatment of the adipocytes with OA only increased PKB activity 2-fold above basal PKB activity. In these studies, the antibody used to immunoprecipitate PKB from the adipocytes immunoprecipitates both PKBα and PKBβ, but not PKBγ. PKBγ is not activated by insulin in adipocytes (Walker *et al.*, 1998) and is therefore an unlikely candidate to be involved in insulin-stimulated GLUT4 translocation to the PM. The possibility that OA stimulates PKBγ cannot be assessed here, and further work would be required to determine whether PKBγ is involved in GLUT4 translocation to the PM. OA treatment of rat adipocytes gave a 2-fold increase in PKB activity, 14% of the insulin-stimulated PKB activity. The OA-stimulated increase in PKB activity corresponded to a 10-fold increase in glucose transport (16% of the insulin-stimulated glucose transport). The OA-stimulated increase in glucose transport is in complete agreement with data obtained by Rondinone *et al.*, (1996).

As discussed in chapter 3, there appears to be spare receptor and signalling capacity in adipocytes in the pathway that leads to the elevation of GLUT4 translocation. Only 14% of the maximal insulin receptor kinase activity in rat adipocytes, and 10% of the insulin-stimulated PI 3-kinase activity in 3T3-L1 adipocytes, is required to activate glucose transport maximally (Klein *et al.* (1991) and unpublished data respectively). Furthermore, the results in chapter 3 suggest that a 2-fold increase in PKB activity in rat adipocytes (after a 24 h chronic-insulin treatment) can still give rise to a normal rate of GLUT4 exocytosis (compared to acutely insulin-stimulated cells). Hence, if PKB is involved in insulin-stimulated GLUT4 translocation to the PM, then a 2-fold OA-stimulated increase in PKB activity, might be expected from data discussed above, to be sufficient to elicit a full insulin-like translocation of

GLUT4 to the PM. However, the OA-stimulated PKB activity in rat adipocytes only corresponds to 16% of the maximal insulin-stimulated glucose uptake. This could suggest that PKB activity is not involved in insulin-stimulated GLUT4 trafficking. Alternatively, OA might be stimulating PKBγ, which is not stimulated by insulin in rat adipocytes, and therefore is unlikely to contribute to insulin-stimulated GLUT4 trafficking. Furthermore, platelet-derived growth factor can stimulate PI 3-kinase to the same extent as insulin, without a significant increase in glucose transport (Wiese *et al.*, 1995). This result suggests that the location of PI 3-kinase is critical for determining its role in GLUT4 trafficking. Similarly, the site of action of PKB activity may also be a determining parameter in eliciting the insulin-stimulated GLUT4 translocation to the PM. OA may inhibit cytosolic phosphatases and hence activate PKB at a membrane site distinct from that activated by insulin which may act on a specific membrane targeted PKB.

It might not be valid to compare the PKB activity in freshly isolated and chronic-insulin treated adipocytes. The chronic-insulin treated cells represents a system whereby processes downstream of PKB might maintain a high 'signalling activity' despite reductions in PKB activity. Furthermore, at concentrations of insulin that stimulate maximal glucose transport (0.7 nM insulin, Satoh *et al.*, 1993) in rat adipocytes, PKBβ activity is 100% of the maximal insulin-stimulated PKBβ activity, and PKBα is ~55% of the maximal insulin-stimulated PKBα activity (Walker *et al.*, 1998), suggesting that PKBβ activity and PM GLUT4 levels correlate.

In contrast to the rat adipocyte data, the small OA activation of PKB activity in human adipocytes was associated with a level of stimulation of 3-OMG uptake that was comparable to insulin stimulation. The differences between the rat and human adipocytes may simply be explained by differences between the two cell types. In human adipocytes, ATB-BMPA studies determined that insulin-stimulated human adipose cells contain approximately 9.9 x 10^4 GLUT4 molecules in the plasma membrane, compared to 195 x 10^4 GLUT4 molecules in the plasma membrane of insulin-stimulated rat adipocytes (Simpson *et al.*, 1983). The low abundance of GLUT4 can account for the low V_{max} for 3-OMG transport in human adipocytes compared to rat adipocytes. Additionally, it was shown that in the basal state of human adipocytes, approximately 25% of the GLUT4 is at the cell surface (compared to 2% for rat adipocytes), whilst in the insulin-stimulated state 50% of the GLUT4 was shown to be at the cell surface (as for rat adipocytes)(Kozka *et al.*, 1995). Furthermore, it was shown by

Kozka *et al.* (1995) that the V_{max} for 3-OMG were very similar in human and rat adipocytes in the basal state. It was therefore suggested that the larger human adipocytes have adapted to release a greater proportion of the total cellular pool of GLUT4, to provide the basal metabolic needs of the adipocyte. Hence, the residual intracellular-pool of GLUT4 that is available to respond to insulin is lower in the human than the rat adipocyte. Therefore, insulin-stimulates glucose transport in human adipocytes by only ~3-fold, in comparison to the 40-fold increase in rat adipocytes. If the same proportion of the intracellular GLUT4 pool were to translocate to the PM upon OA-stimulation in both rat and human adipocytes, then the OA-stimulation in human adipocytes would be more insulin-mimetic, since there is a smaller intracellular-pool of GLUT4 to respond to the OA.

Without further studies, it is unclear to what extent the activation of PKB by OA contributes to OA-stimulated glucose uptake. The 2-fold increase in OA-stimulated PKB activity in both human and rat adipocytes is probably not due to increased phosphorylation of PKB and therefore an increase in its activity. The increased PKB activity more likely represents a situation where activated PKB molecules under basal conditions are prevented from being dephosphorylated in the presence of OA. Hence, the low level of PKB activity in basal cells becomes slightly elevated.

If PKB stimulation by OA does not correspond to elevations in OA-induced glucose transport, then how can the effects of OA be explained? One interesting scenario that would require further investigation, would be the idea that OA stimulates the recycling endosomal pool. The recycling endosomal pool contains the transferrin receptor, GLUT1 and a proportion of the intracellular GLUT4. In 3T3-L1 adipocytes, the recycling endosomal pool contains ~40% of intracellular GLUT4 protein (Livingstone *et al.*, 1996), whereas in rat adipocytes ~10% of the intracellular GLUT4 protein co-localises with the transferrin receptor (Gillingham *et al.*, 1999). Assuming that GLUT4 continuously recycles in human adipocytes as in rat adipocytes, then since 25% of the GLUT4 is on the cell surface in human adipocytes, the recycling endosomal pool may contain a higher proportion of recycling GLUT4 than rat adipocytes. The differences in the quantities of GLUT4 in the recycling endosomal pool could account for the differences observed between the OA-stimulation of glucose transport in human and rat adipocytes. OA stimulation of the rate of exocytosis from the recycling endosomal pool would result in an increase in GLUT4 on the cell surface to a small extent in rat adipocytes, and perhaps to a greater extent in human adipocytes.

Evidence that OA may stimulate the recycling endosomal pool is provided by ablation studies in 3T3-L1 adipocytes (Livingstone *et al.*, 1996). In insulin-stimulated 3T3-L1 adipocytes, the percentage of GLUT1 than can be ablated decreases from 68% to 34% upon insulin stimulation (Livingstone *et al.*, 1996). Similarly, when 3T3-L1 adipocytes were treated with OA, the GLUT4 ablation was decreased from 40% to 26%. The latter result suggests that less GLUT4 is located in the recycling endosomal pool after OA stimulation. This result was explained by the idea that OA inhibited GLUT4 endocytosis in the basal state resulting in increased GLUT4 levels at the cell surface and an increase in glucose transport (Livingstone *et al.*, 1996). However, studies in rat adipocytes have shown that OA stimulates the exocytosis rate constant of GLUT4 trafficking to the PM by ~3-fold, but with no significant changes in the endocytotic rate constant (Rampal *et al.*, 1995). Hence, an alternative explanation for the reduced ablation of GLUT4 upon OA stimulation is that this reagent stimulates the exocytosis of GLUT4 from the recycling endosomal pool in a manner similar to insulin. In human adipocytes, treatment of the cells with both insulin and okadaic acid, does not give an additive effect on glucose transport (figure 36A). This suggests that OA stimulates GLUT4 translocation from an intracellular GLUT4 pool that is also stimulated by insulin. Whilst insulin and OA treatment of human adipocytes does not alter glucose transport in comparison to insulin stimulation alone, the OA and insulin treatment reduces PKB activity. This can be explained by consideration of the observation that OA induces the phosphorylation of serine and threonine residues on IRS-1, and that this reduces insulin-stimulated tyrosine phosphorylation of IRS-1 (Tanti *et al.*, 1994). Therefore, the reduced IRS-1 phosphorylation (and presumably IRS-2) is likely to reduce downstream signalling, such as PI 3-kinase and PKB. In the combined insulin and OA treatment the lowered PKB activity may still be sufficient to elicit GLUT4 translocation to the PM from the recycling endosomal pool. Alternatively, OA may exert its effects downstream of PKB to cause GLUT4 translocation, or the insulin-stimulated translocation of the endosomal recycling pool is a PKB-independent process. This last idea has some precedence from a recent study which has indicated that in 3T3-L1 adipocytes the insulin stimulation of the recycling-endosomal pool does not require PKB activity (Foran *et al.*, 1999).

The observation that insulin-stimulated GLUT1 translocation to the PM is inhibited by wortmannin (Clarke *et al.*, 1994) suggests that the insulin-stimulation of the exocytosis of GLUT1 and GLUT4 from the recycling endosomal pool is dependent upon PI 3-kinase. However, in rat adipocytes wortmannin is not inhibitory to the insulin-mimetic effect of OA on glucose transport activity (Rondinone *et al.*, 1996). This suggests that since PKB requires

activation by PI 3-kinase the action of OA is exerted downstream of, or independent of PKB. Additional serine/threonine kinases may exist, which can be activated by OA-inhibition of a phosphatase activity.

If OA stimulates the exocytosis of GLUT1 and GLUT4 from the recycling endosomal pool independently of PKB, then a serine/threonine kinase is likely to regulate the trafficking of the recycling endosomes. This could possibly explain the effect of phorbol esters on glucose transport. As discussed in the introduction, PMA (an activator of cPKC and nPKC isoforms) has only a small effect on increasing glucose transport in rat adipocytes, similar to OA. cPKC and nPKC isoforms do not appear to play a major role in insulin-stimulated GLUT4 trafficking. A PKC isoform might be involved in regulating the recycling of early-endosomes, since PMA can stimulate GLUT1 exocytosis to the same extent as insulin (Holman *et al.*, 1990; Saltis *et al.*, 1991). Both OA and PMA can cause phosphorylation of GLUT4 (Gibbs *et al.*, 1986; Joost *et al.*, 1987; Lawrence *et al.*, 1990). However, insulin alone does not cause GLUT4 phosphorylation (Gibbs *et al.*, 1986; Joost *et al.*, 1987; Lawrence *et al.*, 1990). GLUT4 phosphorylation induced by OA and PMA may therefore promote its exocytosis to the PM, *via* a pathway not normally stimulated by insulin.

PKB activity in contraction-stimulated muscle. Although muscle contraction does not stimulate glucose transport by a PI 3-kinase-dependent mechanism (Lund *et al.*, 1995; Yeh *et al.*, 1995; Lee *et al.*, 1995), there is some evidence that there may be a common pathway downstream of PI 3-kinase. For example, polymyxin B, an inhibitor of PKC, inhibits both insulin- and contraction-stimulated glucose transport (Henriksen *et al.* 1989). Furthermore, it was shown that the calcium channel blocker verapamil could inhibit both insulin- and contraction-stimulated glucose transport (Cartee *et al.*, 1992). It is therefore possible that insulin and contraction may share some common signalling step. PKB was appealing since PKB has been shown to be activated by cAMP independently of PI 3-kinase (Sable *et al.*, 1997).

Insulin stimulated PKB activity about 4-fold above basal in rat soleus muscles. This is in good agreement with published data achieved in rat skeletal muscles after *in vivo* insulin administration (Cross *et al.*, 1997). The increase in PKB activity was shown to correlate with the fold increase in glucose transport activity and cell surface GLUT4 content observed after insulin stimulation (Lund *et al.*, 1998). Wortmannin treatment of the muscle samples completely abolished the insulin-induced PKB activity, confirming previous reports that the regulation of PKB is mediated by a wortmannin-sensitive PI 3-kinase. However, maximal

electrically stimulated muscle contraction, which increased both glucose transport and cell surface GLUT4 (Lund *et al.*, 1998), did not induce activation of PKB above basal activity. The combined effect of insulin and contraction also failed to affect PKB activity further than that already activated by insulin alone. However, the maximal stimulatory effect of both insulin and muscle contraction were shown to be completely additive on both glucose transport activity and PM GLUT4 content (Lund *et al.*, 1998). These data indicate that at some level in the signalling pathways, there are different mechanisms leading to the stimulatory actions of insulin and muscle contraction. However, the PKB data clearly demonstrates that insulin- and contraction-induced activation pathways do not converge at the level of PKB and that PKB is not involved at all in contraction-induced glucose transport and GLUT4 translocation in rat soleus muscle (Lund *et al.*, 1998). This conclusion is in precise agreement with a subsequent study by Broznick, Jr. & Birnbaum (1998).

CHAPTER 6

PHOSPHATIDYLINOSITIDE-BINDING PROTEINS

Current evidence suggests that insulin-stimulated PI 3-kinase activity is necessary to stimulate GLUT4 translocation to the plasma membrane (*section 1.9*). It is postulated that the lipid products of PI 3-kinase are involved in the route for further downstream processes leading to GLUT4 translocation (*section 1.11*). However, the mechanisms by which PI 3-kinase lipid products stimulate glucose transport are still not clear. Therefore, in order to identify targets of the PI 3-kinase lipid products, a collaboration was established with Professor G. D. Prestwich, University of Utah. The collaboration provided novel photoaffinity probes and affinity resins based upon PI(3,4)P2 and PIP3. The aim of the work described in this chapter was to utilise these photoaffinity probes and affinity resins to identify PI(3,4)P2 and PIP3 binding proteins in rat adipocytes.

6.1 Benzophenone based photolabels

The PI(3,4)P2 and PIP3 photoaffinity probes utilise a photoactivatable benzophenone group, which is chemically more stable than other photolabelling groups such as diazo esters, aryl azides and diazirines. Benzophenone-containing probes also have the advantage of being able to be manipulated in ambient light and activated at wavelengths which avoid protein damage. Additionally the benzophenone-probes react preferentially with unreactive C-H bonds, even in the presence of solvent water and bulk nucleophiles. Incorporation of the photolabel into proteins is achieved by photoactivation of the benzophenone group (figure 39). These processes, and the use of benzophenone photophores in biochemistry, are reviewed by Dormán & Prestwich (1994).

6.2 Synthesis of phosphoinositide-based photolabels and affinity resins

The phosphoinositide based photolabels are formed by a series of chemical syntheses, ultimately generating an ω-aminopropyl tethered analogue of PIP3, PI(3,4)P2 or PIP2 (Prestwich, 1996). Reaction of the terminal amine group with 4-benzoyl-[2,3-^{3}H]-dihydrocinnamoyl *N*-hydroxysuccinimide ([^{3}H]BZDC-NHS) (Olszewski *et al.*, 1995) results in the photolabel (figure 40). By attachment of the photophore *via* a flexible linker at some distance from the ligand recognition site, a photolabel is generated which has ligand-target selectivity and a degree of efficiency similar to that of the benzophenone molecule alone. Alternatively the phosphoinositide analogue is coupled to Affi-Gel 10 (Bio-Rad), where a crosslinked-agarose matrix bearing *N*-hydroxysuccinimide (NHS) functional groups is covalently bound to the amine group resulting in a phosphoinositide affinity matrix (figure 40).

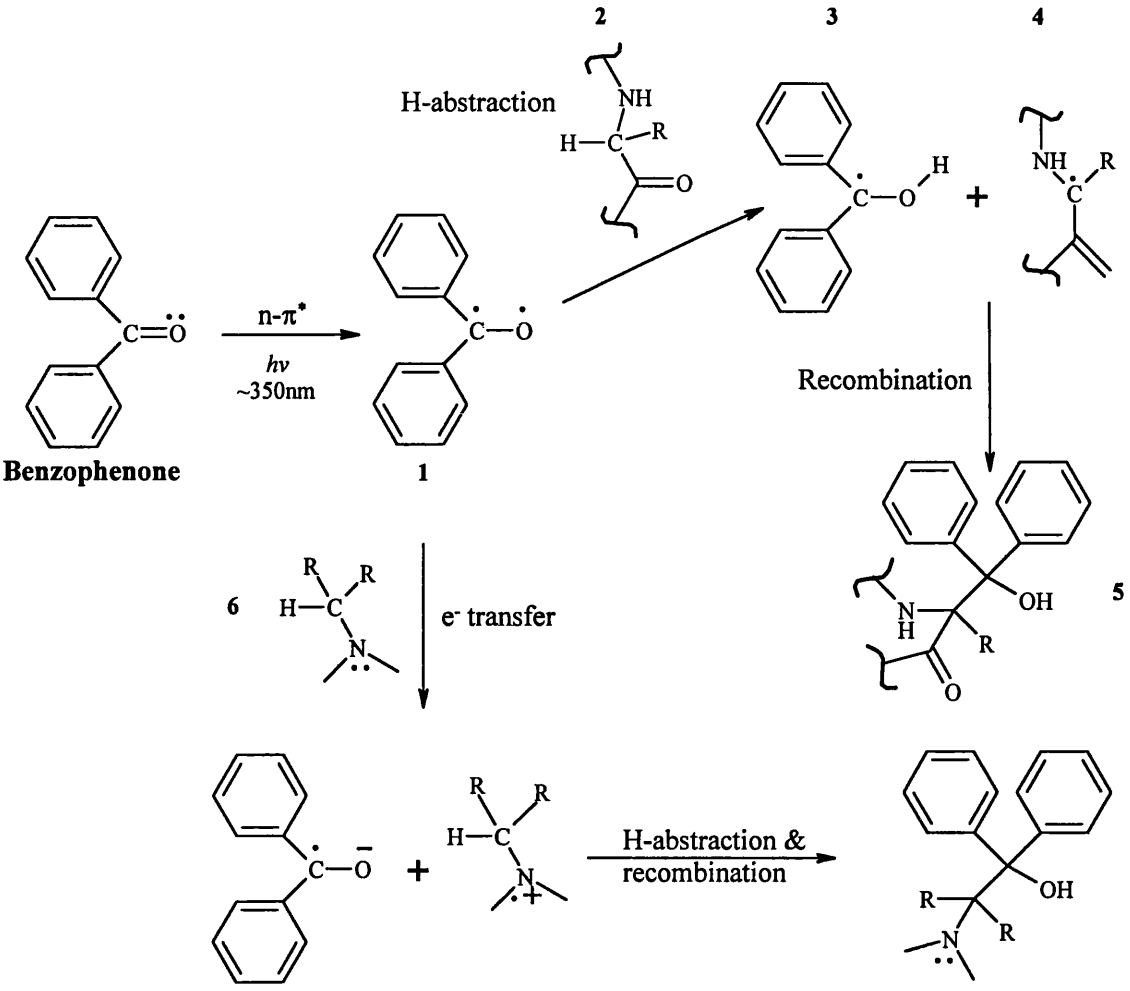

Figure 39. Photochemistry of the benzophenone photophore. Absorption of a photon at ~350 nm results in the promotion of an electron from a non-bonding n-orbital on the oxygen, to an antibonding π^*-orbital of the carbonyl group. This results in a diradical triplet state (**1**) in which the oxygen n-orbital is electrophilic. The excited state may last 80-120 μs, before relaxation back to the ground state and regeneration of the benzophenone moiety. However, if in the excited state the geometry of the electron-deficient oxygen orbital allows interaction with a weak C-H σ-bond, such as those found in the backbone of polypeptides (**2**), then hydrogen abstraction can occur, to complete the half-filled n-orbital. The resulting ketyl (**3**) and alkyl (**4**) radicals that are formed can readily recombine to generate a new C-C bond, producing benzpinacol-type compounds (**5**). Alternatively, if the excited triplet state is proximal to an amine or similar heteroatom, then an electron-transfer step can occur (**6**). This is followed by proton abstraction from an adjacent alkyl group and a radical 1,2-shift. Radical recombination can then occur as previously described. These reactions are the basic processes that follow benzophenone photoactivation, but other radical reaction pathways can exist.

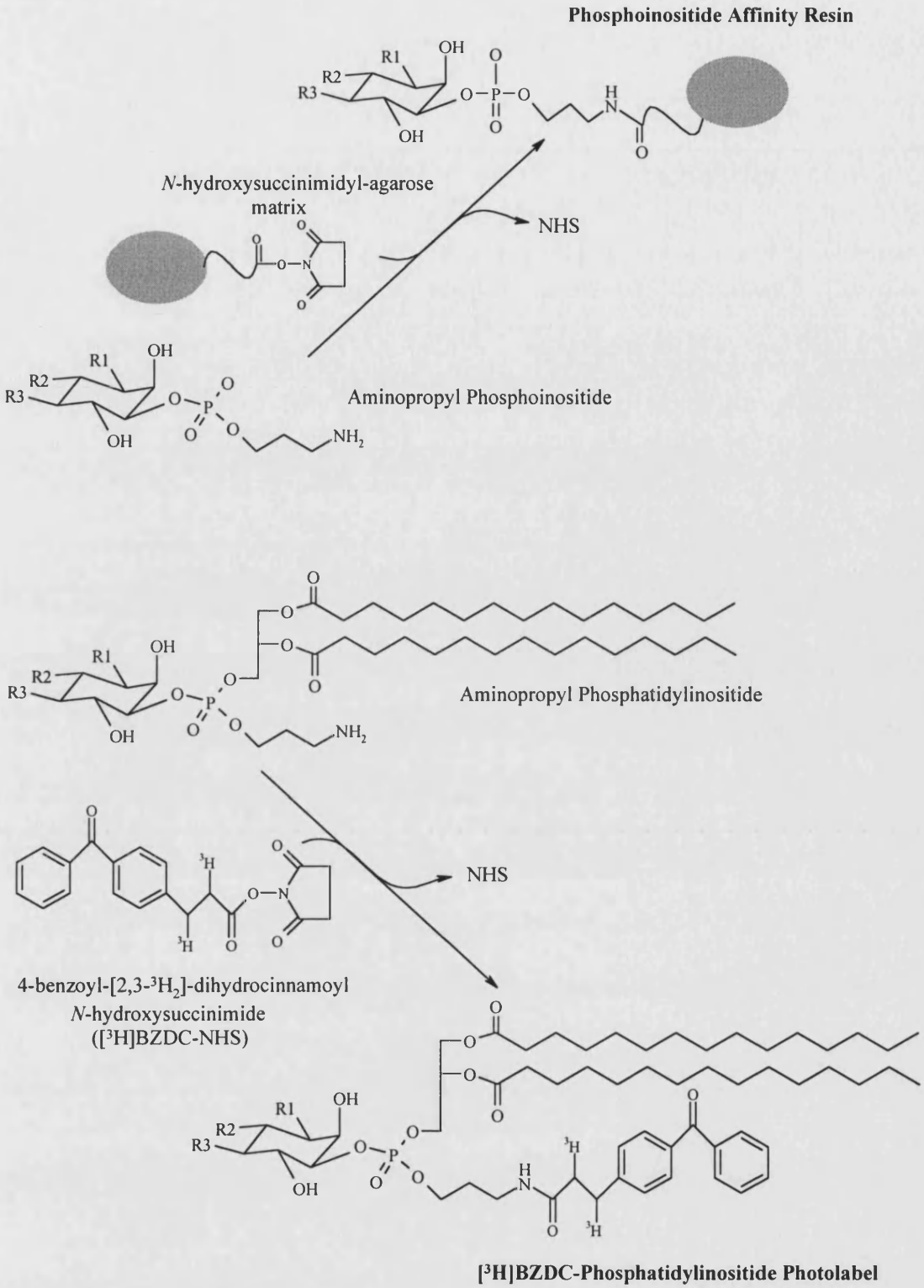

Figure 40. Structures of phosphoinositide analogues bearing either an agarose matrix or [^{3}H]BZDC-photolabelling group. PI(3,4)P2 analogues - $R_1 = R_2 = OPO_3^{-2}$, $R_3 = OH$. PIP3 analogues - $R_1 = R_2 = R_3 = OPO_3^{-2}$. PIP2 analogues - $R_1 = OH$, $R_2 = R_3 = OPO_3^{-2}$

6.3 Photolabelling rat adipocyte whole cell homogenates using [^{3}H]BZDC-phosphatidylinositides

A whole cell lysate was prepared from rat adipocytes and proteins were photolabelled with the PIP2, PIP3 and PI(3,4)P2 [^{3}H]BZDC analogues. After the photolabelling reaction, the radiolabelled proteins were subjected to SDS-PAGE and visualised by fluorography (*section 2.26*). The fluorograph of photolabelled proteins from a whole cell lysate is shown in figure 41. Analysis of the fluorograph revealed labelling of numerous proteins with all three photolabels, with a greater degree of labelling with the PI(3,4)P2-photolabel. The higher degree of photolabelling with the PI(3,4)P2-photolabel probably represents a higher concentration of the photolabel, and not an increased affinity for the PI(3,4)P2 analogue itself, since an overall higher background labelling was observed. Proteins binding phosphatidylinositides phosphorylated at the D-3 position of the inositol ring are proteins of interest. Hence, the fluorograph was analysed for proteins that bound the PIP3- and PI(3,4)P2-photolabels and not the PIP2-photolabel.

At least three proteins appeared to be selectively photolabelled by the PI(3,4)P2- and PIP3-photolabels relative to the PIP2-photolabel (indicated by arrows, figure 41). The proteins uniquely photolabelled by the PIP3 photolabel appeared to run as a doublet with an approximate molecular mass of 38 kDa (lane 3, figure 41). The PIP3 photolabelled protein doublet was therefore termed p38. The proteins uniquely photolabelled by PI(3,4)P2 appeared to run as a doublet with an approximate molecular mass of 37 kDa and a single protein at approximately 39 kDa (indicated by arrows, lane 5, figure 41). These latter proteins were termed p37 and p39.

The photolabelling of p38 was not non-specific labelling since it was reduced by competition of the [^{3}H]BZDC-photolabel with 100 μM dipalmitoyl-PIP3 included into the photolabelling reaction (lane 4, figure 41). Similarly, although dipalmitoyl-PI(3,4)P2 was not available at the time of the experiment, dipalmitoyl-PIP3 was also found to reduce the [^{3}H]BZDC-PI(3,4)P2 photolabelling of both p37 and p39 (lane 6, figure 41). This latter result is not wholly unexpected, since most proteins which bind PI(3,4)P2 are also found to bind PIP3, albeit with varying affinities (*section 1.11*).

Overall, the whole cell lysate photolabelling with the [^{3}H]BZDC-phosphatidylinositides revealed at least three proteins, p37, p38 and p39, which may represent targets of the lipid products of PI 3-kinase.

Since the literature generally indicates that proteins which bind PI(3,4)P2 also bind PIP3 (*section 1.11*), it is possible that due to the additional phosphate group on the PIP3 photolabel compared to the PI(3,4)P2 photolabel, then p37 and p38 may be the same protein.

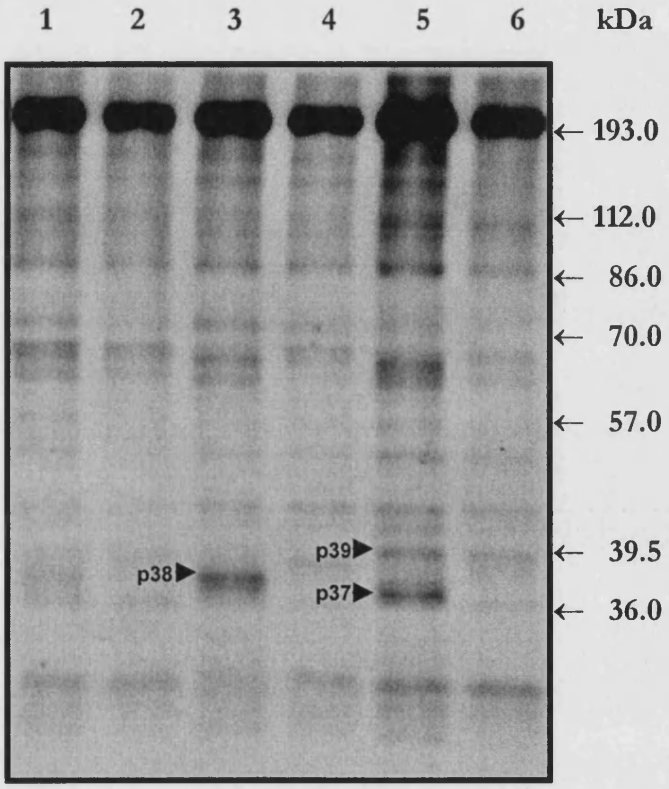

Figure 41. [^{3}H]BZDC-Phosphatidylinositide photolabelling of an adipocyte whole cell homogenate. Basal adipocytes were homogenised and the infranatant removed from the fat. 50 μg aliquots of the homogenate were then photolabelled with 0.2 μCi of [^{3}H]BZDC-PIP2 (lanes 1 and 2), [^{3}H]BZDC-PIP3 (lanes 3 and 4) or [^{3}H]BZDC-PI(3,4)P2 (lanes 5 and 6), in the presence of 100 μM dipalmitoyl-PIP2 (lane 2) or 100 μM dipalmitoyl-PIP3 (lanes 4 and 6). Radiolabelled proteins were analysed by SDS-PAGE and fluorography.

6.4 [^{3}H]BZDC-phosphatidylinositide photolabelling of adipocyte subcellular fractions

Both basal and insulin stimulated rat adipocytes were homogenised and subcellular fractions isolated to determine the cellular location of the PI(3,4)P2 and PIP3 binding proteins, p37, p38 and p39, and whether or not their cellular distribution altered in insulin stimulated cells.

Labelling by the three photolabels was observed in PM, LDM and HDM fractions. However, specific labelling for either PI(3,4)P2 or PIP3 relative to PIP2 was not observed in the PM, LDM or HDM fractions. Furthermore, no differences in labelling due to insulin-stimulation were detected in these fractions.

In the cytosolic fraction, slight differences in labelling were observed between basal and insulin-stimulated samples, but this may have been representative of slight differences in protein loading on the gel (noticeable by observation of the Coomassie Blue stained proteins). A pattern of photolabelling of proteins specific for the PIP3 and PI(3,4)P2 labels, was found in the cytosolic fraction (figure 42) that was similar to that observed in lysates (figure 41). Photolabelling of p37, p38 and p39, are indicated by arrows (figure 42).

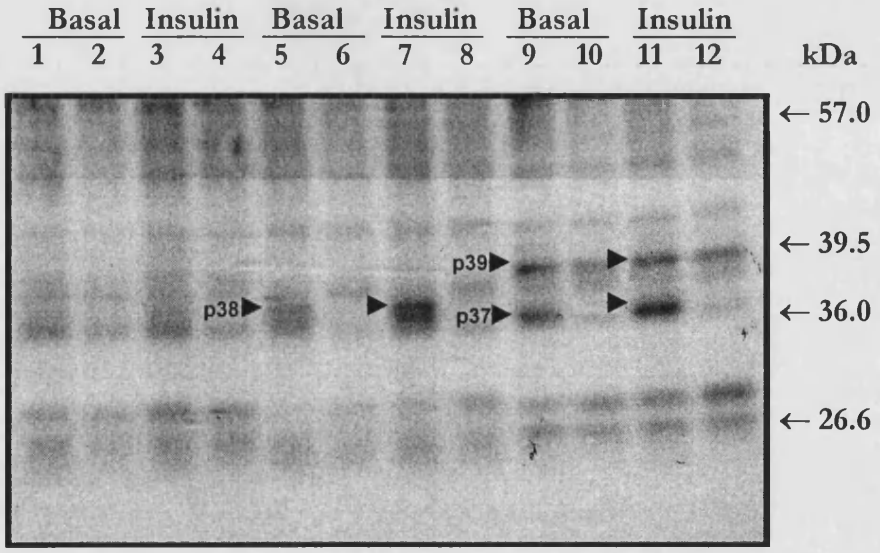

Figure 42. [^{3}H]BZDC-Phosphatidylinositide photolabelling of basal and insulin-stimulated rat adipocyte cytosol. Rat adipocytes were homogenised and the cytosol isolated. 50 μg protein aliquots were photolabelled using 0.2 μCi of [^{3}H]BZDC-PIP2 (lanes 1-4), [^{3}H]BZDC-PIP3 (lanes 5-8) or [^{3}H]BZDC-PI(3,4)P2 (lanes 9-12). Non-specific labelling was determined by the inclusion of 100 μM dipalmitoyl-PIP2 (lanes 2 and 4) or 100 μM dipalmitoyl-PIP3 (lanes 6, 8, 10 and 12) in photolabelling reactions. Radiolabelled proteins were analysed by SDS-PAGE and fluorography.

The photolabelling of p39 by [^{3}H]BZDC-PI(3,4)P2 was not totally reduced in the presence of cold di-palmitoyl-PIP3 (lanes 10 and 12). This was interpreted as being either due to non-specific labelling, or due to a significantly lower K_m for PI(3,4)P2 compared to PIP3.

6.5 Purification of phosphatidylinositide-binding proteins by heparin-agarose chromatography

The [^{3}H]BZDC-photolabels and affinity resins have been used in the detection and purification of the PIP3 binding protein centaurin-α from rat brain (Hammonds-Odie *et al.*, 1996). Communication with G. Prestwich and A. Theibert (co-authors on the aforementioned publication), suggested that a protocol similar to that used for the identification of centaurin-α, would be appropriate to purify the PI(3,4)P2 and PIP3 binding proteins, p37, p38 and p39. Such a protocol requires heparin-agarose chromatography followed by affinity chromatography.

Heparin-agarose chromatography often yields a rapid, efficient initial purification of phosphoinositide-binding proteins (Theibert *et al.*, 1997). It has been proposed that rather than acting as a conventional cation exchange resin (since many of the proteins that interact strongly have neutral pI), heparin-agarose, a polysulfated glycosaminoglycan, may act as a pseudo-affinity resin.

A 5 fold dilution of the cytosol with 10 mM Tris-HCl, pH 7.2, 5 mM EDTA, and incubation with heparin-agarose allowed binding of p37, p38, but not p39 (figure 43) to the heparin-agarose. The dilution of the cytosol is required to lower the concentration of endogenous inositol or phosphate containing compounds that might interfere with binding to the heparin-agarose (personal communication with A. Theibert). Proteins, p37 and p38, were found in the heparin eluate fraction (lanes 3 and 6, figure 43) and were more concentrated relative to the initial cytosol fraction (comparing equivalent amounts of protein). Furthermore, the heparin-agarose step appeared to increase the relative concentration of a protein, designated as p40, that photolabelled with the PI(3,4)P2- but not the PIP3-photolabel (lane 6, figure 43).

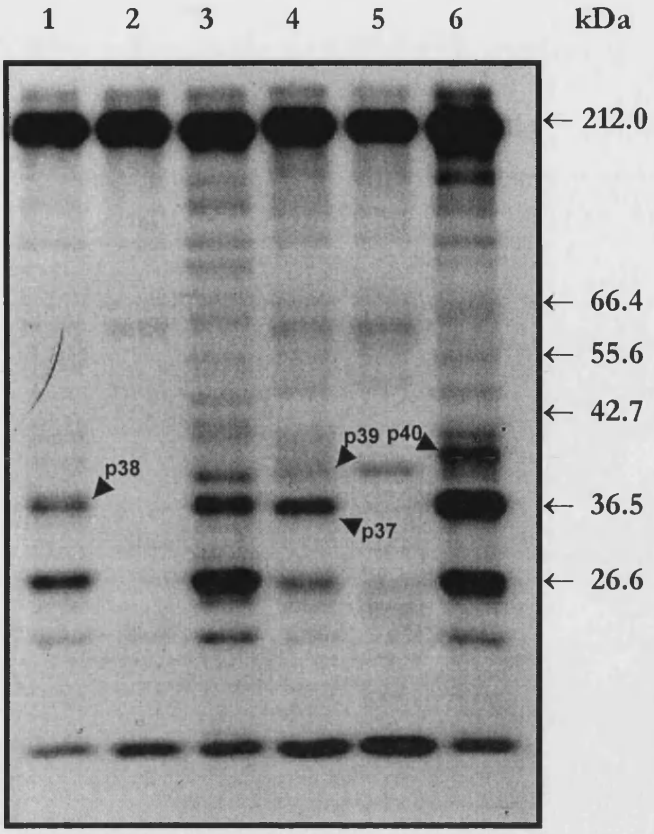

Figure 43. Photolabelling of heparin-agarose eluates. Rat basal cytosol was incubated with heparin-agarose for 2 h in 10 mM Tris-HCl, pH 7.2, 5 mM EDTA. Unbound proteins were removed and bound proteins eluted with 2 M NaCl. Cytosol fraction (lanes 1 and 4), unbound proteins (lanes 2 and 5) and eluted proteins (lanes 3 and 6) were photolabelled with [^{3}H]BZDC-PIP3 (lanes 1-3) or [^{3}H]BZDC-PI(3,4)P2 (lanes 4-6).

Additionally, it was observed that the majority of PI(3,4)P2 and PIP3 photolabelled proteins were in the heparin eluate fraction. Protein measurements indicated that approximately 50% of the cytosolic proteins bound to the heparin-agarose column. This indicated a degree of non-specific binding to the heparin-agarose, so cytosolic proteins were bound to heparin with varying NaCl concentrations (0-250 mM), eluting with 1.5 M NaCl.

Analysis of the profile of binding to the heparin under varying concentrations of NaCl, revealed that p37 and p38 eluted between 50-100 mM NaCl, whereas p40 eluted with 150-200 mM NaCl. A subsequent experiment therefore bound the cytosolic proteins to the heparin in the presence of 50 mM NaCl, then proteins were eluted stepwise with 175 mM NaCl, then 300 mM NaCl. Under these conditions, protein measurements revealed that 90% of the cytosolic protein did not bind to the heparin, and the remaining 10 % was eluted from the

heparin-agarose using 175 mM and 300 mM NaCl. Figure 44 shows part of a Coomassie Blue stained profile of 50 μg of each of these fractions following photolabelling and SDS-PAGE.

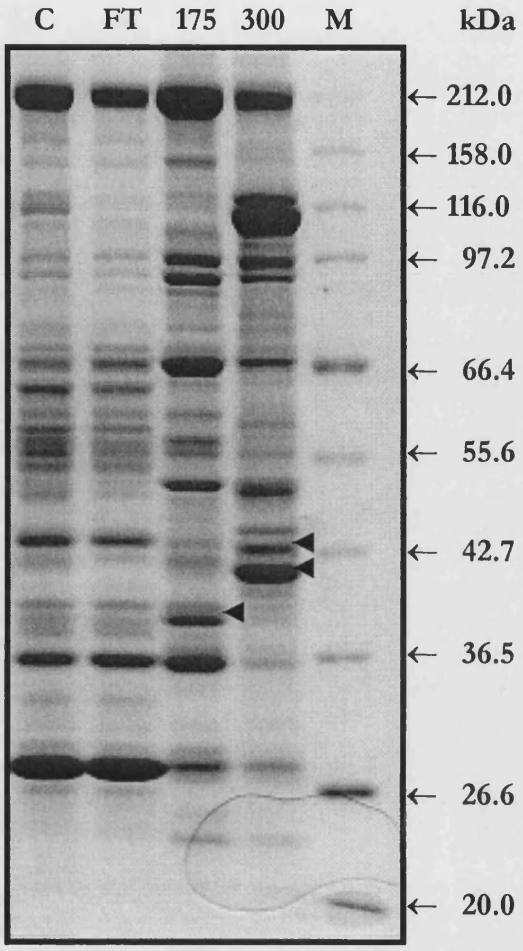

Figure 44. Coomassie Blue stain of cytosolic proteins eluted from heparin-agarose with 175 and 300 mM NaCl. Cytosolic proteins (~ 22 mg) were bound to heparin-agarose in the presence of 50 mM NaCl. Proteins were then eluted stepwise using 175 mM NaCl then 300 mM NaCl. The NaCl was removed from the samples and 50 μg aliquots of cytosol (C), proteins not bound to the heparin-agarose (FT), 175 mM NaCl eluate (175) and 300 mM NaCl elute (300) were photolabelled with the [^{3}H]BZDC-photolabels. Samples were then analysed by SDS-PAGE, stained with Coomassie (as above) and fluorography (figure 45). Broad range markers used in most experiments for approximate molecular mass determination of proteins is shown (M). The fluorography of the above gel is shown by figure 45.

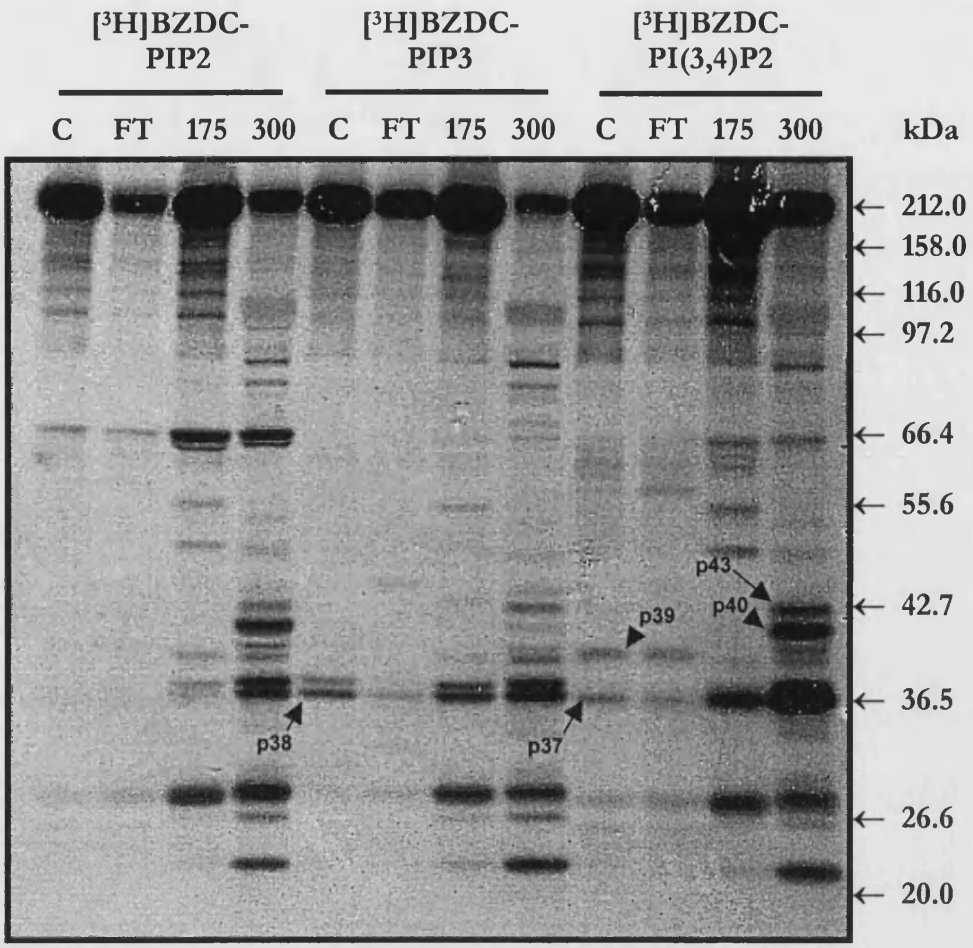

Figure 45. Photolabelling of heparin-agarose 175 mM and 300 mM NaCl eluates. The cytosol was isolated from rat adipocytes. Cytosolic proteins (~ 22 mg) were then bound to heparin-agarose in the presence of 50 mM NaCl. Proteins were then eluted stepwise using 175 mM NaCl then 300 mM NaCl. The NaCl was removed from the samples and 50 μg aliquots of cytosol (C), proteins not bound to the heparin-agarose (FT), 175 mM NaCl eluate (175) and 300 mM NaCl elute (300) were photolabelled with the [³H]BZDC-photolabels (0.1 μCi/ 50μg protein). Samples were then analysed by SDS-PAGE and fluorography.

Analysis of the Coomassie stained proteins (figure 44) shows that amongst other differences, there is a relative increase in the concentration of at least one protein at ~38 kDa in the 175 mM NaCl elution, and an increase in the relative concentration of two proteins at ~ 40 and 43 kDa with the 300 mM NaCl elution (indicated by arrows). The photolabelling of these proteins (figure 45) showed that the p38 doublet labelled by the [³H]BZDC-PIP3 photolabel was high in both the 175 and 300 mM NaCl eluates, more so in the latter eluate. Therefore, the protein seen to increase in its relative concentration by Coomassie Blue staining at ~38 kDa in the 175 mM NaCl eluate (figure 44), probably does not represent the photolabelled protein, p38. Out of the two cytosolic proteins labelled by the [³H]BZDC-PI(3,4)P2

photolabel, p37 and p39, only p37 was concentrated in the NaCl eluates, again to a higher extent in the 300 mM NaCl eluate. The observation that p39 does not bind to the heparin is consistent with data shown in figure 43. Additionally, it was observed that two proteins, p40 and p43, were photolabelled to a greater extent by the [^{3}H]BZDC-PI(3,4)P2 photolabel in the 300 mM NaCl eluate. This photolabelling may correspond to the increase in the proteins seen at these molecular weights by the Coomassie Blue staining of this fraction. Whilst photolabelling of these two proteins was also observed with proteins with similar molecular weights using the [^{3}H]BZDC-PIP2 photolabel, the photolabelling was greater for the [^{3}H]BZDC-PI(3,4)P2 photolabel.

In summary, three cytosolic proteins p37, p38 and p39 showed selective photolabelling for D-3-phosphorylated phosphatidylinositides relative to PIP2. The relative protein concentration of p37 and p38 was increased using a heparin-agarose chromatography step. The heparin-agarose chromatography step also increased the relative concentration of two proteins, p40 and p43, that strongly photolabelled with the PI(3,4)P2-photolabel.

6.6 Purification of phosphatidylinositide-binding proteins by affinity chromatography

To further purify p37, p38, p40 and p43, a phosphoinositide affinity resin based upon Ins(1,3,4)P3 was used. Initially 30 mg of cytosolic protein (40 fat pads) was incubated with heparin-agarose (as described in *section 6.5*) and bound proteins were eluted stepwise with 175 mM NaCl then 300 mM NaCl. The 300 mM NaCl eluate (~ 950 μg protein) was diluted to remove the NaCl (*section 2.20*) then circulated through the Ins(1,3,4)P3 column overnight at 4°C. The column was then washed with 10 mM Tris-HCl, pH 7.2, 1 mM EDTA, and bound proteins were eluted with a NaCl gradient (0 - 2 M NaCl) collecting 30 x 2 ml fractions. The 280nm absorbance of the column eluate was measured. 100 μl of each 2 ml fraction was collected and proteins visualised by SDS-PAGE and silver staining (figure 46).

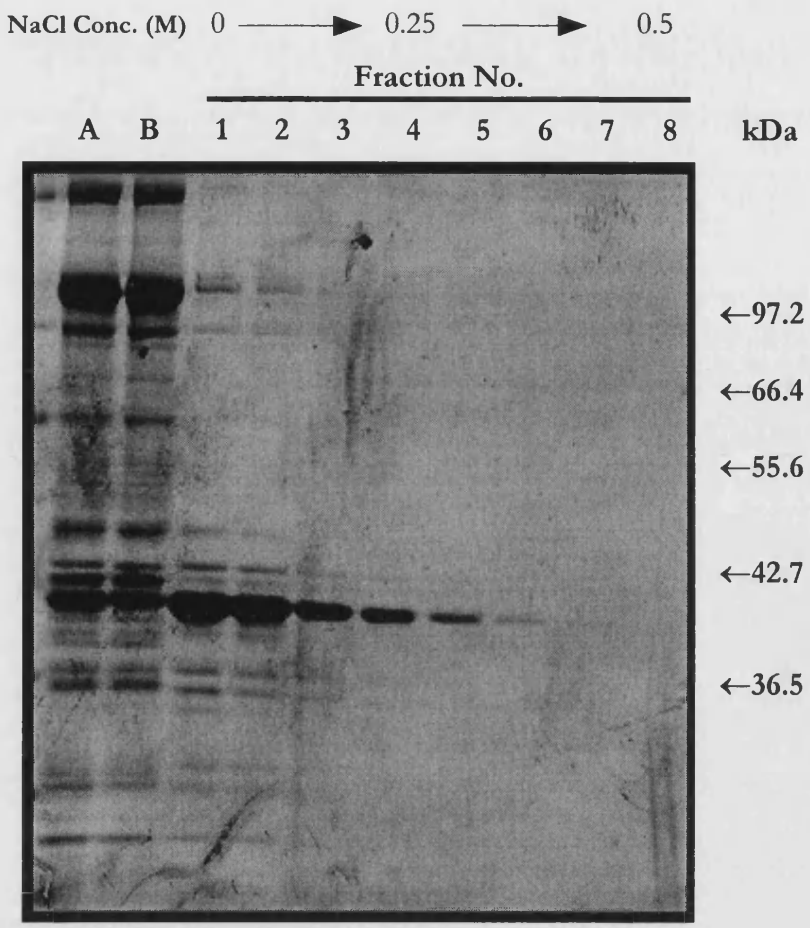

Figure 46. Silver staining of proteins after heparin-agarose and Ins(1,3,4)P3 affinity chromatography. 30 mg of cytosolic protein was incubated with heparin-agarose and bound proteins were eluted stepwise with 175 mM NaCl then 300 mM NaCl. The 300 mM NaCl eluate (~ 950 μg protein) was then circulated through an Ins(1,3,4)P3 affinity resin overnight at 4°C. The column was then washed with 10 mM Tris-HCl, pH 7.2, 1 mM EDTA, and bound proteins eluted with a NaCl gradient (0 - 2 M NaCl) collecting 30 x 2 ml fractions (measuring the absorbance at 280 nm). 100 μl of each 2 ml fraction was collected and proteins visualised by SDS-PAGE and silver staining. 50 μg of the 300 mM NaCl heparin eluate before (A) and after passing through the Ins(1,3,4)P3 affinity column (B) were also included on the gel. No proteins were visualised by silver staining from fraction 8 onwards.

Figure 46 showed no obvious depletion of proteins from the heparin-agarose eluate occurred after Ins(1,3,4)P3 affinity chromatography (compare lanes A and B, figure 46). Some proteins were found to bind to the Ins(1,3,4)P3 column, eluting with a relatively low NaCl concentration. One protein in particular which appeared to bind the Ins(1,3,4)P3 affinity resin relative to other proteins was a protein at ~40 kDa. The silver staining pattern, would suggest that this 40 kDa protein might be p40, identified previously (figure 45). Fractions eluted from the Ins(1,3,4)P3 affinity resin and containing more than one protein (determined by silver staining) were pooled together (fractions 1-3). Additionally, fractions 5-7 which were estimated by silver staining to contain only one protein, ~40 kDa, were also pooled together.

The two pooled fractions were then photolabelled with the three phosphoinositide photolabels. Initially, the pooled fractions which eluted from the Ins(1,3,4)P3 column showed no photolabelling, following a 6 week exposure of the fluor impregnated gel to light sensitive film. However, the amounts of protein photolabelled were very small. The BCA protein assay (sensitive to detecting 20 μg protein /ml) was unable to detect any protein in the pooled fractions used for photolabelling. However, a longer exposure of radiography film to the gel (>6 months), showed a single protein of ~ 43 kDa (possibly p43, as in figure 45) was photolabelled in both of the pooled fractions, but this protein was not the 40 kDa protein observed by silver staining (figure 46). The single protein was found to be photolabelled to a greater extent by the PI(3,4)P2- and PIP3-photolabels than by the PIP2-photolabel (figure 47).

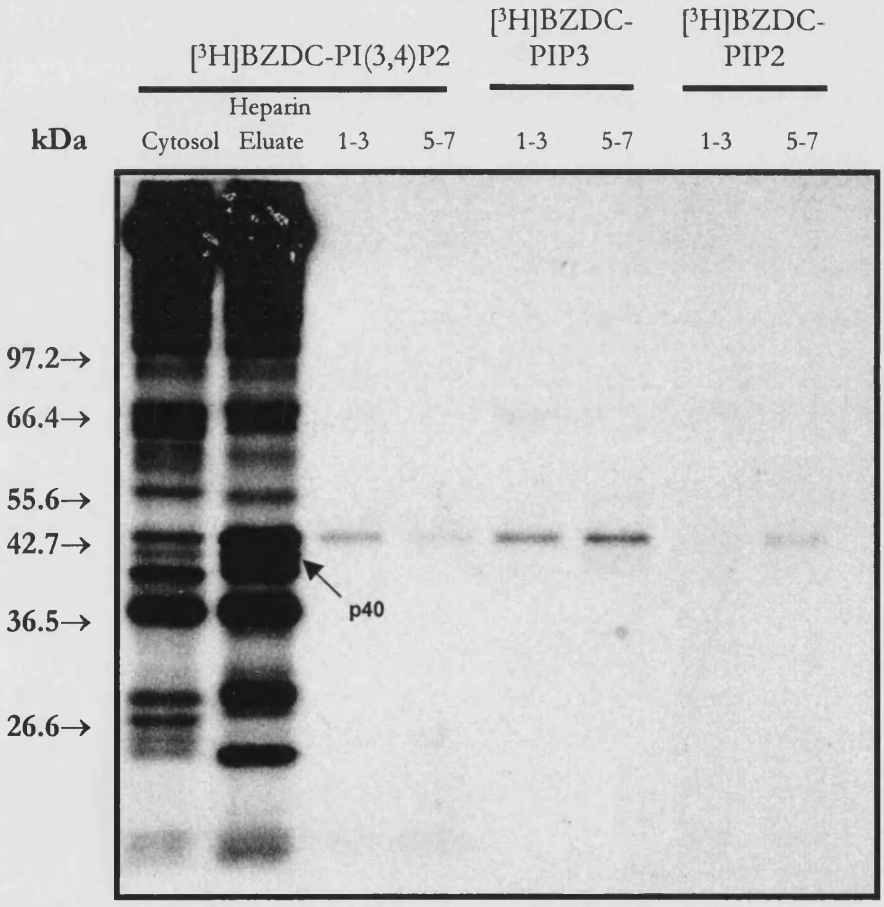

Figure 47. Photolabelling of Ins(1,3,4)P3 affinity column eluates. 50 μg of adipocyte cytosol and a heparin-agarose eluate (300 mM NaCl eluate) were photolabelled with 0.1 μCi [³H]BZDC-PI(3,4)P2. The heparin-agarose eluate was diluted and concentrated to remove the NaCl before photolabelling (*section 2.20*). Subsequent to heparin-agarose chromatography and Ins(1,3,4)P3 affinity chromatography steps, pooled fractions (1-3) and (5-7) eluted from the Ins(1,3,4)P3 affinity column were concentrated to ~200 μl (with NaCl removal by repeated concentration and dilution) and 50 μl aliquots photolabelled with 0.2 μCi of either [³H]BZDC-PI(3,4)P2,-PIP3 or -PIP2. Samples were then subjected to SDS-PAGE and fluorography. The fluorograph represents a >6 month exposure.

Although, p43 appeared to bind to the Ins(1,3,4)P3 affinity column, there was not enough protein to identify p43 by Edman sequencing. Furthermore, neither p37 nor p40 appeared to bind to the Ins(1,3,4)P3 column. Since proteins that bind PI(3,4)P2 are generally found also to bind PIP3 with equal of greater affinity, it was decided to use a Ins(1,3,4,5)P4 affinity column. It was hoped that the Ins(1,3,4,5)P4 column would bind both PIP3 and PI(3,4)P2 binding-proteins. Since only a small quantity of protein bound to the Ins(1,3,4)P3 affinity column, the cytosol from 200 fat pads was isolated, to start with a higher amount of phosphatidylinositide–binding proteins. The isolated cytosol was sequentially applied to heparin-agarose (as for previous experiments), and proteins were eluted with 175 and 300 mM NaCl. The 300 mM NaCl eluate was retained, the NaCl was removed (*section 2.20*) and the eluate applied to a Ins(1,3,4,5)P4 affinity column. Proteins were eluted from the Ins(1,3,4,5)P4 affinity column with a linear NaCl gradient (0 - 2M NaCl). A flow rate of 0.2 ml / min was used and 30 x 1 ml fractions were collected. Silver staining 100 µl aliquots of each fraction revealed that the majority of protein bound to the column eluted at 0.5-1 M NaCl (fractions 9-15). Fractions 9-15 were pooled together, the NaCl removed by repeated dilution with 10 mM Tris-HCl, pH 7.2, 1 mM EDTA, and the proteins concentrated using centrifugal concentrators. From 150 mg of cytosolic protein, 8.7 mg of protein was applied to the Ins(1,3,4,5)P4 column, the pooled proteins eluted from the Ins(1,3,4,5)P4 column gave 280 µg of protein, 0.2% of the starting protein. The protein profile of this fraction, as visualised by Coomassie-Blue staining, after SDS-PAGE, is shown by figure 48.

The fluorograph of the gel shown in figure 48, is shown in figure 49. Comparison of the Coomassie Blue stained proteins eluted from the Ins(1,3,4,5)P4 column (figure 48), and the fluorograph (figure 49), revealed that all the proteins eluted from the Ins(1,3,4,5)P4 affinity column showed some degree of photolabelling. Proteins eluted from the Ins(1,3,4,5)P4 column included proteins p37, p38, p40, which all showed strong photolabelling for PI(3,4,)P2 relative to PIP3 and PIP2. Weaker photolabelling in comparison to p37/38/40 was observed by a protein at ~43 kDa, which may represent p43 (figures 45 & 47).

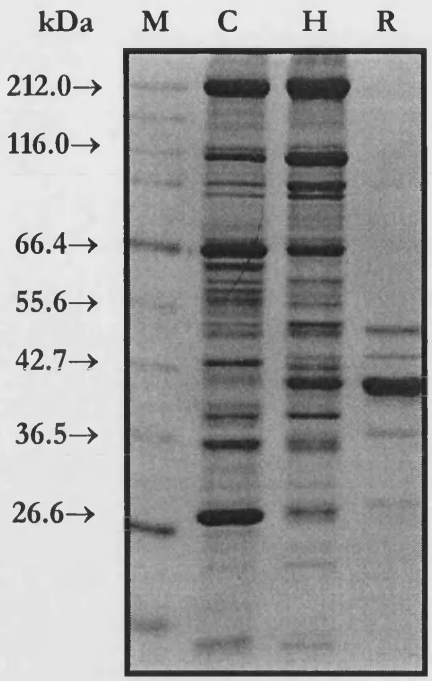

Figure 48. Coomassie Blue staining of the Ins(1,3,4,5)P4 affinity column eluate. Fractions 9-15 which were eluted from the Ins(1,3,4,5)P4 affinity column were pooled and concentrated to ~ 600 µl (280 µg protein). 50 µg aliquots of the original cytosol preparation (C), 50 µg aliquots of the 300 mM heparin-agarose eluate (H), and 10 µg aliquots of the pooled Ins(1,3,4,5)P4 affinity resin eluate (R) were photolabelled with the three phosphatidylinositide photolabels (0.1 µCi photolabel/sample). Samples were subjected to SDS-PAGE, Coomassie Blue staining and fluorography (figure 49). Broad range molecular weight markers (M) are shown on the gel.

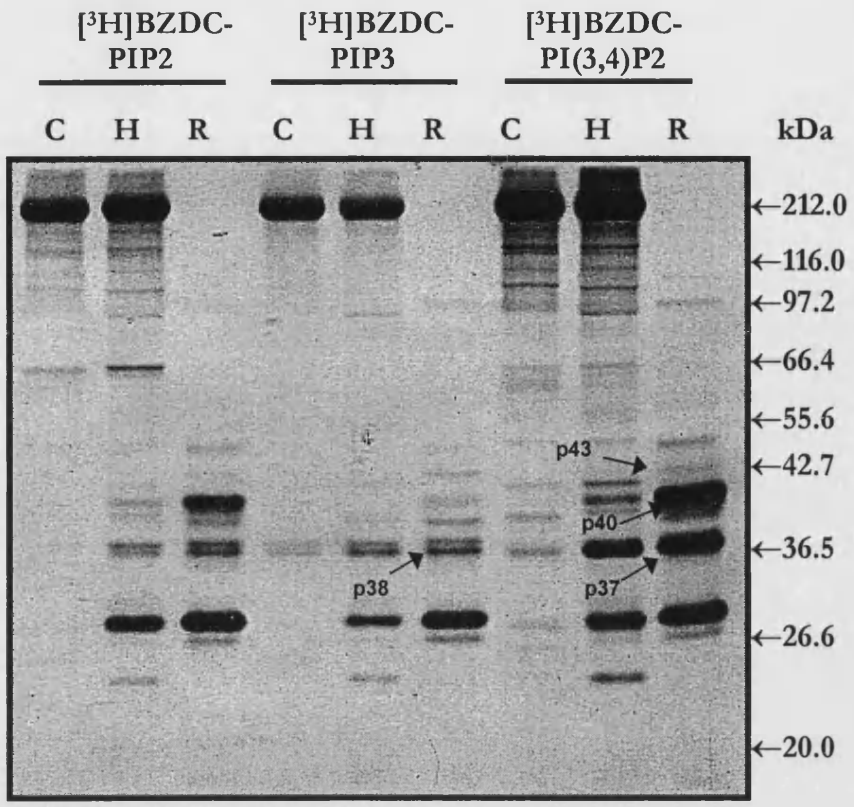

Figure 49. Photolabelling of cytosol, heparin-agarose eluates and Ins(1,3,4,5)P4 affinity column eluates. 50 μg aliquots of either adipocyte cytosol (C) or heparin-agarose 300 mM NaCl eluates (H) were photolabelled with the three [^{3}H]BZDC-phosphatidylinositides. Additionally 10 μg aliquots of Ins(1,3,4,5)P4 affinity resin eluates (R) were photolabelled with the three photolabels. All photolabelling reactions contained 0.1 μCi of the appropriate photolabel (all at 42.5 Ci/mmol). Samples were then subjected to SDS-PAGE and fluorography. The fluorograph represents a 14 day exposure at -70°C.

6.7 Identification of phosphatidylinositide-binding proteins

30 μg of the isolated Ins(1,3,4,5)P4 affinity column eluate fraction was subjected to SDS-PAGE and electrophoretic transfer onto PVDF for protein sequencing. Details of the sequencing results are shown in figure 50 and table 5.

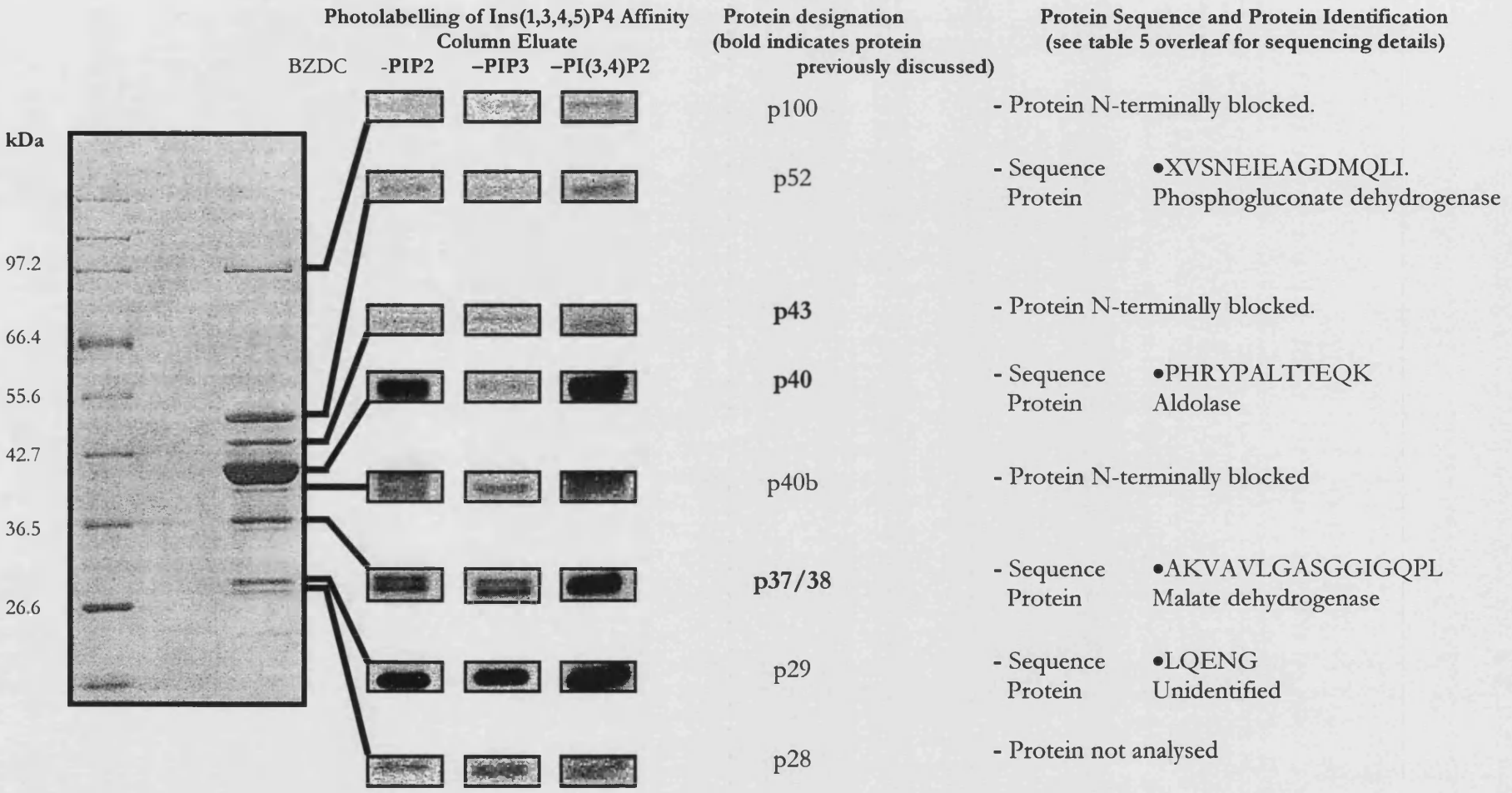

Figure 50. Protein sequencing and identification of Ins(1,3,4,5)P4-binding proteins. 30 μg of Ins(1,3,4,5)P4 protein was subjected to SDS-PAGE and electrophoretically transferred onto PVDF. Ponceau-S staining of the membrane is shown by the left hand panel, indicating molecular weight markers and the Ins(1,3,4,5)P4-binding proteins. Photolabelling of the proteins is shown (data from figure 51). Proteins were sequenced by a variety of methods (see table 5 overleaf).

Protein	Sequencing method
p100	The protein band was initially subjected to automated Edman sequencing with an Applied Biosystems 477A protein sequencer. There was no determinable sequence data, most probably due to a blocked N-terminal residue. Another band was treated by trypsin in-blot digestion. The protein fragments were separated by reverse phase HPLC. Detection of HPLC fractions indicated that the tryptic digest had digested the protein to an unusable state. Further attempts to cleave the protein into fragments using CNBr were also unsuccessful.
p52	The protein band was initially subjected to automated Edman sequencing with an Applied Biosystems 477A protein sequencer. There was no determinable sequence data, most probably due to a blocked N-terminal residue. Another band was treated by trypsin in-blot digestion. The protein fragments were separated by reverse phase HPLC. HPLC fractions were then subjected to MALDI mass spectroscopy. Six peptide fragments were identified by MALDI mass spectroscopy, which gave mass data consistent with that of phosphogluconate dehydrogenase. Edman sequencing of one HPLC fraction gave the sequence XVSNEIEAGDMQLI, consistent with the protein being phosphogluconate dehydrogenase. The molecular weight of phosphogluconate dehydrogenases is typically in the range of 52-53 kDa.
p43	The protein band was initially subjected to automated Edman sequencing with an Applied Biosystems 477A protein sequencer. There was no determinable sequence data, most probably due to a blocked N-terminal residue. Another membrane was subjected to a deblocking method to remove an acetylation group from serine and threonine residues by adding anhydrous trifluoroacetic acid (TFA) to the membrane and incubating for 1 h at 40°C, then allowing the TFA to evaporate then subjecting the membrane to sequencing again. This again provided no sequencing data. Another band was treated by trypsin in-blot digestion. The protein fragments were separated by reverse phase HPLC. HPLC fractions were then subjected to MALDI mass spectroscopy. No masses were detected, this could be due to the lack of material since the HPLC monitoring at 215 and 280 nm indicated that there was not much material. There may have been an over estimation of the amount of protein from the staining of the blot, or the losses by the digestion method may have been greater than expected.
p40	Automated Edman sequencing of the protein band with an Applied Biosystems 477A protein sequencer gave the sequence PHRYPALTTEQK. The sequence indicates that the protein is aldolase.
p40b	The protein band was subjected to automated Edman sequencing with an Applied Biosystems 477A protein sequencer. There was no determinable sequence data. No further attempts at sequencing were made.
p37/38	Sequencing of the protein doublet by automated Edman sequencing gave the sequence AKVAVLGASGGIGQPL for both proteins. This identified the proteins as malate dehydrogenase.
p29	The protein band was initially subjected to automated Edman sequencing with an Applied Biosystems 477A protein sequencer. There was no determinable sequence data, most probably due to a blocked N-terminal residue. Another band was treated by trypsin in-blot digestion. The protein fragments were separated by reverse phase HPLC. HPLC fractions were then subjected to MALDI mass spectroscopy. A partial sequence was obtained. The partial sequence of LQENG did not give protein identification.

Table 5. Sequencing methods used to identify phosphatidylinositide-binding proteins.

6.8 Chapter 6 discussion

Whilst PI 3-kinase activity is necessary to stimulate GLUT4 translocation to the PM (*section 1.9*), details of the intracellular signalling pathway downstream of PI 3-kinase are unclear. The likely route for the generation of subsequent signalling processes is *via* the lipid products formed by the activated PI 3-kinase. PI(3,4)P2 and PIP3 photolabels and affinity resins were therefore employed to identify phosphatidylinositide-binding proteins in rat adipocytes.

Photolabelling experiments indicated that proteins which preferentially bound PI(3,4)P2 and PIP3 in preference to PIP2, appeared to be mainly cytosolic. The observation that apparent PI(3,4)P2-/PIP3-binding proteins were cytosolic was not wholly unexpected. The recruitment of PIP3 binding proteins PKB and PDK1 to membranes upon PIP3 production is well described in the literature. It is therefore possible that the cytosol represents the largest PI(3,4)P2-/3-binding protein pool. If insulin stimulation targets PI(3,4)P2-/PIP3-binding proteins to membranes, then differences in photolabelling between basal and insulin membrane fractions would have been observed. However, no differences in photolabelling were observed between basal and insulin samples. A lack of observable changes in the subcellular distribution of PI(3,4)P2-/PIP3-binding proteins upon insulin treatment, may be explained in a number of ways. Firstly, the photolabelling of proteins may not have been sensitive enough to detect small amounts of protein. Each photolabelling reaction used 50 μg of protein. It is therefore likely that the proportion of true PI(3,4)P2-/PIP3-binding proteins in subcellular fractions such as the PM and LDM would be very small and probably undetectable. For example, labelling of aldolase (p40) was only detectable following heparin-agarose chromatography when its protein concentration relative to other proteins was increased (see figure 45). Hence, these initial experiments may not have identified novel and potentially important PI(3,4)P2-/PIP3-binding proteins in subcellular fractions due to the low levels of protein. It may be necessary to look at the photolabelling of PM and LDM fractions following heparin-agarose chromatography. Secondly, none of the photolabelling experiments takes into account the differences in affinity for the three photolabels utilised. For instance, a protein with a higher affinity for PIP3 than PI(3,4)P2 and PIP2, may not have been directly observed, if the single concentration of the photolabels used was too high to be selective. Important PI(3,4)P2-/PIP3-binding proteins may therefore have been overlooked. Ideally, the experiments would need to be repeated using a concentration range of competitor phosphatidylinositides to obtain a more accurate picture of the affinity of proteins for one phosphatidylinositide over another. Thirdly, the long exposure times might not necessarily

distinguish between strong and weakly photolabelled proteins (minimum exposure times were generally a month). Any small translocation differences may have been missed. Fourthly, phosphatases may have been active in subcellular fractions, and hence any insulin-induced targeting of PI(3,4)P2-/PIP3-binding proteins to membranes may have been lost. Finally, any important PI(3,4)P2-/PIP3-binding protein < 20 kDa would not have been observed, since photolabelled proteins were analysed by 10% SDS-PAGE gels.

Photolabelling of proteins with PI(3,4)P2 and PIP3 analogues therefore has its limitations. Despite the limitations, three cytosolic proteins p37, p38 and p39, seemed to be good candidate PI(3,4)P2-/PIP3-binding proteins. Sequencing of p37/38 revealed the proteins to be malate dehydrogenase, and p52 (figure 50) to be phosphogluconate dehydrogenase. Both these bind phosphate containing substrates and this is possibly the reason why they bind to both the heparin and Ins(1,3,4,5)P4 columns. Malate dehydrogenase photolabelling did not appear to be non-specific (figure 41), it may therefore be necessary to reduce the time of photolabelling to reduce possible aberrant labelling.

There is previous research indicating that aldolase binds Ins(1,4,5)P3 , Ins(1,4)P2 and more importantly Ins(1,3,4,5)P4 (Thieleczek *et al.*, 1989). Furthermore, Ins(3,4)P2 inhibits the binding of Ins(1,4,5)P3 to aldolase (Baron *et al.*, 1995; Baron *et al.*, 1998). It would therefore seem that the Ins(1,3,4,5)P4-affinity column has isolated at least one phosphoinositide-binding protein. The photolabelling of aldolase with PI(3,4)P2 is greater than the photolabelling with PI(4,5)P2 (figure 49). This result is consistent with the reported affinity of aldolase for the different phosphoinositides (Baron *et al.*, 1995; Baron *et al.*, 1998). However, to date there has been no previous evidence for the binding of aldolase to phosphatidylinositides. The specificity of photolabelling of aldolase has not been tested, and further experiments using purified aldolase are needed to examine whether aldolase can also specifically bind phosphatidylinositides. It is generally thought that proteins that bind PI(3,4)P2 also bind PIP3 but with an equal or greater affinity (Rameh *et al.*, 1997; Kavran *et al.*, 1998). However, aldolase clearly photolabels more efficiently with PI(3,4)P2 than PIP3 (figure 49), giving further need for investigating the specificity of phosphatidylinositide binding.

The ability of aldolase to bind F-actin is well documented (Arnold & Pette, 1970; O'Reilly & Clarke, 1993). Interestingly, aldolase has recently been found to associate with the C-terminus of GLUT4 (Kao *et al.*, 1999). Kao *et al.* (1999) observed that an anti-aldolase antibody could

partially inhibit GLUT4 translocation to the PM in 3T3-L1 adipocytes. Additionally, fructose 1,6-bisphosphate can bind to aldolase and disrupt GLUT4/aldolase/F-actin binding. It also inhibits GLUT4 translocation to the PM. It was proposed (Kao *et al.*, 1999) that aldolase mediates the interaction between GLUT4 and F-actin and that glucose metabolism may provide a negative feedback signal for the regulation of glucose transport by insulin. Whilst fructose 1,6-bisphosphate can release aldolase from F-actin, Ins(1,3,4,)P3 is also reported to release aldolase from F-actin (Thieleczek *et al.*, 1989). An interesting speculation is the possibility that PI(3,4)P2 generation may interact with aldolase, thereby releasing GLUT4 vesicles from the cytoskeleton. A tethering of GLUT4 vesicles to an intracellular structure has been proposed by Oatey *et al.* (1997). However destabilisation of actin microfilaments with cytochalasin D was reported to have no effect on green-fluorescent protein(GFP)-GLUT4 translocation to the cell surface. This latter result is in contrast to Wang *et al.* (1998) who observe a 50% decrease in glucose transport and GLUT4 translocation to the PM with cytochalasin D treated 3T3-L1 adipocytes. If PI(3,4)P2 does interact with aldolase bound to GLUT4, then there would be a rationale for the occurrence of PI 3-kinase activity on GLUT4 vesicles. The location of PI 3-kinase activity is an important aspect in GLUT4 trafficking, but it is likely that more than one intracellular site is involved with PI 3-kinase and GLUT4 trafficking.

Western blotting of the Ins(1,3,4,5)P4 eluate, revealed that PKBα/β (a PIP3-binding protein), did not bind to the Ins(1,3,4,5)P4-affinity column (data not shown). It is therefore possible that the Ins(1,3,4,5)P4 moiety of the affinity column is not sufficient to bind phosphatidylinositide-binding proteins. The phosphatidylinositide-binding proteins may also require the recognition of the glycerol backbone and fatty acids of the phosphatidylinositide. Tanaka *et al.* (1997) and Shirai *et al.* (1998) have shown that the glycerol backbone and fatty acids are important for the binding of proteins to the inositide lipid. Tanaka *et al.* (1997) used an IP3 analogue, similar to the one used here, to isolate PIP3-binding proteins (figure 51). The PIP3 analogue used by Tanaka *et al.* (1997) isolated a 43 kDa protein from bovine brain, centaurin-α, which was also isolated by Prestwich and colleagues using the PIP3 analogue used here (Hammonds-Odie *et al.*, 1996). However, the Japanese group subsequently went on to modify the IP3 analogue to contain both a glycerol group and short fatty acid groups (figure 51) (Shirai *et al.*, 1998). Using a protocol identical to the one which identified centaurin-α, the new PIP3 analogue additionally isolated the PIP3 binding proteins, Tec tyrosine kinase, Gap1^{m} and PKBγ (Shirai *et al.*, 1998).

In addition to a partial purification of phosphatidylinositol-binding proteins, heparin-agarose chromatography was used to remove phosphoinositol-phosphatases before these were added to a phosphoinositol-phosphatase sensitive affinity column. Interestingly, Shirai *et al.* (1998) state that their PIP3-affinity resin was reusable and hence insensitive to phosphoinositol-phosphatases, under the conditions used to isolate PIP3-binding proteins. Since the heparin-agarose step led to the loss of p39, it have been worthwhile to add the adipocyte cytosol fraction directly to the Ins(1,3,4,5)P4 resin. However, this would likely result in the isolation of a higher number of non-specific proteins binding to the Ins(1,3,4,5)P4 resin.

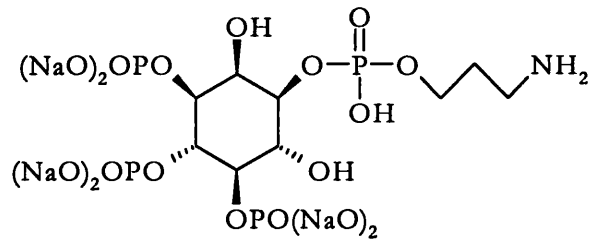

Aminopropyl-Ins(1,3,4,5)P4
Used in this thesis to isolate aldolase and other unknown proteins, and by Hammonds-Odie *et al.* (1996) to isolate centaurin-α.

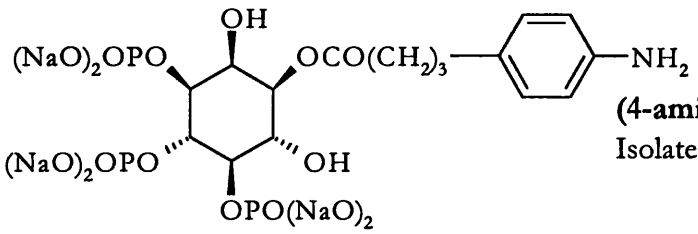

(4-aminophenylbutyryl)-Ins(3,4,5)P3
Isolated centaurin-α (Tanaka *et al.*, 1997).

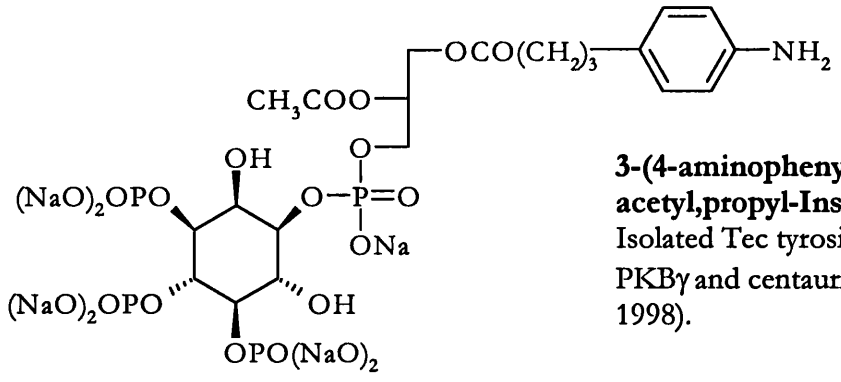

3-(4-aminophenylbutyryl),2-acetyl,propyl-Ins(1,3,4,5)P4
Isolated Tec tyrosine kinase, Gap1^{m}, PKBγ and centaurin-α (Shirai *et al.*, 1998).

Figure 51. PIP3 analogues used to isolate PIP3 binding proteins. All analogues were linked to Affi-Gel 10 (Bio-Rad).

Whilst the binding of phosphogluconate dehydrogenase and malate dehydrogenase to the Ins(1,3,4,5)P4 column is thought to be non-specific binding, proteins p100, p43, p40b, p29 and p28, which remain unidentified, might represent phosphatidylinositide-binding proteins.

Proteins of ~29 kDa were always seen to be photolabelled by all three photolabels and hence p29 was not considered as a possible PI(3,4)P2-/PIP3-binding protein. However as mentioned previously, the photolabelling experiments may not allow discrimination of differences in affinity for the photolabels at a single concentration of photolabel. Hence, it is possible that p29 may be a true PI(3,4)P2-/PIP3-binding protein and further experiments are required to determine whether p29 discriminates between PI(3,4)P2/3 and PIP2 at lower ligand concentrations.

p28 was only seen to be photolabelled following the Ins(1,3,4,5)P4 affinity chromatography step (figure 49). Again, no discrimination between the three photolabels was observed, and further experiments are required to identify whether the photolabelling is specific, and whether p28 binds PI(3,4)P2/3 to a greater extent than PI(4,5,)P2.

A protein ~ 43kDa was found to bind to both the Ins(1,3,4)P3 and Ins(1,3,4,5)P4 column. It is not known whether the 43kDa protein binding to both affinity columns is the same protein, however 43kDa is the molecular mass of centaurin-α, a PIP3 binding protein (Hammonds-Odie *et al.*, 1996; Stricker *et al.*, 1997; Tanaka *et al.*, 1997). The 43 kDa protein was the only protein that appeared to be weakly photolabelled following the Ins(1,3,4)P3 affinity chromatography step, but only a small amount of protein was applied to the Ins(1,3,4)P3 column at the time. In contrast, the p43 that eluted from the Ins(1,3,4,5)P4 column showed relatively weak photolabelling compared to aldolase, malate dehydrogenase, and p29. It is possible, that the adipocyte protein p43, is an isoform of centaurin-α, with a weaker affinity for PI(3,4)P2/3, than previously identified brain forms of centaurin-α.

Finally, p100 is of approximately the right molecular weight as Gap1^{m}, an Ins(1,3,4,5)P4 binding protein (Fukuda & Mikoshiba, 1996), also isolated by Shirai *et al.* (1998). Further work is required to determine whether p100 does represent Gap1^{m}.

In summary, heparin and Ins(1,3,4,5)P4 chromatography have been used to isolate PI(3,4)P2-/PIP3-binding proteins from adipocytes. Using an adipocyte cytosol fraction, the phosphoinositol-binding protein aldolase was isolated. Aldolase, an actin binding protein, has recently been shown to bind to the C-terminus of GLUT4, and hence it is speculated that PI 3-kinase can regulate GLUT4 binding to the cytoskeleton *via* aldolase. Other proteins which bound to the Ins(1,3,4,5)P4 affinity column, were malate dehydrogenase, phosphogluconate

dehydrogenase, and the unidentified proteins p100, p43, p40b, p29 and p28. It is possible that p100 represents Gap1^{m} and p43 represents centaurin-α, but further work is required to identify and characterise these proteins.

CHAPTER 7

CONCLUSION

Using insulin-resistant adipocytes, research described here has indicated that despite reduced activation of early signalling intermediates, a reduction of PM GLUT4 is likely to be a result of increased endocytosis of GLUT4, rather than a reduction in GLUT4 exocytosis. The mechanisms regulating GLUT4 exocytosis are still unclear, and less is known about how insulin may regulate GLUT4 endocytosis. Ultimately, any process that increases PM GLUT4 in NIDDM patients, albeit by increasing GLUT4 exocytosis or decreasing endocytosis, would be of benefit. The work reported here indicates that metformin reduces endocytosis of GLUT4 and this may account for its therapeutic action. If NIDDM patients were also found to show increased GLUT4 endocytosis, particularly in muscle, then the mechanisms regulating GLUT4 endocytosis will be of particular importance, and a shift in current research to study such mechanisms may be appropriate.

Research in this thesis has neither supported or disproved whether PKB is necessary for insulin-stimulated GLUT4 trafficking to the PM in adipocytes. Conclusive evidence that PKB is not required for contraction-stimulated GLUT4 translocation to the PM in muscle is described. Studies looking at the relationship between PKB activity and the serine/threonine phosphatase inhibitor okadaic acid (OA) suggested that OA may stimulate the exocytosis of recycling endosomes in a PKB-independent manner. Whilst this hypothesis needs to be further tested, a very recent study has indicated that the insulin stimulation of the recycling-endosomal pool does not require PKB (Foran *et al.*, 1999). If both PMA and OA act on the recycling of GLUT4 from the recycling-endosomal pool, then it is suggestive of an unidentified serine/threonine kinase regulating this endosomal recycling.

Many aspects of the regulation of GLUT4 exocytosis remain unclear. This includes the precise role of each IRS molecule in GLUT4 trafficking, the site(s) of PI 3-kinase activation, the targets of PIP2/3, whether PKB is involved in GLUT4 trafficking and the precise roles of synip and munc18c in GLUT4 vesicle fusion with the plasma membrane. In an attempt to provide further information into the regulation of GLUT4 trafficking, a significant proportion of the research in this thesis was aimed into identifying regulators of GLUT4 vesicle trafficking, namely GTP- and phosphatidylinositol-binding proteins.

The data using the periodate-oxidised GTP technique indicated that insulin activated GTP-binding proteins which were sensitive to the actions of wortmannin. Identification of these proteins was problematic. It was found that the GTPase ARF can form a strong association

with GLUT4 vesicles. Whilst it is not known which isoform of ARF associates with GLUT4 vesicles, it seems that more than one isoform of ARF regulates GLUT4 trafficking. Since GLUT4 vesicles can associate with adaptor proteins, AP-1 and AP-3 (Gillingham *et al.*, 1999), it is likely that ARF1 associates transiently with GLUT4 vesicles. Hence it is proposed that in addition to the proposed role of ARF6 in GLUT4 endocytosis (Millar *et al.*, 1999) ARF1 can regulate the trafficking of GLUT4 from the PM back to the insulin-responsive GSVs.

Techniques used for attempts at identification of PI(3,4)P2-/PIP3-binding proteins from adipocytes led to the isolation of aldolase, and other PIP3 binding proteins. These currently remain unidentified but might possibly be centaurin-α and Gap1^{m}. Aldolase has been reported to bind phosphoinositides (Thieleczek *et al.*, 1989), actin (Arnold & Pette, 1970), and the C-terminus of GLUT4 (Kao *et al.*, 1999). Whether PI 3-kinase regulates aldolase binding to GLUT4, and hence the cytoskeleton, remains to be determined. The cytoskeleton is likely to play an important role in GLUT4 trafficking by possible tethering of GLUT4 vesicles (Oatey *et al.*, 1997), the localisation of PI 3-kinase (Clark *et al.*, 1998) and by directing the movement of vesicles (Gonzalez & Scheller, 1999).

GLUT4 trafficking and the related signalling processes, are complex. Many aspects of the signalling processes remain unclear. This thesis, has only in part touched upon some of the processes. These require further research in order to provide those elusive answers to the unique trafficking of glucose transporter 4 that can be applied to the study of NIDDM.

CHAPTER 8

REFERENCES

Ahmad, F. & Goldstein, B. J. (1997) Functional association between the insulin receptor and the transmembrane protein-tyrosine phosphatase LAR in intact cells (1997) J Biol Chem **272**: 448-457.

Ahmad, F., Considine, R. V. & Goldstein, B. J. (1995) Increased abundance of the receptor-type protein-tyrosine phosphatase LAR accounts for the elevated insulin receptor dephosphorylating activity in adipose tissue of obese human subjects. J Clin Invest **95**: 2806-2812.

Al Hasani, H., Kinck, C. S. & Cushman, S. W. (1998) Endocytosis of the glucose transporter GLUT4 is mediated by the GTPase dynamin. J Biol Chem **272**: 17504-17510.

Alessi, D. R. & Cohen, P. (1998) Mechanism of activation and function of protein kinase B. Curr Opin Gen & Dev **8**: 55-62.

Alessi, D. R., Andjelkovic, M., Caudwell, B., Cron, P., Morrice, N., Cohen, P. & Hemmings, B. A. (1996) Mechanism of activation of protein kinase B by insulin and IGF-1. EMBO J **15**: 6541-6551.

Alessi, D. R., James, S. R., Downes, C. P., Holmes, A. B., Gaffney, P. R. J., Reese, C. B. & Cohen, P. (1997) Characterisation of a 3-phosphoinositide-dependent protein kinase which phosphorylates and activates protein kinase Bα. Curr Biol **7**: 261269.

Anai, M., Ono, H., Funaki, M., Fukushima, Y., Inukai, K., Ogihara, T., Sadoka, H., Onishi, Y., Yazaki, Y., Kikuchi, M., Oka, Y. & Asano, T. (1998) Different subcellular distribution and regulation of expression of insulin receptor substrate (IRS)-3 from those of IRS-1 and IRS-2. J Biol Chem **273**: 29686-29692.

Anderson, K. E., Coadwell, J., Stephens, L. R. & Hawkins, P. T. (1998) Translocation of PDK-1 to the plasma membrane is important in allowing PDK-1 to activate protein kinase B. Curr Biol **8**: 684-691.

Antonny, B., Beraud-Dufour, S., Chardin, P. & Chabre, M. (1997) N-terminal hydrophobic residues of the G-protein ADP-ribosylation factor-1 insert into membrane phospholipids upon GDP to GTP exchange. Biochem **36**: 4675-4684.

Araki, E., Lipes, M. A., Patti, M-E., Brüning, J. C., Hagg III, B., Johnson, R. S. & Kahn, C. R. (1994) Alternative pathway of insulin signalling in mice with targeted disruption of the IRS-1 gene. Nature **372**: 186-190.

Arnold, H. & Pette, D. (1970) Binding of aldolase and triosephosphate dehydrogenase to F-actin and modification of catalytic properties of aldolase. Eur J Biochem **15**: 360-366.

Balch, W. E., Kahn, R. A. & Schwaninger, R. (1992) ADP-ribosylation factor is required for vesicular trafficking between the endoplasmic reticulum and the *cis*-Golgi compartment. J Biol Chem **267**: 13053-13061.

Baldini, G., Hohman, R., Charron, M. J., Lodish, H. F. (1991) Insulin and nonhydrolyzable GTP analogs induce translocation of GLUT4 to the plasma membrane in α-toxin-permeabilised rat adipose cells. J Biol Chem **266**: 4037-4040.

Bao, S., Smith, R. M., Jarett, L. & Garvey, W. T. (1995) The effects of brefeldin A on the glucose transport system in rat adipocytes. J Biol Chem **270**: 30199-30204.

Baron, C. B., Greeley, P. & Coburn, R. F. (1998) Smooth muscle aldolase C-bound inositol 1,4,5-trisphosphate studied in vitro under physiological conditions. Biochim Biophys Acta **1401**: 81-92.

Baron, C. B., Ozaki, S., Watanabe, Y., Hirata, M., LaBelle, E. F. & Cobum, R. F. (1995) Inositol 1,4,5-trisphosphate binding to porcine tracheal smooth muscle aldolase. J Biol Chem **270**: 20459-20465.

Barr, F. A., Leyte, A. & Huttner, W. B. (1992) Trimeric G proteins and vesicle formation. Trends Cell Biol **2**: 91-94.

Bellacosa, A., Testa, J. R., Staal, S. P. & Tsichlis, P. N. (1991) A retroviral oncogene, *akt*, encoding a serine-threonine kinase containing an SH2-like region. Science **254**: 274-277.

Birnbaum, M. J. (1989) Identification of a novel gene encoding an insulin-responsive glucose transporter protein. Cell **57**: 305-315.

Bjornholm, M., Kawano, Y., Lehtihet, M. & Zierath, J. R. (1997) Insulin receptor substrate-1 phosphorylation and phosphatidylinositol 3-kinase activity in skeletal muscle from NIDDM subjects after in vivo insulin stimulation. Diabetes **46**: 524-527.

Bortoluzzi, M. N., Cormont, M., Gautier, N., Van Obberghen, E. & Le Marchand-Brustel, Y. (1996) GTPase activating protein activity for Rab4 is enriched in the plasma membrane of 3T3-L1 adipocytes. Possible involvement in the regulation of Rab4 subcellular localization. Diabetologia **39**: 899-906.

Brooks, S. P. J. & Storey, K. B. (1992) Bound and determined: A computer program for making buffers of defined ion concentrations. Anal Biochem **201**: 119-126.

Brozinick Jr., J. T. & Birnbaum, M. J. (1998) Insulin, but not contraction activates Akt/PKB in isolated rat skeletal muscle. J Biol Chem **273**: 14679-14682.

Brüning, J. C., Winnay, J., Cheatham, B. & Kahn, C. R. (1997) Differential signaling by insulin receptor substrate 1 (IRS-1) and IRS-2 in IRS-1-deficient cells. Mol CellBiol **17**: 1513-1521.

Bucci, C., Parton, R. G., Mather, I. H., Stunneberg, H., Simons, K., Hoflack, B. & Zerial, M. (1992) The small GTPase rab5 functions as a regulatory factor in the early endocytic pathway. Cell **70**: 715-728.

Burgering, B. M. Th. & Coffer, P. J. (1995) Protein kinase B (c-Akt) in phosphatidylinositol-3-OH kinase signal transduction. Nature **376**: 599-602.

Burks, D. J., Wang, J., Towery, H., Ishibashi, O., Lowe, D., Riede, H. & White, M. F. (1998) IRS Pleckstrin homology domains bind to acidic motifs in proteins. J Biol Chem **273**: 31061-31067.

Cain, C. C., Trimble, W. S. & Lienhard, G. E. (1992) Members of the VAMP family of synaptic vesicle proteins are components of glucose transporter-containing vesicles from rat adipocytes. J Biol Chem **267**: 11681-11684.

Calderhead, D. M., Kitagawa, K., Tanner, L. I., Holman, G. D. & Lienhard, G. E. (1990) Insulin regulation of the two glucose transporters in 3T3-L1 adipocytes. J Biol Chem **265**: 13800-13808.

Calera, M. R., Martinez, C., Liu, H., El Jack, A. K., Birnbaum, M. J. & Pilch P. F. (1998) Insulin increases the association of Akt-2 with Glut4-containing vesicles. J Biol Chem **273**: 7201-7204.

Cartee, G. D., Briggs-Tung, C. & Holloszy, J. O. (1992) Diverse effects of calcium-channel blockers on skeletal muscle glucose-transport. Am J Physiol **263**: 70-75.

Cavenagh, M. M., Whitney, J. A., Carroll, K., Zhang, C-j., Boman, A. L., Rosenwald, A. G., Mellman, I. & Kahn, R. A. (1996) Intracellular distribution of Arf proteins in mammalian cells. Arf6 is uniquely localised to the plasma membrane. J Biol Chem **271**: 21767-21774.

Ceresa, B. P., Kao, A. W., Santeler, S. R. & Pessin, J. E. (1998) Inhibition of clathrin-mediated endocytosis selectively attenuates specific insulin receptor signal transduction pathways. Mol Cell Biol **18**: 3862-3870.

Chakrabarti, R., Buxton, J., Joly, M. & Corvera, S. (1994) Insulin-sensitive association of GLUT4 with endocytic clathrin-coated vesicles revealed with the use of brefeldin A. J Biol Chem **269**: 7926-7933.

Charron, M. J., Brosius III, F. C., Alper, S. L. & Lodish, H. F. (1989) A glucose transport protein expressed predominately in insulin-responsive tissues. Proc Natl Acad Sci USA **86**: 2535-2539.

Cheatham, B., Volchuk, A., Kahn, C. R., Wang, L., Rhodes, C. J. & Klip, A. (1996) Insulin-stimulated translocation of GLUT4 glucose transporters requires SNARE-complex proteins. Proc Natl Acad Sci USA **93**: 15169-15173.

Chen, D. I., Vanhorn, D. J., White, M. F. & Backer, J. M. (1995) Insulin-receptor susbstrate-1 rescues insulin action in CHO cells expressing mutant insulin-receptors that lack a juxtamembrane NPXY motif. Mol Cell Biol **15**: 4711-4717.

Cheng, J. Q., Godwin, A. K., Bellacosa, A., Taguchi, T., Franke, T. F., Hamilton, T. C., Tsichlis, P. N. & Testa, J. R. (1992) *AKT2*, a putative oncogene encoding a member of a subfamily of protein-serine/threonine kinases, is amplified in human ovarian carcinomas. Proc Natl Acad Sci USA **89**: 9267-9271.

Chou, C. K., Dull, T. J., Russell, D. S., Gherzi, R., Lebwohl, D., Ullrich, A. & Rosen, O. M. (1987) Human insulin receptors mutated at the ATP-binding site lack protein tyrosine kinase activity and fail to mediate postreceptor effects of insulin. J Biol Chem **262**: 1842-1847.

Clark, A. E. & Holman, G. D. (1990) Exofacial photolabelling of the human erythrocyte glucose transporter with an azitrifluoroethylbenzoyl-substituted bismannose. Biochem J **269**: 615-622.

Clark, S. F., Martin, S., Carozzi, A. J., Hill, M. M. & James, D. E. (1998) Intracellular localization of phosphatidylinositide 3-kinase and insulin receptor substrate-1 in adipocytes: Potential involvement of a membrane skeleton. J Cell Biol **140**: 1211-1225.

Clarke, J. F., Young, P. W., Yonezawa, K., Kasuga, M. & Holman, G. D. (1994) Inhibition of the translocation of GLUT1 and GLUT4 in 3T3-L1 cells by the phosphatidylinositol 3-kinase inhibitor, wortmannin. Biochem J **300**: 631-635.

Cockcroft, S. (1996) ARF-regulated phospholipase D: a potential role in membrane traffic. Chem & Physics Lipids **80**: 59-80.

Coffer, P. J. & Woodgett, J. R. (1991) Molecular cloning and characterisation of a novel putative protein-serine kinase related to the cAMP-dependent and protein kinase C families. Eur J Biochem **201**: 475-481.

Coffer, P. J., Jin, J. & Woodgett, J. R. (1998) Protein kinase B (c-Akt): a multifunctional mediator of phosphatidylinositol 3-kinase activation. Biochem J **335**: 1-13.

Cormont, M., Bortoluzzi, M-N., Gautier, N., Mari, M., Van Obberghen, E. & Le Marchand-Brustel, Y. (1996a) Potential role of Rab4 in the regulation of subcellular localization of glut4 in adipocytes. Mol Cell Biol **16**: 6879-6886.

Cormont, M., Tanti, J-F., Grémeaux, T., Van Obberghen, E. & Le Marchand-Brustel, Y. (1991) Subcellular distribution of low molecular weight guanosine triphosphate-binding proteins in adipocytes: Colocalization with the glucose transporter glut 4. Endocrinology **129**: 3343-3350.

Cormont, M., Tanti, J-F., Zahraoui, A., Van Obberghen, E., Tavitian, A. & Le Marchand-Brustel, Y. (1993) Insulin and okadaic acid induce Rab4 redistribution in adipocytes. J Biol Chem **268**: 19491-19497.

Cormont, M., Van Obberghen, E., Zerial, M. & Le Marchand-Brustel, Y. (1996b) Insulin induces a change in rab5 subcellular localisation in adipocytes independently of phosphatidylinositol 3-kinase activation. Endocrinol **137**: 3408-3415.

Corvera, S., Jaspers, S. & Pasceri, M. (1991) Acute inhibition of insulin-stimulated glucose transport by the phosphatase inhibitor, okadaic acid. J Biol Chem **266**: 9271-9275.

Cross, D. A. E., Watt, P. W., Morag, S., van der Kaay, J, Downes, C. P., Holder, J. C. & Cohen, P. (1997) Insulin activates protein kinase B, inhibits glycogen synthase kinase-3 and activates glycogen synthase by rapamycin-insensitive pathways in skeletal muscle and adipose tissue. FEBS Lett **406**: 211-215.

Cushman, S. W. & Wardzala, L. J. (1980) Potential mechanism of insulin action on glucose transport in the isolated rat adipose cell. Apparent translocation of intracellular transport systems to the plasma membrane. J Biol Chem **255**: 4758-4762.

D'Souza-Schorey, C., van Donselaar, E., Hsu, V. W., Stahl, P. D. & Peters, P. J. (1998) ARF6 targets recycling vesicles to the plasma membrane: Insights from an ultrastructural investigation. J Cell Biol **140**: 603-616.

D'Souza-Schorey, C., Li, G., Colombo, M. I. & Stahl, P. D. (1995) A regulatory role for Arf6 in receptor-mediated endocytosis. Science **267**: 1175-1178.

Davidson, M. B. & Peters, A. L. (1997) An overview of metformin in the treatment of type 2 diabetes mellitus. Am J Med **102**: 99-110.

De Meyts, P. (1994) The structural basis of insulin and insulin-like growth factor-1 receptor binding and negative co-operativity, and its relevance to mitogenic versus metabolic signalling. Diabetologia **37**: S135-S148.

Denis-Henriot, D., de Mazancourt, P., Goldsmith, P. K. & Giudicelli, Y. (1996) G proteins in adipocytes and preadipocytes: Characterization, subcellular distribution, and potential roles for G_{i2} and/or G_{i3} in the control of cell proliferation. Cell Signal **8**: 225-234.

Didichenko, S. A., Tilton, B., Hemmings, B. A., Ballmer-Hofer, K. & Thelen, M. (1996) Constitutive activation of protein kinase B and phosphorylation of $p47^{pbox}$ by a membrane-targeted phosphoinositide 3-kinase. Curr Biol **6**: 1271-1278.

Domin, J., Dhand, R. & Waterfield, M. D. (1996) Binding to the platelet-derived growth factor receptor transiently activates the p85 alpha-p110 alpha phosphoinositide 3-kinase complex *in vivo*. J Biol Chem **271**: 21614-21621.

Dominguez, L. J., Davidoff, A. J., Srinivas, P. R., Standley, P. R., Walsh, M. F. & Sowers, J. R. (1996) Effects of metformin on tyrosine kinase activity, glucose transport and intracellular calcium in rat vascular smooth muscle. Endocrinology **137**: 113-121.

Dormán, G. & Prestwich, G. D. (1994) Benzophenone photophores in biochemistry. Biochem **33**: 5661-5673.

Downward, J. (1998) Lipid-Regulated Kinases: Some common themes at last. Science **279**: 673-674.

Drake, P. G. & Posner, B. I. (1998) Insulin receptor-associated protein tyrosine phosphatse(s): Role in insulin action. Mol & Cell Biochem **182**: 79-89.

Elazar, Z., Orci, L., Ostermann, J., Amherdt, M., Tanigawa, G. & Rothman, J. E. (1994) ADP-Ribosylation factor and coatomer couple fusion to vesicle budding. J Cell Biol **124**: 415-424.

Elmendorf, J. S., Chen, D. & Pessin, J. E. (1998) Guanosine 5'-*O*-(3-thiotriphosphate)(GTPγS) stimulation of GLUT4 translocation is tyrosine kinase-dependent. J Biol Chem **273**: 13289-13296.

Falck J. R., Shears S. B. & Lafer E. M. (1997) Regulation of AP-3 function by inositides. J Biol Chem **272**: 6393-6398.

Fantin, V. R., Sparling, J. D., Slot, J. W., Keller, S. R., Lienhard, G. E. & Lavan, B. E. (1998) Characterization of insulin receptor substrate 4 in human embryonic kidney 293 cells. J Biol Chem **273**: 10726-10723.

Farese, R. V., Standaert, M. L., Francois, A. J., Ways, K., Arnold, T. P., Hernandez, H. & Cooper, D. R. (1992) Effects of insulin and phorbol esters on subcellular distribution of protein kinase C isoforms in rat adipocytes. Biochem J **288**: 319-323.

Fasshauer, D., Sutton, R. B., Brunger, A. T. & Jahn, R. (1998) Conserved structural features of the synaptic fusion complex: SNARE proteins reclassified as Q- and R-SNAREs. Proc Natl Acad Sci USA **95**: 15781-15786.

Fingar, D. C., Hausdorff, S. F., Blenis, J. & Birnbaum, M. J. (1993) Dissociation of pp70 ribosomal protein S6 kinase from insulin-stimulated glucose transport in 3T3-L1 adipocytes. J Biol Chem **268**: 3005-3008.

Foran, P. G. P., Fletcher, L. M., Oatey, P. B., Mohammed, N., Dolly, J. O. & Tavaré, J. M (1999) Protein kinase B stimulates the translocation of GLUT4 but not GLUT1 or transferrin receptors in 3T3-L1 adipocytes by a pathway involving SNAP-23, synaptobrevin-2, and/or cellubrevin. J Biol Chem **274**: 28087-28095.

Frank, S., Upender, S., Hansen, S. H. & Casanova, J. E. (1998) ARNO is a guanine nucleotide exchange factor for ADP-ribosylation factor 6. J Biol Chem **273**: 23-27.

Frech, M., Andjelkovic, M., Ingley, E., Reddy, K. K., Falck, J. R. & Hemmings, B. A. (1997) High affinity binding of inositol phosphates and phosphoinositides to the plekstrin homology domain of Rac/protein kinase B and their influence on kinase activity. J Biol Chem **272**: 8474-8481.

Frevert, E. U., Bjøbæk, C., Venable, C. L., Keller, S. R. & Kahn, B. B. (1998) Targeting of constitutively active phosphoinositide 3-kinase to GLUT4-containing vesicles in 3T3-L1 adipocytes. J Biol Chem **273**: 25480-25487.

Fujita, Y., Sasaki, T., Fukui, K., Kotani, H., Kimura, T., Hata, Y, Sudhof, T. C., Scheller, R. H. & Takai, Y. (1996) Phosphorylation of Munc-18/n-Sec1/rbSec1 by protein kinase C – Its implication in regulating the interaction of Munc-18/n-Sec1/rbSec1 with syntaxin. J Biol Chem **271**: 7265-7268.

Gaidarov, I. O. & Keen, J. H. (1995) Clathrin adapter protein AP-2 binds phosphatidylinositol 3,4,5-P_3 – Identification of polyphosphoinositol/inositide binding site. Mol Biol Cell **6**:S2368.

Garvey, W. T., Maianu, L., Zhu, J-H., Brechtel-Hook, G., Wallace, P. & Baron, A. D. (1998) Evidence for defects in the trafficking and translocation of GLUT4 glucose transporters in skeletal muscle as a cause of human insulin resistance. J Clin Invest **101**: 2377-2386.

Gibbs, E. M., Allard, W. J. & Lienhard, G. E. (1986) The glucose transporter in 3T3-L1 adipocytes is phosphorylated in response to phorbol ester but not in response to insulin. J Biol Chem **261**: 16597-16603.

Gibbs, E. M., Calderhead, D. M., Holman, G. D. & Gould, G. W. (1991) Phorbol ester only partially mimics the effects of insulin on glucose transport and glucose-transporter distribution in 3T3-L1 adipocytes. Biochem J **275**: 145-150.

Gillingham, A. K., Koumanov, F., Pryor, P. R., Reaves, B. J. & Holman, G. D. (1999) Formation of GLUT4-enriched vesicles by interactions with AP-1 and AP-3 adaptor complexes. *Submitted for publication.*

Goldsmith, P., Gierschik, P., Milligan, G., Unson, C. G., Vinitsky, R., Malech, H. L. & Spiegel, A. M. (1987) Antibodies directed against synthetic peptides distinguish between GTP-binding proteins in neutrophil and brain. J Biol Chem **262**: 14683-14688.

Goldstein, B. J. (1993) Regulation of insulin receptor signalling by protein-tyrosine dephosphorylation. Receptor **3**: 1-15.

Gonzalez, L. Jr. & Scheller, R. H. (1999) Regulation of membrane trafficking: Structural insights from a rab/effector complex. Cell **96**: 755-758.

Goodyear, L. J., Giorgino, F., Sherman, L. A., Carey, J., Smith, R. J. & Dohm, G. L (1995) Insulin receptor phosphorylation, insulin receptor substrate-1 phosphorylation, and phosphatidylinositol 3-kinase activity are decreased in intact skeletal muscle strips from obese subjects. J Clin Invest **95**: 2195-2204.

Gould, G. W. (1997) Trafficking, targeting and translocation of the insulin-regulatable glucose transporter, GLUT4. Facilitative glucose transporters, Ch. 3, Ed. Gould, G. W., R. G. Landes Company.

Gould, G. W. & Holman, G. D. (1993) The glucose transporter family: structure, function and tissue-specific expression. Biochem J **295**: 329-341.

Hall, A. & Self, A. J. (1986) The effect of Mg^{2+} on the guanine nucleotide exchange rate of $p21^{N\text{-}ras}$. J Biol Chem **261**: 10963-10965.

Hammonds-Odie, L. P., Jackson, T. R., Profit, A. A., Blader, I. J., Turck, C. W., Prestwich, G. D. & Theibert, A. B. (1996) Identification and cloning of centaurin-α. A novel phosphatidylinositol 3,4,5-trisphosphate-binding protein from rat brain. J Biol Chem **271**: 18859-18868.

Handgerg, A., Vaag, A., Vinten, J. & Beck-Nielsen, H. (1993) Decreased tyrosine kinase activity in partially purified insulin receptors from muscle of young, non-obese first degree relatives of patients with type 2 (non-insulin-dependent) diabetes mellitus. Diabetologia **36**: 668-674.

Haney, P. M., Levy, M. A., Strube, M. S. & Mueckler, M. (1995) Insulin-sensitive targeting of the GLUT4 glucose transporter in L6 myoblasts is conferred by its COOH-terminal cytoplasmic tail. J Cell Biol **129**: 641-658.

Hara, K., Yonezawa, K., Sakaue, H., Ando, A., Kotani, K., Kitamura, T., Kitamura, Y., Ueda, H., Stephens, L., Jackson, T. R., Hawkins, P. T., Dhand, R., Clark, A. E., Holman, G. D., Waterfield, M. D. & Kasuga, M. (1994) 1-phosphatidylinositol 3-kinase activity is required for insulin-stimulated glucose transport but not for RAS activation in CHO cells. Proc Natl Acad Sci **91**: 7415-7419.

Harlan, J. E., Yoon, H. S., Hadjuk, P. J. & Fesik, S. W. (1995) Structural characterization of the interaction between a pleckstrin homology domain and phosphatidylinositol 4,5-bisphosphate. Biochem **34**: 9859-9864.

Haruta, T., Morris, A. J., Rose, D. W., Nelson, J. G., Mueckler, M. & Olefsky, J. M. (1995) , Insulin-stimulated GLUT4 translocation is mediated by a divergent intracellular signaling pathway. J Biol Chem **270**: 27991-27994.

Haruta, T., Morris, A. J., Vollenweider, P., Nelson, J. G., Rose, D. W., Mueckler, M. & Olefsky, J. M. (1998) Ligand-independent GLUT4 translocation induced by guanosine 5'-*O*-(3-thiotriphosphate) involves tyrosine phosphorylation. Endocrinology **139**: 358-364.

Hausdorff, S. F., Bennett, A. M., Neel, B. G. & Birnbaum, M. J. (1995) Different signaling roles of SHPTP2 in insulin-induced GLUT1 expression and GLUT4 translocation. J Biol Chem **270**: 12965-12968.

Hay, J. C. & Scheller, R. H. (1997) SNAREs and NSF in targeted membrane fusion. Curr Opin Cell Biol **9**: 505-512.

Haystead, T. A. J., Sim, A. T. R., Carling, D., Honnor, R. C., Tsukitani, Y., Cohen, P. & Hardie, D. G. (1989) Effects of the tumour promoter okadaic acid on intracellular protein phosphorylation and metabolism. Nature **337**: 78-81.

Heller-Harrison, R. A., Morin, M. & Czech, M. P. (1995) Insulin regulation of membrane-associated insulin-receptor substrate-1. J Biol Chem **270**: 24442-24450.

Heller-Harrison, R. A., Morin, M., Guilherme, A. & Czech, M. P. (1996) Insulin-mediated targeting of phosphatidylinositol 3-kinase to GLUT4-containing vesicles. J Biol Chem **271**: 10200-10204.

Helms, J. B., Palmer, D. J. & Rothman, J. E. (1993) Two distinct populations of Arf bound to Golgi membranes. J Cell Biol **121**: 751-760.

Henriksen, E. J., Sleeper, M. D., Zierath, J. R. & Holloszy, J. O. (1989) Polymyxin-B inhibits stimulation of glucose transport in muscle by hypoxia or contractions. Am J Physid **256**: 662-667.

Herbst, J. J., Andrews, G., Contillo, L., Lamphere, I., Gardner, J., Lienhard, G. E. & Gibbs, E. M. (1994) Potent activation of phosphatidylinositol 3'-kinase by simple phosphotyrosine peptides derived from insulin-receptor substrate-1 containing 2 YMXM motifs for binding SH2 domains. Biochem **33**: 9376-9381.

Hirst, J. & Robinson, M. S. (1998) Clathrin and adaptors. Biochim Biophys Acta **1404**: 173-193.

Holgado-Madruga, M., Emlet, D. R., Moscatello, D. K., Godwin, A. K. & Wong, A. J. (1996) A Grb2-associated docking protein in EGF- and insulin-receptor signalling. Nature **379**: 560-564.

Holman, G. D., Kozka, I. J., Clark, A. E., Flower, C. J., Saltis, J., Habberfield, A. D., Simpson, I. A. & Cushman, S. W. (1990) Cell surface labeling of glucose transporter isoform GLUT4 by bis-mannose photolabel. Correlation with stimulation of glucose transport in rat adipose cells by insulin and phorbol ester. J Biol Chem **265**: 18172-18179.

Holman, G. D., Leggio, L. L. & Cushman, S. W. (1994) Insulin-stimulated GLUT4 glucose transporter recycling. A problem in membrane protein subcellular trafficking through multiple pools. J Biol Chem **269**: 17516-17524.

Huber, L. A. & Peter, M. E. (1994) Mapping small GTP-binding proteins on high-resolution two-dimensional gels by a combination of GTP binding and labeling with *in situ* periodate-oxidised GTP. Electrophoresis **15**: 283-288.

Huber, L. A., Ullrich, O., Takai, Y., Lütcke, A., Dupree, P., Olkkonen, V., Virta, H., De Hoop, M. J., Alexandrov, K., Peter, M., Zerial, M. & Simons, K. (1994) Mapping of ras-related GTP-binding proteins by GTP overlay following two-dimensional gel electrophoresis. Proc Natl Acad Sci USA **91**: 7874-7878.

Ida, M., Imai, K., Hashimoto, S. & Kawashima, H. (1996) Pervanadate stimulation of wortmannin-sensitive and -resistant 2-deoxyglucose transport in adipocytes. Biochem Pharmacol **51**: 1061-1067.

Inoue, G., Cheatham, B., Emkey, R. & Kahn, C. R. (1998) Dynamics of insulin signaling in 3T3-L1 adipocytes. Differential compartmentalization and trafficking of insulin receptor substrate (IRS)-1 and IRS-2. J Biol Chem **273**: 11548-11555.

James, D. E., Strube, M. & Mueckler, M. (1989) Molecular cloning and characterization of an insulin-regulatable glucose transporter. Nature **338**: 83-87.

James, S. R., Downes, C. P., Gigg, R., Grove, S. J. A., Holmes, A. B. & Alessi, D. R. (1996) Specific binding of the Akt-1 protein kinase to phosphatidylinositol 3,4,5-trisphosphate without subsequent activation. Biochem J **315**: 709-713.

Jhun, B. H., Rampal, A. L., Liu, H. Z., Lachaal, M. & Jung, C. Y. (1992) Effects of insulin on steady-state kinetics of GLUT4 subcellular-distribution in rat adipocytes - evidence of constitutive GLUT4 recycling. J Biol Chem **267**: 17710-17715.

Jones, P. F., Jakubowicz, T., Pitossi, F. J., Maurer, F. & Hemmings, B. A. (1991) Molecular-cloning and identification of a serine threonine protein-kinase of the 2nd-messenger subfamily. Proc Natl Acad Sci USA **88**: 4171-4175.

Joost, H. G., Weber, T. M., Cushman, S. W. & Simpson, I. A. (1987) Activity and phosphorylation state of glucose transporters in plasma membranes from insulin-, isoproterenol-, and phorbol ester-treated rat adipose cells. J Biol Chem **262**: 11261-11267.

Kablaoui, B., Lee, J. & Pilch, P. F. (1995) Dynamics of signaling during insulin-stimulated endocytosis of its receptor in adipocytes. J Biol Chem **270**: 5965.

Kaburagi Y., Satoh S., Tamemoto H., Yamamoto-Honda R., Tobe K., Veki K., Yamauchi T., Kono-Sugita E., Sekihara H., Aizawa S., Cushman S. W., Akanuma Y., Yazaki Y. & Kadowaki T. (1997) Role of insulin receptor substrate-1 and pp60 in the regulation of insulin-induced glucose transport and GLUT4 translocation in primary adipocytes. J Biol Chem **272**: 25839-25844.

Kaburagi, Y., Momomura, K., Yamamoto-Honda, R., Tobe, K., Tamori, Y., Sakura, H., Akanuma, Y., Yazaki, Y. & Kadowaki, T. (1993) Site-directed mutagenesis of the juxtamembrane domain of the human insulin receptor. J Biol Chem **268**: 16610-16622.

Kaestner, K. H., Christy, R. J., McLenithan, J. C., Braiterman, L. T., Cornelius, P., Pekala, P. H. & Lane, M. D. (1989) Sequence, tissue distribution, and differential expression of mRNA for a putative insulin-responsive glucose transporter in mouse 3T3-L1 adipocytes. Proc Natl Acad Sci USA **86**: 3150-3154.

Kahn, C. R. (1994) Insulin action, diabetogenes, and the cause of type II diabetes. Diabetes **43**: 1066-1084.

Kandror, K. V. & Pilch, P. F. (1998) Multiple endosomal recycling pathways in rat adipose cells. Biochem J **331**: 829-835.

Kao, A. W., Noda, Y., Johnson, J. H., Pessin, J. E. & Saltiel, A. R. (1999) Aldolase mediates the association of F-actin with the insulin-responsive glucose transporter GLUT4. J Biol Chem **274**: 17742-17747.

Karnam, P., Standaert, M. L., Galloway, L. & Farese, R. V. (1997) Activation and translocation of Rho (and ADP ribosylation factor) by insulin in rat adipocytes. J Biol Chem **272**: 6136-6140.

Katagiri, H., Asano, T., Inukai, K., Ogihara, T., Ishihara, H., Shibasaki, Y., Murata, T., Terasaki, J., Kikuchi, M., Yazaki, Y. & Oka, Y. (1997) Roles of PI 3-kinase and Ras on insulin-stimulated glucose transport in 3T3-L1 adipocytes. Am J Physio-Endocrin Metab **35**: E326-E331.

Katagiri, H., Asano, T., Ishihara, H., Inukai, K., Shibasaki, Y., Kikuchi, M., Yazaki, Y. &Oka, Y. (1996) Overexpression of catalytic subunit p110 alpha of phosphatidylinositol 3-kinase increases glucose transport activity with translocation of glucose transporters in 3T3-L1 adipocytes. J Biol Chem **271**: 16987-16990.

Kavran, J. M., Klein, D. E., Lee, A., Falasca, M., Isakoff, S. J., Skolnik, E. Y. & Lemmon, M. A. (1998) Specificity and promiscuity in phosphoinositide binding by pleckstrin homology domains. J Biol Chem **272**: 30497-30508.

Keller, S. R., Scott, H. M., Corley Mastick, C., Aebersold, R. & Lienhard, G. E. (1995) Cloning and characterization of a novel insulin-regulated membrane aminopeptidase from GLUT4 vesicles. J Biol Chem **270**: 23612-23618.

Kelly, K. L. & Rudeman, N. B. (1993) Insulin-stimulated phosphatidylinositol 3-kinase. Association with a 185-kDa tyrosine phosphorylated protein (IRS-1) and localization in a low density membrane vesicle. J Biol Chem **268**: 4391-4398.

Kelly, K. L., Rudeman, N. B. & Chen, K. S. (1992) Phosphatidylinositol 3-kinase in isolated rat adipocytes. Activation by insulin and subcellular distribution. J Biol Chem **267**: 3423-3428.

Kitamura, T., Ogawa, W., Sakaue, H., Hino, Y., Kuroda, S., Takata, M., Matsumoto, M., Maeda, T., Konishi, H., Kikkawa, U. & Kasuga, M. (1998) Requirement for activation of the serine-threonine kinase Akt (protein kinase B) in insulin stimulation of protein synthesis but not of glucose transport. Mol & Cell Biol **18**: 3708-3717.

Klarlund, J. K., Guilherme, A., Holik, J. J., Vibasius, J. V., Chawla, A. & Czech, M. P. (1997) Signaling by phosphoinositide-3,4,5-trisphosphate through proteins containing pleckstrin and Sec7 homology domains. Science **275**: 1927-1930.

Klein, H. H., Matthaei, S., Drenkham, M., Ries, W. & Scriba, P. C. (1991) The relationship between insulin binding, insulin activation of insulin-receptor tyrosine kinase, and insulin stimulation of glucose uptake in isolated rat adipocytes - effects of isoprenaline. Biochem J **274**: 787-792.

Klippel, A., Kavanaugh, W. M., Pot, D. & Williams, L. T. (1997) A specific product of phosphatidylinositol 3-kinase directly activates the protein kinase Akt through its plekstrin homology domain. Mol & Cell Biol **17**: 338-344.

Kohn, A. D., Kovacina, K. S. & Roth, R. A. (1995) Insulin stimulates the kinase activity of RAC-PK, a plekstrin homology domain containing ser/thr kinase. EMBO J **14**: 4288-4295.

Kohn, A. D., Summers, S. A., Birnbaum, M. J. & Roth, R. A. (1996b) Expression of a constitutively active ser/thr kinase in 3T3-L1 adipocytes stimulates glucose uptake and glucose transporter 4 translocation. J Biol Chem **271**: 31372-31378.

Kohn, A. D., Takeuchi, F. & Roth, R. A. (1996a) Akt, a plekstrin homology domain containing kinase, is activated primarily by phosphorylation. J Biol Chem **271**: 21920-21926.

Konishi, H., Kuroda, S., Tanaka, M., Matsuzaki, H., Ono, Y., Kameyama, K., Haga, T. & Kikkawa, U. (1995) Molecular cloning and characterization of a new member of the rac protein kinase family: association of the plekstrin homology domain of three types of rac protein kinase with protein kinase C subspecies and βγ subunits of G proteins. Biochem Biophys Res Comm **216**: 526-534.

Kono-Sugita, E., Satoh, S., Suzuki, Y., Egawa, M., Udaka, N., Ito, T. & Sekihara, H. (1996) Insulin-induced GLUT4 recycling in rat adipose cells by a pathway insensitive to brefeldin A. Eur J Biochem **236**: 1033-1037.

Kotani, K., Ogawa, W., Matsumoto, M., Kitamura, T., Sakaue, H., Hino, Y., Miyake, K., Sano, W., Akimoto, K., Ohno, S. & Kasuga, M. (1998) Requirement of atypical protein kinase Cλ for insulin stimulation of glucose uptake but not for Akt activation in 3T3-L1 adipocytes. Mol Cell Biol **18**: 6971-6982.

Kozka, I. J. & Holman, G. D. (1993) Metformin blocks downregulation of cell surface GLUT4 caused by chronic insulin treatment of rat adipocytes. Diabetes **42**: 1159-1165.

Kozka, I. J., Clark, A. E., Reckless, J. P. D., Cushman, S. W., Gould, G. W. & Holman, G. D. (1995) The effects of insulin on the level and activity of the GLUT4 present in human adipose cells. Diabetologia **38**: 661-666.

Krook, A., Roth, R. A., Jiang, X. J., Zierath, J. R. & Wallberg-Henriksson, H. (1998) Insulin-stimulated Akt kinase activity is reduced in skeletal muscle from NIDDM subjects. Diabetes **47**: 1281-1286.

Ktistakis, N. T., Brown, A., Waters, M. G., Sternweis, P. C. & Roth, M. G. (1996) Evidence that phospolipase D mediates ADP ribosylation factor-dependent formation of Golgi coated vesicles. J Cell Biol **134**: 295-306.

Kublaoui, B., Lee, J. & Pilch, P. F. (1995) Dynamics of signaling during insulin-stimulated endocytosis of its receptor in adipocytes. J Biol Chem **270**: 5965.

Kukuda, M. & Mikoshiba, K. (1996) Structure-function relationships of the mouse Gap1^{m}. Determination of the inositol 1,3,4,5-tetrakisphosphate-binding domain. J Biol Chem **271**: 18838-18842.

Kukumoto, H., Kayano, T., Buse, J. B., Edwards, Y., Pilch, P. F., Bell, G. I. & Seino, S. (1989) Cloning and characterisation of the major insulin-responsive glucose transporter expressed in human skeletal muscle and other insulin-responsive tissues. J Biol Chem **264**: 7776-7779.

Kulas, D. T., Zhang, W-R., Goldstein, B. J., Furlanetto, R. W. & Mooney, R. A. (1995) insulin receptor signaling is augmented by antisense inhibition of the protein tyrosine phosphatase LAR. J Biol Chem **270**: 2435-2438.

Lachaal, M., Moronski, C., Liu, H. & Jung, C. Y. (1994) Brefeldin A inhibits insulin-induced glucose transport stimulation and GLUT4 recruitment in rat adipocytes. J Biol Chem **269**: 23689-23693.

Lavan, B. E., Fantin, V. R., Chang, E. T., Lane, W. S., Keller, S. R. & Lienhard, G. E. (1997) A novel 160-kDa phosphotyrosine protein in insulin-treated embryonic kidney cells is a new member of the insulin receptor substrate family. J Biol Chem **272**: 21403-21407.

Lavan, B. E., Lane, W. S. & Lienhard, G. E. (1997) The 60-kDa phosphotyrosine protein in insulin-treated adipocytes is a new member of the insulin receptor substrate family. J Biol Chem **272**: 11439-11443.

Lavan, E. & Lienhard, G. E. (1993) The insulin-elicited 60-kDa phosphotyrosine protein in rat adipocytes is associated with phosphatidylinositol 3-kinase. J Biol Chem **268**: 5921-5928.

Lawrence Jr., J, C, Hiken, J. F. & James, D. E. (1990) Stimulation of glucose transport and glucose transporter phosphorylation by okadaic acid in rat adipocytes. J Biol Chem **265**: 19768-19776.

Lee, A. D., Hansen, P. A. & Holloszy, J. O. (1995) Wortmannin inhibits insulin-stimulated but not contraction-stimulated glucose transport activity in skeletal muscle. FEBS Lett **361**: 51-54.

Lee, J., O'Hare, T., Pilch, P. F. & Shoelson, S. E. (1993) Insulin receptor autophosphorylation occurs asymmetrically. J Biol Chem **268**: 4092-4098.

Lemmon, M. A. & Schlessinger, J. (1994) Regulation of signal transduction and signal diversity by receptor oligomerization. TIBS **19**: 459-463.

Lenhard, J. M., Kahn, R. A. & Stahl, P. D. (1992) Evidence for ADP-ribosylation factor (Arf) as a regulator of *in vitro* endosome-endosome fusion. J Biol Chem **267**: 13047-13052.

Li, G., D'Souza-Schorey, C., Barbieri, M. A., Roberts, R. L., Klippel, A., Williams, L. T. & Stahl, P. D. (1995) Evidence for phosphatidylinositol 3-kinase as a regulator of endocytosis via activation of Rab5. Proc Natl Acad Sci USA **92**: 10207-10211.

Lippincott-Schwartz, J., Yuan, L., Tipper, C., Amherdt, M., Orci, L. & Klausner, R. D. (1991) Brefeldin A's effects on endosomes, lysosomes, and the TGN suggest a general mechanism for regulating organelle structure and membrane traffic. Cell **67**: 601-616.

Livingstone, C., James, D. E., Rice, J. E., Hanpeter, D. & Gould, G. W. (1996) Compartment ablation analysis of the insulin-responsive glucose transporter (GLUT4) in 3T3-L1 adipocytes. Biochem J **315**: 487-495.

Longo, N., Shuster, R. C., Griffin, L. D., Langley, S. D. & Elsas L. J. (1992) Activation of insulin receptor signaling by a single amino acid substitution in the transmembrane domain. J Biol Chem **267**: 12416-12419.

Losonczi, J. A. & Prestegard, J. H. (1998) Nuclear magnetic resonance characterization of the myristoylated, N-terminal fragment of ADP-ribosylation factor 1 in a magnetically oriented membrane array. Biochem **37**: 706-716.

Löw, A., Sprinzl, M. & Faulhammer, H. G. (1993) Affinity labeling of c-H-ras p21 consensus elements with periodate-oxidised GDP and GTP. Eur J Biochem **215**: 473-479.

Lu, P-J. & Chen, C-S. (1997) Selective recognition of phosphatidylinositol 3,4,5-trisphosphate by a synthetic peptide. J Biol Chem **272**: 466-472.

Lund, S., Holman, G. D., Schmitz, O. & Pederson, O. (1995) Contraction stimulates translocation of glucose transporter GLUT4 in skeletal-muscle through a mechanism distinct from that of insulin. Proc Natl Acad Sci USA **92**: 5817-5821.

Lund, S., Pryor, P. R., Ostergaard, S., Schmitz, O., Pederson, O. & Holman, G. D. (1998) Evidence against protein kinase B as a mediator of contraction-induced glucose transport and GLUT4 translocation in rat skeletal muscle. FEBS Lett **425**: 472-474.

Lupashin, V. V. & Waters, M. G. (1997) t-SNARE activation through transient interaction with a Rab-like guanosine triphosphatase. Science **276**: 1255-1258.

Ma, L., Cantley, L. C., Janmey, P.A. & Kirschner, M. W. (1998) Corequirement of specific phosphoinositides and small GTP-binding protein Cdc42 in inducing actin assembly in *Xenopus* egg extracts. J Cell Biol **140**: 1125-1136.

Macaulay, S. L., Hewish, D. R., Gough, K. H., Stoichevska, V., Macpherson, S. F., Jagadish, M. & Ward, C. W. (1997) Functional studies in 3T3L1 cells support a role for SNARE proteins in insulin stimulation of GLUT4 translocation. Biochem J **324**: 217-224.

Machesky, L. M. & Hall, A. (1996) Rho: a connection between membrane receptor signalling and the cytoskeleton. Trends Cell Biol **6**: 304-310.

Malide, D. & Cushman, S. W. (1997) Morphological effects of wortmannin on the endosomal system and GLUT4-containing compartments in rat adipose cells. J Cell Sci **110**: 2795-2806.

Malide, D., Dwyer, N. K., Blanchette Mackie, E. J. & Cushman, S. W. (1997) Immunocytochemical evidence that GLUT4 resides in a specialised translocation post-endosomal VAMP2-positive compartment in rat adipose cells in the absence of insulin. J Histochem & Cytochem **45**: 1083-1096.

Marshall, S., Green, A. & Olefsky, J. M. (1981) Evidence for recycling of insulin receptors in isolated rat adipocytes. J Biol Chem **256**: 11464-11470.

Martin, L. B., Shewan, A., Millar, C. A., Gould, G. W. & James, D. E. (1998) Vesicle-associated membrane protein 2 plays a specific role in the insulin-dependent trafficking of the facilitative glucose transporter GLUT4 in 3T3-L1 adipocytes. J Biol Chem **273**: 1444-1452.

Martin, S. S., Haruta, T., Morris, A. J., Klippel, A., Williams, L. T. & Olefsky, J. M. (1996a) Activated phosphatidylinositol 3-kinase is sufficient to mediate actin rearrangement and GLUT4 translocation in 3T3-L1 adipocytes. J Biol Chem **271**: 17605-17608.

Martin, S., Reaves, B., Banting, G. & Gould, G. W. (1994) Analysis of the co-localization of the insulin-responsive glucose transporter (GLUT4) and the *trans* Golgi network marker TGN38 within 3T3-L1 adipocytes. Biochem J **300**: 743-749.

Martin, S., Tellam, J., Livingstone, C., Slot, J. W., Gould, G. W. & James, D. E. (1996b) The glucose transporter (GLUT4) and vesicle-associated membrane protein-2 (VAMP-2) are segregated from recycling endosomes in insulin-sensitive cells. J Cell Biol **134**: 625-635.

Matthaei, S., Hamann, A., Klein, H. H., Benecke, H., Kreymann, G., Fliers, J. S. & Greten, H. (1991) Association of metformin's effect to increase insulin-stimulated glucose

transport with potentiation of insulin-induced translocation of glucose transporters from intracellular pool to plasma membrane in rat adipocytes. Diabetes 40: 850-857.

Matthaei, S., Reibold, J. P., Hamann, A., Benecke, H., Haring, H. U., Greten, H. &Klein, H. H. (1993) *In vivo* metformin treatment ameliorates insulin resistance: evidence for potentiation of insulin-induced translocation and increased functional activity of glucose transporters in obese (fa/fa) Zucker rat adipocytes. Endocrinology 133: 304-311.

McClain, D. A., Maegawa, H., Lee, J., Dull, T. J., Ullrich, A., Olefsky, J. M. (1987) A mutant insulin receptor with defective tyrosine kinase displays no biological activity and does not undergo endocytosis. J Biol Chem 262: 14663-14671.

McCollam, L., Bonfini, L., Karlovich, C. A., Conway, B. R., Kozma, L. M, Banerjee, U. & Czech, M. P. (1995) Functional roles for the pleckstrin and Dbl homology regions in the Ras exchange factor son-of-sevenless. J Biol Chem 270: 15954-15957.

Meacci, E., Tsai, S-C., Adamik, R., Moss, J. & Vaughan, M. (1997) Cytohesin-1, a cytosolic guanine nucleotide-exchange protein for ADP-ribosylation factor. Proc Natl Acad Sci USA 94: 1745-1748.

Meier, R., Alessi, D. R., Cron, P., Andjelkovic, M. & Hemmings, B. A. (1997) Mitogenic activation, phosphorylation, and nuclear translocation of protein kinase Bβ. J Biol Chem 272: 30491-30497.

Melvin, D. R., Marsh, B. J., Walmsley, A. R., James, D. E. & Gould, G. W. (1999) Analysis of amino and carboxy terminal GLUT-4 targeting motifs in 3T3-L1 adipocytes using an endosomal ablation technique. Biochem 38: 1456-1462.

Michiels, F., Habets, G. G. M., Stam, J. C., van der Kammen, R. A. & Collard, J. G. (1995) A role for rac in Tiam1-induced membrane ruffling and invasion. Nature375: 338-340.

Millar, C. A., Powell, K. A., Hickson, G. R. X., Bader, M-F. & Gould, G.W. (1999) Evidence for a role for ADP-ribosylation factor 6 in insulin-stimulated glucose transporter-4 (GLUT4) trafficking in 3T3-L1 adipocytes. J Biol Chem 274: 1761917625.

Min, J., Okada, S., Kanzaki, M., Elmendorf, J. S., Coker, K. J., Ceresa, B. P., Syu, L-J., Noda, Y., Saltiel, A. R. & Pessin, J. E. (1999) Synip: A novel insulin-regulated syntaxin 4-binding protein mediating GLUT4 translocation in adipocytes. Mol Cell3: 751-760.

Moller, N. P. H., Moller, K. B., Lammers, R., Kharitonenkov, A., Hoppe, E., Wiberg, F. C, Sures, I., Ullrich, A. (1995) Selective down-regulation of the insulin receptor signal by protein-tyrosine phosphatases α and ε. J Biol Chem 270: 23126-23131.

Mooney, R. A., Kulas, D. T., Bleyle, L. A. & Novak, J. S. (1997) The protein tyrosine phosphatase LAR has a major impact on insulin receptor dephosphorylation. Biochem Biophys Res Comm **235**: 709-712.

Mora, S., Monden, I., Zorzano, A. & Keller, K. (1997) Heterologous expression of rab4 reduces glucose transport and GLUT4 abundance at the cell surface in oocytes. Biochem J **324**: 455-459.

Morris, A. J., Martin, S. S., Haruta, T., Nelson, J. G., Vollenweider, P., Gustafson, T. A., Mueckler, M., Rose, D. W. & Olefsky, J. M. (1996) Evidence for an insulin receptor substrate 1 independent insulin signaling pathway that mediates insulin-responsive glucose transporter (GLUT4) translocation. Proc Natl Acad Sci USA **93**: 8401-8406.

Moxham, C. M. & Malbon, C. C. (1996) Insulin action impaired by deficiency of the G-protein subunit $G_{i\alpha 2}$. Nature **379**: 840-844.

Murakami, M. S. & Rosen, O. M. (1991) The role of insulin receptor autophosphorylation in signal transduction. J Biol Chem **266**: 22653-22660.

Myers, M. G., Grammer, T. C., Brooks, J., Glasheen, E. M., Wang, L-M, Sun, X. J., Blenis, J., Pierce, J. H. & White, M. F. (1995) The pleckstrin homology domain in insulin receptor substrate-1 sensitizes insulin signaling. J Biol Chem **270**: 11715-11718.

Nakanishi, H., Brewer, K. A. & Exton, J. H. (1993) Activation of the ζ isozyme of protein kinase C by phosphatidylinositol 3,4,5-trisphosphate. J Biol Chem **268**: 13-16.

Nave, B. T., Siddle, K. & Shepherd, P. R. (1996) Phorbol esters stimulate phosphatidylinositol 3,4,5-trisphosphate production in 3T3-L1 adipocytes: implications for stimulation of glucose transport. Biochem J **318**: 203-205.

Nishimura, H., Pallardo, F. V., Seidner, G. A., Vannucci, S., Simpson, I. A. & Birnbaum, M. J. (1993) Kinetics of GLUT1 and GLUT4 glucose transporters expressed in Xenopus oocytes. J Biol Chem **268**: 8514-8520.

Norris, K., Norris, F., Kono, D. H., Vestergaard, H., Pedersen, O., Theofilopoulos, A. N. & Møller, N. P. H. (1997) Expression of protein-tyrosine phosphatases in the major insulin target tissues. FEBS Letts **415**: 243-248.

Novick, P. & Zerial M. (1997) The diversity of Rab proteins in vesicle transport. Curr Opin Cell Biol **9**: 496-504.

O'Reilly, G. & Clarke, F. (1993) Identification of an actin binding region in aldolase. FEBS Lett **321**: 69-72.

Oatey, P. B., Van Weering, D. H., Dobson, S. P., Gould, G. W. & Tavaré, J. M. (1997) GLUT4 vesicle dynamics in living 3T3-L1 adipocytes visualized with green-fluorescent protein. Biochem J **327**: 637-642.

Odorizzi, G., Cowles, C. R. & Emr, S. D. (1998) The AP-3 complex: a coat of many colours. Trends Cell Biol **8**: 282-288.

Okada, T., Kawano, T., Sakakibara, T., Hazeki, O. & Ui, M. (1994) Essential role of phosphatidylinositol 3-kinase in insulin-induced glucose transport and anti-lipolysis in rat adipocytes - studies with a selective inhibitor wortmannin. J Biol Chem **269**: 3568-3573.

Olszewski, J. D., Dorman, G., Elliott, J. T., Hong, Y., Ahern, D. G. & Prestwich, G. D. (1995) Tethered benzophenone reagents for the synthesis of photoactivatable ligands. Biconjugate Chem **6**: 395-400.

Omata, W., Shibata, H., Suzuki, Y., Tanaka, S., Suzuki, T., Takata, K., Kojima, I. (1997) Subcellular distribution of GLUT4 in Chinese hamster ovary cells overexpressing mutant dynamin: Evidence that dynamin is a regulatory GTPase in GLUT4 endocytosis. Biochem Biophys Res Comm **241**: 401-406.

Ooi, C. E., Dell'Angelica, E. C. & Bonifacino, J. S. (1998) ADP-ribosylation factor 1 (ARF1) regulates recruitment of the AP-3 adaptor complex to membranes. J Cell Biol **142**: 391-402.

Palfreyman, R. W., Clark, A. E., Denton, R. M. & Holman, G. D. (1992) Kinetic resolution of the separate GLUT1 and GLUT4 glucose transport activities in 3T3-L1 cells. Biochem J **284**: 275-281.

Palmer, R. H., Dekker, L. V., Woschlolski, R., Le Good, J. A., Gigg, R. & Parker, P. J. (1995) Activation of PRK1 by phosphatidylinositol 4,5-bisphosphate and phosphatidylinositol 3,4,5-trisphosphate. A comparison with protein kinase C isotypes. J Biol Chem **270**: 22412-22416.

Paris, S., Béraud-Dufour, S., Robineau, S., Bigay, J., Antonny, B., Chabre, M. & Chardin, P. (1997) Role of protein-phospholipid interactions in the activation of ARF1 by the guanine nucleotide exchange factor Arno. J Biol Chem **272**: 22221-22226.

Patki, V., Virbasius, J., Lane, W. S., Toh, B-H., Shpetner, H. S. & Corvera, S. (1997) Identification of an early endosomal protein regulated by phosphatidylinositol 3-kinase. Proc Natl Acad Sci USA **94**: 7326-7330.

Pawson, T. (1995) Protein modules and signalling networks. Nature **373**: 573-580.

Pedersen, O., Bak, J. F., Andersen, P. H., Lund, S., Moller, D. E., Flier, J. S. & Kahn, B. B. (1990) Evidence against altered expression of GLUT1 or GLUT4 in skeletal muscle of patients with obesity or NIDDM. Diabetes **39**: 865-870.

Pelicci, G., Lanfrancone, L., Grignani, F., McGlade, J., Cavallo, F., Forni, G., Nicoletti, I., Grignani, F., Pawson, T. & Pelicci, P. G. (1992) A novel transforming protein (SHC) with an SH2 domain is implicated in mitogenic signal transduction. Cell **70**: 93-104.

Peter, M. E., She, J., Huber, L. A. & Terhorst, C. (1993) Labeling of adenine and guanine nucleotide-binding proteins in permeabilised cells with *in situ* periodate-oxidised nucleotides. Anal Biochem **210**: 77-85.

Peyroche A., Paris S. & Jackson C. L. (1996) Nucleotide exchange on ARF mediated by yeast Gea1 protein. Nature **384**: 479-484.

Pfeffer, S. R. (1992) GTP-binding proteins in intracellular transport. Trends Cell Biol **2**: 41-45.

Pfeffer, S. R. (1999) Transport-vesicle targeting: tethers before SNAREs. Nature Cell Biol **1**: E17-E22.

Prestwich, G. D. (1996) Touching all the bases: Synthesis of inositol polyphosphate and phosphoinositide affinity probes from glucose. Acc Chem Res **29**: 503-513.

Pronk, G. J., McGlade, J., Pelicci, G., Pawson, T. & Bos, J. L. (1993) Insulin-induced phosphorylation of the 46- and 52-kDa Shc proteins. J Biol Chem **268**: 5748-5753.

Pryor, P. R., Liu, S. C. H., Clark, A. E., Yang, J., Holman, G. D. & Tosh, D. (1999) Chronic-insulin effects on insulin signaling and GLUT4 endocytosis are reversed by metformin. *Submitted for publication.*

Quon, M. J., Chen, H., Ing, B. L., Liu, M-L., Zarnowski, M. J., Yonezawa, K., Kasuga, M., Cushman, S. W. & Taylor, S. I. (1995) Roles of 1-phosphatidylinositol 3-kinase and ras in regulating translocation of GLUT4 in transfected rat adipose cells. Mol Cell Biol **15**: 5403-5411.

Ralston, E. & Ploug, T. (1996) GLUT4 in cultured skeletal myotubes is segregated from the transferrin receptor and stored in vesicles associated with the TGN. J Cell Sci **109**: 2967-2978.

Rameh, L. E. & Cantley, L. C. (1999) The role of phosphoinositide 3-kinase lipid products in cell function. J Biol Chem **274**: 8347-8350.

Rameh, L. E., Arvidsson, A-K., Carraway III, K. L., Couvillon, A. D., Rathbun, G., Crompton, A., VanRenterghem, B., Czech, M. P., Ravichandran, K. S., Burakoff, S. J., Wang, D-S., Chen, C-S. & Cantley, L. C. (1997) A comparative analysis of the

phosphoinositide binding specificity of pleckstrin homology domains. J Biol Chem **272**: 22059-22066.

Rampal, A. L., Jhun, B. H., Kim, S., Liu, H., Manka, M., Lachaal, M., Spangler, R. A. & Jung, C. Y. (1995) Okadaic acid stimulates glucose transport in rat adipocytes by increasing the externalization rate constant of GLUT4 recycling. J Biol Chem **270**: 3938-3943.

Rapoport, I., Chen, Y. C., Cupers, P., Shoelson, S. E. & Kirchhausen, T. (1998) Dileucine-based sorting signals bind to the β chain of AP-1 at a site distinct and regulated differently from the tyrosine-based motif-binding site. EMBO J **17**: 2148-2155.

Rea, S. & James, D. E. (1997) Moving GLUT4. The biogenesis and trafficking of GLUT4 storage vesicles. Diabetes **46**: 1667-1677.

Rea, S., Martin, L. B., McIntosh, S., Macaulay, S. L., Ramsdale, T., Baldini, G. & James, D. E. (1998) Syndet, an adipocyte target SNARE involved in the insulin-induced translocation of GLUT4 to the cell surface. J Biol Chem **273**: 18784-18792.

Rondinone, C. M. & Smith, U. (1996) Okadaic acid exerts a full insulin-like effect on glucose transport and glucose transporter 4 translocation in human adipocytes. Evidence for a phosphatidylinositol 3-kinase-independent pathway. J Biol Chem **271**: 18148-18153.

Rondinone, C. M., Wang, L-M., Lonnroth, P., Wesslau, C., Pierce, J. H. & Smith, U. (1997) Insulin receptor substrate (IRS) 1 is reduced and IRS-2 is the main docking protein for phosphatidylinositol 3-kinase in adipocytes from subjects with non-insulin-dependent diabetes mellitus. Proc Natl Acad Sci USA **94**: 4171-4175.

Rondinone, C. M., Zarnowski, M. J., Londos, C. & Smith, U. P. G. (1996) The inhibitory effect of staurosporine on insulin action is prevented by okadaic acid. Evidence for an important role of serine/threonine phosphorylation in eliciting insulin-like effects. Biochim Biophys Acta - Mol Cell Res **1314**: 49-56.

Rossetti, L., DeFronzo, R. A., Gherzi, R., Stein, P., Andraghetti, G., Falzetti, G., Schulman, G. I., Klein-Robbenhaar, E. & Cordera, R. (1990) Effect of metformin treatment on insulin action in diabetic rats: *in vivo* and *in vitro* correlations. Metabolism **39**: 425-435. S2-S17.

Saad, M. J. A., Maeda, L., Brenelli, S. L., Carvalho, C. R. O., Paiva, R. S. & Velloso, L. A. (1997) Defects in insulin signal transduction in liver and muscle of pregnant rats. Diabetologia **40**: 179-186.

Sable, C. L., Filippa, N., Hemmings, B. & Obberghen E. V. (1997) cAMP stimulates protein kinase B in a wortmannin-insensitive manner. FEBS Lett **409**: 253-257.

Saltis, J., Habberfiled, A. D., Egan, J. J., Londos, C., Simpson, I. A. & Cushman, S. W. (1991) Role of protein kinase C in the regulation of glucose transport in the rat adipose cell. Translocation of glucose transporters without stimulation of glucose transport activity. J Biol Chem **266**: 261-267.

Sanchez, P., De Carcer, G., Sandoval, I. V., Moscat, J. & Diaz-Meco, M. T. (1998) Localization of atypical protein kinase C isoforms into lysosome-targeted endosomes through interaction with p62. Mol Cell Biol **18**: 3069-3080.

Sancho, J., Peter, M. E., Franco, R., Danielian, S., Kang, J. S., Fagard, R., Woods, J., Reed, J. C., Kamoun, M. & Terhorst, C. (1993) Coupling of GTP-binding to the T cell receptor (TCR) ξ-chain with TCR-mediated signal transduction. J Immunol **150**: 3320-3242.

Santos, R. F., Nomizo, R., Wajhenberg, B. L., Reaven, G. M. & Azhar, S. (1995) Changes in insulin receptor tyrosine kinase activity associated with metformin treatment of type 2 diabetes. Diabete & Metabolisme **21**: 274-280.

Satoh, S., Nishimura, H., Clark, A. E., Kozka, I. J., Vannucci, S. J., Simpson, I. A., Quon, M. J., Cushman, S. W. & Holman, G. D. (1993) Use of bismannose photolabel to elucidate insulin-regulated GLUT4 subcellular trafficking kinetics in rat adipose cells. J Biol Chem **268**: 17820-17829.

Sawke-Verhelle, D., Tartare-Deckert, S., White, M. F. & Van Obberghen, E. (1996) Insulin receptor substrate-2 binds to the insulin receptor through its phosphotyrosine-binding domain and through a newly identified domain comprising amino acids 591-786. J Biol Chem **271**: 5980-5983.

Scheffzek, K., Ahmadian, M. R. & Wittinghofer, A. (1998) GTPase-activating proteins: helping hands to complement an active site. TIBS **23**: 257-262.

Schiavo, G., Gu, Q-M., Prestwich, G. D., Söllner, T. H. & Rothman, J. E. (1996) Calcium-dependent switching of the specificity of phosphoinositide binding to synaptotagmin. Proc Natl Acad Sci USA **93**: 13327-13332.

Seely, B. L., Staubs, P. A., Reichart, D. R., Berhanu, P., Milarski, K. L., Saltiel, A. R., Kusari, J. & Olefsky, J. M. (1996) Protein tyrosine phosphatase 1B interacts with the activated insulin receptor. Diabetes **45**: 1379-1385.

Sharma, P. M., Egawa, K., Gustafson, T. A., Martin, J. L. & Olefsky, J. M. (1997) Adenovirus-mediated overexpression of IRS-1 interacting domains abolishes insulin-stimulated mitogenesis without affecting glucose transport in 3T3-L1 adipocytes. Mol Cell Biol **17**: 7386-7397.

Shepherd, P. R., Withers, D. J. & Siddle, K. (1998) Phosphoinositide 3-kinase: the key switch mechanism in insulin signalling. Biochem J **333**: 471-490.

Shibata, H., Omata, W. & Kojima, I. (1997) Insulin stimulates guanine nucleotide exchange on Rab4 via a wortmannin-sensitive signaling pathway in rat adipocytes. J Biol Chem **272**: 14542-14546.

Shibata, H., Omata, W., Suzuki, Y., Tanaka, S. & Kojima, I. (1996) A synthetic peptide corresponding to the rab4 hypervariable carboxyl-terminal domain inhibits insulin action on glucose transport in rat adipocytes. J Biol Chem **271**: 9704-9709.

Shibata, H., Suzuki, Y., Omata, W., Tanaka, S. & Kojima, I. (1995) Dissection of GLUT4 recycling pathway into exocytosis and endocytosis in rat adipocytes. Evidence that GTP-binding proteins are involved in both processes. J Biol Chem **270**: 11489-11495.

Shirai, T., Tanaka, K., Terada, Y., Sawada, T., Shirai, R., Hashimoto, Y., Nagata, S., Iwamatsu, A., Okawa, K., Li, S., Hattori, S., Mano, H. & Fukui, Y. (1998) Specific detection of phosphatidylinositol 3,4,5-trisphosphate binding proteins by the PIP_3 analogue beads: An application for rapid purification of the PIP_3 binding proteins. Biochim Biophys Acta **1402**: 292-302.

Shisheva, A. & Czech, M. P. (1997) Association of cytosolic Rab4 with GDI isoforms in insulin-sensitive 3T3-L1 adipocytes. Biochem **36**: 6564-6570.

Shisheva, A. & Shechter, Y. (1993) Mechanism of pervanadate stimulation and potentiation of insulin-activated glucose transport in rat adipocytes: Dissociation from vanadate effect. Endocrinology **133**: 1562-1568.

Simonsen A., Lippé R., Christoforidis S., Gaullier J-M., Brech A., Callaghan J., Toh B-H., Murphy C., Zerial M. & Stenmark H. (1998) EEA1 links PI(3)K function to Rab5 regulation of endosome fusion. Nature **394**: 494-498.

Simpson, I. A., Yver, D. R., Hissin, P. J., Wardzala, L. J., Karnieli, E., Salans, L. B. &Cushman S. W. (1983) Insulin-stimulated translocation of glucose transporters in the isolated rat adipose cells: Characterization of subcellular fractions. Biochim Biophys Acta **763**: 393-407.

Skolnik, E. Y., Lee, C. H., Batzer, A., Vicentini, L. M., Zhou, M., Daly, R., Myers, M. J., Backer, J. M., Ullrich, A., White, M. F. & Schlessinger, J. (1993) The SH2/SH3 domain-containing protein GRB2 interacts with tyrosine-phosphorylated IRS1 and Shc: implications for insulin control of *ras* signalling. EMBO J **12**: 1929-1936.

Slot, J. W., Garruti, G., Martin, S., Oorschot, V., Posthuma, G., Kraegen, E. W., Laybutt, R., Thibault, G. & James, D. E. (1997) Glucose transporter (GLUT-4) is targeted to secretory granules in rat atrial cardiomyocytes. J Cell Biol **137**: 1243-1254.

Slot, J. W., Geuze, H. J., Gigengack, S., Lienhard, G. E. & James, D. E. (1991) Immuno-localization of the insulin regulatable glucose transporter in brown adipose tissue of the rat. J Cell Biol **113**: 123-135.

Söllner, T., Whiteheart, S. W., Brunner, M., Erdjument-Bromage, H., Geromanos, S., Tempst, P. & Rothman, J. E. (1993) SNAP receptors implicated in vesicle targeting and fusion. Nature **362**: 318-323.

Sprang, S. R. & Coleman, D. E. (1998) Invasion of the nucleotide snatchers: Structural insights into the mechanism of G protein GEFs. Cell **95**: 155-158.

Stack, J. H., Herman, P. K., Schu, P. V. & Emr, S. D. (1993) A membrane-associated complex containing the vps15 protein-kinase and the vps34 PI 3-kinase is essential for protein sorting to the yeast lysosome-like vacuole. EMBO J **12**: 2195-2204.

Stamnes, M. A. & Rothman, J. E. (1993) The binding of AP-1 clathrin adaptor particles to Golgi membranes requires ADP-ribosylation factor, a small GTP-binding protein. Cell **73**: 999-1005.

Standaert, M. L., Galloway, L., Karnam, P., Bandyoppadhyay, G., Moscat, J. & Farese, R. V. (1997) Protein kinase C-ζ as a downstream effector of phosphatidylinositol 3-kinase during insulin stimulation in rat adipocytes. Potential role in glucose transport. J Biol Chem **272**: 30075-30082.

Standaert, M., Bandyopadhyay, G., Galloway, L., Ono, Y., Mukai, H. & Farese, R. (1998) Comparative effects of GTPγS and insulin on the activation of Rho, phosphatidylinositol 3-kinase, and protein kinase N in rat adipocytes. J Biol Chem **273**: 7470-7477.

Stephens, L., Anderson, K., Stokoe, D., Erdjument-Bromage, H., Painter, G. F., Holmes, A. B., Gaffney, P. R. J., Reese, C. B., McCormick, F., Tempst, P., Coadwell, J. & Hawkins, P. T. (1998) Protein kinase B kinases that mediate phosphatidylinositol 3,4,5-trisphosphate-dependent activation of protein kinase B. Science **279**: 710-714.

Stith, B. J., Goalstone, M. L., Espinoza, R., Mossel, C., Roberts, D. & Wiernsperger, N. (1996) The antidiabetic drug metformin elevates tyrosine kinase activity and inositol 1,4,5-trisphosphate mass in *Xenopus* oocytes. Endocrinology **137**: 2990-2999.

Stricker, R., Husler, E., Fischer, J., Jarchau, Th., Walter, U., Lottspeich, F. & Reiser, G. (1997) cDNA cloning of porcine $p42^{IP4}$, a membrane-associated and cytosolic 42 kDa

inositol(1,3,4,)tetrakisphosphate receptor from pig brain with similarly high affinity for phosphatidylinositol (3,4,5)P_3. FEBS Lett **405**: 229-236.

Sun, X. J., Crimmins, D. L., Myers Jr., M. G., Miralpeix, M. & White, M. F. (1993) Pleiotropic insulin signals are engaged by multisite phosphorylation of IRS-1. Mol Cell Biol **13**: 7418-7428.

Sun, X. J., Pons, S., Asano, T., Myers Jr., M. G., Glasheen, E. & White, M. F. (1996) The fyn tyrosine kinase binds IRS-1 and forms a distinct signaling complex during insulin stimulation. J Biol Chem **271**: 10583-10587.

Sun, X. J., Rothenberg, P., Kahn, C. R., Backer, J. M., Araki, E., Wilden, P. A., Cahill, D. A., Goldstein, B. J. & White, M. F. (1991) Structure of the insulin receptor substrate IRS-1 defines a unique signal transduction protein. Nature **352**: 73-77.

Sun, X. J., Wang, L-M., Zhang, Y., Yenush, L., Myers Jr., M. G., Glasheen, E., Lane, W. S., Pierce, J. H. & White, M. F. (1995) Role of IRS-2 in insulin and cytokine signalling. Nature **377**: 173-177.

Suzuki, K. & Kono, T. (1980) Evidence that insulin causes translocation of glucose transport activity to the plasma membrane from an intracellular storage site. Proc Natl Acad Sci USA **77**: 2542-2545.

Tamemoto, H., Kadowaki, T., Tobe, K., Yagi, T., Sakura, H., Hayakawa, T., Terauchi, Y., Ueki, K., Kaburagi, Y., Satoh, S., Sekihara, H., Yoshioka, S., Horikoshi, H., Furuta, Y., Ikawa, Y., Kasuga, M., Yazaki, Y. & Aizawa, S. (1994) Insulin resistance and growth retardation in mice lacking insulin receptor substrate-1. Nature **372**: 182-186.

Tamori, Y., Kawanishi, M., Niki, T., Shinoda, H., Araki, S., Okazawa, H. & Kasuga, M. (1998) Inhibition of insulin-induced GLUT4 translocation by Munc18c through interaction with syntaxin4 in 3T3-L1 adipocytes. J Biol Chem **273**: 19740-19746.

Tanaka, K., Imajoh-Ohmi, S., Sawada, T., Shirai, R., Hashimoto, Y., Iwasaki, S., Kaibuchi, K., Kanaho, Y., Shirai, T., Terada, Y., Kimura, K., Nagata, S. & Fukui, Y. (1997) A target of phosphatidylinositol 3,4,5-trisphosphate with a zinc finger motif similar to that of the ADP-ribosyation factor GTPase-activating protein and two pleckstrin homology domains. Eur J Biochem **245**: 512-519.

Tanti, J. F., Gremeaux, T., Grillo, S., Calleja, V. & Klippel, A., Williams, L. T., Van Obberghen, E. & Le Marchand-Brustel, Y. (1996) Overexpression of a constitutively active form of phosphatidylinositol 3-kinase is sufficient to promote glut 4 translocation in adipocytes. J Biol Chem **271**: 25227-25232.

Tanti, J-F., Gremeaux, T., Van Obberghen, E. & Le Marchand-Brustel, Y. (1994) Serine/threonine phosphorylation of insulin receptor substrate 1 modulates insulin receptor signalling. J Biol Chem **269**: 6051-6057.

Taylor, L. P. & Holman, G. D. (1981) Symmetrical kinetic parameters for 3-O-methyl-D-glucose transport in adipocytes in the presence and in the absence of insulin. Biochim Biophys Acta **642**: 325-335.

Tellam, J. T., Macaulay, S. L., McIntosh, S., Hewish, D. R., Ward, C. W. & James, D. E. (1997) Characterization of Munc-18c and Syntaxin-4 in 3T3-L1 adipocytes. J Biol Chem **272**: 6179-6186.

Tellam, J. T., McIntosh S. & James, D. E. (1995) Molecular identification of two novel Munc-18 isoforms expressed in non-neuronal tissues. J Biol Chem **270**: 5857-5863.

Thiebert, A. B., Prestwich, G. D., Jackson, T. R. & Hammonds-Odie, L. P. (1997) The purification and assay of inositide binding proteins. Signalling by inositides. A practical approach. Edited by Shears, S. Oxford University Press.

Thieleczek, R., Mayr, G. W. & Brandt, N. R. (1989) Inositol polyphosphate-mediated repartitioning of aldolase in skeletal muscle triads and myofibrils. J Biol Chem **264**: 7349-7356.

Timmers, K. I., Clark, A. E., Omatsu-Kanbe, M., Whiteheart, S. W., Bennett, M. K., Holman, G. D. & Cushman, S. W. (1996) Identification of SNAP receptors in rat adipose cell membrane fractions and in SNARE complexes co-immunoprecipitated with epitope-tagged N-ethylmaleimide-sensitive fusion protein. Biochem J **320**: 429-436.

Tobe, K., Sabe, H., Yamamoto, T., Yamauchi, T., Asai, S., Kaburagi, Y., Tamemoto, H., Ueki, K., Kiura, H., Akanuma, Y., Yazaki, Y., Hanafusa, H. & Kadowaki, T. (1996) Csk enhances insulin-stimulated dephosphorylation of focal adhesion proteins. Mol Cell Biol **16**: 4765-4722.

Tyers, M., Rachubinski, R. A., Stewart, M. I., Varrichio, A. M., Shorr, R. G. L., Haslam, R. J. & Harley, C. B. (1988) Molecular-cloning and expression of the major protein kinase-c substrate of platelets. Nature **333**: 470-473.

Uphues, I., Kolter, T., Goud, B. & Eckel, J. (1994) Insulin-induced translocation of the glucose transporter GLUT4 in cardiac muscle: studies on the role of small-molecular mass GTP-binding proteins. Biochem J **301**: 177-182.

Vanhaesebroeck, B., Leevers, S. J., Panayotou, G. & Waterfield, M. D. (1997) Phosphoinositide 3-kinases: a conserved family of signal transducers. TIBS **22**: 267-272.

Venkateswarlu, K., Oatey, P. B., Tavaré, J. M. & Cullen, P. J. (1998) Insulin-dependent translocation of ARNO to the plasma membrane of adipocytes requires phosphatidylinositol 3-kinase. Curr Biol **8**: 463-466.

Verhage, M., deVries, K. J., Roshol, H., Burbach, J. P. H., Gispen, W. H. & Sudhof, T. C. (1997) DOC2 proteins in rat brain: Complementary distribution and proposed function as vesicular adapter proteins in early stages of secretion. Neuron **18**: 453-461.

Virbasius, J. V., Guilherme, A. & Czech, M. P. (1996) Mouse p170 is a novel phosphatidylinositol 3-kinase containing a C2 domain. J Biol Chem **271**: 13304-13307.

Volchuk, A., Narine, S., Foster, L. J., Grabs, D., DeCamilli, P. & Klip, A. (1998) Perturbation of dynamin II with an amphiphysin SH3 domain increases GLUT4 glucose transporters at the plasma membrane in 3T3-L1 adipocytes - Dynamin II participates in GLUT4 endocytosis. J Biol Chem **273**: 8169-8176.

Volchuk, A., Sargeant, R., Sumitani, S., Liu, Z., He, L. & Klip A. (1995) Cellubrevin is a resident protein of insulin-sensitive GLUT4 glucose transporter vesicles in 3T3-L1 adipocytes. J Biol Chem **270**: 8233-8240.

Voliovitch, H., Schindler, D. G., Hadari, Y. R., Taylor, S. I., Accili, D. & Zick, Y. (1995) Tyrosine phosphorylation of insulin receptor substrate-1 *in vivo* depends upon the presence of its pleckstrin homology region. J Biol Chem **270**: 18083-18087.

Walaas, O., Horn, R. S. & Walaas, S. I. (1997) The protein kinase C pseudosubstrate peptide (PKC19-36) inhibits insulin-stimulated protein kinase activity and insulin-mediated translocation of the glucose transporter glut 4 in streptolysin-O permeabilised adipocytes. FEBS Lett **413**: 152-156.

Walker, K. S., Deak, M., Paterson, A., Hudson, K., Cohen, P. & Alessi, D. R. (1998) Activation of protein kinase B β and γ isoforms by insulin *in vivo* and by 3-phosphoinositide-dependent protein kinase-1 *in vitro*: comparison with protein kinase B α. Biochem J **331**: 299-308.

Wang, Q., Bilan, P. J., Tsakiridis, T., Hinek, A. & Klip, A. (1998) Actin filaments participate in the relocalization of phosphatidylinositol 3-kinase to glucose transporter-containing compartments and in the stimulation of glucose uptake in 3T3-L1 adipocytes. Biochem J **331**: 917-928.

Waters, S. B., D'Auria, M., Martin, S. A., Nguyen, C., Kozma, L. M. & Luskey, K. L. (1997) The amino terminus of insulin-responsive aminopeptidase causes GLUT4 translocation in 3T3-L1 adipocytes. J Biol Chem **272**: 23323-23327.

Weber, T. M., Joost, H., Simpson, I. A. & Cushman, S. W. (1988) Methods for assessment of glucose transport activity and the number of glucose transporters in isolated rat adipose cells and membrane fractions. The Insulin Receptor, part B (ed. Kahn, C. R & Harrison, L. C.): 171-187. Liss, A. R. Inc, New York.

West, M. A., Bright, N. A. & Robinson, M. S. (1997) The role of ADP-ribosylation factor and phospholipase D in adaptor recruitment. J Cell Biol **138**: 1239-1254.

White, M. F. & Kahn, C. R. (1994) The insulin signaling system. J Biol Chem **269**: 1-4.

White, M. F. (1997) The insulin signaling system and the IRS proteins. Diabetologia **40**: S2-S17.

White, M. F., Livingstone, J. N., Backer, J. M., Lauris, V., Dull, T. J., Ullrich, A. & Kahn, C. R. (1988) Mutation of the insulin-receptor at tyrosine-960 inhibits signal transmission but does not affect its tyrosine kinase-activity. Cell **54**: 641-649.

Wiese, R. J., Mastick, C. C., Lazar, D. F. & Saltiel, A. R. (1995) Activation of mitogen-activated protein-kinase and phosphatidylinositol 3'-kinase is not sufficient for the hormonal-stimulation of glucose uptake, lipogenesis, or glycogen synthesis in 3T3-L1 adipocytes. J Biol Chem B **270**: 3442-3446.

Withers, D. J., Gutierrez, J. S., Towery, H., Burks, D. J., Ren, J-M., Previs, S., Zhang, Y., Berna,l D., Pons, S., Shulman, G. I., Bonner-Weir, S. & White, M. F. (1998) Disruption of IRS-2 causes type 2-diabetes in mice. Nature **391**: 900-904.

Xiao, S., Rose, D. W., Sasaoka, T., Maegawa, H., Burke Jr., T. R., Roller, P. P., Shoelson, S. E. & Olefsky, J. M. (1994) Syp (SH-PTP2) is a positive mediator of growth factor-stimulated mitogenic signal transduction. J Biol Chem **269**: 21244-21248.

Yamaguchi, T., Yamamoto, A., Furuno, A., Hatsuzawa, K., Tani, K., Himeno, M. & Tagaya, M. (1997) Possible involvement of heterotrimeric G proteins in the organization of the Golgi apparatus. J Biol Chem **272**: 25260-25266.

Yamamoto-Honda, R., Kadowaki, T., Momomura, K., Tobe, K., Tamori, Y., Shibasaki, Y., Mori, Y., Kaburagi, Y., Koshio, O., Akanuma, Y., Yazaki, Y. & Kasuga, M. (1993) Normal insulin receptor substrate-1 phosphorylation in autophosphorylation-defective truncated insulin receptor. J Biol Chem **268**: 16859-16865.

Yang, J. & Holman, G. D. (1993) Comparison of GLUT4 and GLUT1 subcellular trafficking in basal and insulin-stimulated 3T3-L1 cells. J Biol Chem **268**: 4600-4603.

Yang, J., Clark, A. E., Harrison, R., Kozka, I. J. & Holman, G. D. (1992) Trafficking of glucose transporters in 3T3-L1 cells. Inhibition of trafficking by phenylarsine oxide

implicates a slow dissociation of transporters from trafficking proteins. Biochem J **281**: 809-817.

Yang, J., Clarke, J. F., Ester, C. J., Young, P. W., Kasuga, M. & Holman, G. D. (1996) Phosphatidylinositol 3-kinase acts at an intracellular membrane site to enhance GLUT4 exocytosis in 3T3-L1 cells. Biochem J **313**: 125-131.

Yeh, J. I., Gulve, E. A., Rameh, L. & Birnbaum, M. J. (1995) The effects of wortmannin on rat skeletal muscle - dissociation of signaling pathways for insulin-activated and contraction-activated hexose transport. J Biol Chem **270**: 2107-2111.

Yenush, L. & White, M. F. (1997) The IRS-signalling system during insulin and cytokine action. BioEssays **19**: 491-500.

Zhang, W-R., Li, P-W., Oswald, M. A. & Goldstein, B. J. (1996) Modulation of insulin signal transduction by eutopic overexpression of the recptor-type protein tyrosine phosphatase LAR. Mol Endocrinol **10**: 575-584.

Zhu, Y., Traub, L. M. & Kornfeld, S. (1998) ADP-ribosylation factor 1 transiently activates high-affinity adaptor protein complex AP-1 binding sites on Golgi membranes. Mol Biol Cell **9**: 1323-1337.

Zor, T., Halifa, I., Kleinhaus, S., Chorev, M. & Selinger, Z. (1995) m-Acetylanilido-GTP, a novel photoaffinity label for GTP-binding proteins: synthesis and application. Biochem J **306**: 253-258.

Zorzano, A., Wilkinson, W., Kotliar, N., Thoidis, G., Wadzinkski, B. E., Ruoho, A. E. & Pilch, P. F. (1989) Insulin-regulated glucose uptake in rat adipocytes is mediated by two transporter isoforms present in at least two vesicle populations. J Biol Chem **264**: 12358-12363.